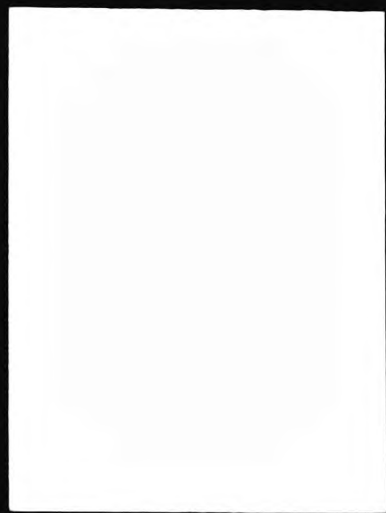


This PDF was created from the British Library's microfilm copy of the original thesis. As such the images are greyscale and no colour was captured.

Due to the scanning process, an area greater than the page area is recorded and extraneous details can be captured.

This is the best available copy



DX

189641

THE BRITISH LIBRARY

BRITISH THESIS SERVICE

TITLE AN ANALYTICAL STUDY OF THE ROLE SELECTED METAL IONS IN BONE AND JOINT DISEASES

AUTHOR Alexandra
FURST

DEGREE Ph.D

AWARDING BODY University of North London

DATE 1995

THESIS NUMBER DX189641

THIS THESIS HAS BEEN MICROFILMED EXACTLY AS RECEIVED

The quality of this reproduction is dependent upon the quality of the original thesis submitted for microfilming. Every effort has been made to ensure the highest quality of reproduction. Some pages may have indistinct print, especially if the original papers were poorly produced or if awarding body sent an inferior copy. If pages are missing, please contact the awarding body which granted the degree.

Previously copyrighted materials (journals articles, published texts etc.) are not filmed.

This copy of the thesis has been supplied on condition that anyone who consults it is understood to recognise that its copyright rests with its author and that no information derived from it may be published without the author's prior written consent.

Reproduction of this thesis, other than as permitted under the United Kingdom Copyright Designs and Patents Act 1988, or under specific agreement with the copyright holder, is prohibited.

**AN ANALYTICAL STUDY OF THE ROLE OF SELECTED METAL IONS IN
BONE AND JOINT DISEASES**

ALEXANDRA FURST

**A thesis submitted in partial fulfillment of the requirements of the University of
North London for the degree of Doctor of Philosophy**

The research work was carried out in collaboration with the Royal London Hospital

JULY 1995

ABSTRACT

Metal ions play a major role in a wide range of biological processes in the human body. Metal ions in low-molecular weight complexes are of particular interest because of their greater 'mobility' and 'reactivity' compared to the high-molecular weight protein-bound metal ions. In this project, low-molecular weight metal ions encountered *in vivo* due to bone and joint disease are studied, namely gold, titanium and iron metal ions.

Gold compounds such as disodium aurothiomalate (Myocrisin) have been used for over 50 years in the treatment of rheumatoid arthritis (RA). As gold (I) acts like a soft Lewis acid, it possesses a high affinity for thiol ligands and therefore primarily distributes itself amongst protein and to some extent non-protein thiol groups *in vivo*. Most of the gold is bound to the protein serum albumin, principally at the sulphhydryl site Cys(34)-SH, and a smaller amount is bound to immunoglobulins. A small amount of the total circulating gold is present as low-molecular weight or "free" gold, which is likely to play an important role in gold transportation processes and the attainment of chemical equilibrium of gold between the protein binding sites.

In this study the concentration of low-molecular weight gold in the biological fluids of RA patients undergoing gold drug therapy (chrysotherapy) was analysed. The biological samples were centrifuged in order to obtain ultrafiltrate which would be free of high-molecular weight gold. The ultrafiltrate, containing the low-molecular gold was treated with potassium cyanide to facilitate the production of an auro(I)cyanide complex which could be detected and quantified by the use of high pressure liquid chromatography (HPLC) in conjunction with ultra-violet (UV) detection at a wavelength of 211 nm. HPLC provided a method that was sensitive to the low concentrations found. The results obtained were backed up by measuring the "free" gold concentration by means of flameless atomic absorption spectrometry (AAS).

In addition the chemical nature of titanium ions found in localised darkly stained tissue adjacent to titanium-aluminium-vanadium hip implants was investigated. The production of the dark blue/black complex seen in the affected tissue was simulated *in vitro* by synthetic pathways. The speciation of the titanium (III)/titanium (IV) complexes in the biological matrices was investigated with Fourier transform infra red (FTIR) spectroscopy and high field proton nuclear magnetic resonance (NMR) with a Hahn spin echo pulse sequence.

The chemical nature of non-protein bound iron present in knee joint synovial fluid obtained from RA patients was also investigated by use of NMR.



Dedicated to Those I Love

*'Whatever you can do or dream you can,
begin it'.*

Goethe



Acknowledgements

I would like to express my heartfelt gratitude to my supervisor, Dr D.E.M. Spillane for his guidance, encouragement and moral support, as well as for endless proof reading. I would also like to thank Dr M. Grootveld for his help and ideas on the project.

My thanks are extended to Wimal Dissanayake for his invaluable technical help and also to Alan Bashall for running of the AA samples.

A special thanks goes to Dr D.R. Blake and his group, at the Bone and Joint Research Unit at the Royal London Hospital, for supplying the biological samples.

I would like to thank Pete Haycock at Queen Mary College and Harry Parkes at Birkbeck College for running the NMR spectra.

I would like to thank my colleagues and friends Reetu and Ismail for sharing and understanding the trials and tribulations.

I would like to wholeheartedly express my gratitude to Panos for the kind loan of a computer and printer, and most of all, to Dimitri, for his tireless printing and photocopying, and endless patience and encouragement.

My final thanks go to my dearest mother, Dusanka, for her boundless encouragement and support.

CONTENTS

ABSTRACT	1
CHAPTER 1 INTRODUCTION	8
1. INTRODUCTION	9
1.1 METAL IONS IN BIOLOGICAL SYSTEMS	9
a) Trigger and Control Mechanisms	9
b) Structural Influences	10
c) Lewis acid behaviour	10
d) Redox behaviour	10
1.2 METAL IONS IN BONE AND JOINT DISEASE	11
1.3 RHEUMATOID ARTHRITIS	13
1.3.1 Histology of Rheumatoid Arthritis	15
1.3.2 Treatment of Rheumatoid Arthritis	16
1.4 GOLD DRUGS IN RHEUMATOID ARTHRITIS	18
1.4.1 History of Gold Treatment	18
1.4.2 Chrysotherapy and Structure of Gold (I) Thiolates	20
1.4.3 Distribution of Gold (I) Thiolate Drugs <i>in vivo</i>	22
1.4.4 Mechanism of Action of Gold Drugs	23
1.5 TITANIUM IMPLANTS IN BONE AND JOINT DISEASE	26
1.5.1 Introduction	26
1.5.2 General Chemistry of Titanium	27
1.5.2.1 The Aqueous +4 Oxidation State	28
1.5.2.2 The Aqueous +3 Oxidation State	28

1.5.3.	Titanium Alloys	30
1.5.4.	The Tissue Environment	31
1.5.5.	Use of Titanium Implants	31
1.6	IRON IN THE RHEUMATOID JOINT	33
1.6.1	The Role of Iron in the Body	33
1.6.2	Iron Storage and Transport	34
1.7	AIMS OF THIS PROJECT	35
CHAPTER 2	ANALYTICAL TECHNIQUES	38
2.1	ANALYTICAL TECHNIQUES EMPLOYED	39
2.2	LIQUID CHROMATOGRAPHY	40
2.2.1	Introduction	40
2.2.2	Development of Chromatography	41
2.2.3	Classification of Liquid Chromatography	42
	a) Adsorption Chromatography	42
	b) Liquid-Liquid Partition Chromatography	42
	c) Bonded Phase Chromatography (BPC)	43
2.2.4	Classification of Non Polar Bonded Phases	44
	2.2.4.1 Siloxane Type Bonded Phases	45
2.2.5	Monomeric Phases	45
2.2.6	Polymeric Phases	46
2.2.7	General Theory of Chromatography	47
	2.2.7.1 Molecular Interactions	47
	2.2.7.2 Dispersive Interactions	47
	2.2.7.3 Polar Interactions	48
	2.2.7.4 Hydrogen Bonding	49
	2.2.7.5 Ionic Interactions	50
	2.2.7.6 Acid-Base Reactions	50

2.2.8	Chromatographic Behaviour of Solutes	51
	2.2.8.1 Retention Behaviour	51
	2.2.8.2 Distribution Coefficient	53
2.2.9	Band Broadening	53
	2.2.9.1 Eddy Diffusion	54
	2.2.9.2 Longitudinal Diffusion	55
	2.2.9.3 Mass Transfer	55
2.2.10	HPLC Instrumentation	58
	2.2.10.1 HPLC Detectors	58
2.3	ELECTROMAGNETIC RADIATION	60
	2.3.1 Properties of Electromagnetic Radiation	61
2.4	INFRARED SPECTROSCOPY	62
	2.4.1 Fourier Transform Infrared (FTIR) Spectroscopy	63
2.5	ATOMIC ABSORPTION SPECTROSCOPY (AAS)	65
	2.5.1 Instrumentation	66
2.6	NUCLEAR MAGNETIC RESONANCE (NMR) SPECTROSCOPY	69
	2.6.1 General Principles of NMR	69
	2.6.2 Pulse NMR	73
	2.6.2.1 Hahn Spin-Echo	75
CHAPTER 3 THE DEVELOPMENT OF AN ANALYTICAL METHOD FOR THE DETECTION OF GOLD (I) PRESENT AS THE ANTI-RHEUMATIC DRUG DISODIUM AUROTHIOMALATE BY HPLC		78

3.1	INTRODUCTION	79
3.1.1	Dithizone as a Complexing Agent	79
3.1.2	Formation of Dicyanoaurate	81
3.2	MATERIALS AND METHODS	81
3.2.1	Materials	81
3.2.2	Dithizone Experiments	82
3.2.2.1	Spectrophotometric Titration	82
3.2.2.2	Extraction of Au (I) with Dithizone	83
3.2.2.3	Dithizone Spectrophotometric Results	84
3.2.2.4	Dithizone HPLC Results	88
3.3	FORMATION OF GOLD CYANIDE	91
3.3.1	Materials	91
3.3.2	Standard Curve of Potassium Dicyanide	92
3.3.3	Chromatogram of a RA Blood Serum Ultrafiltrate	94
3.3.3	Obtaining an Internal Standard	95
3.3.4	Standard Curve of Potassium Dicyanoaurate	98
3.4	RESULTS AND DISCUSSION	100
3.5	CONCLUSION	110
CHAPTER 4 DEVELOPMENT OF AN ANALYTICAL METHOD FOR THE DETECTION OF LOW MOLECULAR WEIGHT GOLD (I) PRESENT IN BIOLOGICAL FLUID OF RHEUMATOID ARTHRITIS PATIENTS UNDERGOING CHRYSOTHERAPY		111
4.1	INTRODUCTION	112
4.2	MATERIALS AND METHODS	114
4.2.1	Instrumentation	114
4.2.2	Preparation of Biological Samples	115

4.2.3	Method	115
4.2.4	HPLC Procedure	117
4.2.5	Atomic Absorption	118
4.3	RESULTS AND DISCUSSION	120
4.3.1	Quantitative Analysis	123
4.3.2	Atomic Absorption Results	125
4.3.3	Analysis of Plasma	127
4.4	CONCLUSION	132
CHAPTER 5 INVESTIGATION OF THE MOLECULAR NATURE OF IMPLANT-DERIVED TITANIUM (III) AND TITANIUM (IV) IONS IN TISSUE AND SYNOVIAL FLUID ADJACENT TO TITANIUM-ALLOY HIP PROSTHESES		134
5.1	INTRODUCTION	135
5.1.1	Black Staining	135
5.1.2	Oxide Needle Model	137
5.1.3	Titanium Gels	138
5.2	MATERIALS AND METHODS	141
5.2.1	Reagents	141
5.2.2	Methods	141
5.2.2.1	Reduction of Titanium (IV) Complexes	141
5.2.2.1.1	Preparation with Ti (IV) Oxysulphate	141
a)	Precipitation with Sodium Hydroxide	141
b)	Measurement of Titanium Concentration	142
c)	Precipitation with Sodium Carbonate	144
d)	Precipitation // Inorganic Phosphate	146
5.2.2.1.2	Preparations Using Ti (IV) Potassium Oxalate	146

	a) Precipitation with Sodium Carbonate	146
	b) Precipitation with Sodium Hydroxide	148
	c) Removal of Ti (IV) Oxalate	152
	d) Addition of Citrate	152
	e) Precipitation with Phosphate	153
	5.2.2.2 Tissue Samples	153
	5.2.2.3 Synovial Fluid Samples	154
	5.2.2.4 FTIR Spectroscopic Analysis	154
	5.2.2.5 NMR Measurements	155
5.3	RESULTS AND DISCUSSIONS	156
	5.3.1 FTIR Spectroscopic Analysis	159
	5.3.2 High Field Proton Hahn Spin-echo NMR Analysis	164
5.4	CONCLUSION	169
CHAPTER 6 SPECIATION OF NON-TRANSFERRIN BOUND IRON IN SYNOVIAL FLUID OF RHEUMATOID ARTHRITIS PATIENTS BY PROTON HAHN SPIN-ECHO NMR		173
6.1	INTRODUCTION	174
6.2	MATERIALS AND METHODS	177
	6.2.1 Materials	177
	6.2.2 Methods	177
	6.2.3 NMR Measurements	178
6.3	RESULTS AND DISCUSSION	179
6.4	CONCLUSION	184
CHAPTER 7 CONCLUSIONS		185
REFERENCES		189

CHAPTER 1

INTRODUCTION


1. INTRODUCTION

1.1 METAL IONS IN BIOLOGICAL SYSTEMS

Metal ions play an important role in a wide range of biological processes. The function of the ion varies considerably depending on the process involved. There are four major ways in which the metal ions can act in the body:

- a) in trigger and control mechanisms,
- b) in a structural context,
- c) as Lewis acids,
- d) as Redox catalysts¹.

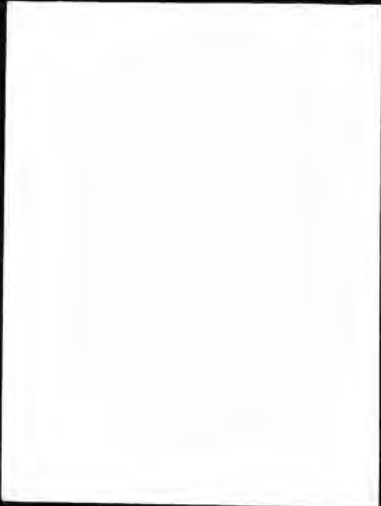
a) **Trigger and Control Mechanisms** - The cations sodium (Na^+), potassium (K^+), magnesium (Mg^{2+}), and calcium (Ca^{2+}) are responsible for a number of trigger and control mechanisms, acting as charge carriers. Sodium and potassium ions act to provide osmotic balance and electrolyte current. Sodium ions are found outside the cell and potassium ions within the cell. The sodium-potassium concentration gradient across the cell membrane is important physiologically. The difference in the concentration results in the generation of potential difference between the two sides of the membrane. A nerve impulse is conducted along the membrane when there is a rapid influx of sodium ions into the nerve cells resulting from a temporary reversal of the membrane's selectivity towards sodium and potassium ions. An example of the trigger mechanism is provided by the sudden influx of calcium ions into muscle cells. Normally calcium is excluded from the cells and magnesium ions are present, but the influx of calcium ions results in the activation of certain enzymes and hence muscle contraction.



b) **Structural Influences** - Metal ions stabilise certain protein configurations so affecting the physical and biological properties of the protein. Calcium, magnesium and manganese can influence the equilibrium between the native and reversibly denatured protein. Metal ions such as nickel (II) act as templates, bringing reacting groups into a correct orientation for reaction. The presence of metal ions is also important in the maintaining of the structure of the cell walls. Calcium and magnesium are both present in the body at a greater concentration than expected if their roles were purely those of enzyme activators. It is probable that these divalent ions participate in a stiffening mechanism for the lipoprotein membranes by bridging neighbouring carboxylate groups.

c) **Lewis acid behaviour** - Metal ions in biological systems can accept electron pairs and so act as Lewis acids catalysing certain enzyme reactions. Calcium, manganese and particularly magnesium act by activating enzymes associated with the phosphate system. Magnesium is required in all stages of vitamin B₁ biosynthesis. Zinc is associated with hydrolytic enzymes.

d) **Redox behaviour** - In redox reactions the metal ions catalyse valance changes in the substrates. Specificity of the enzyme for the metal tends to be much higher. The transition metal ions are involved in a wide range of catalytic functions, whilst zinc also acts as a catalyst of hydride transfer. Ten trace metals are essential to warm blooded animals, these are copper, iron, zinc, cobalt, molybdenum, chromium, tin, vanadium and nickel. The more important metals in biological redox processes are iron, copper and cobalt with molybdenum involved to a lesser extent. The processes range from electron transfer, oxygen atom and hydroxyl group incorporation to hydrogen atom and hydride removal. Iron is involved in the respiratory process, binding oxygen when incorporated in haemoglobin and myoglobin. It is also a component of various cytochromes,



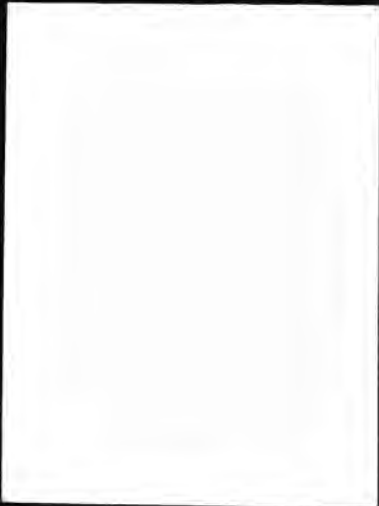
peroxidases and catalases. In the body there is an iron transport system controlled by the iron enzymes ferritin and transferrin. Copper is present in about 12 enzymes whose functions range from the utilisation of iron to the pigmentation of the skin. Two copper containing enzymes of importance are amine oxidase which is necessary for the formation of elastin and bone collagen, and tyrosinase utilised in the formation of melanin. Copper is also required for the release of iron from its storage protein ferritin.

As well as native metal ions *in vivo*, there can be present those such as gold, titanium, mercury, etc., which do not occur naturally but are introduced deliberately for therapeutic reasons or accidentally with deleterious effect.

1.2 METAL IONS IN BONE AND JOINT DISEASE

The metal ions encountered in bone and joint disease can be found naturally *in vivo* like copper and iron or can be present due to introduction into the body for medical reasons. In this study gold, titanium and iron metal ions encountered *in vivo* due to bone and joint disease are of interest. Gold and titanium are introduced into the biological system of diseased patients for medicinal purposes.

Gold-containing drugs have been used therapeutically to treat rheumatoid arthritis for 55 years². Whilst not curing the disease, they can produce remission. The treatment usually involves weekly injections of gold drugs, followed by maintenance therapy at less regular intervals. The majority of gold drugs administered contain sulphur bound gold. Although there is no single mechanism to completely explain the action of antiarthritic drugs in this as yet not fully understood inflammatory disease, their action is thought to involve the blocking of reactive thiol sites on the membrane proteins such as albumin and immunoglobulin G^{3,4}. The gold



administered is widely distributed in the plasma and serum, reflecting the lack of natural systems for transport and storage. The tissue distribution of gold shows that the greatest concentrations occur in the liver, kidney, spleen and lymph node. The levels of gold present in the body vary from patient to patient, however, unfortunately, the gold blood levels do not correlate with either clinical benefits or with toxicity⁵.

Titanium metal ions are introduced into the body by way of titanium alloy hip implants. The titanium implants or prostheses are used in standard hip replacement operations which are performed when the patient's hip joint is badly eroded or broken due to the thinning and increased brittleness of the bone from osteoporosis or erosion from rheumatoid arthritis. Titanium has been used as a surgical implant material because of its excellent mechanical properties, resistance to corrosion and biocompatibility^{6,7,8}. However recently a number of workers have reported the presence of dark staining around the titanium alloy prostheses upon revision surgery due to loosening of the implant^{9,10,11}. This dark staining is found to be due to titanium. This suggests that titanium is not as inert as originally thought and that the metal interacts with the biological environment.

It is known that rheumatoid arthritis leads to altered serum levels of copper and iron¹². There are raised levels of copper in the serum of rheumatoid arthritis sufferers¹³. The chief source of serum copper is ceruloplasmin, which though not an oxygen carrier has important oxidase activity. The increase in copper is mainly due to an increase in the ceruloplasmin content of the serum. The ceruloplasmin is a protein responsible for copper transfer to apoenzymes and also for the mobilisation of iron from the liver to the blood. Since the levels of copper in the liver actually fall in the diseased state, with a rise in the serum level, it has been suggested that the rise in copper levels is a physiological response to the disease.

Iron is naturally present in human serum, however it has been previously reported that low molecular weight redox active iron complexes are present in the knee joint synovial fluid of patients with rheumatoid arthritis. These iron complexes can readily promote the generation of highly reactive free radical species which can attack a wide range of endogenous molecules to produce modified chemical species. These degradation products can themselves stimulate synovitis and progressive joint destruction.

A speciation of these metal ions would lead to a greater understanding of their roles and modes of action in bone and joint disease. Due to lack of time speciation of copper within the rheumatoid arthritis patients was not investigated in this study.

1.3 RHEUMATOID ARTHRITIS

Rheumatoid arthritis is a chronic inflammatory disease that primarily affects peripheral joints and is characterised by inflammation of the synovium which leads to destructive, erosive changes in the joint. The exact causes of rheumatoid arthritis are not known. In general females are three times as likely to be affected as males. It is a common disease with overall 2% of males and 5% of females affected in the United Kingdom. The age of onset ranges from childhood to over 75 years of age, however rheumatoid arthritis mainly develops between 35 to 50 years of age¹⁴. The onset of the disease primarily affects the hands and feet, with new joint involvement developing irregularly to include the larger limb joints such as ankles, knees, elbows, shoulders and often later the hip joints. Movable joints are all synovial joints (Figure 1.1), possessing a synovial membrane which produces a synovial fluid to lubricate the movement of the joint. It is these joints that are affected by rheumatoid arthritis.

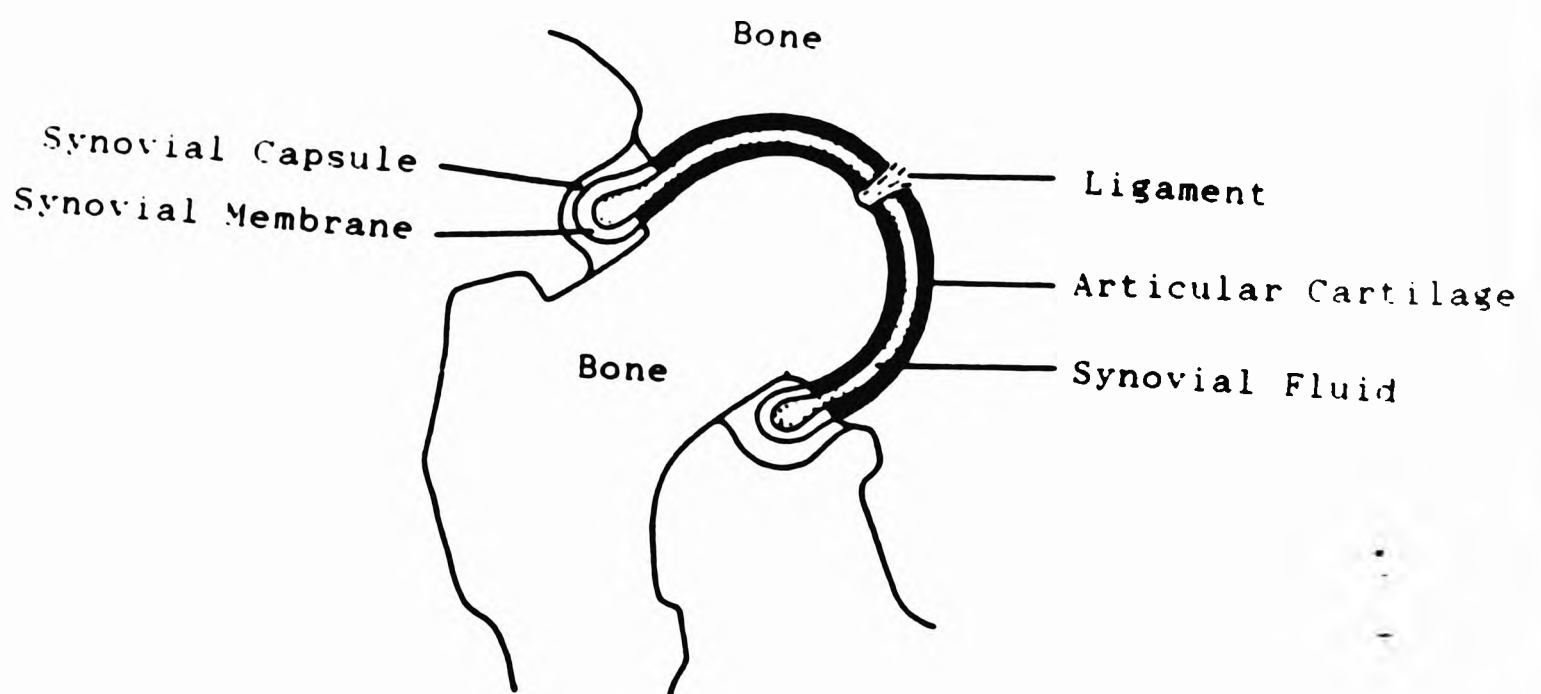


Figure 1.1 Section Through a Synovial Joint

The disease is characterised by remissions that occur spontaneously for no known reasons. Very little joint pain can be experienced over many years, only to enter another phase with severe joint swelling and disability. Rheumatoid arthritis affects mainly joints and synovial tissue, subsequently destroying the tissue, cartilage or bone irreversibly¹⁵. The production of synovial fluid, the natural joint lubricant, is increased but its viscosity is much below normal. The decrease in viscosity is due

to the breakdown of the polysaccharide hyaluronic acid to lower molecular weight moieties. It has been postulated that the derogatory action of free radical reactions leads to the degradation of the hyaluronic acid¹⁶.

1.3.1 Histology of Rheumatoid Arthritis

Rheumatoid arthritis is a chronic and acute inflammation of the joints, with eventual proteolytic degradation of the affected tissue. Inflammation encompasses a dynamic mixed response of chemical, cellular and extracellular changes in the body due to many different inciting agents¹⁷⁻²⁰. The first sign of inflammation is the dilation of the arteries and veins in the affected tissue, resulting in increased blood circulation. The white blood corpuscles, the leucocytes, begin to adhere to the inner surface of the blood vessels. Gradually the leucocytes push their way through the walls of the smaller capillaries, migrating into the surrounding tissue along with fluid material from the blood and a few red blood cells, erythrocytes. This process is known as diapedesis and is responsible for the swelling which is a characteristic sign of inflammation.

The immunological events occurring in synovial tissue affected by rheumatoid arthritis are not completely understood and the onset of this inflammatory disease appears as yet to have no causative stimulus¹⁵. Rheumatoid arthritis is thought to arise due to biphasic processes; the first exudation and the second granulation. The exudative stage involves the action of inflammatory mediators, such as kinins and prostglandins, which lead to an alteration of the permeability of the synovial membrane blood vessels. This change in vascular permeability allows various cell types, including phagocytic cells such as polymorphnuclear leucocytes (PMN) and lymphocytes, to traverse and migrate into the extracellular spaces in the synovial fluid. The polymorphnuclear leucocytes (PMN), including neutrophils, contain

both proteolytic (elastase and cathepsin G) and oxidative (myeloperoxidase) enzymes which are normally stored in cytoplasmic granules. However on encountering immune complexes or antigens, rapid degranulation associated with phagocytosis occurs and this is known as the granulation phase. With phagocytosis, the proteolytic and oxidative enzymes are often released into the tissues themselves. Normally it is the major plasma inhibitor, alpha-1-proteinase inhibitor (α -1-PI) that can also penetrate vascular walls, which exerts control on connective tissue proteolysis²¹. However, because of the massive infiltration of PMN leucocytes and the inactivation of the α -1-PI by the myeloperoxidase-H₂O₂-Cl⁻ system²² which occurs during phagocytosis, the ability of the tissue levels of this inhibitor to protect the tissues from proteolysis are markedly reduced. Hence the uncontrolled digestion of connective tissues may occur resulting in severe damage associated with diseases such as rheumatoid arthritis. Free radical damage of the connective tissue has also been implicated more recently²³⁻²⁵. The myeloperoxidase enzyme is particularly deleterious since it generates the powerful oxidant hypochlorite ion (OCl⁻) from hydrogen peroxide (H₂O₂) and the chloride ion. Also the activated neutrophils produce low levels of the superoxide radical anion (O₂⁻) and hydrogen peroxide which must be released into the synovial fluid. These highly reactive free radicals can attack biomolecules with deleterious effect leading to eventual connective tissue destruction.

1.3.2 Treatment of Rheumatoid Arthritis

In view of the incomplete understanding of the causes of rheumatoid arthritis, there are no preventative measures that can be applied to halt the onset of the disease. Treatment is designed to modify the course of this inflammatory joint disease and to reduce its structural consequences, which lead to deformity and

consequent disability. The drug treatments currently utilised can broadly be classified into four groups; analgesics, corticosteroids, immunosuppressive drugs and slow acting drugs such as gold compounds^{14,15}.

Analgesics are essential as they provide pain relief and can be used in conjunction with more specific treatment. They are the most widely used of the antirheumatic drugs and include chiefly the salicylates such as aspirin. Paracetamol may occasionally be preferred but is usually less effective. The analgesics provide pain relief at low doses and are anti-inflammatory after repeated administration of high doses. Their anti-inflammatory action may be due to inhibition of prostglandin and hence reduction of vascular permeability. They act rapidly and their clinical effects decline promptly after the cessation of therapy. The analgesics do not prevent the progression of rheumatoid arthritis nor do they induce remission.

Corticosteroids administered at low levels have anti-inflammatory effects. They act on the blood vessel walls leading to decreased vascular permeability. They block the accumulation of polymorphnuclear leucocytes and monocytes at inflammatory sites. At high doses the corticosteroids are immunosuppressive as they redistribute the lymphocytes into the bone marrow. Corticosteroid dose levels must be restricted to those which will produce some level of suppression without, even over a long period, causing the patient to develop unacceptable features of overdose. The beneficial effects of corticosteroids such as cortisone are only temporary and cease when treatment is stopped.

Immunosuppressive drugs include alkylating agents such as cyclophosphamide and chlorambucil. Despite differences in their site and mode of action the immunosuppressive drugs share many features with respect to their use in the treatment of rheumatoid arthritis. They are all slow acting, with several weeks being taken before their clinical effects are apparent and they may induce

remission. They have a wide range of complex immunosuppressive effects. Their mechanism of action is unknown but they probably interfere with lymphocyte populations.

Slow acting drugs include mainly the gold compounds but also D-penicillamine. Treatment with gold containing drugs such as disodium aurothiomalate should be initiated once diagnosis is firmly established and when there is evidence of progressive disease. These drugs have a slow onset of action (6-8 weeks) with the clinical benefit improving over a period of months. They induce remission and may slow the progression of the erosive disease. The gold compounds distribute themselves rapidly throughout the body with a tendency to concentrate in the areas of inflammation as well as within the lysosomal membranes of phagocytic cells. Gold compounds are thought to act by the blocking of some reactive thiol groups on membranes and by interfering directly with the ability of macrophages to behave as effector cells. The beneficial effects of gold compounds may endure after the cessation of treatment.

The final treatment is surgery. During surgery a badly worn joint can be replaced with an artificial implant such as a titanium alloy hip prosthesis. These operations serve to prevent later disability and are often salvage operations.

1.4 GOLD DRUGS IN RHEUMATOID ARTHRITIS

1.4.1 History of Gold Treatment

Gold was probably one of the first metals to attract the attention of man due to it being one of the few metals that exists in its elemental state in nature, as well as to the attraction of its scarcity, lustre and its non-oxidising properties. Gold was

chiefly used for ornamental purposes, however as early as 2500 BC the Chinese used gold for biological benefit. The Roman historian Pliny described the use of gold in ashen form as a treatment for fistulas and discharges. In the thirteenth century gold, dissolved in aqua regia and diluted with oil, was recommended for the treatment of leprosy. However it was Robert Koch who reported the first experimental antibacterial activity of gold salts in 1890 and paved the way for a sounder basis for gold therapy. Koch described *in vitro* antitubercular activity of gold cyanide and other workers reported beneficial results with the use of inorganic gold compounds in the treatment of skin tuberculosis, syphilis and lupus²⁶. After intensive efforts in synthesis in the 1920s several gold (I) thiols were prepared which were stable in solution and biologically active and were less toxic. The development of gold thiosulphate (Sanochrisin) as a therapeutic agent for tuberculosis by Mollgaard in 1924, sparked off what was later termed the "Gold Decade" (1925-1935) as clinical gold therapy flourished²⁷.

Lande first introduced aurothioglucose (Solganol) for the treatment of rheumatoid arthritis noting a significant loss of joint pain in affected patients. This treatment was popularised by Forestier²⁸ who reported the beneficial action of gold salts in chronic rheumatoid arthritis. He employed a range of gold thiolates including disodium aurothiomalate (Myocrisin) which were administered intramuscularly²⁹. In 1960 controlled trials by the Empire Rheumatism Council³⁰ were carried out which confirmed the efficacy of gold drugs in patients suffering from rheumatoid arthritis. Although some patients can safely undergo gold therapy for many years, about 35% can suffer toxic side effects. However medical opinion remains that gold drugs are as effective as any other drug used to treat difficult cases of rheumatoid arthritis and that they are one of the few drugs that can alter the course of the disease³¹.

1.4.2 Chrysotherapy and Structure of Gold (I) Thiolates

Today, gold drug treatment (chrysotherapy), is still employed as it is one of the few regimes that can produce remission from rheumatoid arthritis. The gold (I) thiolates in common use in chrysotherapy include aurothiopropansulphonate (Allochrysine) and particularly aurothiomalate (Myocrisin) and aurothioglucose (Solganol) (Figure 1.2). Aurothiomalate and aurothiopropansulphonate are water soluble whilst aurothioglucose is oil soluble and is injected in to the body in the form of an oil suspension. In this study particular interest will be devoted to disodium aurothiomalate and its use in chrysotherapy.

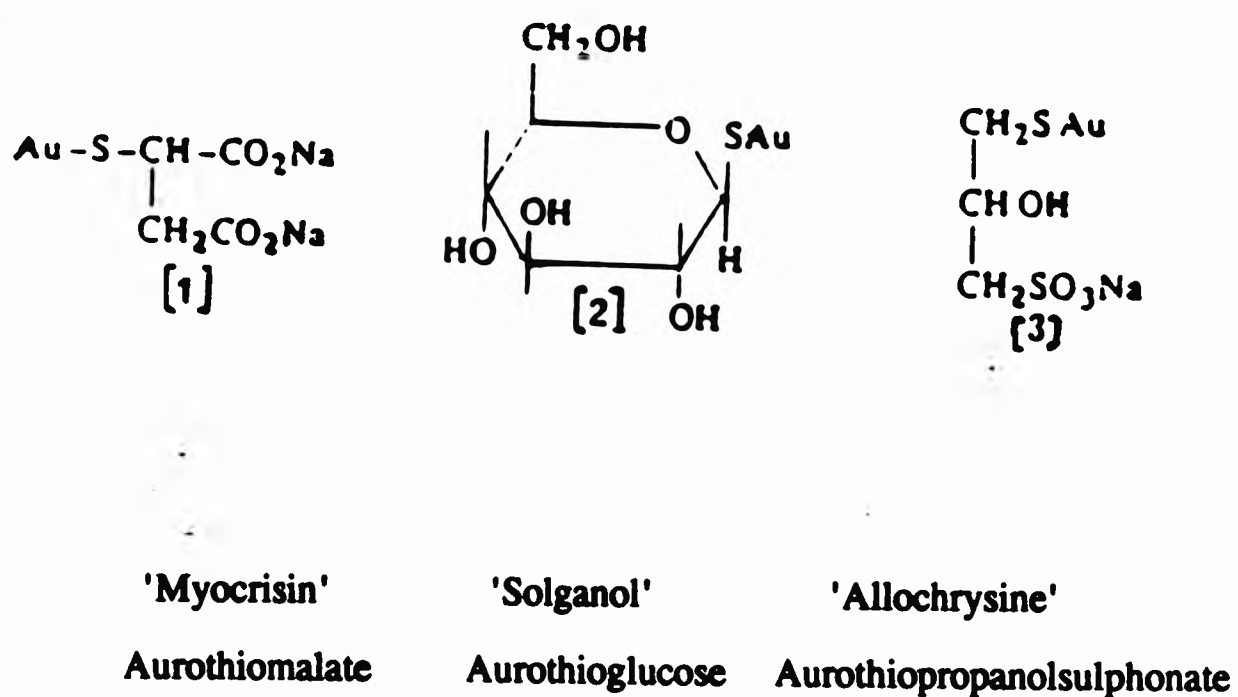


Figure 1.2 Structure of Gold (I) Thiolates Used in Chrysotherapy

Present conventional chrysotherapy involves giving a deep intramuscular injection of a solution of gold drug to the patient. An initial injection of a gold compound containing 10 mg of gold is given to test the patient's tolerance to the drug. The dose is increased stepwise in the next 2-3 weeks to 25-50 mg (based on the gold content of the drug) and thereafter weekly 50 mg doses are administered. The whole course of treatment usually involves 2 g of gold. Maintenance therapy may be instituted consisting of 20-50 mg every 2-4 weeks³².

The structural nature of 1:1 gold (I) thiolate drugs has previously been poorly defined and it is only relatively recently that work has been done to investigate their chemistry³³⁻³⁶. The complexes have often been formulated as simple monomers, $[\text{Au}(\text{SR})]$, but it has been demonstrated that the gold (I) thiolate complexes exist as polymeric rings (Figure 1.3), with gold achieving a linear two-coordination via bridging thiolate sulphur ligands i.e $[\text{Au}(\text{SR})]_6$ ³³. However the exact structural composition is dependant on pH, ionic strength and temperature³⁷.

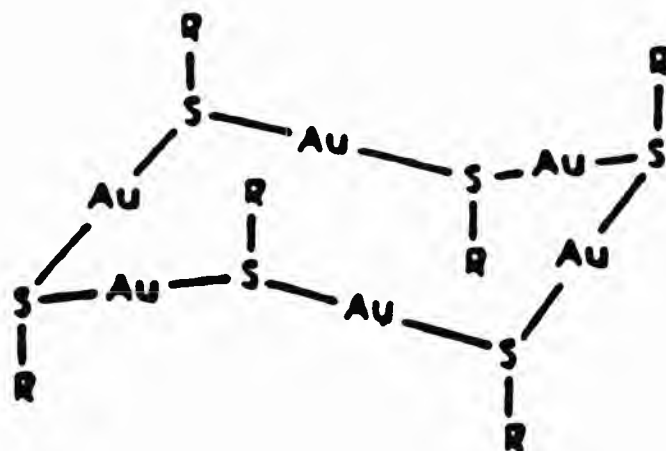


Figure. 1.3 Polymeric Ring Structure for 1:1 Gold (I) Thiolate Complexes

Present conventional chrysotherapy involves giving a deep intramuscular injection of a solution of gold drug to the patient. An initial injection of a gold compound containing 10 mg of gold is given to test the patient's tolerance to the drug. The dose is increased stepwise in the next 2-3 weeks to 25-50 mg (based on the gold content of the drug) and thereafter weekly 50 mg doses are administered. The whole course of treatment usually involves 2 g of gold. Maintenance therapy may be instituted consisting of 20-50 mg every 2-4 weeks³².

The structural nature of 1:1 gold (I) thiolate drugs has previously been poorly defined and it is only relatively recently that work has been done to investigate their chemistry³³⁻³⁶. The complexes have often been formulated as simple monomers, $[\text{Au}(\text{SR})]$, but it has been demonstrated that the gold (I) thiolate complexes exist as polymeric rings (Figure 1.3), with gold achieving a linear two-coordination via bridging thiolate sulphur ligands i.e $[\text{Au}(\text{SR})]_6$ ³³. However the exact structural composition is dependant on pH, ionic strength and temperature³⁷.

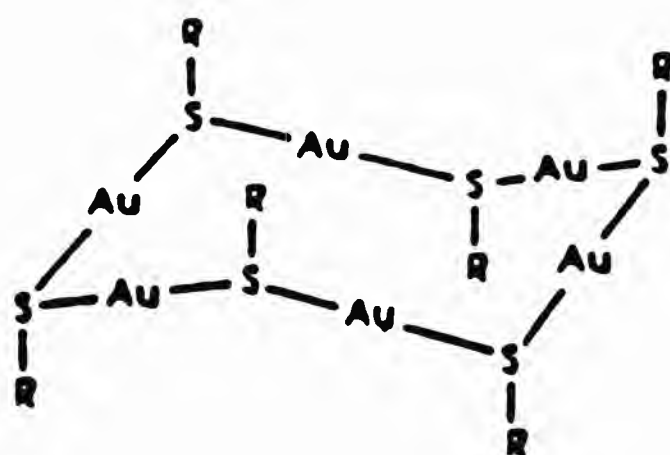


Figure. 1.3 Polymeric Ring Structure for 1:1 Gold (I) Thiolate Complexes

1.4.3 Distribution of Gold (I) Thiolate Drugs *in vivo*

Gold (I) is a soft Lewis acid with a low affinity for nitrogen and oxygen donor ligands and a high affinity for ligands which contain a thiol moiety. It is therefore likely that the gold from gold (I) thiolate drugs administered during chrysotherapy will primarily distribute itself amongst protein and non-protein thiol groups *in vivo*. Work done on the distribution of gold (I) *in vivo* shows that in human plasma where the principal source of thiol groups is albumin (cysteine-34 residue), the gold is predominantly albumin bound (80-90%) with smaller amounts bound to immunoglobulins^{38,39}. Although gold reacts slowly with albumin the gold-albumin complexes formed are very stable⁴⁰. The binding plateau for albumin is not reached until 5 hours whereas the binding to globulins is completed in 3 minutes³⁸. Approximately 5-10% of total circulating gold is non-protein bound, low molecular mass or 'free reactive' gold. Despite their low concentration, low molecular mass gold species such as monomeric (L-cysteinato)gold (I) complexes $[\text{Au}(\text{SCys})_2]^-$ ⁴¹ are likely to play a vital part in the attainment of chemical equilibria and various transport processes. An important part of gold (I) chemistry is its ability to undergo thiolate exchange and release reactions as shown in Figure 1.4 which depicts a reaction between aurothiomalate and a non-protein bound thiol and the formation of a gold (I) albumin complex.

The injected gold is widely distributed in the plasma and serum, reflecting the lack of a natural transport and storage system. The serum half-life of aurothiomalate (Myocrisin) is 5.5 days. Gold may persist in the body for months after treatment and is mainly deposited in lysosomes which upon accumulating the metal become electron dense and are called aurosomes⁴².

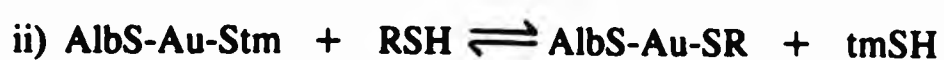
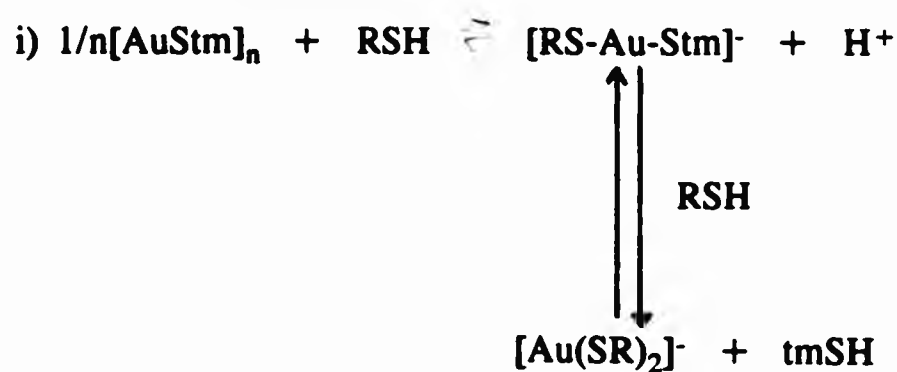


Figure. 1.4 Scheme for the Release of Thiomalate (tmS) from Gold (I) *in vivo* by i) Direct Attack of a Non-Protein Bound Thiol (RSH, e.g Cysteine or Glutathione) on the 1:1 Gold (I) Thiomalate Complex ($\frac{1}{n}[\text{AuStm}]_n$) and ii) Interaction of the Non-Protein Bound Thiol with Gold (I) Thiomalate Bound to the Cysteine-34 Residue of Human Serum Albumin (AlbA-Au-Stm).

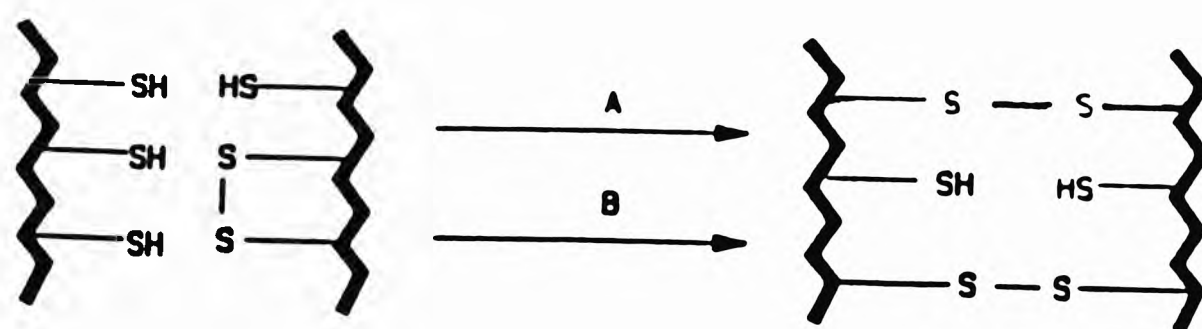
Gold is also present in the synovial fluid and research into the slow development of synovial aurosomes has been carried out because initial arthritic damage is localised in the synovium⁴³. Synovial levels of gold (I) are approximately half those of serum⁴⁴. Equilibration between the two is thought possible.

Gold is mainly excreted through urine but also through faeces. Gold excreted in urine is predominantly protein bound, mainly bound to serum albumin as in blood serum⁴⁵. The presence of proteins in the urine following gold injections are due to proteinuria, a common side effect of gold.

1.4.4 Mechanism of Action of Gold Drugs

There is no unique mechanism of action for gold containing antiarthritic drugs reflecting the diffuse nature of the initiation of the disease. The correction of the imbalance in the immune system as witnessed by remission during chrysotherapy,

implies modulation of the immune response and may be linked to the regulation of the thiol/disulphide (RSH/RSSR) balance in the cell. It is thought that the delayed favourable response following injections of gold (I) thiolate drugs results from the ability of gold (I) to block some critical thiol groups, such as in immunoglobulin G^{46,47}. Figure 1.5 depicts a possible mechanism for the alteration of the complex thiol-disulphide equilibria *in vivo* by polymeric 1:1 gold (I) thiolates such as disodium aurothiomalate.



A = Oxidation of sulphydryl group (brought about by oxygen or superoxide).

B = Intermolecular sulphydryl-disulphide interchange reaction.

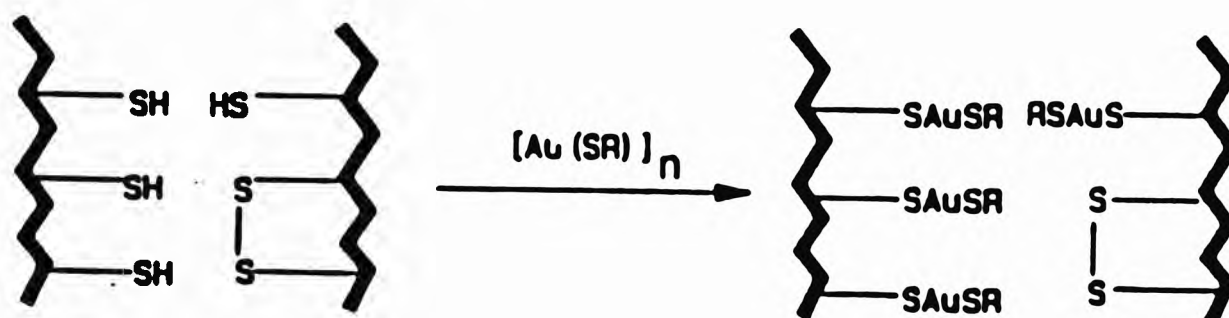
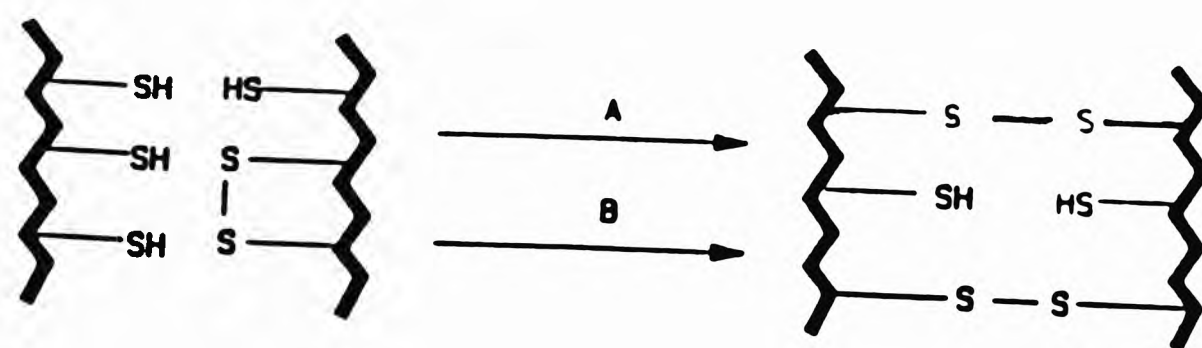


Figure. 1.5 Possible Mechanism for the Regulation of the Complex Thiol-Disulphide Equilibria *in vivo* by Gold (I) Thiolate Drugs.

implies modulation of the immune response and may be linked to the regulation of the thiol/disulphide (RSH/RSSR) balance in the cell. It is thought that the delayed favourable response following injections of gold (I) thiolate drugs results from the ability of gold (I) to block some critical thiol groups, such as in immunoglobulin G^{46,47}. Figure 1.5 depicts a possible mechanism for the alteration of the complex thiol-disulphide equilibria *in vivo* by polymeric 1:1 gold (I) thiolates such as disodium aurothiomalate.



- A = Oxidation of sulphhydryl group (brought about by oxygen or superoxide).
 B = Intermolecular sulphhydryl-disulphide interchange reaction.

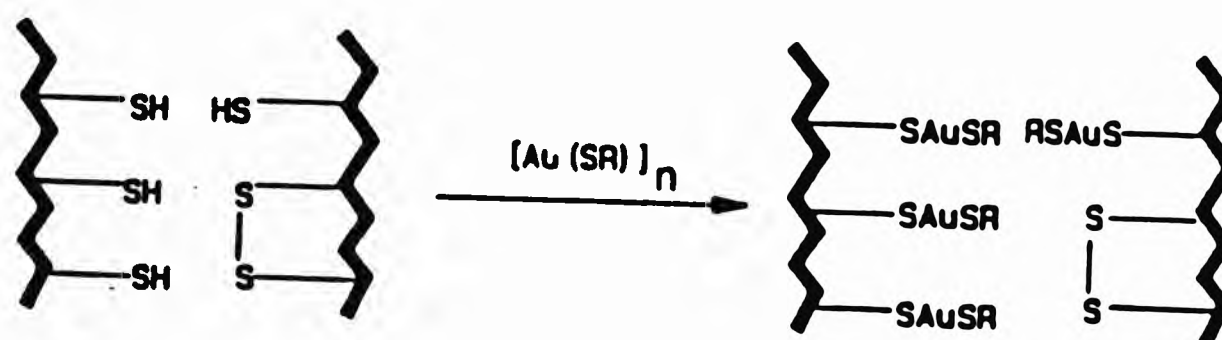


Figure. 1.5 Possible Mechanism for the Regulation of the Complex Thiol-Disulphide Equilibria *in vivo* by Gold (I) Thiolate Drugs.

There are many proposed modes of action of gold drugs which may also involve the blockage of sulphhydryl activity. These include an induced decrease in immunoglobulin G and suppression of lymphocyte proliferation^{17,48}. Gold also seems to enter pre-existing lysosomes and alters their behaviour so as to prevent the release of enzymes which would perpetuate the inflammatory process⁴⁹⁻⁵². Other proposed modes of action of gold drugs include the inhibition of the myeloperoxidase system²¹, inhibition of human neutrophil collagenase⁵³, inhibition of prostaglandin biosynthesis⁵⁴ and of mast cell histamine release⁵⁵, or the possible stimulation by gold of the T effector as well as T suppressor cells⁵⁶.

It has been reported that there is oxidative damage to the synovial fluid and the lipids within an inflamed rheumatoid joint⁵⁷⁻⁶⁰. Disodium aurothiomalate (myocrisin) inhibits oxy radical generation *in vitro*, a deleterious reaction which can lead to depolymerisation of hyaluronic acid, disruption of lysosomal and cellular membranes and degradation of DNA^{61,62}. Gold (I) thiolate drugs *in vivo* are thought to limit the oxidative damage by controlling enzyme systems involved in the production of reactive oxygen species (ROS) and by protecting proteins and enzymes against oxidative damage^{63,64}. One possible action of gold (I) is that it protects unsaturated membrane lipids and proteins against oxidative degradation caused by activated phagocytes that are not properly regulated. Superoxide ion (O_2^-), a product of activated phagocytes can be oxidised to an electronically excited singlet oxygen capable of peroxidation of unsaturated fatty acid derivatives. Gold (I) has been shown to be a deactivator of singlet oxygen⁶⁵.

The ability of gold (I) to transport electron-donating thiolate ligands to certain intra- or extracellular 'target' sites is likely to be an important mechanism in the metals control of oxygen radical-mediated oxidative damage. Although the thiolate

ligands in 1:1 gold (I) thiolate may exert a therapeutic effect on the release from gold (I) *in vivo*⁶⁶, it is clear that the gold metal centre is an essential pre-requisite for the ability of gold drugs to suppress active rheumatoid arthritis.

The mechanism of action of gold drugs may not be known with certainty but a reasonable postulate to their chemical activity can be put forward. Much work still needs to be done to define the various hypotheses of chrysotherapy efficacy and indeed a greater understanding of rheumatoid arthritis itself and its onset and progression needs to be reached.

1.5 TITANIUM IMPLANTS IN BONE AND JOINT DISEASE

1.5.1 Introduction

Titanium (Ti) has been employed successfully as an implant material in medicine for many years⁶⁷⁻⁶⁹. In 1940 Bothe, Beaton and Davenport⁷⁰ studied local tissue response to various metals including commercially pure titanium (cp Ti). They found that it was well tolerated, and that bone, perhaps even had a tendency to grow into contact with the metal. Through the years titanium and titanium alloys have been used increasingly in medical devices such as heart valves, cardiac plates, dental implants, bone plates and artificial joints. The main reason for the use of titanium is its resistance to the highly corrosive fluids in which an implant must survive. The resistance to corrosion is due to a tenacious passive oxide layer, which forms a thin coating on the surface of the metal.

The surface of any biomaterial is of vital importance, because it determines the biocompatibility and corrosion resistance of the prosthesis. In joint prostheses, low friction and good wear characteristics are of importance. At room temperature,

oxidation occurs on the titanium metal surface forming an oxide layer which is 1-5 nm thick. The oxide forms a protective layer and prevents direct contact of the metal with its tissue environment. The surface of the alloy usually used for titanium implants, Ti-6Al-4V (6% aluminium, 4% vanadium), consists of the oxides of titanium (TiO_2) and aluminium (Al_2O_3), whilst pure titanium has a TiO_2 layer only. The surface chemical composition and surface microstructure of the implant strongly influence the chemical reactions that will take place at the prostheses-tissue interface⁷¹.

1.5.2 General Chemistry of Titanium

Titanium is the most naturally abundant transition metal after iron and the ninth most common element in the earth's crust (average 0.6%), present in small amounts in practically all silicate minerals and in almost all soils. It is found in its oxidic mineral form (rutile, ilmenite and sphene). The metal is lustrous white, with a density of 4.5 g cm^{-3} and is malleable when not contaminated with oxygen. It is very reactive, being the only metal to burn in nitrogen. When it forms an oxide layer on exposure to oxygen, it becomes resistant to most chemicals and is considered physiologically inert.

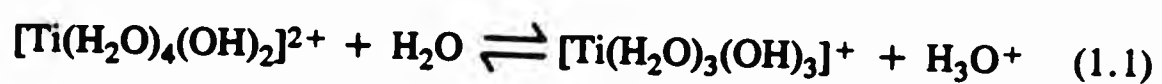
The problems of 'working' titanium are caused by its hardness, brittleness and rather poor ductility. As titanium is becoming an increasingly important structural metal, these problems are being overcome by alloying it with other metals. Dilute mineral acids have little effect at room temperature but the metal dissolves in hot dilute hydrochloric acid or cold dilute hydrofluoric acid. Hot concentrated nitric acid slowly attacks the metal with the formation of insoluble hydrated titanium dioxide, $\text{TiO}_2 \cdot n\text{H}_2\text{O}$.

The ground state outer electronic configuration is $3d^2 4s^2$. The maximum oxidation state is +4 (titanic) and it is the commonest state found as it is the most stable. The +3 (titanous) and +2 states are also formed.

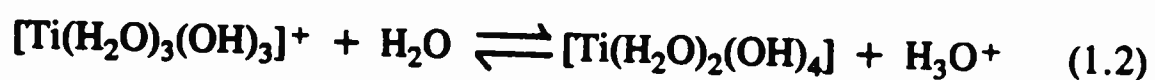
1.5.2.1 The Aqueous +4 Oxidation State

The +4 titanium oxidation state gives rise to largely covalent compounds. The titanium hexaaqua-ion ($[\text{Ti}(\text{H}_2\text{O})_6]^{4+}$) is unknown, as the high charge-to-size ratio leads to great acidity so that only hydrolysed derivatives are obtained in aqueous solution^{72,73}.

With dilute acids, such as perchloric acid (HClO_4), the thermodynamic equilibrium will lie as follows:



Addition of a base gives the hydrous oxide precipitate:



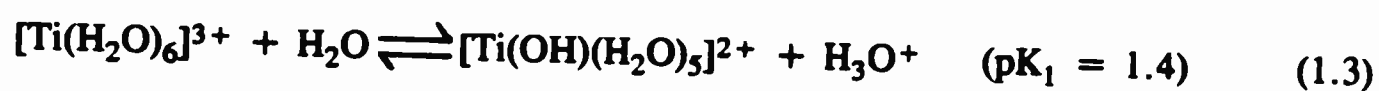
The hydrous oxide is normally regarded as $\text{TiO}_2 \cdot n\text{H}_2\text{O}$ as there is no evidence of hydroxide ($\text{Ti}(\text{OH})_4$) formation.

1.5.2.2 The Aqueous +3 Oxidation State

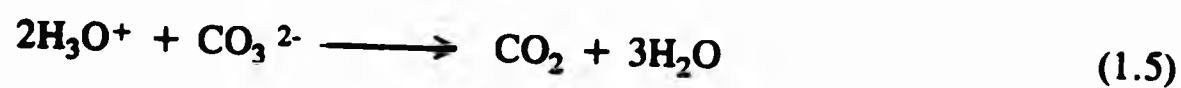
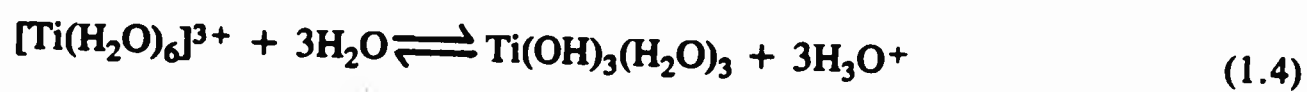
In its ground state the +3 oxidation state, has an outer configuration of $3d^1$. Unlike titanium (IV), the Ti (III) compounds are paramagnetic ($\mu_{\text{eff}} \approx 1.7 \text{ B.M}$)

and coloured through d-d absorption even when charge-transfer absorptions are absent. This oxidation state is less acidic than the +4 state, and its compounds show a considerably greater degree of ionic character.

The hexaaqua-ion $[\text{Ti}(\text{H}_2\text{O})_6]^{3+}$ is readily prepared by either reducing solutions containing titanium (IV) with zinc and hydrochloric acid, or by electrolysis. There is however some substitution of the water molecules by chloride ions in high acid concentrations, species such as $[\text{Ti}(\text{H}_2\text{O})_5\text{Cl}]^{2+}$ and $[\text{Ti}(\text{H}_2\text{O})_4\text{Cl}_2]^+$ being predominant in these solutions. Solutions containing Ti (III) are readily obtained by dissolving the metal in hydrochloric acid. The violet aqua-ion is strongly acidic:-



The addition of salts of weak acids to titanium (III) solutions thus results in the precipitation of the hydrous oxide. The reaction with sodium hydroxide or for example carbonate solution results in the evolution of carbon dioxide.



Water soluble titanium (III) salts are therefore limited to salts of strong nonoxidising acids, that is halides and sulphates. The dark purple hydrous oxide is often written as $\text{Ti}(\text{OH})_3$ but since there is considerable evidence for "polymerisation", in the formation of this product, it is best considered as $\text{Ti}_2\text{O}_3(\text{aq})$.

In acidic solution Ti^{3+} is a strong reducing agent (slightly stronger than the tin ion, Sn^{2+}).



The solution is oxidised by air and must be kept under nitrogen.

1.5.3. Titanium Alloys

At room temperature titanium forms a hexagonal close packed structure (α -Ti) which at $882^\circ C$ is transformed into a body-centered cubic structure (β -Ti) which in turn melts at $1,678^\circ C$.

The addition of an alloying element, either stabilises the hexagonal α -Ti form or promotes the existence of the cubic β -Ti structure. When titanium is alloyed with oxygen or aluminium, it gives rise to a material of the cubic β -Ti structure which has improved mechanical properties. The tensile strength is increased by 35-70% for an additional 1% of alloying element. However if the aluminium content is over 9% by weight, the alloy becomes brittle due to the precipitation of Ti_3Al . Brittle fracture may also occur as a consequence of titanium hydride (TiH_2) formation. Alpha-beta alloys have a hexagonal α -Ti structure and a cubic β -Ti structure, so alleviating the Ti_3Al formation problem. The α - β -alloy, Ti-6Al-4V (6% aluminium, 4% vanadium) accounts for over 50% of world titanium production and is the chief alloy used for the manufacture of joint prostheses. It gives a high tensile strength (1000 MPa) with improved formability⁷⁴.

1.5.4. The Tissue Environment

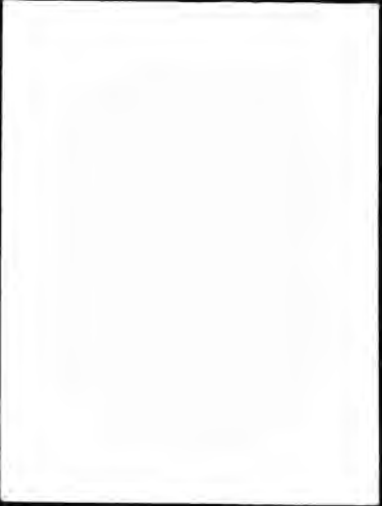
The tissue environment together with blood and intestinal liquor are aqueous electrolytic media (approx. 1% sodium chloride solution) at a constant temperature (37°C) of about neutral or slightly acidic pH and a moderate redox potential that varies with pH and oxygen tension. Organic species present may act as strong complexing agents. Implant materials are found among the transition metals and fall into 3 categories:

- i) the noble metals, e.g. gold, platinum etc. which are immune to oxidation in the tissue environment
- ii) metals in group 4A and 5A e.g. titanium, vanadium and zirconium which readily form impenetrable surface oxides.
- iii) the 6A-8 groups e.g. iron.

The ii) category provides the best implants.

1.5.5. Use of Titanium Implants

Implants serve a mechanical function, and will therefore be subjected to stress over a long period of time whilst functioning as an integrated part of the skeleton during a patient's lifetime. The prosthesis, or implant must be biocompatible, that is it must not attack or itself be attacked by the hosting tissue. Titanium has continually been found to be biocompatible, and commercially pure titanium (c.p Ti) and alumina ceramics have been proposed as reference standards for biocompatible materials⁷⁵.



Animal experiments have shown that titanium implants can be hosted by the organism for up to 10 years without any detectable or systematic reactions⁷⁶. Albrektsson *et al*⁷⁷ reported that implanted commercially pure titanium, after up to 90 months within the organism was characterised by normal lamellar bone in direct contact with the metal. An interface zone of 20-50 nm between the implant and bone collagen filaments has been reported⁷⁸. This type of bone-implant interface seems to be particular to titanium.

Unalloyed titanium is used for the prosthesis where biocompatibility of the implant is the highest priority. However by far the most commonly used titanium implant material is achieved by alloying titanium to 6% aluminium and 4% vanadium. This leads to an improvement of the implant's mechanical and wear properties without seriously jeopardizing its biocompatibility. The fatigue strength of the Ti-6Al-4V alloy is 49% greater than that of commercially pure titanium and has approximately half the elasticity modulus (E modulus) of stainless steel or a Co-Cr-Mo alloy. This low modulus may be advantageous in reducing the stress shielding of the femur and reducing strain at the bone implant interface. The oxide layer, approximately 10 nm thick, that forms on the implant surface represents the ultimate goal for prostheses as it marries the inertness of ceramics with the strength of a metal. Titanium is therefore expected to resist physiologic chloride solutions at body temperature indefinitely.

However in recent years the presence of dark staining of the tissue adjacent to titanium prostheses has been noted during some revision surgery. This may point to the fact that titanium implants are not as biocompatible and inert within the biological environment as originally thought.

1.6 IRON IN THE RHEUMATOID JOINT

As already mentioned there is little doubt that free radical reactions take place in the rheumatoid joint, leading to the degradation of the synovial fluid and the breakdown of hyaluronic acid. The formation of free radicals, such as the highly reactive hydroxyl radical ($\cdot\text{OH}$) from hydrogen peroxide present in the cells, is iron mediated. The presence of iron in rheumatoid synovium is therefore of interest.

Rheumatoid arthritis is accompanied by abnormalities in the iron metabolism of the body. The plasma 'total iron' concentration level at the onset of inflammation is lowered and there is an increase in iron protein deposition in the synovial membranes. The drop in serum iron concentration correlates closely with inflammation⁷⁹. The total iron concentration in rheumatoid synovial fluid has been found to be $20\text{-}40 \times 10^{-6} \text{ mol dm}^{-3}$ ⁸⁰. Gutteridge *et al* reported that the "free" iron concentration of rheumatoid synovial fluid was $2\text{-}3 \times 10^{-6} \text{ mol dm}^{-3}$ ⁸¹. Most of the iron is protein bound, however there is sufficient 'free' iron present in the synovium to lead to the formation of deleterious free radical species which lead to the degradation of synovial fluid characteristic of rheumatoid arthritis.

1.6.1 The Role of Iron in the Body

The two principle functions of iron in the body are i) transport of oxygen and ii) mediation in electron transfer reactions. Oxygen is transported around the body by haemoglobin, an iron-containing protein. Haemoglobin has a molecular weight of 64,500 and consists of four subunits or haeme groups which contain a central iron atom. The haemoglobin has two functions; it binds oxygen molecules to its iron

atoms and transports them from the lungs to the muscles where they are delivered to another iron containing protein, myoglobin, and the haemoglobin also binds carbon dioxide produced as waste from the cells and carries it back to the lungs.

Cytochromes are also haeme proteins, present in both plants and animals, which are involved in electron transfer chains in the mitochondria. The electron transfer is associated with the presence of iron (II)-iron (III) redox couple which act as electron carriers in various metabolic pathways. The peroxidase and catalase enzymes are both haeme proteins. Peroxidases catalyse oxidations by hydrogen peroxide, whilst catalases catalyse the disproportionation of hydrogen peroxide (1.7, 1.8 (S = substrate)).



Iron therefore plays a very important role in the body metabolism and a chemical system for the storing and transfer of iron is required.

1.6.2 Iron Storage and Transport

An average adult male contains about 4.5g of iron. Iron not required in haemoglobin and various enzymes is stored as ferritin and haemosiderin. Ferritin consists of a protein shell surrounding an iron core that holds up to 4,500 atoms of iron per molecule of protein⁸². Iron enters ferritin as Fe(II), becomes oxidised to Fe(III) by the protein and deposited inside the core. The ferritin can be converted into an insoluble product known as haemosiderin. Iron ingested is taken up by the gut, transferred to the circulation and enters the plasma bound to transferrin, a

carrier protein molecule. Transferrin is a glycoprotein and each molecule has two separate binding sites to which iron(III) attaches itself firmly at physiological pH. Tight binding requires the presence at each site of an anion, usually bicarbonate (HCO_3^-). When the iron is needed, acidification of the environment facilitates the release of the transferrin bound iron. Under normal conditions, the transferrin present in the human bloodstream is only about 30% loaded with iron on average, so that the amount of free iron salts in blood plasma would be expected to be virtually zero.

1.7 AIMS OF THIS PROJECT

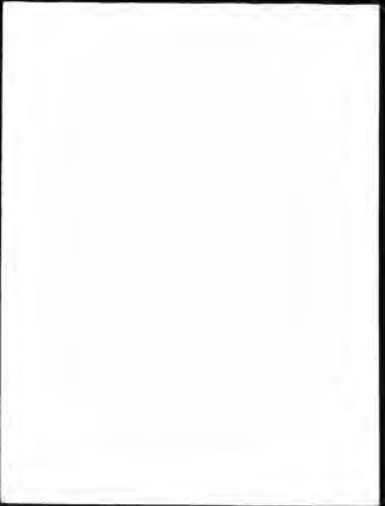
Bone and joint disease, including rheumatoid arthritis, is prevalent in today's population as longevity is increased. Rheumatoid arthritis is a chronic and acute inflammation of the joints and the onset and course of the disease is not well understood. As a result of this, treatment involves, at best, a remission. As yet no cure or preventative action has been found. In this project specific low molecular weight or 'free' metal ions encountered in bone and joint disease either introduced for therapeutic purposes, such as gold and titanium, or present naturally, such as iron, will be studied. Their speciation will lead to a greater elucidation of their role and action in the diseased joint environment, and might lead to a greater understanding of the disease itself.

Treatment with gold drugs is one of the few therapeutic regimes that can produce remission of rheumatoid arthritis. Most of the gold becomes protein bound in the body, but a small amount is present as low molecular 'free' gold. This gold is probably of vital importance in gold transport systems and helps in the achievement of equilibria. There is a need to develop a relatively quick

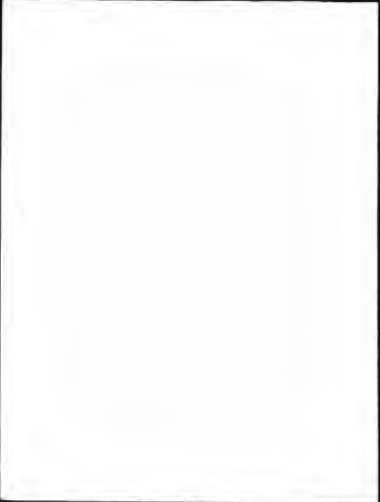
qualitative and quantitative analytical method to measure the low molecular weight gold from patients undergoing chrysotherapy which involves very little pretreatment. This project aims to develop a HPLC method for the determination of 'free' gold from the serum and synovial fluid of rheumatoid patients undergoing gold treatment. This would lead to a better understanding of the action and efficacy of gold drugs.

Up until recently it has been thought that titanium alloy implants, introduced during surgery after the extraction of broken or badly damaged hip joints, are completely inert in the biological environment. However in recent years there have been reports of dark staining of tissue adjacent to the titanium prostheses, noted during revision surgery of failed hip implants. This staining is thought to be due to titanium. Until now, no work has been done on the speciation and possible complex formation that gives rise to the staining. The aim of this study was to determine the possible cause of the dark pigmentation and the possible titanium complexes formed. A variety of analytical methods were used including FTIR and NMR.

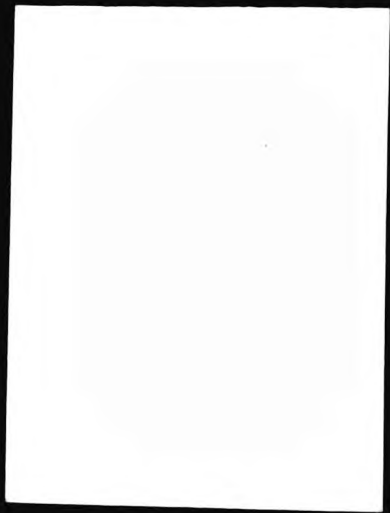
A possible cause of rheumatoid arthritis is the destruction and degradation of the synovial fluid and connective tissue by highly reactive free radicals. It is known that hydrogen peroxide is produced in the cells during inflammation. The deleterious hydroxyl radical ($\cdot\text{OH}$) is readily formed from the hydrogen peroxide in the presence of low molecular weight iron. There is a deposition of iron in the rheumatoid diseased joints and this can accelerate free radical reactions. The amount of 'free' non-transferrin bound iron in rheumatoid arthritis has been measured, but to date no investigation has been made of the precise chemical nature of the iron. This study aims to investigate the nature of the low molecular weight iron present in rheumatoid synovial fluid by means of NMR spectroscopy.



Understanding the chemical nature of the low molecular weight metal ions encountered in bone and joint disease will lead to increased awareness of the action of therapeutic agents and any needs to modify them. It will also go some way to elucidate the disease itself.



Understanding the chemical nature of the low molecular weight metal ions encountered in bone and joint disease will lead to increased awareness of the action of therapeutic agents and any needs to modify them. It will also go some way to elucidate the disease itself.



CHAPTER 2

ANALYTICAL TECHNIQUES

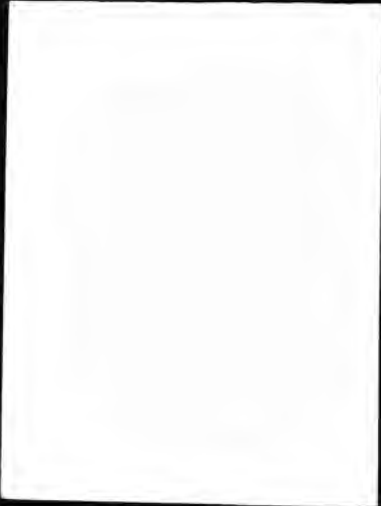
2.1 ANALYTICAL TECHNIQUES EMPLOYED

A number of analytical techniques have been employed in the analysis of the metal ions in biological fluids and tissues relevant to this study. These include chiefly, reversed phase HPLC, with the use of atomic absorption spectroscopy (AAS) as a means for corroboration, Fourier Transform infrared spectroscopy (FTIR) and nuclear magnetic resonance (NMR) spectroscopy. Ultra-violet (UV) spectrophotometry was also employed.

The metal ions found *in vivo* are present in very small concentrations, usually in $\mu\text{mol dm}^{-3}$ quantities. For this reason the analytical techniques used must be very sensitive.

A relatively rapid and sensitive analytical method with minimal pre-treatment was required for the detection of gold in blood plasma and synovial fluid from rheumatoid patients undergoing chrysotherapy. In the following work, separation and detection of gold was very effectively achieved by the development of an HPLC method which required little pre-treatment, exhibited a high level of sensitivity (detection limit $1.00 \times 10^{-6} \text{ mol dm}^{-3}$) and was relatively rapid. A UV detector was used in conjunction with the HPLC chromatograph. Atomic absorption was employed as a corroborative analytical method.

Fourier Transform infrared spectroscopy was employed to speciate the titanium ions within a piece of dark stained tissue obtained during revision surgery for a failed titanium alloy prostheses by comparing the tissue FTIR spectra with spectra of synthesised suspected titanium compounds.



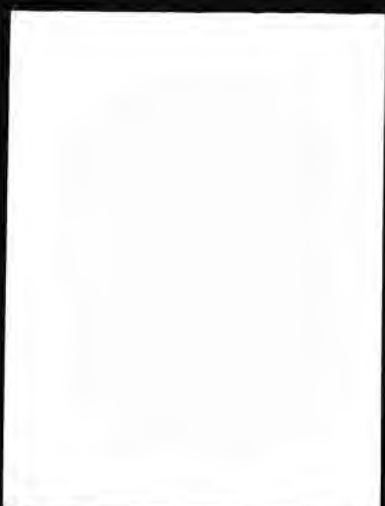
Proton Hahn spin-echo NMR spectroscopy provided a highly effective analytical tool to study low levels of metal ions in biological media. It was employed to define the precise chemical nature of both titanium and iron metal ions as encountered in bone and joint disease.

2.2 LIQUID CHROMATOGRAPHY

2.2.1 Introduction

The separation of compounds of interest is a vitally important step in chemical analysis. The most widely used and successful method of separation is chromatography. This technique relies on two mutually immiscible phases being brought into contact as one phase (the mobile phase) flows over the other phase (the stationary phase). The sample mixture introduced into the mobile phase, achieves an equilibrium distribution between the two phases many times as it migrates through the column system. These interactions make use of the difference of the chemical and physical properties of the sample components.

The separated components emerge in order of increasing interaction with the stationary phase. Those components or solutes preferentially distributed in the mobile phase elute first, and those more strongly retained by the stationary phase elute last. Separation is achieved when one component is retarded to such an extent so as to prevent overlap with the zone of an adjacent solute as the sample components elute from the column.



In liquid chromatography (LC) the stationary phase is contained within a column and the mobile phase is forced under pressure or by gravity through the column. The sample is introduced at the head of the column using a suitable introduction system. After passing through the column, the separated components are recorded using an appropriate detector.

2.2.2 Development of Chromatography

The first acknowledged chromatographic system was demonstrated by Day⁸³ in 1897, when he used a column packed with Fullers earth to separate the components of crude oil. However, the discovery of the technique of chromatography is generally attributed to the Russian botanist Mikhail Tswett⁸⁴, who in 1906 reported the separation of pigments found in green plants (chlorophyll, xanthophyll, etc.) by means of a calcium carbonate column, where the pigments were retained at different levels of the column giving rise to coloured bands (Greek; chroma-colour, graphein-to write). Although experimental research using chromatography followed, it was not until 1941 that Martin and Synge⁸⁵ developed a basic chromatographic theory. Other milestones in the advancement of chromatography were brought about by other workers. In 1952 James and Martin⁸⁶ developed gas chromatography and Howard and Martin⁸⁷ reported reversed phase chromatography (RPC) in 1950, so called because the polarities of the mobile and stationary phase are reversed. In the late 1960's high pressure liquid chromatography (HPLC) was developed by Snyder, Scott and Kirkland⁸⁸⁻⁹⁰ where the mobile phase is actually pumped through the stationary phase within the chromatography column.

2.2.3 Classification of Liquid Chromatography

Liquid column chromatography, LCC, can be classified according to several modes of interaction:-

a) Adsorption Chromatography

Adsorption chromatography or liquid-solid chromatography as it is known, achieves separation of the sample components by selective adsorption of the solute on to the surface of the stationary phase adsorbent. Silica gel is the most widely used adsorbent, although alumina can also be used. The adsorbent possesses active sites upon its surface, on to which solute molecules will adsorb to different extents. The active sites on the silica surface are hydroxyl groups which can be activated by prolonged heating. The exact conditions of activation depend upon the nature of the surface hydroxyls. The active sites can be deactivated by controlled addition of water or other polar organic solvents.

This technique was the one used by Tswett⁸⁴ in 1906, and is usually employed for the separation of relatively non-polar organic molecules. Compounds which are highly polar can be bound on to the adsorbent too strongly, even irreversibly.

b) Liquid-Liquid Partition Chromatography

In 1941 Martin and Synge⁸⁵ introduced the theory of partition or liquid-liquid chromatography (LCC). Separation is achieved by the partitioning of the solutes between two immiscible liquid phases, one held stationary on a solid support and the other mobile. As opposed to adsorption chromatography in LLC the solid support has an inert role and merely provides a large surface area on to which the

stationary phase is absorbed. The solutes to be analysed are separated by selective retention, which results from their different distribution coefficients between the mobile and stationary phase.

LLC offers a high selectivity for various solute compounds because of the wide range of liquids that can be employed for the stationary phase. NORMAL-PHASE LLC involves separation using a polar stationary phase, and a relatively non-polar mobile phase. In REVERSED-PHASE LLC the stationary phase is less polar than the mobile phase. Reversed-phase LLC is generally used to separate solutes with a low water solubility, whereas the normal-phase mode is employed when dealing with more polar, water soluble solutes.

c) Bonded Phase Chromatography (BPC)

Bonded phase chromatography forms a branch of solid-liquid chromatography in which organic functions are covalently bound on to the surface of a support, usually silica gel. Bonded phases are the most widely used column packings in LC, accounting for over 80% use in all high pressure liquid chromatography (HPLC) separations. Such stationary phases give rise to high efficiencies, selectivity control and reproducible results. The high efficiency obtained is partly due to the uniform rigid pore structure and chemical stability of the support, as well as to the thermodynamic and kinetic properties of the bonded phase.

Chemically bonded phases can be divided into two main categories:

- i) normal phase
- ii) reversed phase

The term normal phase describes the use of a polar bonded phase in conjunction with a less polar mobile phase. Polar bonded phases are made from silica gel by the covalent attachment of a polar organic functional group (e.g an amino, cyano or hydroxy group) to the surface of the support (adsorbent). The term reversed

phase describes a hydrophobic, non-polar stationary phase, which consists, most commonly, of octyl (C8) or octadecyl (C18) hydrocarbon chains, attached to the silica support. In the reversed phase mode, the mobile phase used is very polar, usually aqueous. 90% of bonded phases are reversed phase.

In 1968 Stewart and Perry⁹¹ reported their success in preparing a packing material for gas chromatography, made by reacting octadecylchlorosilane with silica gel by hydrolytic polymerisation, and suggested its potential use in liquid chromatography. It was Halasz and Sebastian⁹² who popularised chemically bonded phases, when in 1969 they reported the preparation of a column packing by the esterification of silica gel with alcohols, followed by the extraction of the esterified product with methylene chloride. The phase produced was "brush" like, the organic functions of the stationary phase, protruding like bristles from the silica gel surface. New bonding techniques have developed. Currently, most bonded phases are prepared by reacting organosilane compounds with the silanol (Si-OH) groups on the silica gel.

2.2.4 Classification of Non Polar Bonded Phases

Silica gel is used in almost all current stationary bonded phases as the support matrix. Essentially four types of bonds between an organic moiety and the silica gel surface, are used to prepare bonded phases; i) ester type (\equiv Si-O-R), ii) amino type (\equiv Si-NR₂), iii) carbon type (\equiv Si-CR₃) and, iv) siloxane type (\equiv Si-O-Si-CR₃) (R = organic groups). The siloxane bonded phase is the most commonly encountered phase.

2.2.4.1 Siloxane Type Bonded Phase (Si-O-Si-CR₃)

The siloxane type bond (Si-O-Si-CR₃) has become the most widely used bonded phase. It is formed by the reactions of the surface silanol groups with organosilanes of the type:



R = Organic Moiety

Most commonly in the reversed phase bonded preparations R is a linear hydrocarbon chain, usually an octadecyl (C₁₈) or octyl (C₈) chain. One of the X substituents must be a reactive group, usually a chloride, even though both may be reactive. Methyl groups if present, are used as non-reactive substituents because of their small size and the stability of their Si-C bond. Organoalkoxysilane reagents can also be used but particle aggregation has been reported with this method⁹³. with this method. Siloxane-type bonded phases are hydrolytically stable over a pH range of 2-8.5. The siloxane coating can either be made as a monomolecular layer, or as a polymerised multilayer, depending on the silanizing agent and on the conditions. The two types of coating formed are known as monomeric and polymeric phases, respectively.

2.2.5 Monomeric Phases

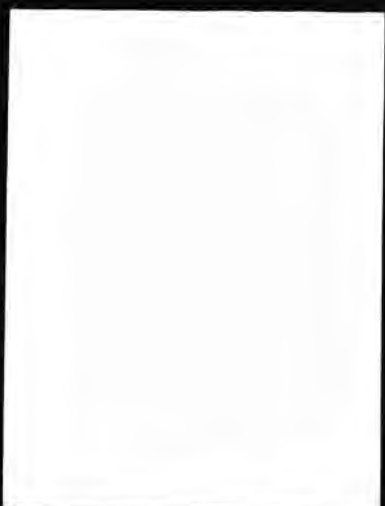
Brush-type phases or monomeric phases as they are more commonly known, are used to a greater extent than polymeric phases. The term "monomeric" is used to indicate that the surface of the silica is covered with a monomolecular layer of hydrocarbonaceous functions, which are attached to the surface via siloxane

bridges. The phases are prepared by reacting the organosilanes, most commonly chlorosilanes, with activated silica. If the reagent is a di- or tri- chlorosilane, absence of water is vital in order to avoid crosslinking polymerisation.

With monosubstituted reagents e.g. monochlorosilanes, it is obviously impossible for polymerisation to occur and they are therefore the most commonly used reagents in the synthesis of monomeric phases. When multifunctional reagents such as di and trichlorosilane are used, not all the reactive chloro- groups will react with the silica, due to steric hindrance. These residual $\equiv\text{Si-Cl}$ groups can be hydrolysed to form silanols ($\equiv\text{Si-OH}$). These free hydroxyl groups are undesirable, as they can hinder chromatographic separation due to mixed retention mechanisms. The reaction should therefore take place in dry solvents to stop hydrolysis. The silica should also be heat treated to remove water bound to it. The presence of free hydroxyl groups after bonding of the stationary phase, can be determined by methyl red adsorption. A red colour is seen in the presence of the mildly acidic hydroxyl groups. To reduce significantly the silanols that are accessible to the sample components, the bonded phase is treated with trimethylchlorosilane (Me_3SiCl) or hexamethyldisilazane ($(\text{CH}_3)_3\text{SiNHSi}(\text{CH}_3)_3$). This reaction is known as "endcapping".

2.2.6 Polymeric Phases

Polymeric phases are formed by the treatment of silica with di- or tri-chlorosilanes in the presence of water. The first reaction step is identical with that for the preparation of a monomeric phase. The unreacted groups e.g. Cl, are then hydrolysed with traces of water present in the reaction mixture. These newly



formed silanols can then either undergo a condensation reaction with surface hydroxyl groups and/or they can react with excess organosilane. In this way a cross-linked polymeric phase is produced.

Columns packed with a polymeric packing can suffer from poor reproducibility because of the uncontrollable and unpredictable nature of the polymerisation reaction.

2.2.7 General Theory of Chromatography

2.2.7.1 Molecular Interactions

The distribution of a solute between two phases results from the balance of interactive forces between the solute molecules and molecules of each phase⁹⁴. It reflects the relative attraction or repulsion that molecules or ions of the two phases show for the solute and for themselves. These forces can be polar, arising from the permanent or induced electric fields associated with the solute and the solvent, dispersive or ionic.

2.2.7.2 Dispersive Interactions

Van der Waals forces are relatively weak forces that exist between any adjacent pair of atoms or molecules. The dispersion forces account for a major part of the total attractive energy.

The interaction occurs due to the formation of a transient dipole between adjacent molecules. An alignment of the molecules occurs due to the unequal distribution of electrons within the atom or molecule, at any given instant. The attractive interaction energy $(E_{ij})_d$ between two atoms i' and j' as a result of these dispersion forces can be expressed as :

$$(E_{ij})_d = -3/2 (I_i I_j / I_i + I_j) (\alpha_i \alpha_j / r^6) \quad (2.2)$$

Here I_i and I_j refer to the first ionisation potentials of the atoms i' and j' , r is the distance between the two atoms and α_i and α_j are their respective polarisabilities.

2.2.7.3 Polar Interactions

Polar interactions can arise from the presence of permanent and induced dipoles within the molecule. When two adjacent molecules possess permanent dipoles, dipole orientation occurs, in which the positive end of one dipole is positioned close to the negative end of the other. For a maximum energy of attraction, orientation of the two dipoles should be linear, however thermal motion causes this linear arrangement to be disrupted. On average a net attractive energy $(E_{ij})_o$ occurs between the positive and negative ends of the two dipoles:

$$(E_{ij})_o = -2/3 (\mu_i^2 \mu_j^2 / kTr^6) \quad (2.3)$$

Here μ_i and μ_j refer to the permanent dipole moments of the adjacent molecules i and j , k is the Boltzmann constant, r the intermolecular distance and T is the absolute temperature. The forces between two permanent dipole containing molecules are known as Keeson forces.

A molecule i with a permanent dipole can also induce temporary dipoles in adjacent molecules j (whether or not j possess a permanent dipole). The net attractive energy $(E_{ij})_i$ resulting from this dipole or Debye interaction is given by:

$$(E_{ij})_i = -\mu_i^2 \alpha_j / r^6 \quad (2.4)$$

When both molecules i and j have permanent dipoles, the total induction interaction is obtained from the above equation by summing the terms of each dipole:

$$-(\mu_i^2 \alpha_j + \mu_j^2 \alpha_i) / r^6 \quad (2.5)$$

where μ_i and μ_j are the permanent dipole moments of molecules i and j , and α_j and α_i are their polarisabilities.

2.2.7.4 Hydrogen Bonding

The basis of hydrogen bonding is largely electrostatic, the normally small O-H or N-H dipole being effectively magnified by the small radius of the hydrogen atom. This allows the hydrogen end of the dipole to approach an interacting proton acceptor more closely, leading to a smaller value of r and a larger interaction energy. The energy of the bond can be determined by the various factors such as acid-base character and stereo chemistry. Polar molecules are attracted to hydrogen bonded solvents.

2.2.7.5 Ionic Interactions

Ions or ionic molecules having a net positive or negative charge exhibit ionic interactions, which are utilised when separating by ion-exchange or ion-pair chromatography.

2.2.7.6 Acid-Base Reactions

Acid-base or electron donor-acceptor reactions of the form: $A + :B \rightleftharpoons A:B$ involve hydrogen bonding, Lewis acid-base reactions and the combination of ions to form salts or complex ions. Pearson⁹⁵ surveyed the overall scheme of these acid-base bonds in terms of the so called soft interactions. Hard interactions being regarded as predominantly electrostatic in character and soft interactions as mainly covalent. The interaction energy E_{ab} of these various acid interactions can be expressed as:

$$E_{ab} = E_A^* E_B^* + C_A^* C_B^* \quad (2.6)$$

Here E_A^* and E_B^* measure the hard (electrostatic) acid and the base strengths of a given molecule, and C_A^* and C_B^* measure the corresponding soft (covalent) acid and base strengths.

The total energy of interaction of a molecule i , surrounded by phase j , is a sum of all the possible interactions: dispersion E_d , dipole orientation E_o and induction E_i and acid-base type interactions. Thus the total interaction energy E_{ij} , between non-bonding species can be written as:

$$E_{ij} = E_d + E_o + E_i + E_{AB} \quad (2.7)$$

2.2.8 Chromatographic Behaviour of Solutes

2.2.8.1 Retention Behaviour

The retention of solute molecules reflects their distribution between the mobile and stationary phases. Figure 2.1 depicts the parameters that are measured from a chromatogram obtained from the separation of two components.

The volume of the mobile phase needed to carry a solute band from the point of injection through the column and to the detector (to the apex of the solute peak) is defined as the retention volume, V_R . It may be directly obtained by the measurement of the retention time, t_R , of the solute. Retention time is defined as the time taken for a solute band to elute (at peak height maximum) from the point of injection. Retention volume may be obtained by multiplying the retention time with the flow rate of the mobile phase, F_C .

$$V_R = t_R F_C \quad (2.8)$$

$$V_M = t_M F_C \quad (2.9)$$

V_M is known as the dead volume, and is a measure of the volume of mobile phase that is needed for an unretained component to pass through the column. t_M is the transit time of a non-retained solute. The adjusted retention volume, V_R' , or time, t_R' is given by:

$$V_R' = V_R - V_M \text{ or } t_R' = t_R - t_M \quad (2.10)$$

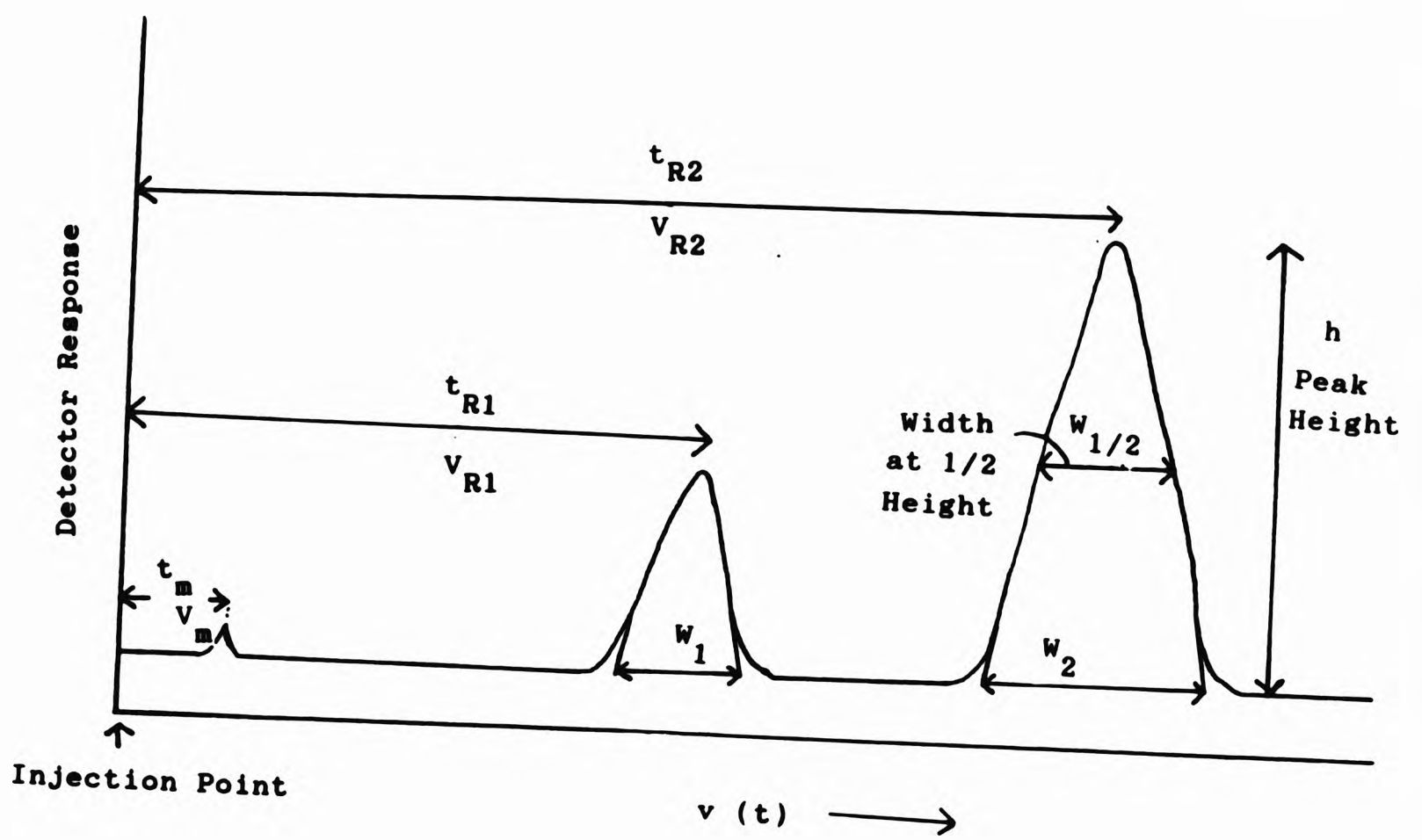


Figure 2.1 Chromatographic Parameters

2.2.8.2 Distribution Coefficient

A solute on entering a chromatography column, distributes itself between the stationary and mobile phase. If at some point the mobile phase is stopped, the sample components will very rapidly achieve an equilibrium distribution between the two phases. In this state the concentration of solute in each phase is given by the distribution coefficient, K:

$$K = C_S / C_M \quad (2.11)$$

C_S and C_M are the concentrations of the solute in the stationary and mobile phases respectively. The distribution coefficient determines the average velocity of the solute in each zone.

2.2.9 Band Broadening

As a solute migrates along the column, the band width increases as a result of the kinetic processes occurring within the column. Whilst working on gas chromatography (GC) van Deemter et al⁹⁶ attributed this band broadening to three factors related to plate height, H, by postulating the van Deemter equation:

$$H = 2\lambda d_p + 2\gamma D_M / \mu + 2/3 K'/(1+K')^2 \cdot D_M d_f^2 \mu / D_S \quad (2.12)$$

Stated in its simplified form:

$$H = A + B/\mu + C\mu \quad (2.13)$$

where H is the plate height, μ the average linear mobile phase velocity, and the A , B and C terms express the kinetic contributions from eddy diffusion, longitudinal or axial diffusion and mass transfer between the mobile and stationary phases. Variables such as particle size of the packing, thickness of the stationary phase, and the flow rate determine the value of these effects.

2.2.9.1 Eddy Diffusion

Eddy diffusion constitutes the A term in the van Deemter equation, and results from the inhomogeneity of flow velocities and path lengths around the packing particles.

$$A = 2\lambda d_p \quad (2.14)$$

d_p is the particle diameter of the packing and λ is an unspecified constant that is a function of packing uniformity and column geometry. λ usually has a value of 1-6.

If the packing is anything less than perfect, the flow paths of the solute molecules will be of unequal length. So some molecules of a single species, will flow close to the column wall, where the packing density is relatively low, whilst other molecules will pass through the more tightly packed centre of the column, at a lower velocity. Therefore molecules following an easier flow path will elute sooner than ones following a more difficult flow path, leading to band broadening.

The A term is therefore a measure of how well a column is packed and it can be minimised by making the mean particle diameter, d_p as small as possible and by obtaining a uniformly packed column.

2.2.9.2 Longitudinal Diffusion

The B term in the van Deemter equation accounts for longitudinal or axial diffusion, that is random molecular migration. It is expressed as:

$$B = 2\tau D_M \quad (2.15)$$

where τ is known as a tortuosity constant which accounts for restriction to diffusion by particles and ranges between 0.01 and 1.0. D_M is the solute diffusion coefficient in the mobile phase and is concerned with the diffusion of the sample in the mobile phase. High diffusion rates in the mobile phase make the solute bands disperse axially along the column, especially at low mobile phase velocities, which leads to band broadening.

In the van Deemter equation B is divided by the mobile phase velocity, B/μ . So to minimise the B term, the mobile phase velocity should be as high as possible and the diffusion rate, D_M should be low.

2.2.9.3 Mass Transfer

The C term in the van Deemter equation is expressed as:

$$C = \frac{2}{3} \frac{K'}{(1 + K')^2} \cdot D_M d_f^2 / D_s \quad (2.16)$$

where K' is the capacity ratio which is related to the distribution coefficient, d_f is the film thickness of the stationary phase coating and D_s is the diffusion coefficient of the solute in the stationary phase. The C term describes dispersion

due to slow mass transfer which occurs because of the slow equilibrium of the solute between the mobile and stationary phases. As solute molecules move through the column, they suffer random displacements (changes in position) away from the centre of this molecular assembly. Displacements in the direction of flow are responsible for band spreading, since these displacements can be regarded as a number of forward and backward random walks, relative to the band centre.

To minimise the C term, a high diffusion coefficient term is desirable, and so is a thin film coating, d_f . However if the film thickness is decreased so is retention.

In the van Deemter equation, the term C is multiplied by the average linear velocity ($C\mu$). Therefore as slow a linear velocity as possible should be used to minimise the C term. So terms B and C contradict each other as to the optimum linear velocity for minimising the terms. This is indicated in the HETP graph in Figure 2.2.

Taking into account all the terms, the best overall linear velocity is μ_{opt} (see figure 2.2). At μ_{opt} (flow rate approximately 0.1 ml/min) maximum efficiency is achieved. However as this minimum (H) region is quite broad for a usual LC column, efficiency can be traded for speed, and the work can be carried out at higher μ values (of around 1 ml/min flow rate).

For well packed columns the A term is 1, B is 2 and C is about 0.05.

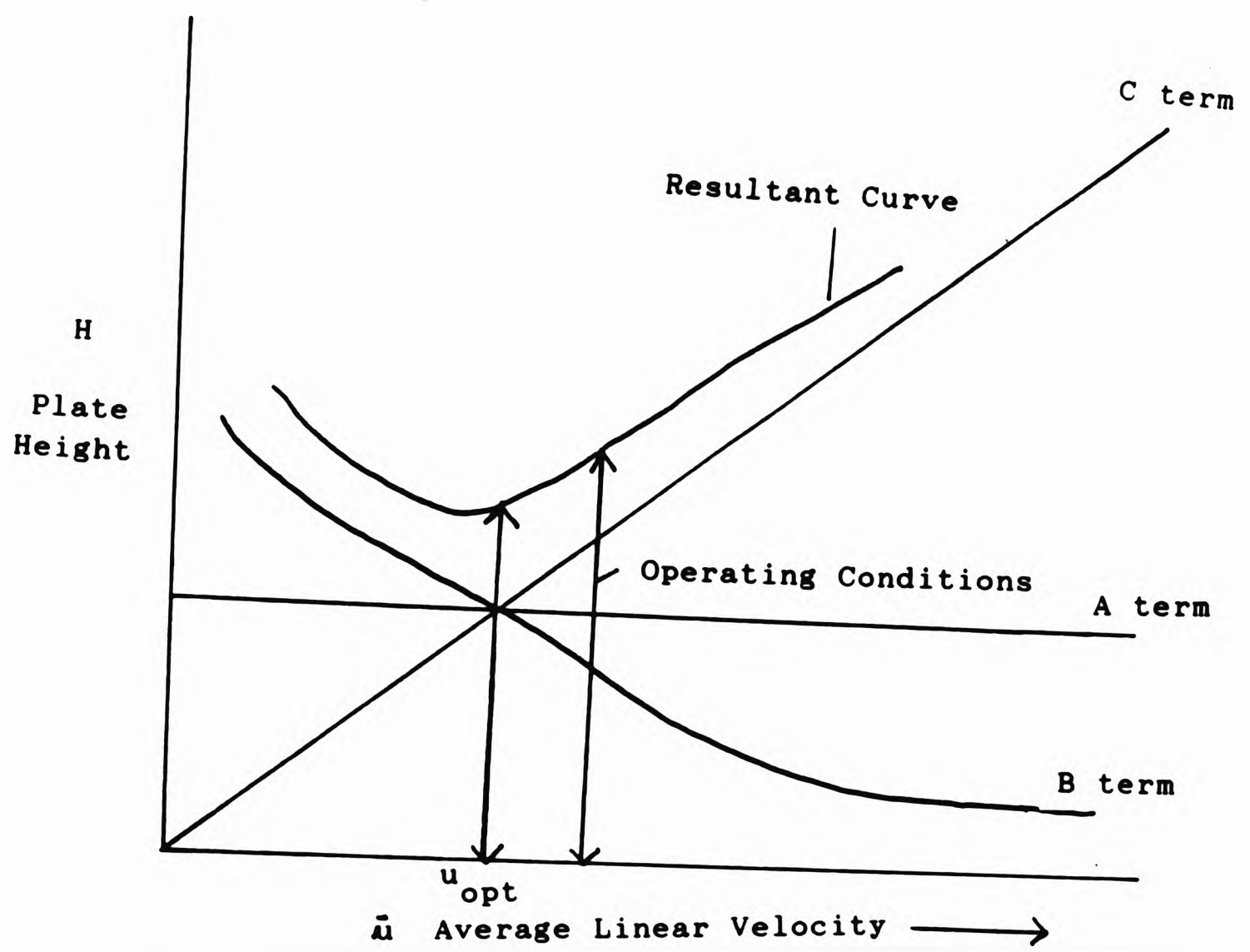


Figure 2.2 Van Deemter H/u Plot (HETP) in Liquid Chromatography

2.2.10 HPLC Instrumentation

The general instrumentation for HPLC consists of a solvent pump, an injection device to introduce the sample onto the column, the separation column, and a detector with recorder readout. The high pressure pumping system delivers the mobile phase solvent from the solvent reservoir to the column through stainless steel tubing and fittings (Figure 2.3). The stainless steel columns usually used for analytical separations have small internal diameters (2 to 5 mm).

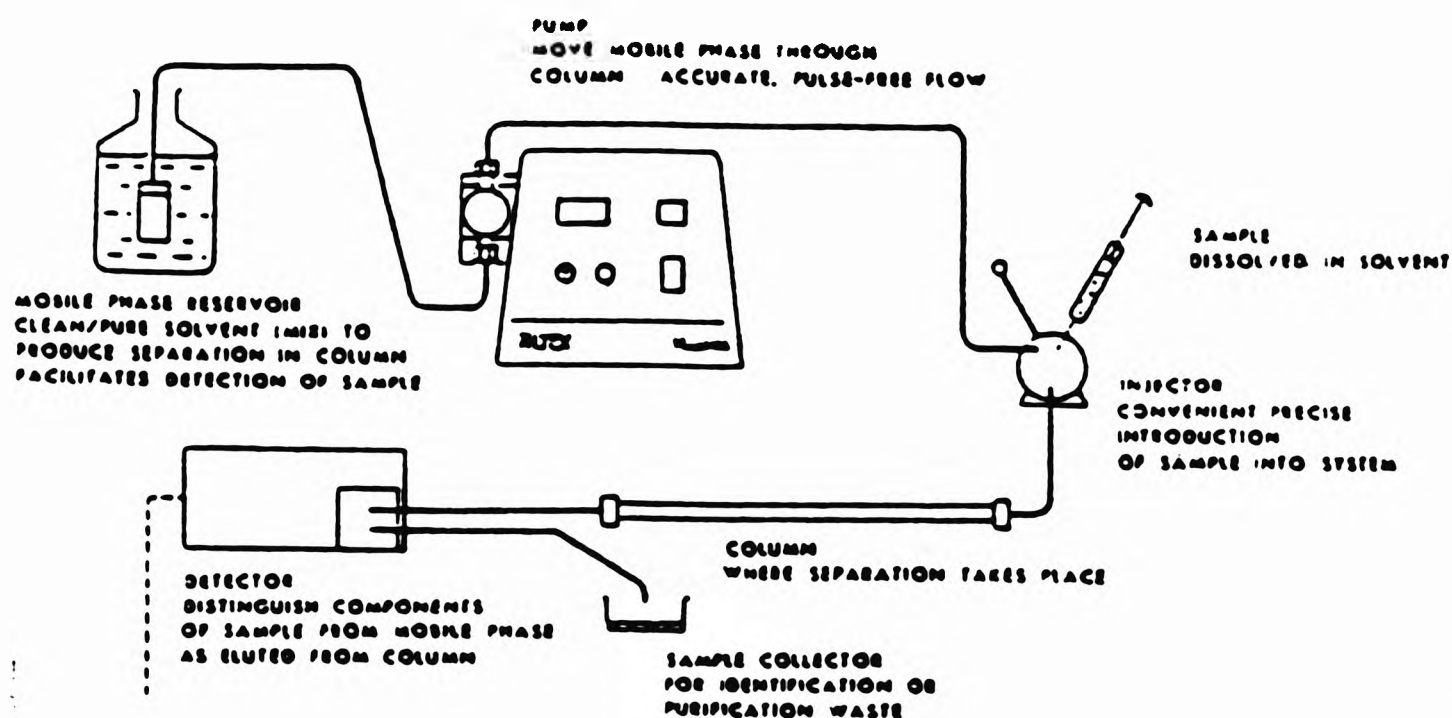


Figure 2.3 Schematic Diagram of HPLC Apparatus

2.2.10.1 HPLC Detectors

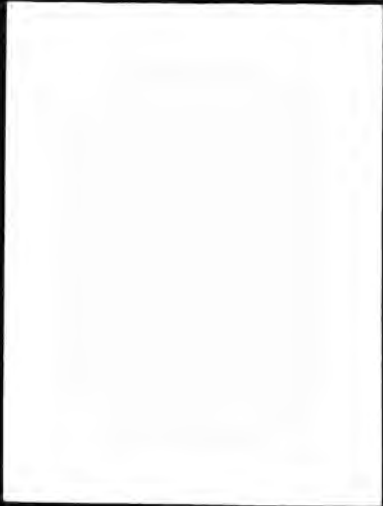
Detectors which can be used in liquid chromatography include ultraviolet (UV)/visible, fluorometric, infrared (IR), and electrochemical (EC) detectors and differential refractometers. These detectors can be categorized as being either bulk property or specific property detectors. Bulk property detectors, typified by the refractive index monitor, compare an overall change in a physical property of the mobile phase with and without the eluting solute. Although universal, this detector

tends to be relatively insensitive. The specific property detectors respond to a physical property of the solute not exhibited by the mobile phase. Solute property detection is roughly 1000 times more sensitive than mobile phase detection. Ultraviolet/visible absorption, fluorescence and electrochemical detectors are examples of specific property detectors. Precolumn and postcolumn derivitisation expands their applicability.

The UV/visible detector can either be a fixed wavelength detector, which operates at wavelengths of 240 or 280 nm, or a variable wavelength detector. The fixed wavelength detector is the most widely used in LC. Its main advantages are its relatively low cost, high sensitivity for compounds of both chemical and biological interest that absorb light in the UV region and its insensitivity to changes in temperature, flow rate and mobile phase composition. The variable wavelength detector operates by rotating a diffraction grating to the appropriate incidence angle to give the desired wavelength. The advantages of this detector are the availability of a wide range of wavelengths, the ability to alter wavelengths without changing filters or lamps, and the ability to operate at wavelengths below 254 nm. All compounds that have one or more double bonds, or have unshared unbonded electrons (e.g aromatics and compounds with carbonyl, thiocarbonyl, nitroso and azo groups) will absorb in the UV region.

Fluorometric detectors are sensitive to compounds that are inherently fluorescent or that can be converted to fluorescent derivatives by either chemical transformation of the compounds or by the coupling at specific functional groups with fluorescent tagging reagents. Turbidity of the sample will present a problem to fluorescence.

Infrared detectors are particularly useful when the compound of interest is not active in the UV region.



Electrochemical detectors can be used where the compound of interest can be oxidised at a suitable electrode present in the detector. Once the operating potential has been chosen, chromatograms are plotted showing current as a function of time. Compounds typically detected by electrochemical means include aromatic amines and their derivatives, ascorbic and uric acid, and phenolics and carboxylic acids.

The differential refractometer detects differences between the refractive indexes of the pure solvent and of a solution of the solute of interest in the solvent. The response is affected by small changes in the solvent composition, flow rate and temperature.

In general the signal output from the detector is amplified before it is fed to a suitable automatic recording device, usually a strip chart potentiometric recorder, where the signal is plotted against time.

2.3 ELECTROMAGNETIC RADIATION

Spectroscopy involves the measurement and interpretation of electromagnetic radiation absorbed or emitted when molecules, atoms or ions of a substance transfer from energy level to another, in absorption spectroscopy this involves excitation from the ground state to an excited state. Each substance has a characteristic interaction with the electromagnetic radiation.

2.3.1 Properties of Electromagnetic Radiation

A beam of light may be viewed as a collection of photons of energy that move at the speed of light. A photon has both wave and particle properties. A photon originating from a point in space, radiates from that point in the form of a spherical wave which has periodic maxima perpendicular to its direction of travel. The distance between two maxima is deemed the wavelength (λ). The frequency (ν) is the number of waves that pass a given point in a unit length of time.

The energy of light is given by Planck's equation:

$$E = h\nu = hc/\lambda \quad (2.17)$$

where c is the speed of light in a vacuum ($3.00 \times 10^8 \text{ m sec}^{-1}$) and h is Planck's constant. The shorter the wavelength of the radiation the higher its energy.

Interaction with matter occurs throughout a broad range of radiations to give the electromagnetic spectrum (Figure 2.5). The radiations all travel with the speed of light but differ in their wavelengths, frequencies and the effects they produce. Radiation in the ultraviolet (UV) region is high energy and can excite electrons away from the nucleus to an excited state. Infrared (IR) radiation has only enough energy to excite vibrational and rotational energy. Microwave radiation is involved with changes in electron spin states and the low energy radio waves are involved with the flipping of nuclear spins^{97,98}.

2.3.1 Properties of Electromagnetic Radiation

A beam of light may be viewed as a collection of photons of energy that move at the speed of light. A photon has both wave and particle properties. A photon originating from a point in space, radiates from that point in the form of a spherical wave which has periodic maxima perpendicular to its direction of travel. The distance between two maxima is deemed the wavelength (λ). The frequency (ν) is the number of waves that pass a given point in a unit length of time.

The energy of light is given by Planck's equation:

$$E = h\nu = hc/\lambda \quad (2.17)$$

where c is the speed of light in a vacuum ($3.00 \times 10^8 \text{ m sec}^{-1}$) and h is Planck's constant. The shorter the wavelength of the radiation the higher its energy.

Interaction with matter occurs throughout a broad range of radiations to give the electromagnetic spectrum (Figure 2.5). The radiations all travel with the speed of light but differ in their wavelengths, frequencies and the effects they produce. Radiation in the ultraviolet (UV) region is high energy and can excite electrons away from the nucleus to an excited state. Infrared (IR) radiation has only enough energy to excite vibrational and rotational energy. Microwave radiation is involved with changes in electron spin states and the low energy radio waves are involved with the flipping of nuclear spins^{97,98}.

2.4 INFRARED SPECTROSCOPY

The IR region of the electromagnetic spectrum crosses the wavelengths between 0.7 and 500 μm or in wave numbers ($1/\lambda$) between 14,000 and 20 cm^{-1} . Infrared spectroscopy is concerned with the excitation of mechanical motions within a molecule. These motions involve stretching, or deformation of bonds. These observed motions are rarely pure and due to singular vibrations. Usually coupled motions have to be observed. These fall into three groups: i) coupling between two fundamentals e.g symmetric and asymmetric stretches of a C-H bond, ii) overtones and combinations iii) Fermi resonance; a combination of coupling between an overtone and a fundamental.

As a large number of vibrations occur simultaneously, a complex absorption spectrum is obtained, which gives an indication of the overall configuration of the atoms as well as the functional groups present within the molecule.

These vibrational motions are quantised and at room temperature the molecules will be present mostly in the lowest vibrational state. However when the molecule absorbs light of an appropriate wavelength and energy, it will become excited and will move to a higher energy level. In IR spectrophotometry, the absorption of such a quantum of energy can only occur if the dipole moments differ in the two vibrational energy levels. When bonds stretch or bend in a vibrating molecule the dipole moment may vary. This oscillating dipole shakes the electromagnetic field into oscillation and so radiation may be absorbed. Therefore only vibrations that are accompanied by a changing dipole moment can be excited by electromagnetic radiation. The necessity for absorption of a vibrational quantum to be accompanied by a change in dipole moment is known as the selection rule. Then the molecule is said to be infrared active.

An infrared spectrum is obtained by plotting the wavelength against per cent transmittance of the sample. Absorption of light is manifested as a trough in a curve. Zero transmittance corresponds to 100% absorption of light of that wavelength. Of the IR ranges, the mid-infrared region, also known as the "fingerprint" region ($1300-650\text{ cm}^{-1}$) is the most valuable in compound identification, as absorption in this region is highly characteristic of certain molecules.

2.4.1 Fourier Transform Infrared (FTIR) Spectroscopy

An FTIR spectrophotometer, consists of three main parts; a radiation source, an optical system and a detector (Figure 2.4). A half reflecting mirror splits the beam from a light source (a glowbar) into two equal parts. The two beams traverse different paths, being reflected by different mirrors, before coming together again just before passing through the sample and into the detector. The distance travelled by one of the beams is oscillated by moving one of the mirrors (M4).

If the lengths of the two optical paths are identical then there will be no phase difference between the beams and they will combine constructively. If there is a difference between the two optical paths, the beam may recombine destructively. For different interferometer path lengths, the amplitude of the recombined signals will depend on the frequency and distance moved by the mirror M4. For instance low frequencies will give destructive interference, with phase shifts of the order of about 100° , with large movements of the mirror. High frequencies need only a small movement of the mirror M4 to achieve the same interference. The beam focused on the sample is a complex mixture of modulation frequencies, which on passing through the sample is collected by the detector. The detector signal is

sampled at precise intervals during the scan. A reference laser beam is passed through the system to oversee the whole process by controlling the sampling rate and the mirror velocity. The resulting signal is known as an interferogram and contains the information necessary to construct a spectrum using a mathematical process known as a Fourier transformation.

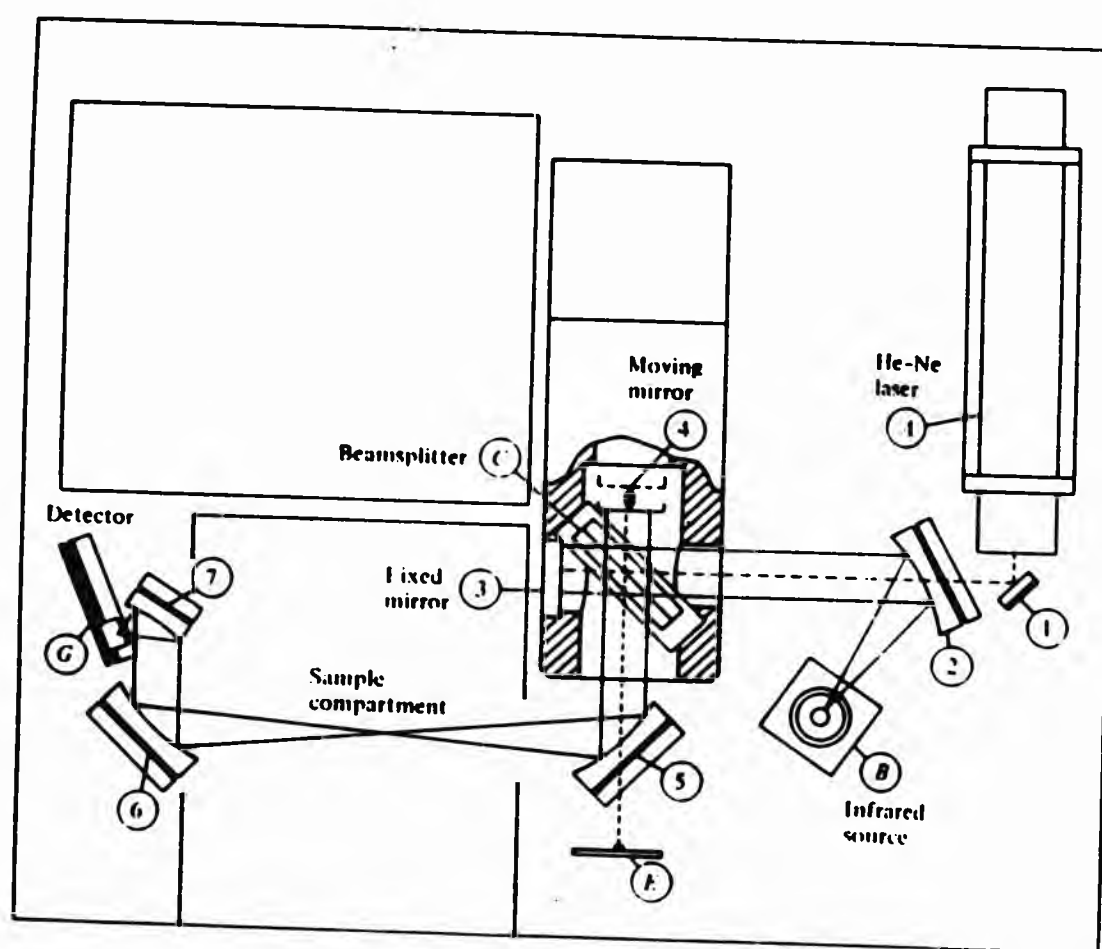


Figure 2.4 Diagram of Infrared Fourier Transform Interferometric Spectrometer

FTIR has five main advantages over conventional infrared techniques;

- i) mechanically there is only one moving part, M4,
- ii) Jacquinot's advantage - there are very few optical surfaces and no gratings or prisms which leads to fewer monochromator losses,
- iii) Fellgett's advantage - all the wavelengths are detected simultaneously. At any

- one wavelength the detector has more time to accumulate signals,
- iv) The computational power offers signal averaging - as the signal to noise ratio (S/N) is proportional to the square root of the number of scans. Therefore four scans give a half the noise. Usually 32 scans are made (approximately 60 seconds) to produce an averaged interferogram.
 - v) Connes' advantage - the FTIR spectrophotometer is continually calibrated with reference to the laser beam, therefore wavelength accuracy and precision is excellent.

2.5 ATOMIC ABSORPTION SPECTROSCOPY (AAS)

Atomic absorption spectroscopy is based on the absorption of ultraviolet or visible light by gaseous free atoms⁹⁸. The compound to be analysed must first absorb enough energy to be vaporised, and to form a molecular gas, where the molecules have dissociated to form free atoms. An absorption spectrum is obtained when the free atoms absorb radiant energy at characteristic wavelengths.

In order to vaporise the sample, the solution is aspirated into a flame, where the solvent is evaporated and the sample compounds become thermally decomposed and converted to a gas of individual free atoms. The free atoms are mostly in a ground state and absorb radiation from a light source when the radiation corresponds exactly to the transition of the element of interest from the ground state to a higher excited state. Some of the light will be absorbed by the free atoms of the sample, and the rest will pass through. The spectral line of interest is isolated from the emerging beam by a monochromator and the ratio of the

intensity of the line to that of its source is measured by a photocell or photomultiplier. Therefore the ratio between the incident beam (P_0) and the transmitted beam (P) is measured.

A hollow cathode lamp containing the element to be analysed is used as the light source, so that the atoms of the analyte metal absorb at exactly the same wavelength emitted by the light source. As the cathode lamp has narrow band emissions, virtually complete specificity for the element is provided. Therefore there is hardly any interference from the spectral lines of other elements.

The amount of light absorbed by the sample depends on the number of atoms found in the path of the light. Provided that the flame is hot enough to convert the aspirated solution to free atoms, the light absorbed is almost independent of the flame temperature and the wavelength of absorption.

If the flame conditions are kept fairly constant as well as the rate of sample aspiration, then the absorbance ($\log P_0/P$) is directly proportional to the concentration of a given metal in the sample.

2.5.1 Instrumentation

An AA spectrophotometer consists of a light source (the hollow cathode lamp), a burner-nebuliser and a monochromator and detector (Figure 2.5). The hollow cathode lamp is evacuated, but contains some argon or neon gas. The cathode contains the element to be determined e.g. if gold is to be determined a gold cathode is used. A high voltage of about 400 volts ionises the atoms of argon,

which bombard the cathode. This bombardment leads to the expulsion of the metal atoms into the atmosphere of the tube, where they collide and become excited, emitting light at wavelengths that are characteristic of the cathode metal.

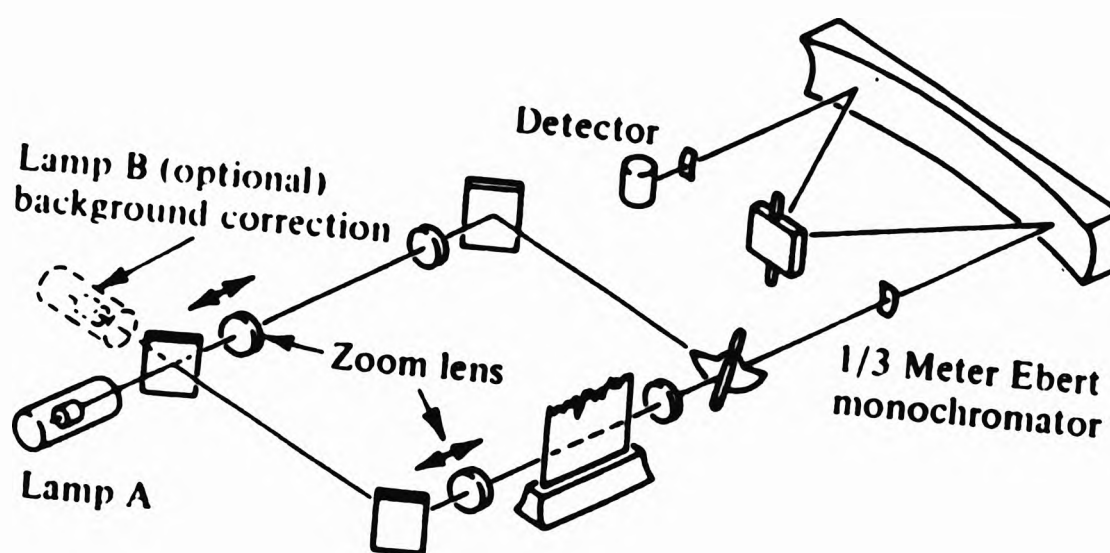
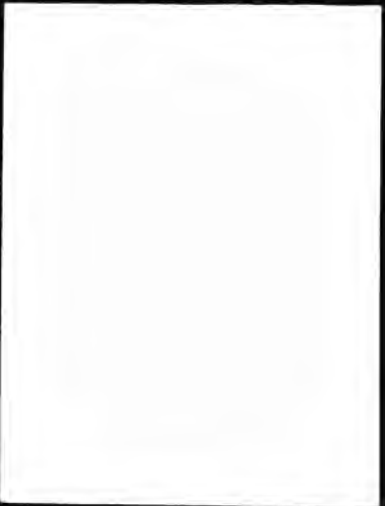


Figure 2.5 A Double-beam Atomic Absorption Spectrometer.

The burner-nebuliser produces a flame, most commonly an air-acetylene flame. Some metals are refractory and are difficult to convert to gaseous atoms. Among these are boron and titanium, as they form very strong metal to oxygen bonds which are difficult to decompose thermally. This problem is overcome by the use of a fuel rich oxy-acetylene or nitrous oxide-acetylene flame. The height of the flame and the rate of aspiration can be adjusted to achieve maximum sensitivity for particular elements.



Another way of producing gaseous free atoms is by the use of an electric furnace, where no flame is used. In this technique a few microlitres of the sample are placed in a graphite tube, which is heated electrically until the gaseous free atoms are produced. A beam of monochromatic radiation from the hollow cathode lamp traverses the tube and is partly absorbed by some of the gaseous atoms. The sample element is analysed and calculated as in the flame atomic absorption spectrophotometer.

The graphite furnace removes the requirement for the nebulisation of the sample as occurs in flame AA. This is not a very efficient process and the free gaseous atoms only stay in the beam for a fraction of a second. However, liquid samples need three heating stages. At the first stage the solvent is removed, the second stage involves the ashing of the sample, and at the final heating stage the analyte is converted to free gaseous atoms.

The sensitivity of the graphite furnace depends on the metal being analysed, but it usually achieves a greater sensitivity than the flame AA.

The monochromator selects the spectral line of interest, as the lines of the source are narrow and there is almost zero background interference.

The concentration of the element of interest in the sample is obtained by the preparation of a calibration curve from serial dilutions of a standard solution of the metal salt of interest.

The accuracy and precision of the AA spectrophotometer depend on the element analysed.

2.6 NUCLEAR MAGNETIC RESONANCE (NMR) SPECTROSCOPY

Nuclear magnetic resonance (NMR) spectroscopy allows elucidation of the configuration of molecules by investigating nuclear spins when the molecule is placed in a strong magnetic field. In the magnetic field, the nucleus can have quantised nuclear energy levels, corresponding to certain orientations of the spin magnetic moment. Absorption of radiation is detected when the difference between the nuclear levels corresponds to absorption of a quantum of radiation. In NMR the sample is placed in a magnet and the nuclei in the molecule generate a bulk macroscopic magnetisation (Figure 2.6).

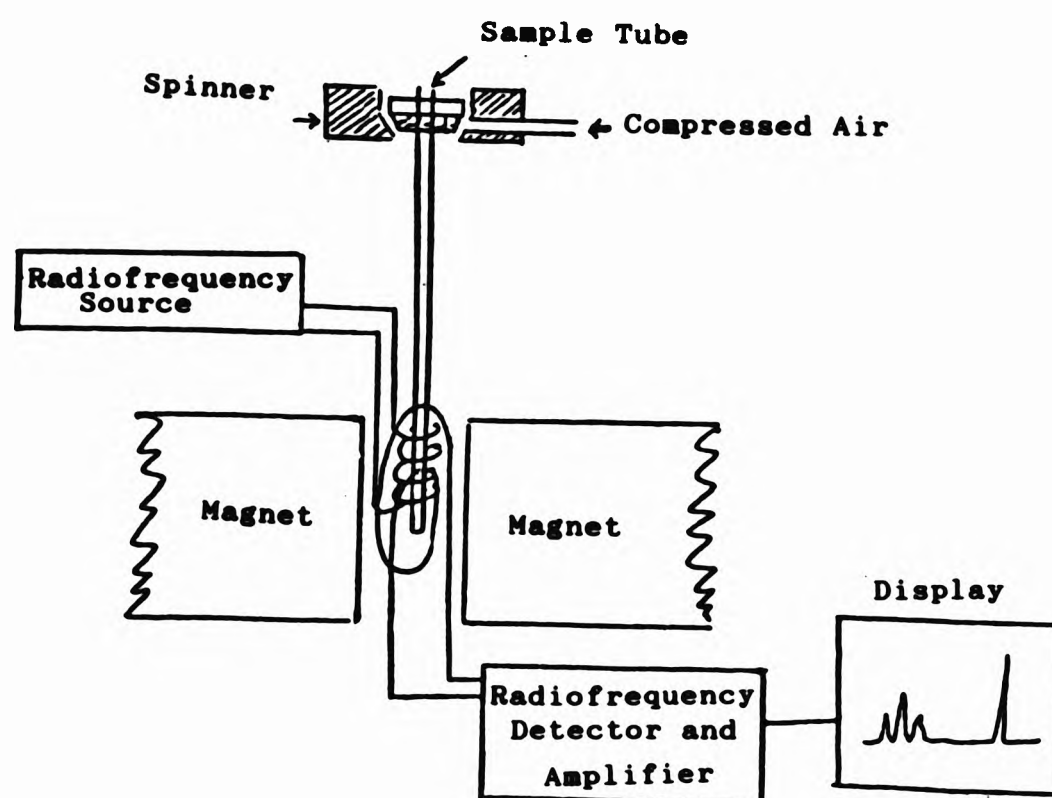


Figure 2.6 A Schematic Diagram of an NMR Spectrophotometer.

2.6.1 General Principles of NMR

The nucleus of certain isotopes, for example protons in a water sample, possess an intrinsic spinning motion around their axes, which will interact with an applied magnetic field. The nuclear spins will either align with the magnetic field, which

is the more stable configuration, or against it, which is less stable as energy has to be absorbed to flip over the proton. The proton has a spin quantum number, $I=1/2$, which in a magnetic field generates two energy levels (Figure 2.7). These energy levels can be characterised by the nuclear spin number m_I , and they are separated by the difference in energy states δE . The difference between the energy states is dependant upon the magnetic field:

$$\delta E = h\gamma B_0/2\pi \quad (2.18)$$

where γ is the magnetogyric ratio and B_0 is the magnitude of the applied magnetic field.

The lower energy state, where the magnetic moment is parallel to the applied magnetic field, B_0 , has the magnetic spin number $m_I = +1/2$, and is usually known as the α state. The upper energy state, β , in which the magnetic moment is antiparallel to B_0 , has the magnetic spin number $m_I = -1/2$.

Transitions can occur when the gap between the energy levels is exactly the same as the incoming frequency ($E=h\nu$).

The frequency of observation can be expressed as:

$$\nu = \gamma B_0/2\pi \quad (2.19)$$

ν is the resonant frequency in hertz. The difference in the magnetogyric ratio γ , gives different observation frequencies for differing nuclei. ν for carbon 13 (^{13}C), is one quarter of that for protons, ^1H . Therefore a signal for ^{13}C is seen at a frequency of 50.3 MHz, whilst for a proton it is seen at 200 MHz in the same magnetic field.

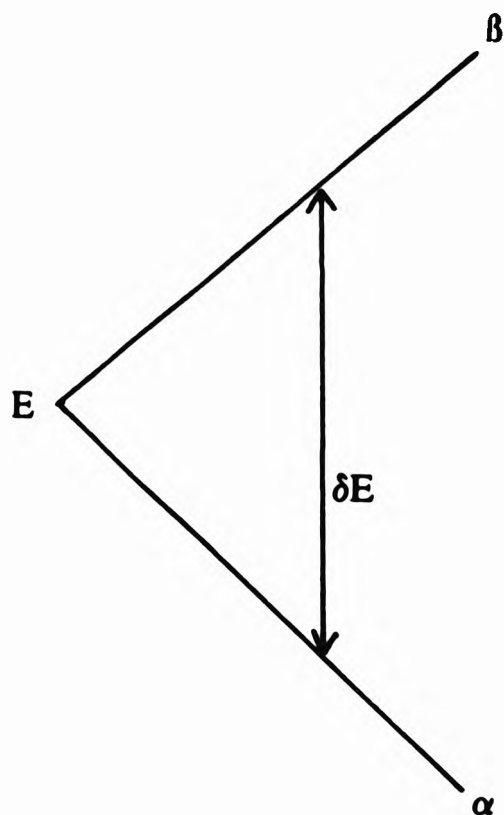


Figure 2.7 Energy level diagram for spin with $I=1/2$ in a magnetic field B

In proton NMR, the frequency of the absorption depends on the magnetic and electric environment of the nuclei. These environments generally determine the position of the signals in an NMR proton spectrum. The electrons around the proton nucleus begin to precess when placed in an applied magnetic field B_0 . This motion induces a magnetic field which opposes the applied magnetic field. As a result, the net magnetic field experienced by the proton is said to be "shielded" and absorption occurs upfield. If the induced magnetic field enhances the applied field, then "deshielding" occurs and the absorption is downfield. These movements in absorption are known as chemical shifts. As a general rule, as the electronegativity of the surrounding atom increases, so the electron density decreases and deshielding occurs.

The appearance of a resonance in proton NMR is influenced by the neighbouring hydrogen nuclei of the molecule. Resonances appearing as peaks have the form of doublets, triplets etc.; that is to say that peak splitting occurs. This phenomenon arises from the magnetic field that is associated with each individual neighbouring spinning proton. These magnetic fields will alter the total magnetic field experienced by another proton. The signal will split into two, giving a doublet if influenced by one neighbouring proton, and if influenced by two protons it will split into a triplet.

The magnetic field experienced by the secondary proton is influenced by the adjacent tertiary proton (Figure 2.8). By way of shared electrons, the magnetic field will be increased when the tertiary proton is aligned with the field, and decreased when aligned against it. As a result the absorption by the secondary proton is shifted slightly downfield for half the molecule and for the other half it is shifted upfield.

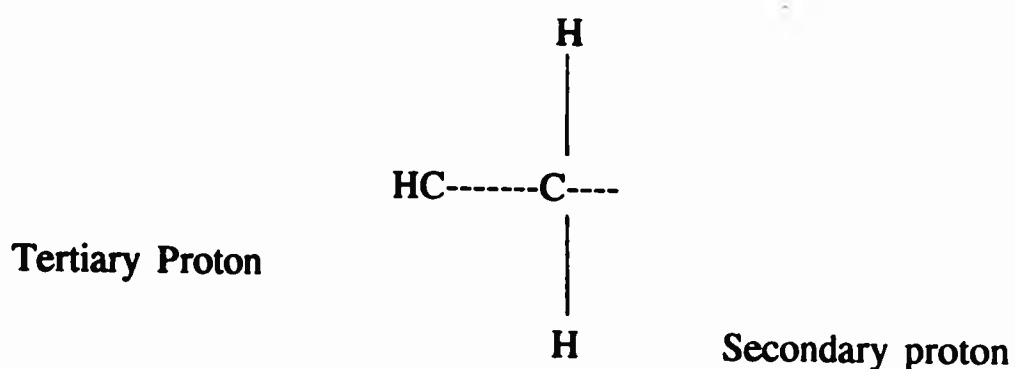


Figure 2.8 Positions of Secondary and Tertiary Protons

If the tertiary proton has a β -spin, the effect is as if the total magnetic field experienced is greater than that supplied by the applied magnetic field generated by the NMR instrument. Therefore less applied field is needed to achieve a resonance, than in the absence of the tertiary proton and a slight downfield shift is experienced. Only half of the tertiary protons have a β -spin, the rest having an α -spin. As a result these molecules feel as if the magnetic field is weaker at the

secondary proton than that of the applied field. A greater magnetic field must therefore be supplied by the NMR spectrophotometer. This results in an upfield shift. The secondary and tertiary protons are said to be coupled. For one half of the molecule, the absorption for the secondary proton is shifted slightly downfield, and for the other half of the molecule it is shifted slightly upfield. The signal is therefore split into two peaks giving a doublet of a 1:1 intensity. Similarly, the magnetic field experienced by the tertiary proton is influenced by the spin of two neighbouring protons and the NMR signal splits into a triplet of intensity 1:2:1.

2.6.2 Pulse NMR

The proton NMR spectra of biological samples usually exhibit broad overlapping resonances attributable to the presence of relatively immobile macromolecular species such as proteins. Application of a pulse NMR technique, suppresses the broad resonances, giving a clearer NMR spectrum with well resolved resonances arising from the low-molecular mass components of the sample⁹⁹.

The pulse NMR technique involves disturbing the system from equilibrium by the application of a pulse and then following the response of the system to the disturbance. The magnetisation of a sample is achieved by application of a magnetic field. This magnetisation can be perturbed by a second field oscillating with the appropriate radiofrequency. This disturbance of the magnetic field generates the nuclear magnetic spectrum. In continuous wave (CW) NMR the disturbance is measured as either the radiofrequency is varied or the field is swept, only one single frequency being excited and at the same time detected. In pulsed FT NMR, the entire spectrum is excited by a pulse of radiofrequency energy, and the response of the sample to the pulse is measured as a function of time and is converted to the frequency domain by a computer^{100,101}.

The NMR pulse technique is best described by use of a vector diagram (Figure 2.9).

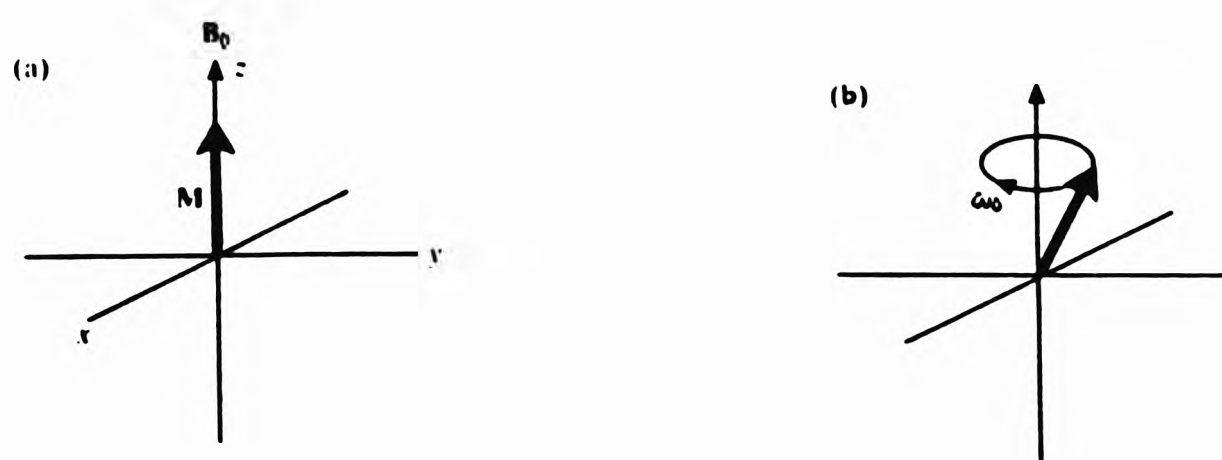


Figure 2.9 Vector Diagram Showing Behaviour of the Bulk Magnetization M a) at Equilibrium, and b) after Perturbation by a Pulse

The net magnetisation of the sample (M) will align with the magnetic field initially. The applied field (B_0) will be in the z direction. The net magnetisation can be moved from its equilibrium, by a second magnetic field or pulse, to the xy axis. This NMR signal can be detected. However the net magnetisation will return to its equilibrium position and the signal will gradually decay. This signal is called a free induction decay (FID). In order for the spin to return to equilibrium, there must be interaction between the spins and the surroundings or "lattice", which leads to the loss of excess energy. The time for the spin system to return to the equilibrium by this method is known as the spin-lattice or longitudinal (i.e along the z axis) relaxation time (T_1) and is of the order of seconds. When the net magnetisation is disturbed from equilibrium, it may also have components in the xy -plane which will also relax to zero. Magnetisation in the xy -plane may also be

lost by additional processes which cause the xy components to fan out or dephase. These processes do not necessarily need an energy change, so the xy relaxation rate may be faster than the z relaxation. The time for the xy relaxation to occur is known as the spin-spin or transverse (perpendicular to z axis) relaxation time (T_2).

2.6.2.1 Hahn Spin-Echo

The pulse sequence most commonly used is the two pulse Hahn spin-echo experiment¹⁰². In its simplest form it can be written as:

$$\pi/2 - t_D - \pi - t_D - \text{Echo} \quad (2.20)$$

A schematic representation of the Hahn spin-echo is shown in Figure 2.10 by using vector diagrams.

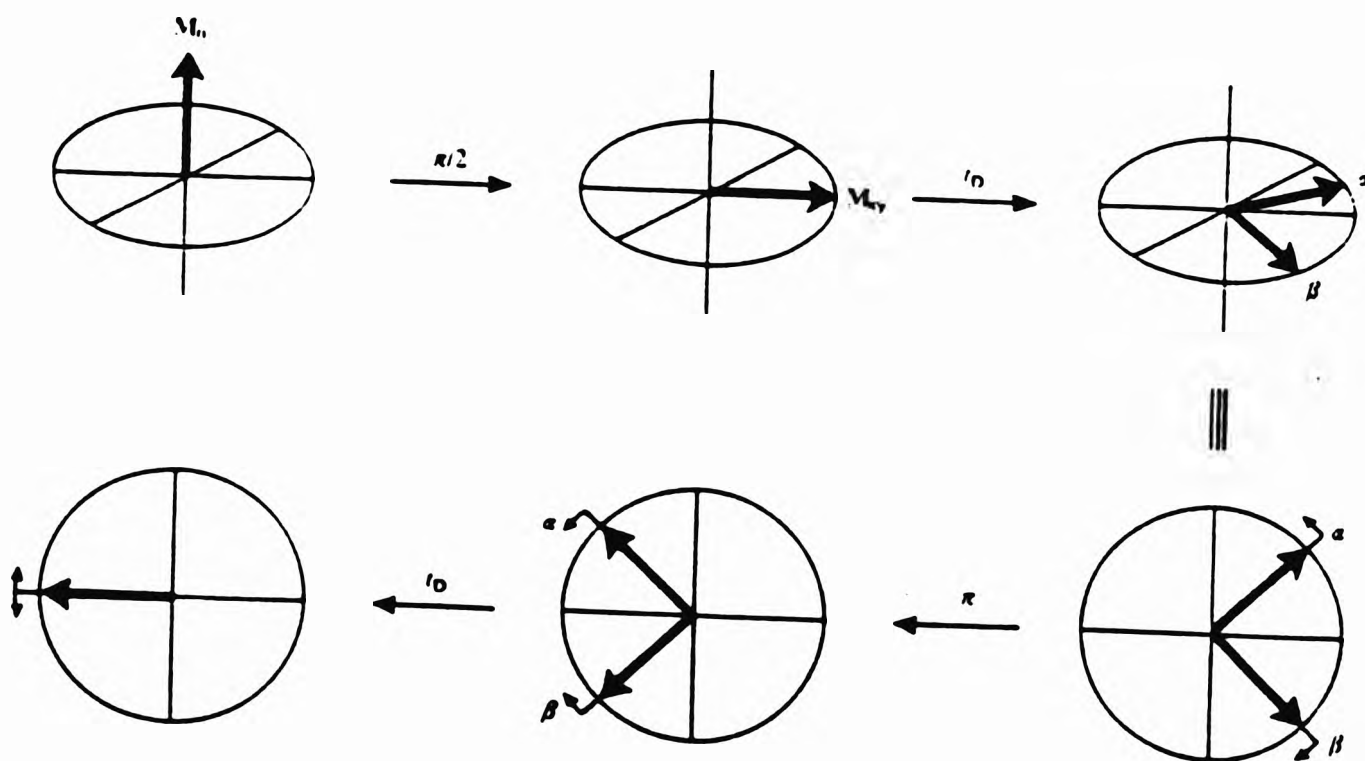
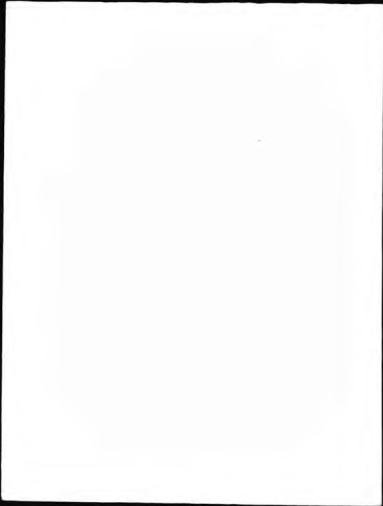


Figure 2.10 Vector Diagram of Hahn Spin Echo Sequence

If we consider a sample with resonance at the z axis. The chemically identical spins of the sample are found in different parts of the the NMR tube, and as such will experience different affective magnetic fields. Field inhomogeneity will therefore result and the spins will precess at a range of frequencies, rather than at a single frequency. A $\pi/2$ or 90° pulse is applied to the sample and the magnetisation vectors are tipped into the xy-plane, where due to the loss of phase coherence the vectors fan out. The main contributing factors to the dephasing are the loss of phase coherence from spin-spin relaxation and the inhomogeneity of the applied magnetic field (B_0). The fanning out occurs as the nuclei precess at different rates within the sample, some slower and some faster. The signal observed will result from the vector sum of the components, but as the components fan out the vector sum decreases and the net signal decays rapidly. A π pulse (180°) is applied after a time delay, t_D . This has the effect of rotating all the magnetisation vectors by 180° about the y axis. The magnetisation will be in the xy axis as before but it will now be displaced from the -y axis by an amount which depends on the time delay, t_D , and the precession frequency. However, as the magnetisation is still precessing in the same direction as before, it is now moving towards the -y axis. After a second identical time delay (t_D), the magnetisation will converge and refocus at the -y axis. The vector sum and the resulting signal intensity will increase to form an echo of maximum amplitude at the moment when the second time delay t_D equals the first time delay. After that moment, the signal will decay again, but at the peak of the echo, when the signal is collected, all effects of field inhomogeneity, will have been eliminated.

Resolution of the NMR spectrum is also enhanced by the Hahn spin-echo technique due to the fact that different molecules have different spin-spin relaxation times (T_2). High molecular weight molecules usually possess short spin-spin relaxation times (T_2) compared with the T_2 value of smaller, more mobile



molecules. If, therefore, the time delay t_D of the spin-echo sequence is made longer than the T_2 of the macromolecules, the large overlapping molecule resonances can be eliminated to leave a well resolved, cleaner NMR spectrum.

CHAPTER 3

**THE DEVELOPMENT OF AN ANALYTICAL METHOD FOR
THE DETECTION OF GOLD (I) PRESENT AS THE ANTI-
RHEUMATIC DRUG DISODIUM AUROTHIOMALATE BY
HPLC**

3.1 INTRODUCTION

About 5% of the total circulating gold present in rheumatoid arthritis patients undergoing chrysotherapy is present as "free" gold, or gold that is unbound to protein. This unbound gold could play an important part in the attainment of an equilibrium of the gold within a number of biological protein binding sites, and could also play a part in transportation processes and, as such, needs to be accurately quantified by a reliable method. In this chapter a procedure is sought, in which gold present in the drug myocrisin, can be complexed, in order to form a stable compound that can be analysed, quantified and standardised by reversed-phase HPLC. Complexing with the reagent dithizone, as well as with cyanide is carried out to this purpose.

3.1.1 Dithizone as a Complexing Agent

Dithizone, also known as 1,5-diphenylthiocarbazone, was first prepared by Emil Fischer in 1882, who remarked on the compound's ability to form strongly chelated complexes with many heavy metals. Fischer¹⁰³ carried out extensive work on dithizone and utilised its heavy metal complex forming properties to detect and determine trace levels of metals. Dithizone has been used for the determination of trace levels of gold both by extractive titration¹⁰⁴, where the end point is indicated by colour change, and by spectrophotometry¹⁰⁵. In this work the complexation and extraction of trace levels of gold (I) by dithizone, from standard solutions of the anti-arthritic drug disodium aurothiomalate have been attempted. Dithizone was used to form gold (I) dithizonate which when extracted and reconstituted can be introduced onto a HPLC column, where it was separated out and detected at the appropriate wavelength by an UV detector. Standard work was done with a view

to formulating a method for the quantification of the unbound ("free") gold that is present in the biological fluids of rheumatoid arthritis patients undergoing gold drug therapy.

Dithizone is a violet-black solid which is soluble in most organic solvents such as chloroform and carbon tetrachloride. Two main structures have been proposed for dithizone; namely a thione and a thiol form (Figure 3.1). Dilute solutions of dithizone are intensely green, whilst more concentrated solutions are dichroic (red in transmitted, green in reflected light).

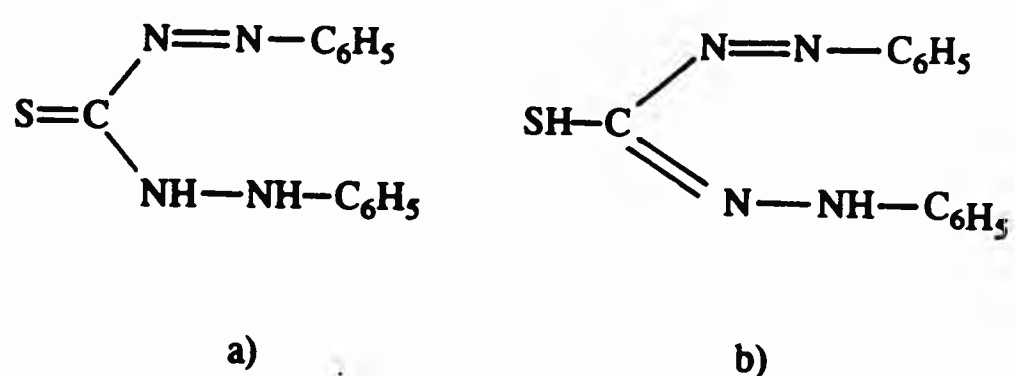


Figure 3.1 The a) Thione and b) Thiol Structures of Dithizone

When an organic solution of dithizone is shaken with an aqueous solution of a reacting metal, a metal dithizonate complex is formed. The dithizonate is usually formed in the organic layer, to which it imparts a violet, red, orange or yellow colour depending on the metal involved. The organic layer can be removed, evaporated and reconstituted to extract the metal dithizonate.

The metal can displace either one or both of the acidic hydrogens of the dithizone to give the keto (or primary) dithizonate, or the enol (or secondary) dithizonate.

3.1.2 Formation of Dicyanoaurate

The linear complex ion dicyanoaurate $[\text{Au}(\text{CN})_2]^-$ is a very stable gold (I) complex. It has been reported^{106,107} that tobacco smoking produces an increased uptake of gold by blood cells of patients treated with aurothiomalate; this effect being due to the inhalation of cyanide. Studies¹⁰⁸ indicate that cyanide converts the aurothiomalate to dicyanoaurate which is rapidly taken up by the cells. Graham *et al*¹⁰⁹ carried out ^1H and ^{13}C NMR and UV spectroscopic studies to elucidate the interaction of cyanide with aurothiomalate, and reported that excess cyanide levels led to the sole production of $[\text{Au}(\text{CN})_2]^-$. Haddad *et al*¹¹⁰ detected trace levels of gold (I) as its cyano complex by ion-interaction reversed-phase HPLC. UV spectra of the dicyanoaurate give rise to peak maxima at 209.5, 228, and 239 nm¹¹¹.

Since cyanide forms such a stable complex with gold (I) and one, moreover, which is active in the UV region, in this work, the formation of dicyanoaurate, from aurothiomalate in the presence of excess potassium cyanide has been utilised to detect low, biologically relevant concentrations of gold (I) by reversed-phase HPLC with UV detection. An attempt to standardise the method is carried out with a view to its use on appropriate RA biological samples.

3.2 MATERIALS AND METHODS

3.2.1 Materials

The disodium aurothiomalate used was purchased from Rhone-Poulenc (Dagenham, Essex). All solvents were of HPLC grade and were purchased from BDH Chemicals (Poole, Dorset).

3.1.2 Formation of Dicyanoaurate

The linear complex ion dicyanoaurate $[\text{Au}(\text{CN})_2]^-$ is a very stable gold (I) complex. It has been reported^{106,107} that tobacco smoking produces an increased uptake of gold by blood cells of patients treated with aurothiomalate; this effect being due to the inhalation of cyanide. Studies¹⁰⁸ indicate that cyanide converts the aurothiomalate to dicyanoaurate which is rapidly taken up by the cells. Graham *et al*¹⁰⁹ carried out ^1H and ^{13}C NMR and UV spectroscopic studies to elucidate the interaction of cyanide with aurothiomalate, and reported that excess cyanide levels led to the sole production of $[\text{Au}(\text{CN})_2]^-$. Haddad *et al*¹¹⁰ detected trace levels of gold (I) as its cyano complex by ion-interaction reversed-phase HPLC. UV spectra of the dicyanoaurate give rise to peak maxima at 209.5, 228, and 239 nm¹¹¹.

Since cyanide forms such a stable complex with gold (I) and one, moreover, which is active in the UV region, in this work, the formation of dicyanoaurate, from aurothiomalate in the presence of excess potassium cyanide has been utilised to detect low, biologically relevant concentrations of gold (I) by reversed-phase HPLC with UV detection. An attempt to standardise the method is carried out with a view to its use on appropriate RA biological samples.

3.2 MATERIALS AND METHODS

3.2.1 Materials

The disodium aurothiomalate used was purchased from Rhone-Poulenc (Dagenham, Essex). All solvents were of HPLC grade and were purchased from BDH Chemicals (Poole, Dorset).

Chromatographic experiments were performed using a Philips PU 4100 liquid chromatograph pump in conjunction with a Philips PU 4110 ultraviolet/visible detector. Electronic absorption spectra were recorded on a Philips PU 8740 ultraviolet/visible scanning spectrophotometer. Standard quartz cells (1.0 cm³ pathlength) were used for these measurements.

3.2.2 Dithizone Experiments

The HPLC column used was a reversed phase C18 Spherisorb 5 ODS with an i.d. 4.5 mm and of a length of 250 mm. The solutes were introduced onto the column using a Rheodyne 7125 valve fitted with a 10 μ L injection loop. The absorbance of the emerging eluant was monitored at 450 nm. The mobile phase employed was 60:40 (v/v) acetonitrile (ACN) : citrate/acetate buffer. The citrate / acetate buffer was of a pH of 4.75 and contained sodium citrate of a concentration of 3.00×10^{-2} mol dm⁻³ and sodium acetate of a concentration of 2.72×10^{-2} mol dm⁻³. The flow rate was 1.00 ml/min unless otherwise stated.

The signal from the photometric detector was recorded on a ChemLab CH-4002 chart recorder. The chart speed was normally 0.5 cm/min unless otherwise stated. A full scale deflection of 10 mV was generally employed.

3.2.2.1 Spectrophotometric Titration of Dithizone with Disodium Aurothiomalate

The reaction of the dithizone with disodium aurothiomalate was followed by means of a spectrophotometric titration. A standard solution of dithizone (5.00×10^{-5} mol dm⁻³) was prepared in the mobile phase (60:40 (v/v) acetonitrile: citrate/acetate (pH 4.75)). To 2.00 mL of the dithizone solution, ten successive 50.0 μ L

aliquots of disodium aurothiomalate ($5.00 \times 10^{-5} \text{ mol dm}^{-3}$) were added. After the addition of each aliquot, a UV spectrum was run in overlay mode, scanning from 230-670 nm. The final ratio of dithizone to disodium aurothiomalate was 4:1.

3.2.2.2 Extraction of Au (I) with Dithizone

An aqueous stock solution of disodium aurothiomalate containing $1.00 \times 10^{-3} \text{ mol dm}^{-3}$ gold was prepared in degassed sodium hydroxide ($1.00 \times 10^{-2} \text{ mol dm}^{-3}$). By serial dilutions a series of aurothiomalate standard solutions at concentrations of 5.0, 10.0, 25.0, 50.0, 100.0, 250.0, and $500.0 \times 10^{-6} \text{ mol dm}^{-3}$ were also prepared in $1.0 \times 10^{-2} \text{ mol dm}^{-3}$ NaOH. The aqueous aurothiomalate standard solutions (1.00 ml) were added to equal volumes of dithizone prepared in chloroform ($1.00 \times 10^{-3} \text{ mol dm}^{-3}$). The dithizone solution was initially dark green in colour. The two layers which formed were rotamixed for 20 minutes in glass stoppered test tubes. In the lower (chloroform) layer, a gradual colour change from dark green to deep red was noted. At high aurothiomalate concentrations the chloroform layer was deep red in colour and at low aurothiomalate concentrations the chloroform layer remained virtually unchanged in colour (dark green). This procedure was carried out with the addition of a further two 1.00 mL aliquots of dithizone to the aurothiomalate solution. The combined chloroform layers (total volume 3.00 mL) were evaporated to dryness under an atmosphere of nitrogen at ambient temperature. The residue was then reconstituted in $500.00 \mu\text{L}$ of the mobile phase and injected onto the column. Reconstituted samples with a high gold (I) concentration were yellow in colour, whilst samples containing a large excess of dithizone were green.

A control sample was prepared by the same method, where sodium hydroxide solution ($1.0 \times 10^{-2} \text{ mol dm}^{-3}$) was used instead of the disodium aurothiomalate standard solutions.

3.2.2.3 Dithizone Spectrophotometric Results

The spectrum of the dithizone solution displays two major peaks; one at 474 nm and one at 596 nm (Figure 3.2, page 84). The presence of these two absorption bands in the spectrum of dithizone points to the existence of two tautomeric forms; the thione form (λ_{max} 596 nm) and the thiol form (λ_{max} 474 nm). The dithizone solution probably contains the thiol and thione forms in a tautomeric equilibrium (Figure 3.3).

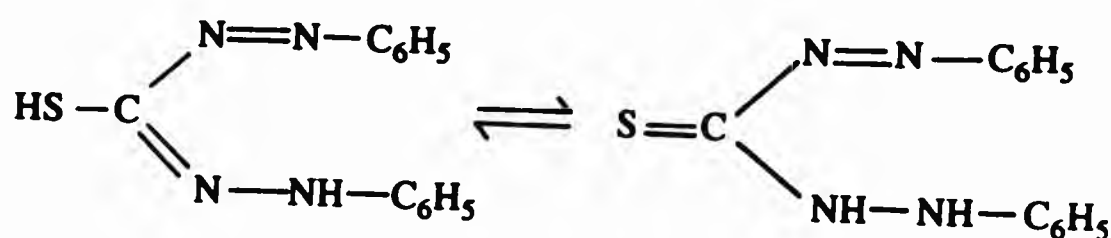
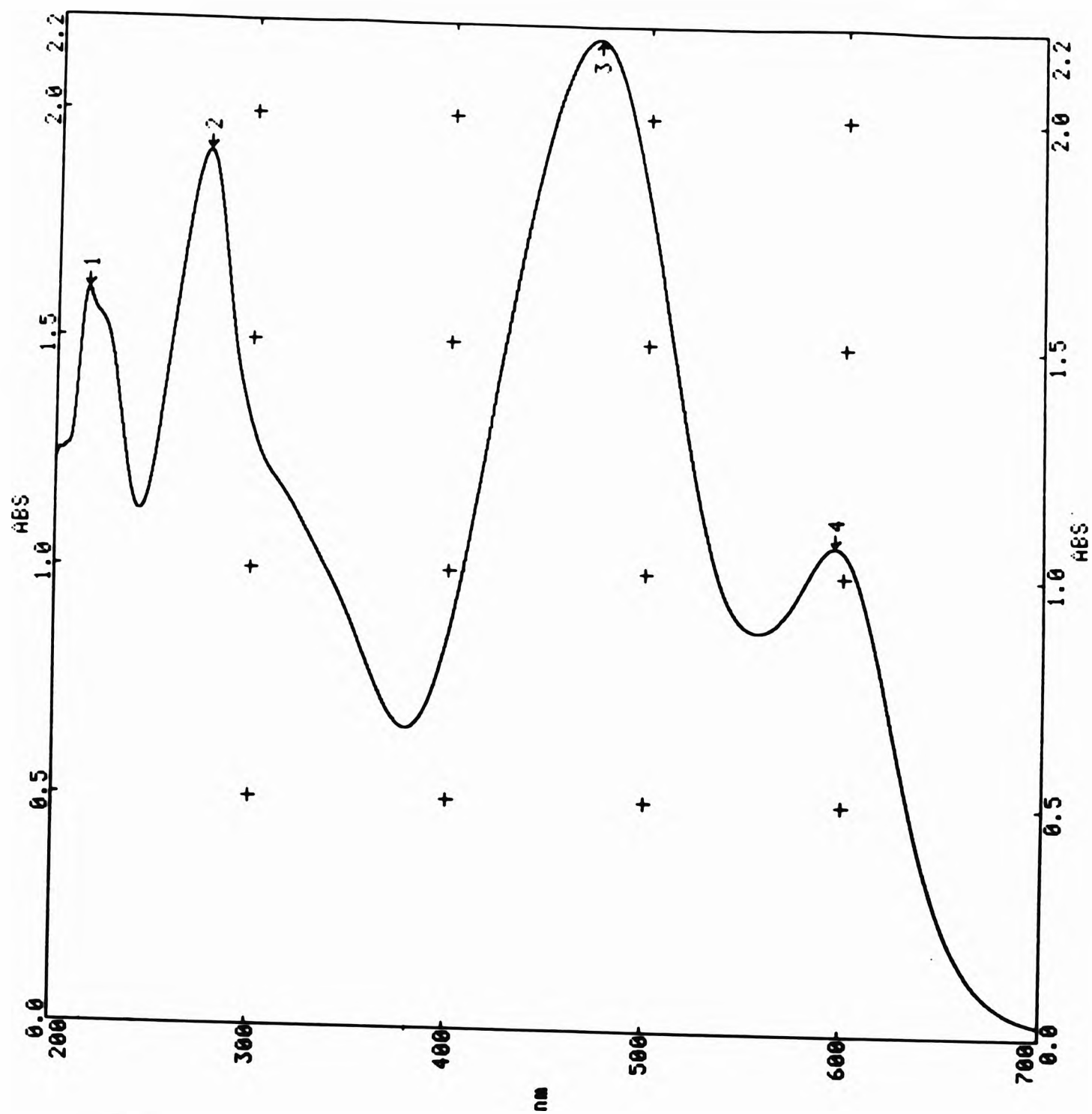


Figure 3.3 Tautomeric Equilibrium of Dithizone

Results of the spectrophotometric titration show that with the addition of each successive aliquot of disodium aurothiomalate the peak at 593 nm diminishes in intensity (Figure 3.4). At the final aliquot addition ($1.00 \times 10^{-5} \text{ mol dm}^{-3}$ aurothiomalate, $4.00 \times 10^{-5} \text{ mol dm}^{-3}$ dithizone) the peak at 593 nm due to the thione form nearly disappears (Figure 3.5), indicating the complete conversion of dithizone from its thione to its thiolate form. The peak at 466 nm is seen to shift to a lower wavelength of 443 nm.



1 DITHIZONE		1	2	3	4
λ		215.9	276.1	473.6	595.7
ABS		1.604	1.913	2.173	1.066

Figure 3.2 UV Spectrum of Dithizone

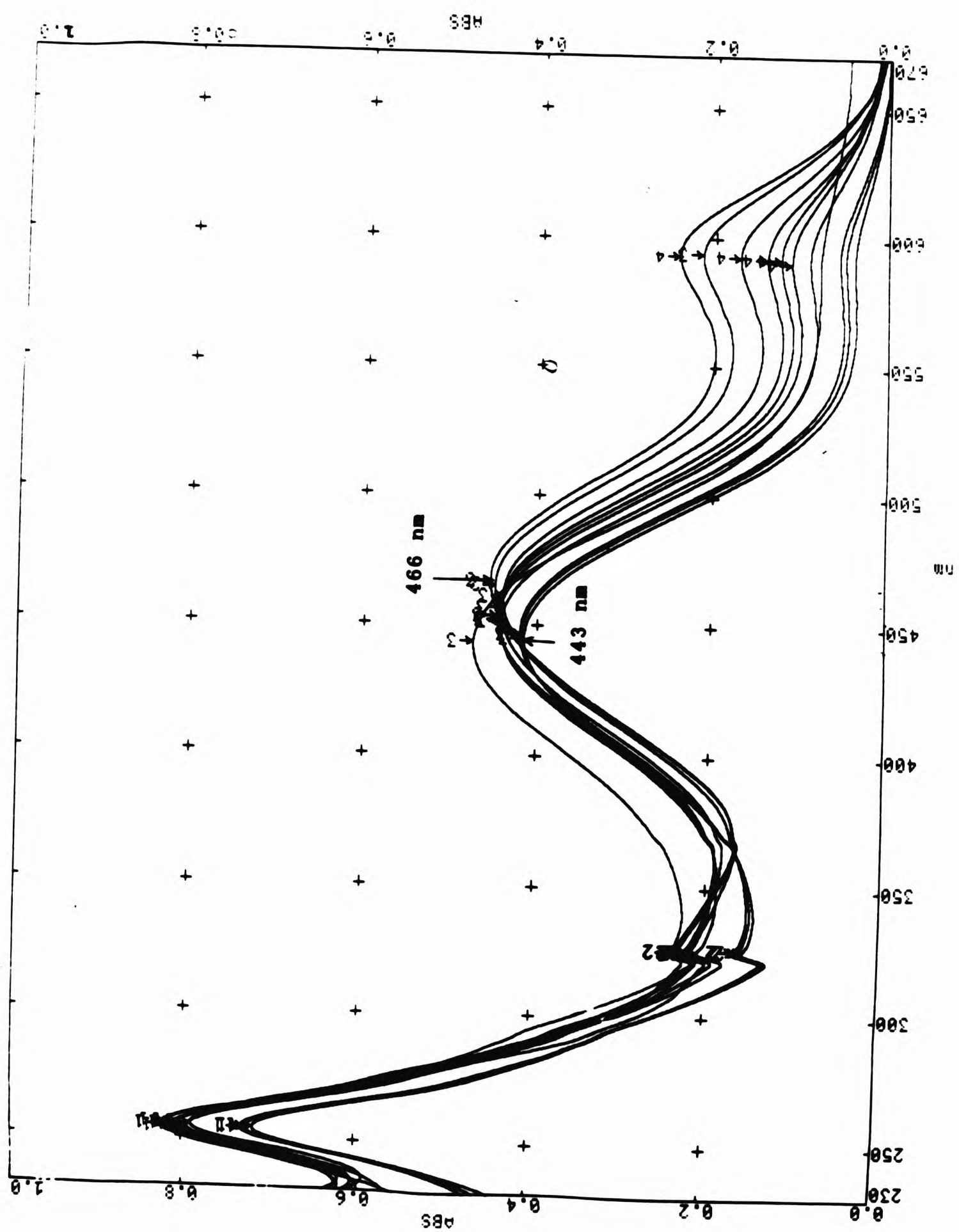
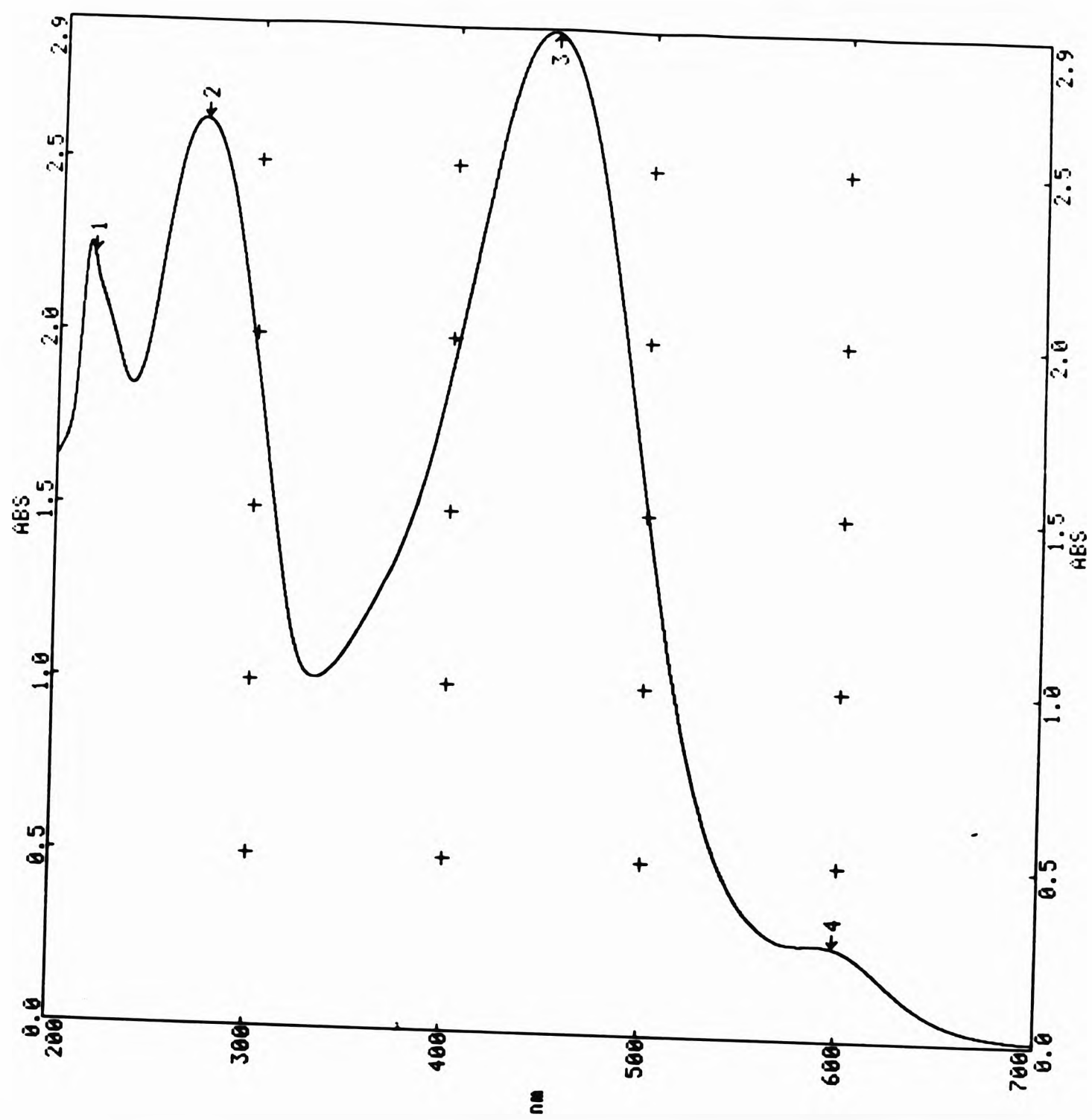


Figure 3.4 UV Spectrophotometric Titration of Dithizone with Disodium Aurothiomalate



1 Au DITHIZONE				
	1	2	3	4
λ	217.4	272.2	449.4	598.6
ABS	2.222	2.618	2.892	0.269

Figure 3.5 UV Spectrum of Gold [I] Dithizonate

It can therefore be concluded that the gold (I) must be interacting with the thiol or secondary tautomeric form in which the hydrogen of the sulphhydryl group, as well as the hydrogen of the imide group is replaced by the metal (Figure 3.6).

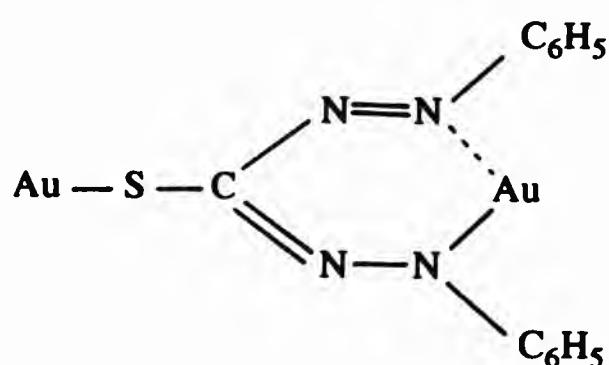


Figure 3.6 Structure of Gold Dithizonate

3.2.2.4 Dithizone HPLC Results

In the preliminary chromatography work, two peaks were detected by the on-line UV/vis detector at 450 nm (Figure 3.7B) The average retention times of the peaks were $t_R = 3.6$ minutes and $t_R = 4.6$ minutes. The control solution (A) (prepared without disodium aurothiomalate) gave rise to only one eluting solute peak at $t_R = 3.6$ minutes (Figures 3.7A and 3.8). This peak can therefore be assigned to dithizone. As the peak eluting at $t_R = 4.6$ minutes increased in height with increasing disodium aurothiomalate concentrations, it can be concluded to be due to the formation of the gold (I) dithizonate complex (B). No peaks were detected on injecting a solution of disodium aurothiomalate alone.

2-mercaptosuccinic acid was added to the reaction mixtures of disodium aurothiomalate and dithizone to investigate its effect on the gold dithizonate complex formation. The resulting peak, attributable to the metal dithizonate complex, was seen to be noticeably diminished in the presence of the 2-mercaptosuccinic acid (Figure 3.7C). The presence of the acid within the reaction

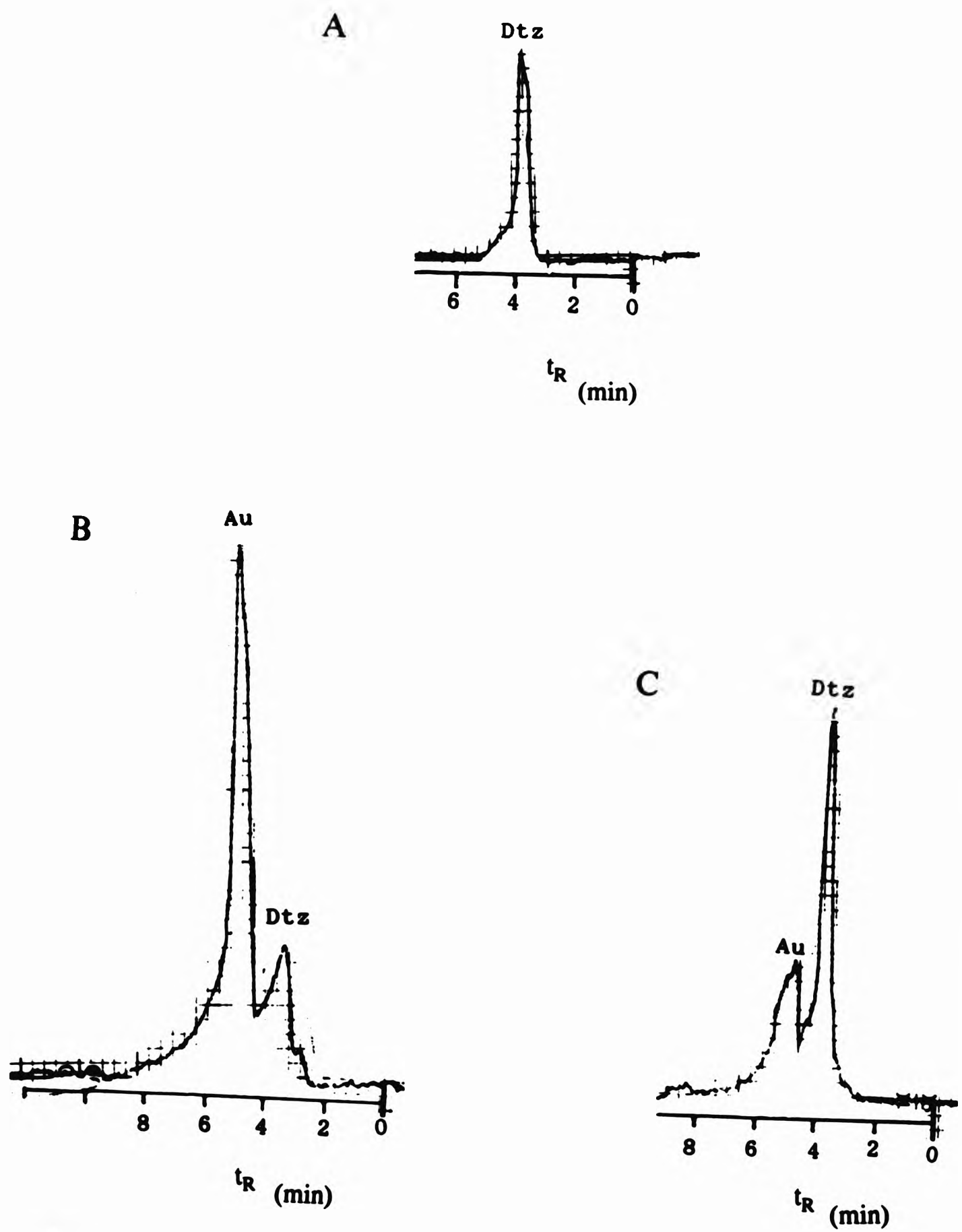


Figure 3.7 A) Chromatogram of Control Sample where Dithizone is Extracted without the Presence of Disodium Aurothiomalate. B) Chromatogram of Disodium Aurothiomalate Extracted in the Presence of Excess Dithizone. C) Chromatogram of Disodium Aurothiomalate with Dithizone in the Presence of 2-Mercaptosuccinic Acid.

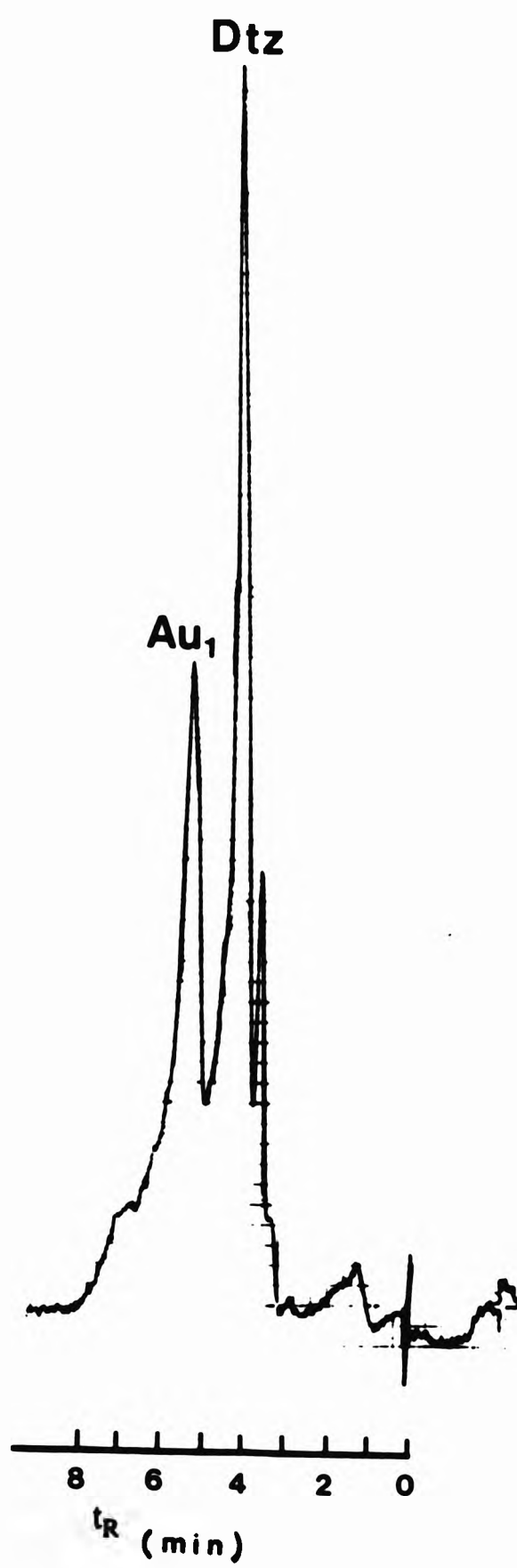
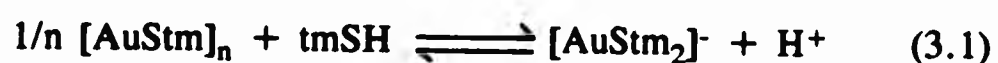


Figure 3.8 Chromatogram of Gold (I) Dithizonate Formed in the Presence of Excess Dithizone.

medium obviously suppressed the peak. This is attributable to the preferential interaction of the gold (I) in the disodium aurothiomalate with the 2-mercapto-succinic acid (thiomalate moiety) instead of the dithizone (Equation 3.1).



It was noticed that the gold dithizonate peaks were neither stable nor reproducible. The complex was therefore unstable. The rate of formation of the extracted complex depends on the amount of gold present in the aqueous phase and the instability of the colour of the complex leads to errors in spectrophotometric analysis and detection¹¹². Dithizone is very sensitive to oxidation and the oxidation product formed, carbodiazone $\text{S}=\text{C}(\text{N}=\text{NAr})_2$ (which is insoluble in alkali), can be present as an impurity. For these reasons further work to standardise the HPLC gold dithizone method was abandoned. Dithizone was deemed to be an unsuitable reagent with which to complex gold (I) for purposes of detection and quantification by HPLC.

3.3 FORMATION OF GOLD CYANIDE

3.3.1 Materials

The potassium dicyanoaurate was obtained from Fluka (Gillingham, Dorset) and resorcinol, potassium cyanide and potassium dihydrogen phosphate were purchased from Sigma Chemical Company. The HPLC column was a Techsphere 50DS (octadecyl silyl) column (i.d 4.5 mm, length 250 mm) purchased from HPLC Technology. All the other chemicals and instrumentation was as described in section 3.2.1.

3.3.2 Standard Curve of Potassium Dicyanide Obtained by Reacting Disodium Aurothiomalate with Potassium Cyanide

A reliable analytical method that can be used to detect low-molecular weight gold in biological fluids of rheumatoid arthritis patients undergoing gold therapy needs to be developed. For a successful HPLC method, a stable gold (I) complex that can be separated and absorbs well in the UV/vis region would be desirable. The formation of the complex potassium dicyanoaurate by addition of excess potassium cyanide to the gold drug disodium aurothiomalate was investigated for this purpose.

A UV spectrum of standard commercial potassium dicyanoaurate ($\text{KAu}(\text{CN})_2$) was run to record the absorbance maxima for the purpose of setting the HPLC UV detector at the optimum wavelength (Figure 3.9). Water was used as the blank. It was seen that there are 5 absorbance maxima at 196.5 nm, 204.3 nm, 211.1 nm, 229.9 nm and 239.2 nm. The maximum absorbance occurred at 211 nm and so the HPLC UV detector was set at this wavelength.

Standard solutions of disodium aurothiomalate of concentrations 10.0, 25.0, 50.0, 100.0 and 200.0 $\times 10^{-6}$ mol dm^{-3} were prepared, to each 1.0 mL aliquot an equal volume of 5.00×10^{-4} mol dm^{-3} of KCN was added. The mixtures were left for 40 minutes in a fume cupboard prior to injection on to the HPLC column. A control was set up by injecting separately a 1.00×10^{-4} mol dm^{-3} solution of disodium aurothiomalate, and then a 5.00×10^{-4} mol dm^{-3} solution of KCN.

With lower concentrations of aurothiomalate no peaks were seen in the chromatograms, therefore the sensitivity had to be increased. However the 10 fold increase in sensitivity, from $R = 0.1$ to $R = 0.01$, coupled with the low UV

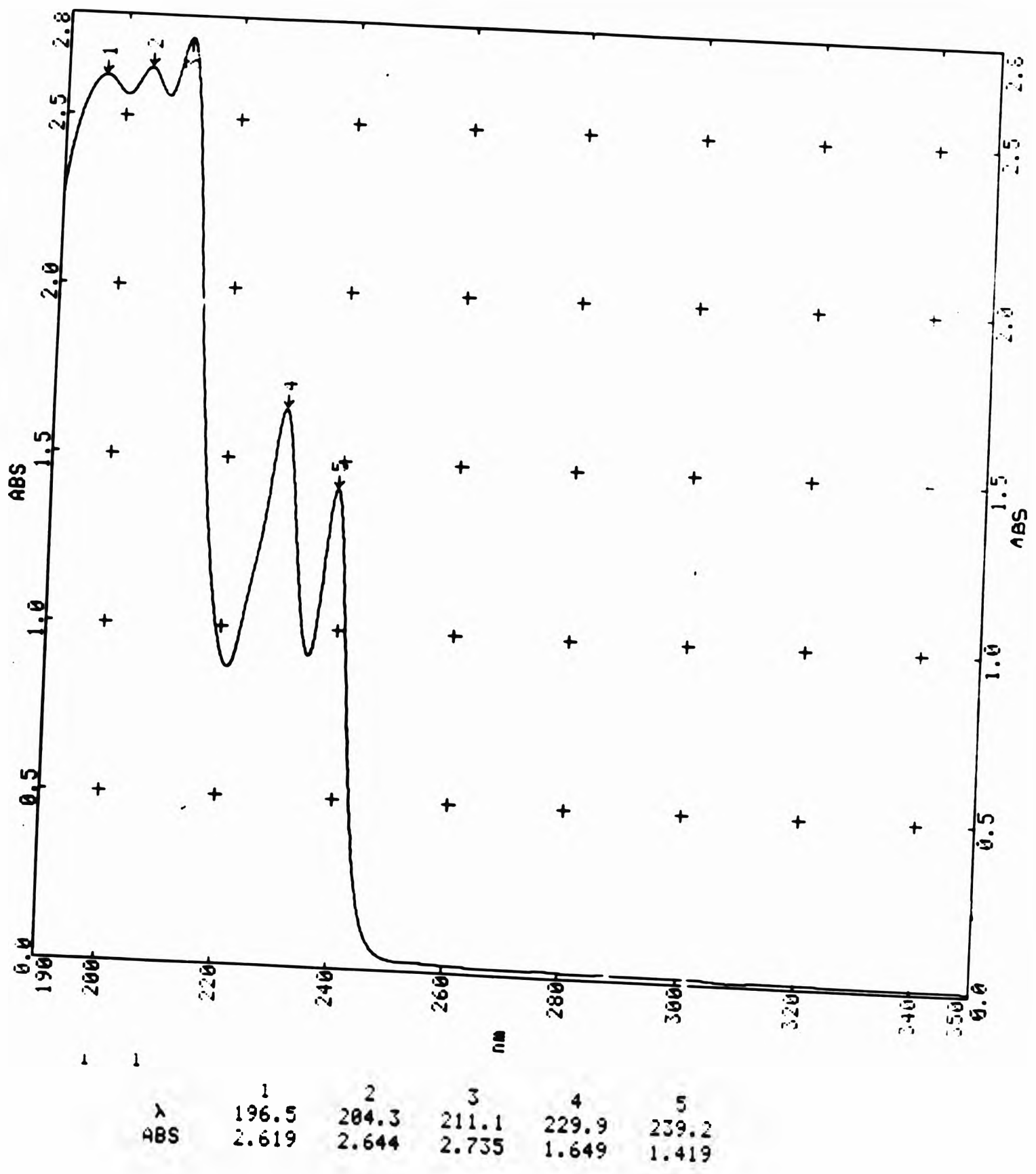


Figure 3.9 UV Spectrum of $5.00 \times 10^{-4} \text{ mol dm}^{-3}$ Potassium Dicyanoaurate (I).

wavelength gave rise to a very noisy baseline. The HPLC column had to be washed through with deionised water for 4 days to allow the baseline to become steady at the higher sensitivity. The mobile phase used was a 0.15 mol dm⁻³ potassium dihydrogen phosphate (pH 6.5) (KH₂PO₄). All the mobile phases used were degassed for 20 minutes prior to use. This was done mainly to prevent air bubbles forming within the column and also to expel oxygen as dissolved oxygen can lead to reaction and deterioration of the stationary phase as well as to the alteration of the sample components. The temperature of the column was kept as constant as possible at room temperature.

3.3.3 Chromatogram of a RA Blood Serum Ultrafiltrate Sample

Before finding an appropriate internal standard, a chromatogram of a rheumatoid arthritis blood serum ultrafiltrate sample needed to be run in order to see where all the major peaks (components) would elute. This was necessary to make sure that the chosen internal standard would elute in a gap in the biological chromatogram and not be masked by any major biological components.

The blood serum samples were obtained from the Royal London Hospital Medical College from rheumatoid arthritis patients. The samples were kept frozen at -34°C until they were ready for use. The serum was allowed to thaw out at room temperature and then 1.00 mL of it was pipetted into an ultrafiltration device. The ultrafiltration device was a centrifree micropartiton system manufactured by Amicon (Stonehouse, Gloucestershire). The sample was then centrifuged at 2000 g for 30 minutes. The micropartition device works on the principle that the biological sample is filtered through a anisotropic, hydrophilic ultrafiltration

membrane by the pressure provided by centrifugation. The membrane has a molecular weight cut-off of 30,000 so that only molecules with a molecular weight lower than that are allowed to pass through and are collected as the ultrafiltrate. As macromolecular molecules, proteins are prevented from passing through the membrane, so the collected ultrafiltrate is free from protein-bound ligands and contains only lower molecular weight molecules.

The rheumatoid arthritis blood serum ultrafiltrate was injected onto the HPLC column using the usual operating conditions. A representative chromatogram of serum ultrafiltrate is shown in figure 3.10. It is seen that nearly all the components in the serum ultrafiltrate have eluted after 16 minutes. Therefore the internal standard used needs to elute after this.

3.3.3 Obtaining an Internal Standard

In HPLC it is very important to have an internal standard, as it allows for fluctuations in operating conditions from sample to sample. An internal standard must meet several criteria; it must be spectrophotometrically active at the wavelength at which the UV detector is set, it has to be completely resolved and not be overlapping or masked by any other peak, it should not be present in the sample and should not react or interfere with the sample.

Known concentrations of the internal standard are chromatographed and a plot of peak area against concentration was set up. On chromatographing the unknown sample a known concentration of the internal standard is added to it. Therefore any variation in the sample size, or any temperature or pressure changes are

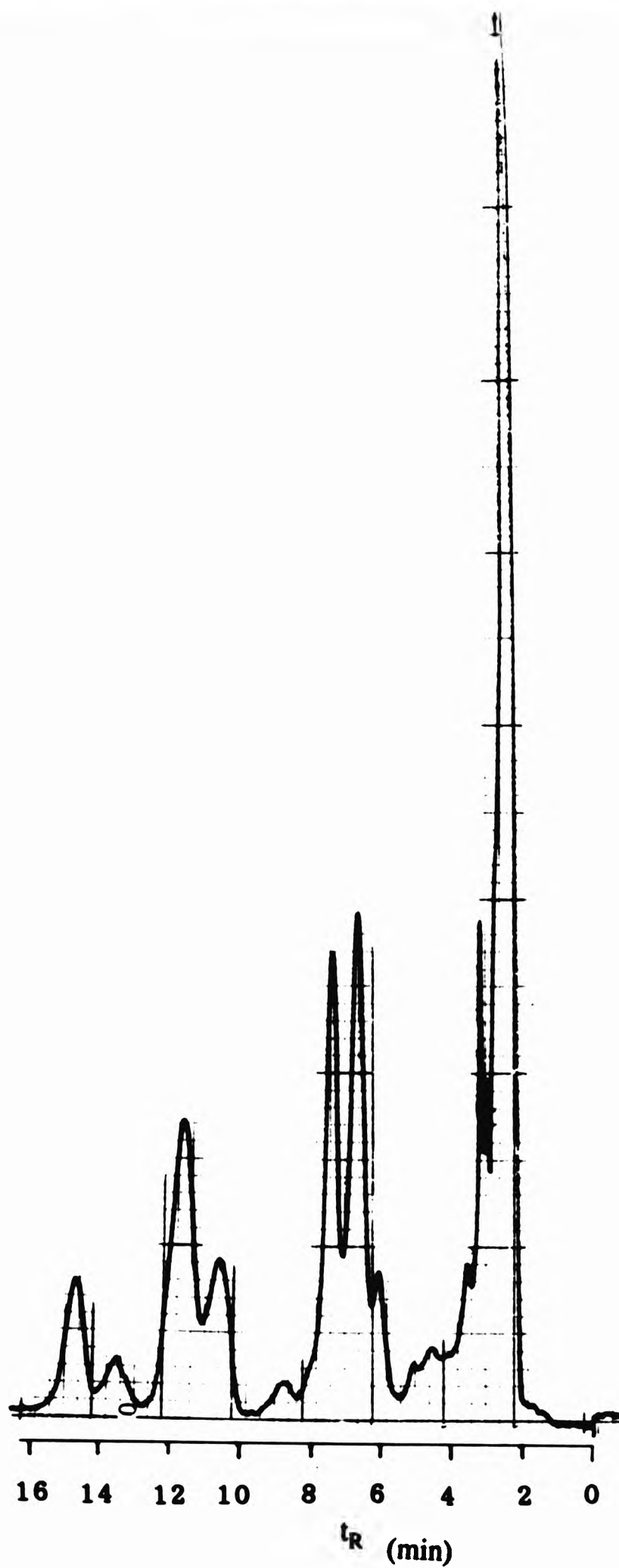


Figure 3.10 Reversed Phase HPLC Chromatogram of a Typical Blood Serum Ultrafiltrate Sample from a RA Patient. Mobile Phase $0.15 \text{ mol dm}^{-3} \text{ KH}_2\text{PO}_4$, Flow Rate: 1.0 ml/min , Detector Wavelength: 211 nm , Response Factor, R : 0.05 , Chart Speed: 0.5 cm/min .

immediately apparent by comparing the peak areas of the internal standard from run to run. A correction factor can therefore be applied on determining the concentration of unknown in the sample. Therefore when a standard curve of the sample is produced, the correction factor is applied by plotting the area of the unknown sample peak (A_x) divided by the area of the internal standard peak (A_{IS}) against concentration.

In this particular case, an internal standard was needed that eluted after the low-molecular weight components present in the biological fluid ultrafiltrate samples but that did not have too long a retention time. Various chemicals were tested for this purpose, some of which were not spectrophotometrically active at the desired wavelength of 211 nm. Caffeine and catechol were found to elute too soon and potassium ferrocyanide eluted with the solvent front at about $t_R = 1.8$ min. Quinol gave rise to a peak at $t_R = 8.0$ min which was not suitable since the compound of interest, potassium aurocyanide eluted at the same retention time. The aromatic aldehyde vanillin was found to have too long a retention time, eluting well after all the other components present in the ultrafiltrate. Rhodamine was found to have a suitable retention time of $t_R = 18.0$ min but it was deemed inappropriate for use as an internal standard as it reacts with gold. Finally the compound resorcinol (1,3-dihydroxybenzene), was injected and it gave rise to an eluting peak with an average retention time of $t_R = 16.0$ minutes, appearing after nearly all the biological fluid ultrafiltrate components have eluted, therefore making it suitable for an internal standard (Figure 3.11).

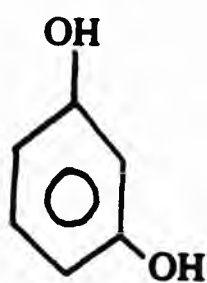


Figure 3.11 Resorcinol

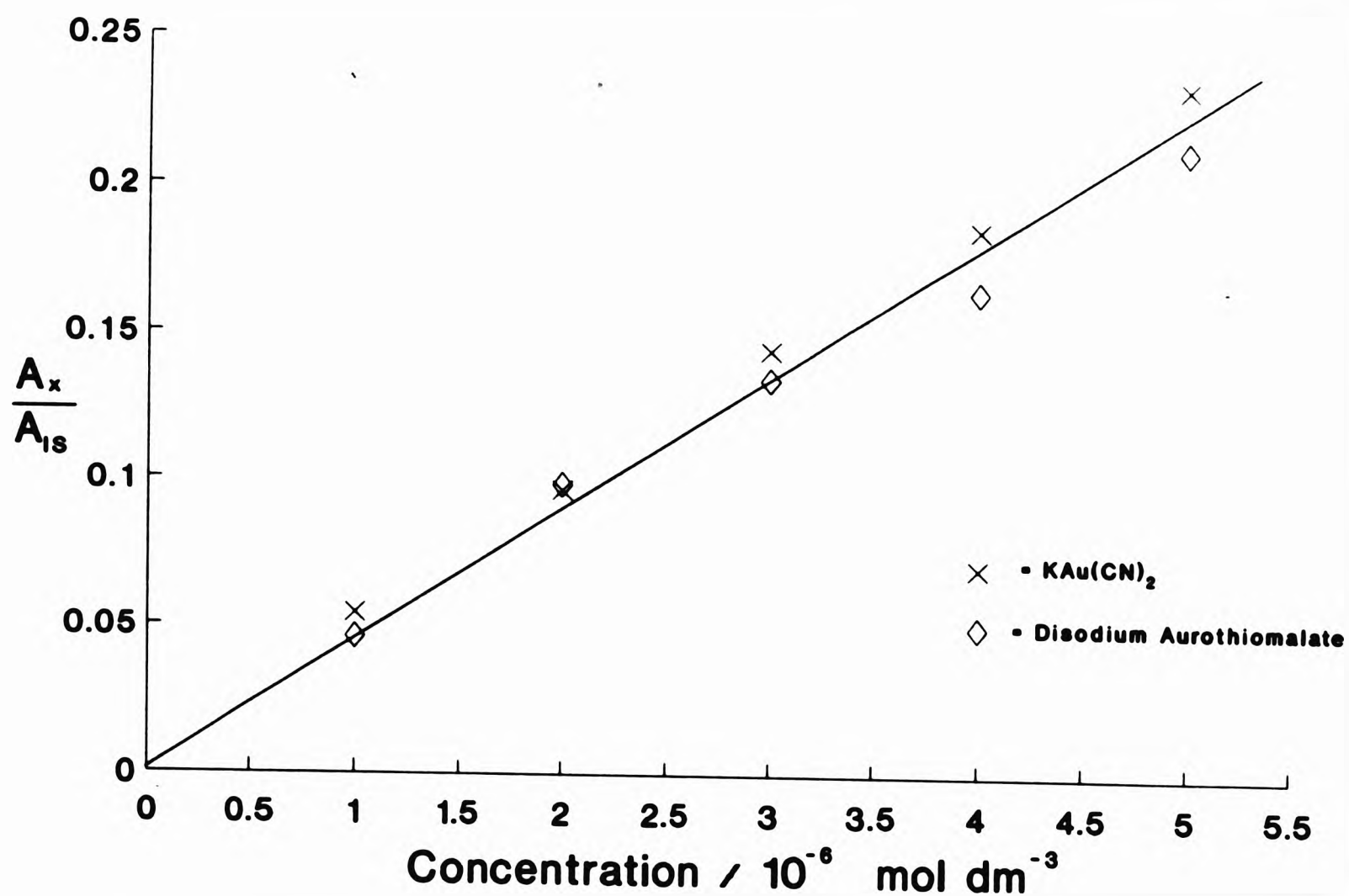
A standard calibration curve for resorcinol was set up by injecting concentrations of 2.0, 4.0, 5.0, 6.0, 7.0, 8.0 and 10.0 x 10⁻⁵ mol dm⁻³ into the HPLC column. The mobile phase used was 0.15 mol dm⁻³ KH₂PO₄.

3.3.4 Standard Curve of Potassium Dicyanoaurate with Resorcinol as Internal Standard

A working baseline was attained with the higher sensitivity of R = 0.01, therefore another potassium dicyanoaurate standard curve was constructed with lower concentrations more applicable to the level of "free" gold present in biological samples of RA patients undergoing chrysotherapy. Standard solutions of disodium aurothiomalate of concentrations 2.0, 4.0, 6.0, 8.0 and 10.0 x 10⁻⁶ mol dm⁻³ were prepared. 0.5 ml of potassium cyanide (0.5 x 10⁻⁴ mol dm⁻³) was respectively added to 0.5 ml of each aurothiomalate standard solution. The mixture was left for 30 minutes to allow the formation of potassium dicyanoaurate to go to completion. Resorcinol was then added to the mixture as an internal standard (final concentration 2.5 x 10⁻⁵ mol dm⁻³).

A standard curve of commercial potassium aurocyanide was also constructed with concentrations of 1.0 x 10⁻⁶ mol dm⁻³, 2.0 x 10⁻⁶ mol dm⁻³, 3.0 x 10⁻⁶ mol dm⁻³, 4.0 x 10⁻⁶ mol dm⁻³ and 5.0 x 10⁻⁶ mol dm⁻³, with resorcinol (final concentration 2.5 x 10⁻⁵ mol dm⁻³) included as the internal standard. The two standard curves obtained were very similar and the best straight line is drawn through them (Graph 3.1).

In the calibration graph below, the ratio of the HPLC peak area of potassium dicyanoaurate (A_x) compared with the internal standard area (A_{IS}), was plotted against concentration. The potassium dicyanoaurate peak was either produced by the addition of excess KCN to given concentrations of disodium aurothiomalate (\diamond), or by injection of commercially obtained potassium dicyanoaurate (\times). Both sets of results were plotted on the graph and one straight line was drawn (Beer's law assumed), as it is assumed that the concentration of disodium aurothiomalate is equivalent to the concentration of $\text{KAu}(\text{CN})_2$ formed in excess KCN.



Graph 3.1 Standard Calibration Graph for both Disodium Aurothiomalate and Potassium Dicyanoaurate.

3.4 RESULTS AND DISCUSSION

A clear peak at an average retention time of $t_R = 8.0$ minutes is seen (Figure 3.12). No peaks were seen to elute at 211 nm on injecting either potassium cyanide or disodium aurothiomalate on their own. These controls prove that the presence of the peak at $t_R = 8.0$ min is due to the formation of potassium dicyanoaurate on addition of excess cyanide to the gold drug disodium aurothiomalate. This was further verified by eluting a commercial solution of $\text{KAu}(\text{CN})_2$, which also exhibited a peak at $t_R = 8.0$ min. Indeed, on addition of commercial $\text{KAu}(\text{CN})_2$ to the cyanide-aurothiomalate mixture the peak was seen to increase in size, retaining its symmetry. This is known as "spiking" and is a common chromatographic tool for confirming suspected identity of an unknown compound and is very important method in qualitative HPLC analysis.

The linear complex ion $[\text{Au}(\text{CN})_2]^-$ is perhaps the most stable formed by gold (I), the stability constant has been estimated in aqueous solution as:



The metal-carbon bond strength in $[\text{Au}(\text{CN})_2]^-$ is high compared to other similar metal cyanides such as $[\text{Ag}(\text{CN})_2]^-$ and this is probably at least partially responsible for the overall stability constant for the formation of $[\text{Au}(\text{CN})_2]^-$.

It is therefore expected that the dicyanoaurate ion should form on addition of excess cyanide to the aurothiomalate (Autm) as has been previously reported¹¹³. When there is an equal 1:1 ratio of gold (I) to cyanide, intermediates such as $[\text{tmAuCN}]^-$ form. On addition of excess cyanide the thiomalate is displaced.

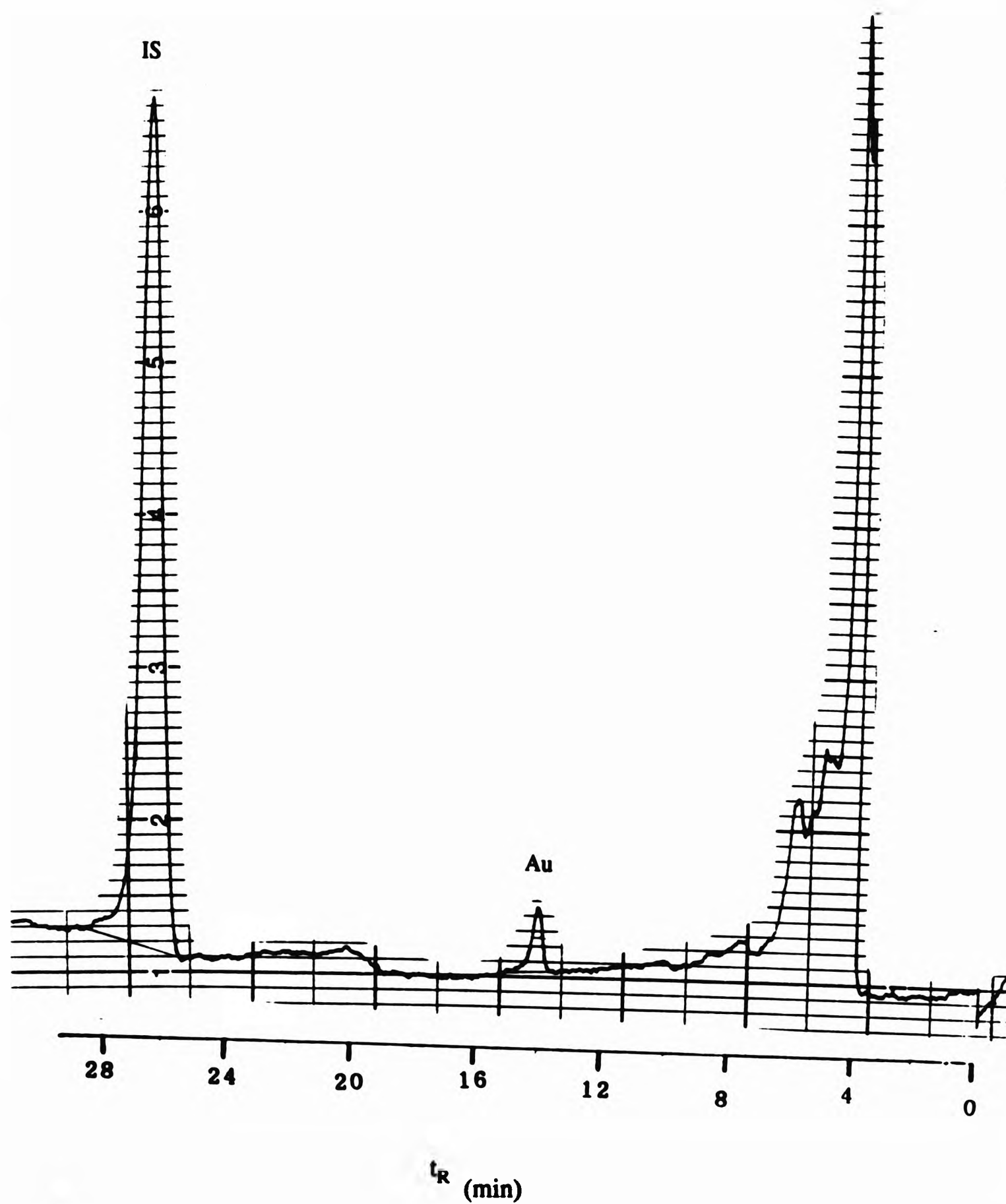
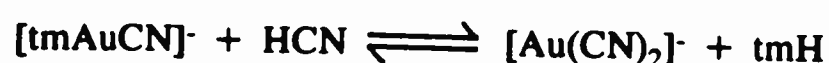
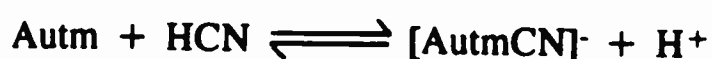


Figure 3.12 HPLC Chromatogram of $1.00 \times 10^{-6} \text{ mol dm}^{-3}$ Aurothiomalate Reacted with $1.25 \times 10^{-4} \text{ mol dm}^{-3}$ KCN and $2.50 \times 10^{-5} \text{ mol}$ Resorcinol (Internal Standard). Mobile Phase: 0.15 mol dm^{-3} Potassium Dihydrogen, Flow Rate: 1 ml/min , Detector Wavelength: 211 nm , Chart Speed: 0.5 cm/min , Response Factor: $R = 0.1$.



The peaks assigned to $[\text{Au}(\text{CN})_2]^-$ in the chromatogram were not detected at lower aurothiomalate concentrations at the first working sensitivity of $R = 0.1$. Since the levels of "free" gold generally encountered in blood plasma of patients undergoing treatment with disodium aurothiomalate is low, as it is approximately 5% of the total circulating gold⁴¹, a higher sensitivity needed to be achieved. The sensitivity was increased to $R = 0.01$ giving a noisy baseline but after equilibrating the column with water for a few days, a good working baseline was achieved. The standard curve for aurothiomalate was reconstructed at a lower and therefore more applicable concentration range. Sharp, symmetrical well resolved peaks were obtained down to a concentration of $1.0 \times 10^{-6} \text{ mol dm}^{-3}$. An example of the chromatograms obtained is seen in Figures 3.12-3.15. The standard curve for commercial $\text{K}[\text{Au}(\text{CN})_2]$ was reconstructed in the same concentration range. It can be seen that the slopes of the two curves are very similar. From this it can be concluded that virtually all the gold in the disodium aurothiomalate is being converted into the detectable potassium dicyanoaurate in the presence of excess cyanide. There is a very slightly greater response for commercial standard $\text{K}[\text{Au}(\text{CN})_2]$ than for the $\text{K}[\text{Au}(\text{CN})_2]$ formed from the disodium aurothiomalate at the same concentration.

To investigate how the formation of the $\text{K}[\text{Au}(\text{CN})_2]$ from action of excess cyanide on aurothiomalate alters with time, UV spectra at 211 nm were repeatedly run at increasing time intervals. The results can be seen from Figures 3.16a-h). The second derivative of the UV absorbance spectra was displayed in order that the intensities of the peaks could be followed at the exact peak maxima. It can be seen

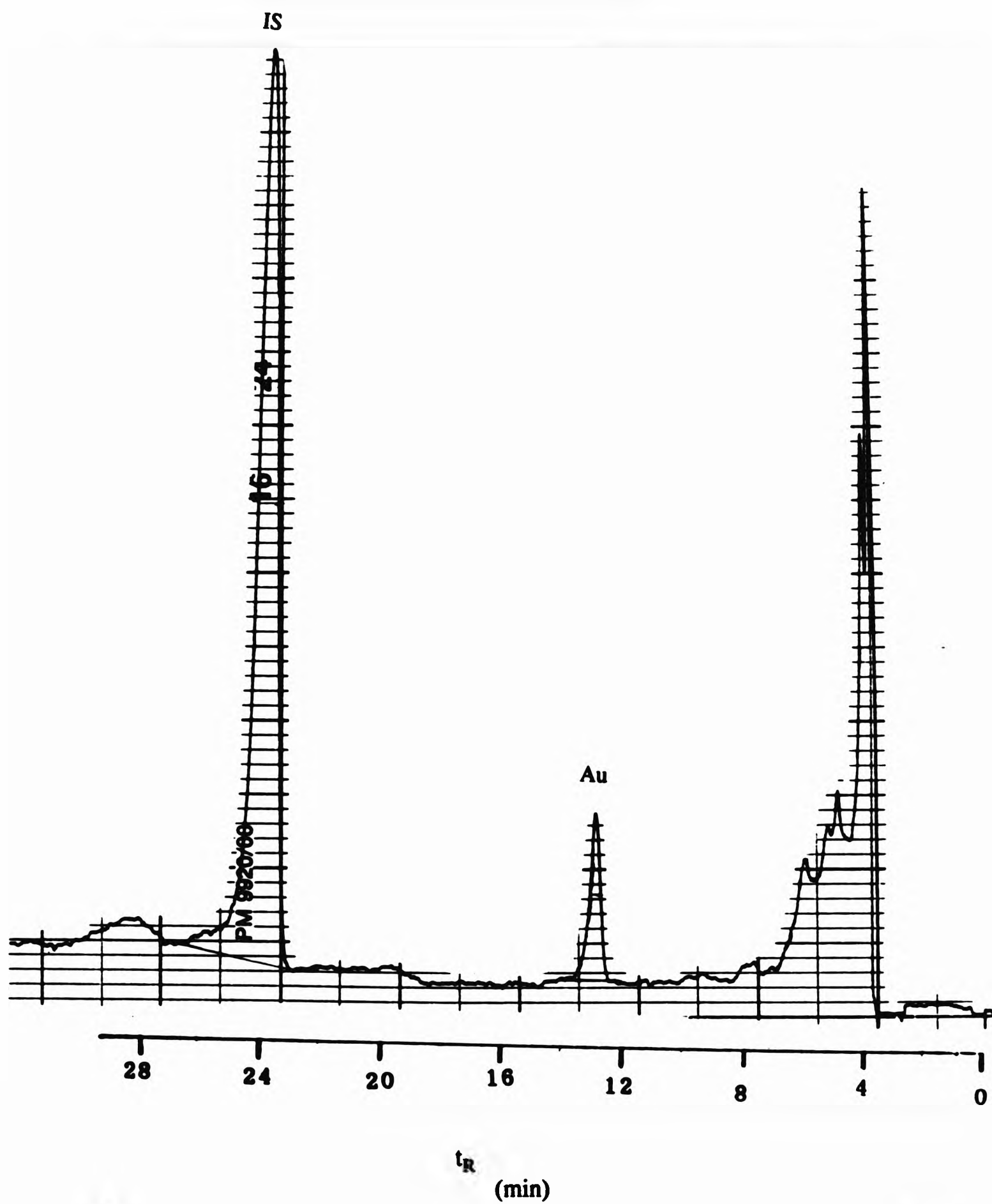


Figure 3.13 HPLC Chromatogram of $2.00 \times 10^{-6} \text{ mol dm}^{-3}$ Aurothiomalate Reacted with $1.25 \times 10^{-4} \text{ mol dm}^{-3}$ KCN and $2.50 \times 10^{-5} \text{ mol}$ Resorcinol (Internal Standard). Mobile Phase: 0.15 mol dm^{-3} Potassium Dihydrogen, Flow Rate: 1 ml/min, Detector Wavelength: 211 nm, Chart Speed: 0.5 cm/min, Response Factor: $R = 0.1$.

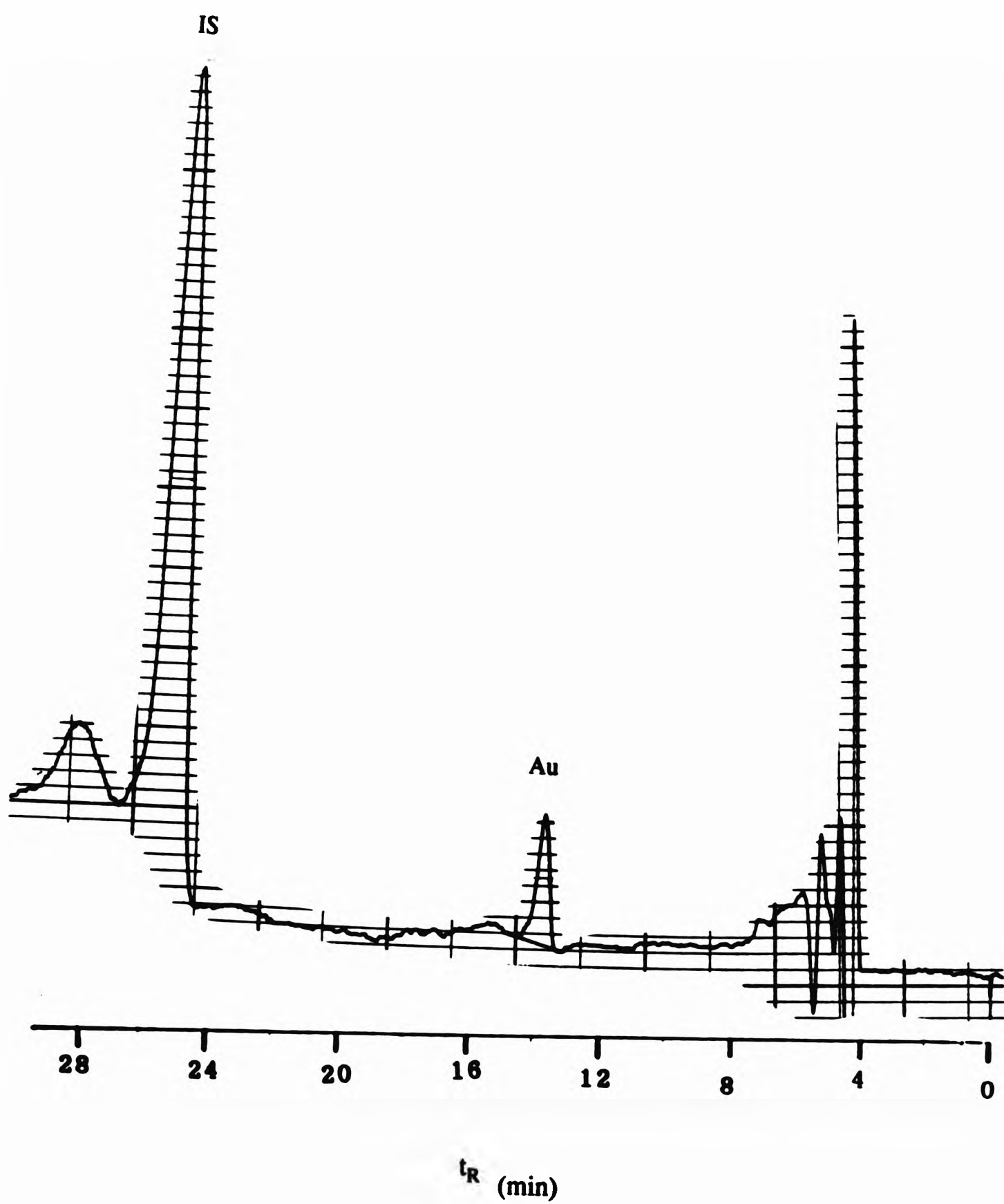


Figure 3.14 HPLC Chromatogram of 2.00×10^{-6} mol dm^{-3} Potassium Dicyanoaurate and 2.50×10^{-5} mol Resorcinol (Internal Standard). Mobile Phase: 0.15 mol dm^{-3} Potassium Dihydrogen, Flow Rate: 1 ml/min, Detector Wavelength: 211 nm, Chart Speed: 0.5 cm/min, Response Factor: $R = 0.1$.

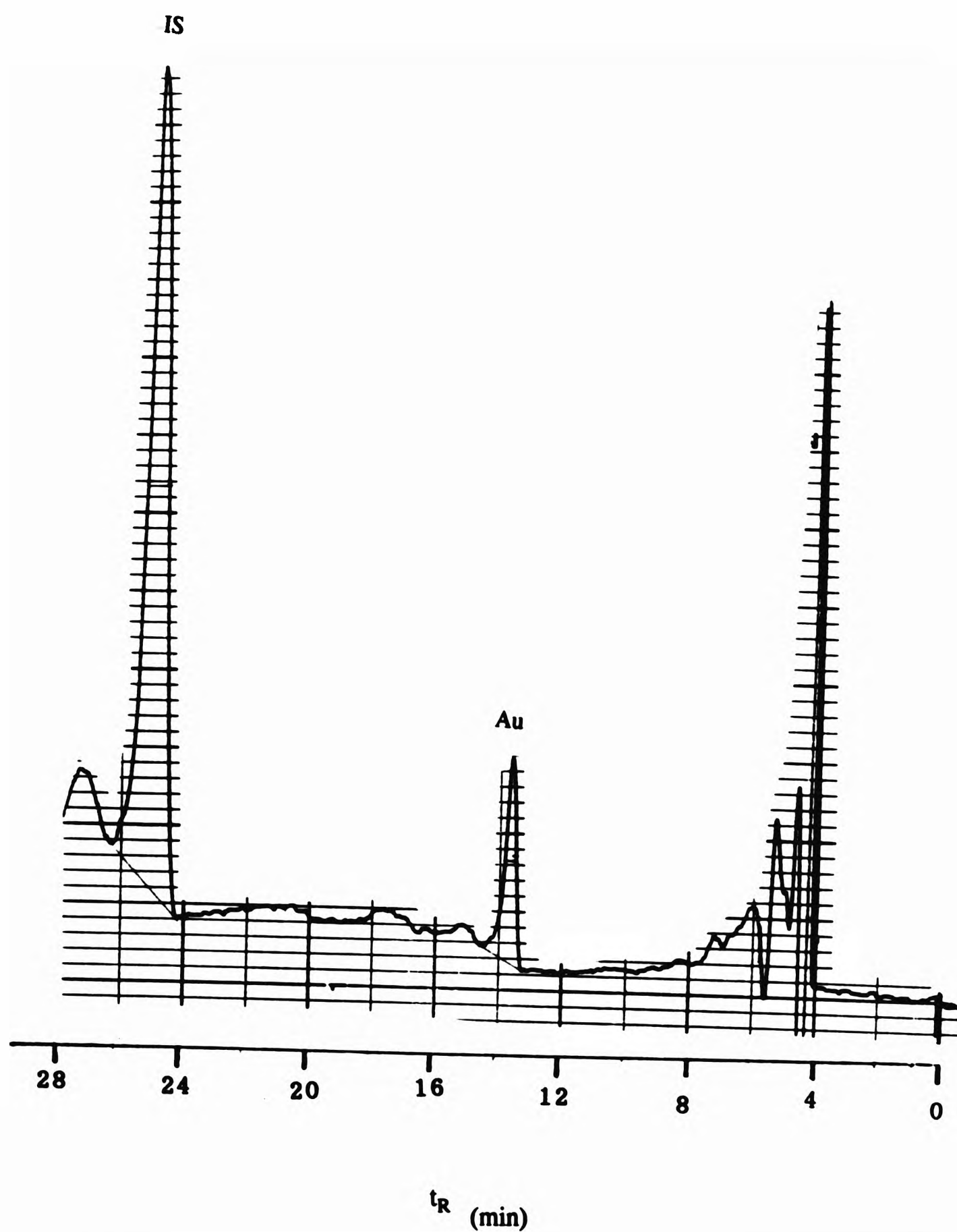
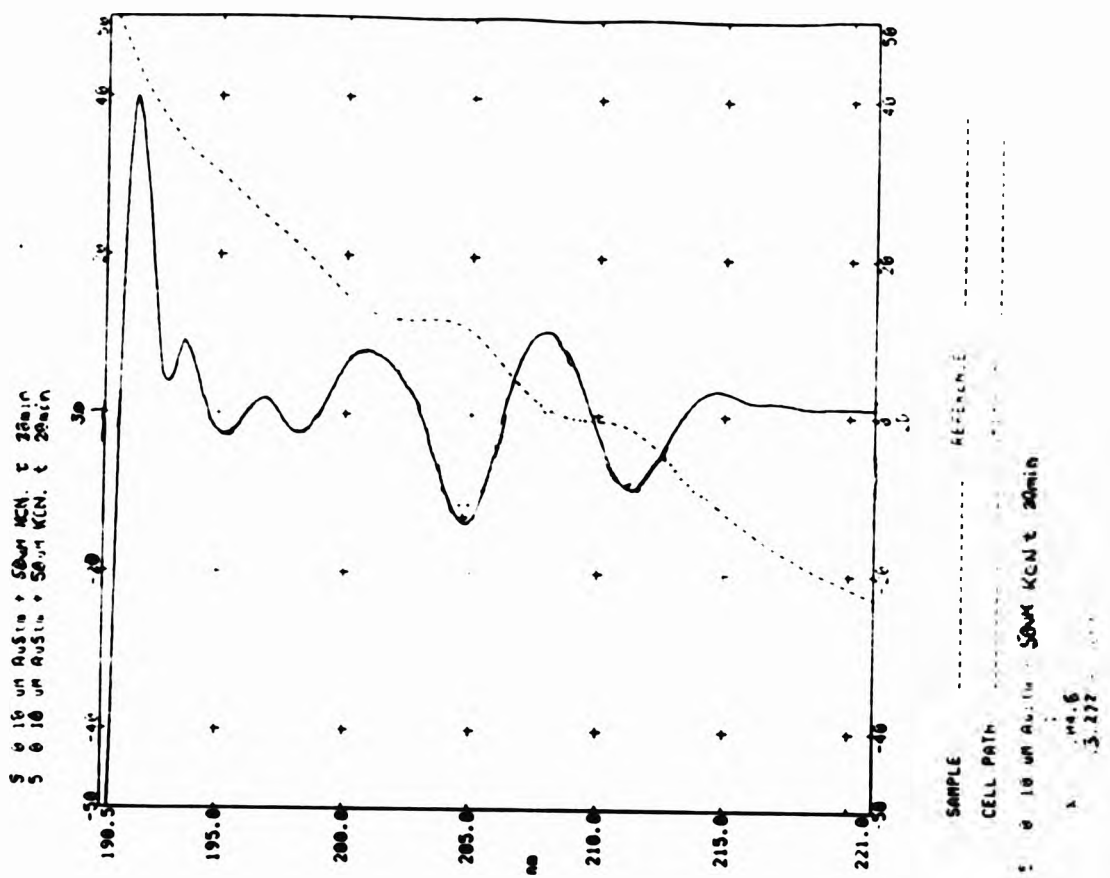


Figure 3.15 HPLC Chromatogram of $3.00 \times 10^{-6} \text{ mol dm}^{-3}$ Potassium Dicyanoaurate and $2.50 \times 10^{-5} \text{ mol}$ Resorcinol (Internal Standard). Mobile Phase: 0.15 mol dm^{-3} Potassium Dihydrogen, Flow Rate: 1 ml/min , Detector Wavelength: 211 nm , Chart Speed: 0.5 cm/min , Response Factor: $R = 0.1$.

a)



b)

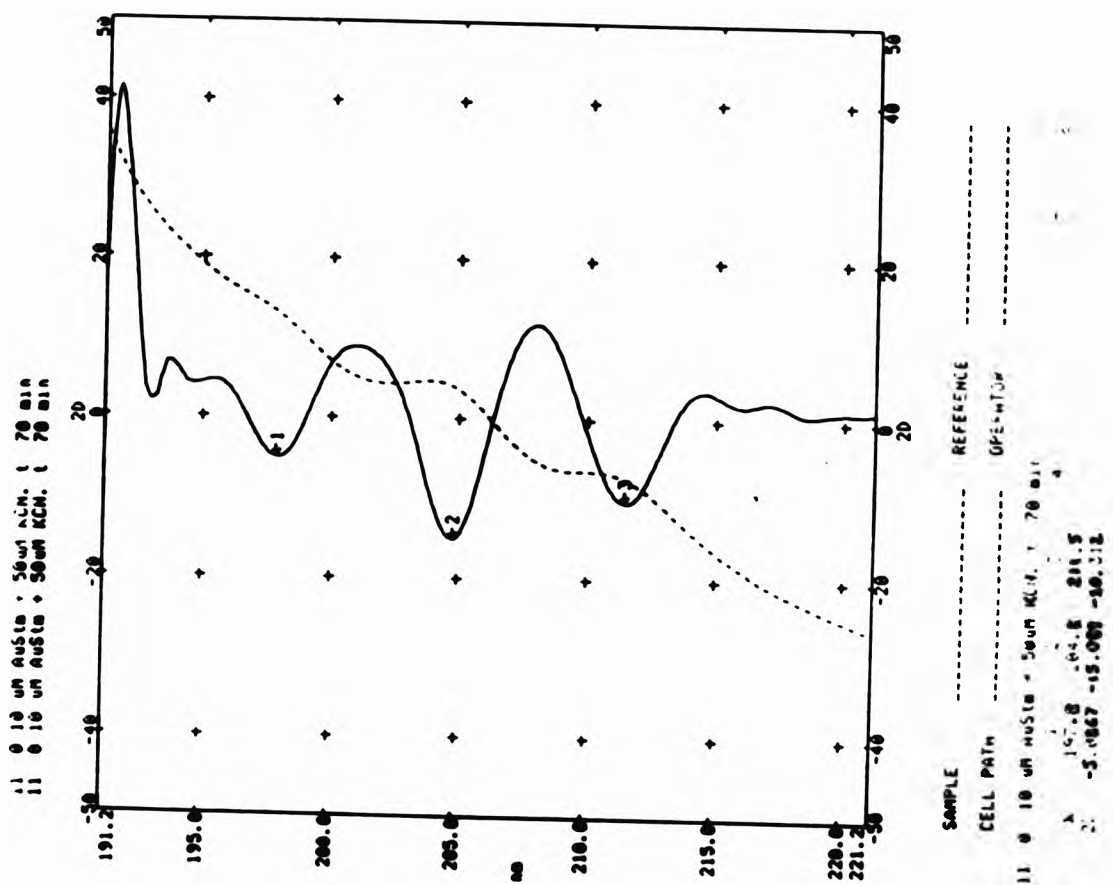
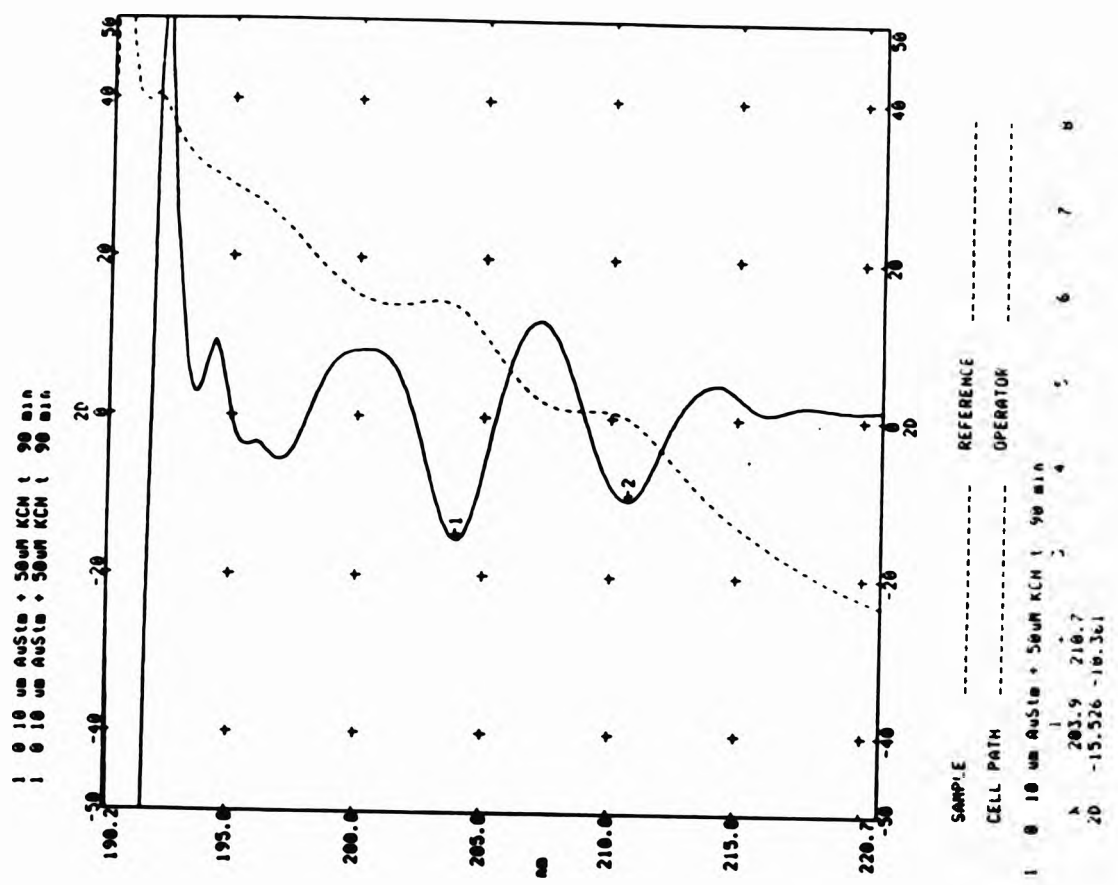
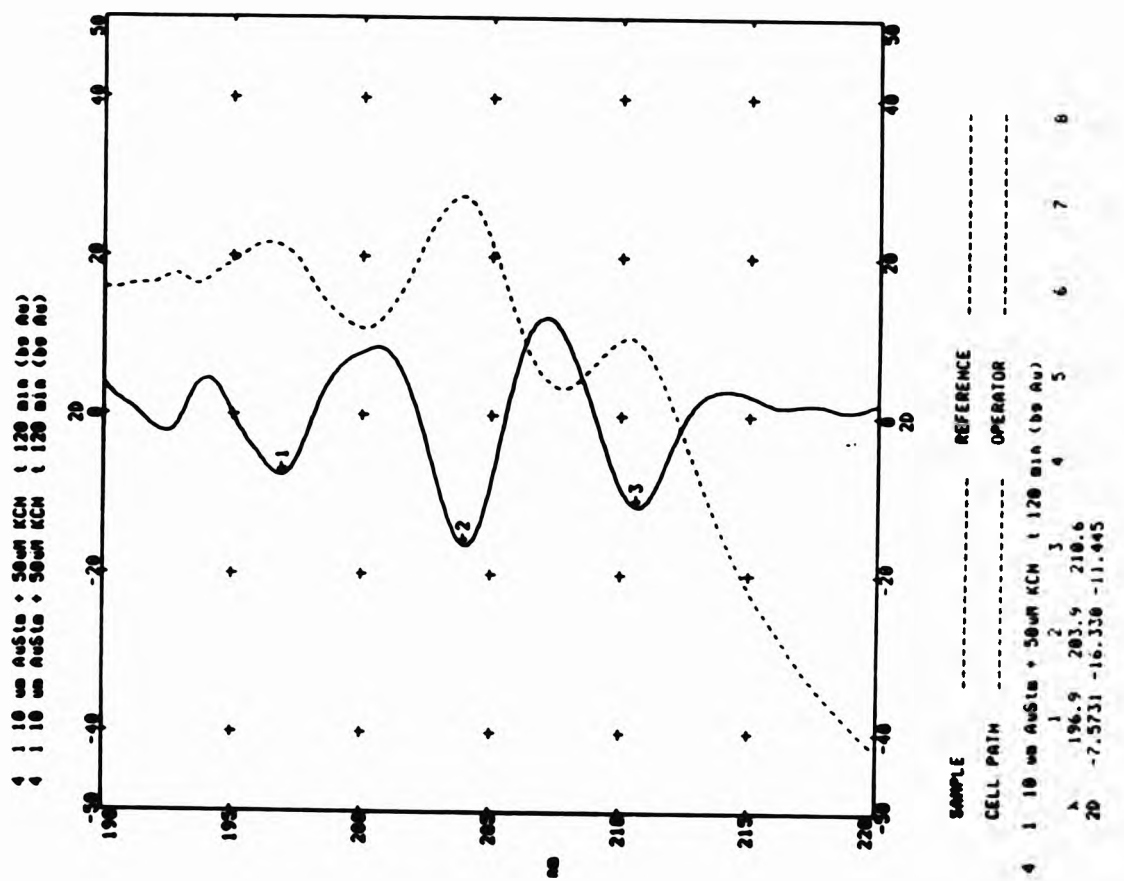


Figure 3.16a-h UV Spectra Showing how the Action of Excess Cyanide (5.00×10^{-6} mol dm $^{-3}$) reacted with Aurothiomalate (1.0×10^{-6} mol dm $^{-3}$) Changes with Time. a) After 20 mins b) After 70 mins.

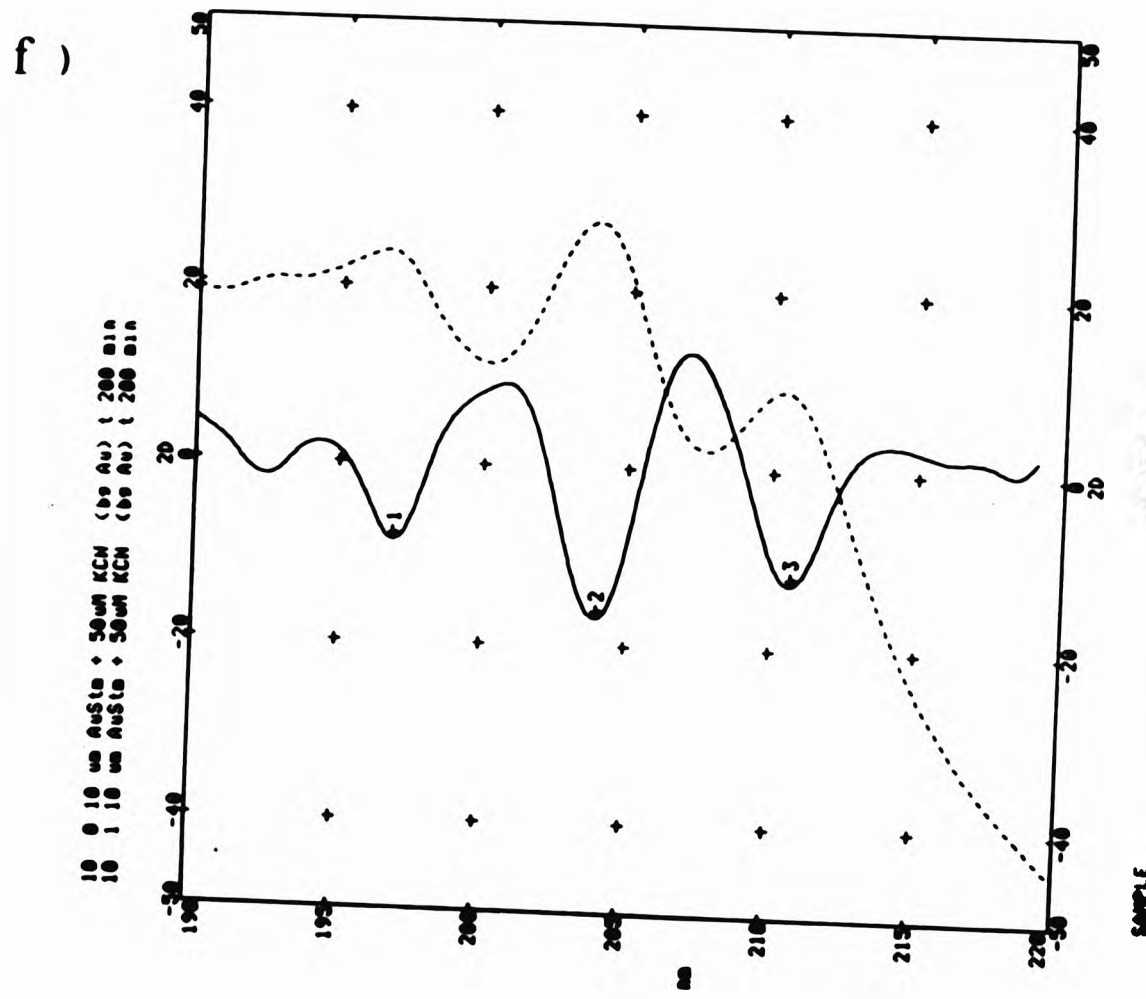
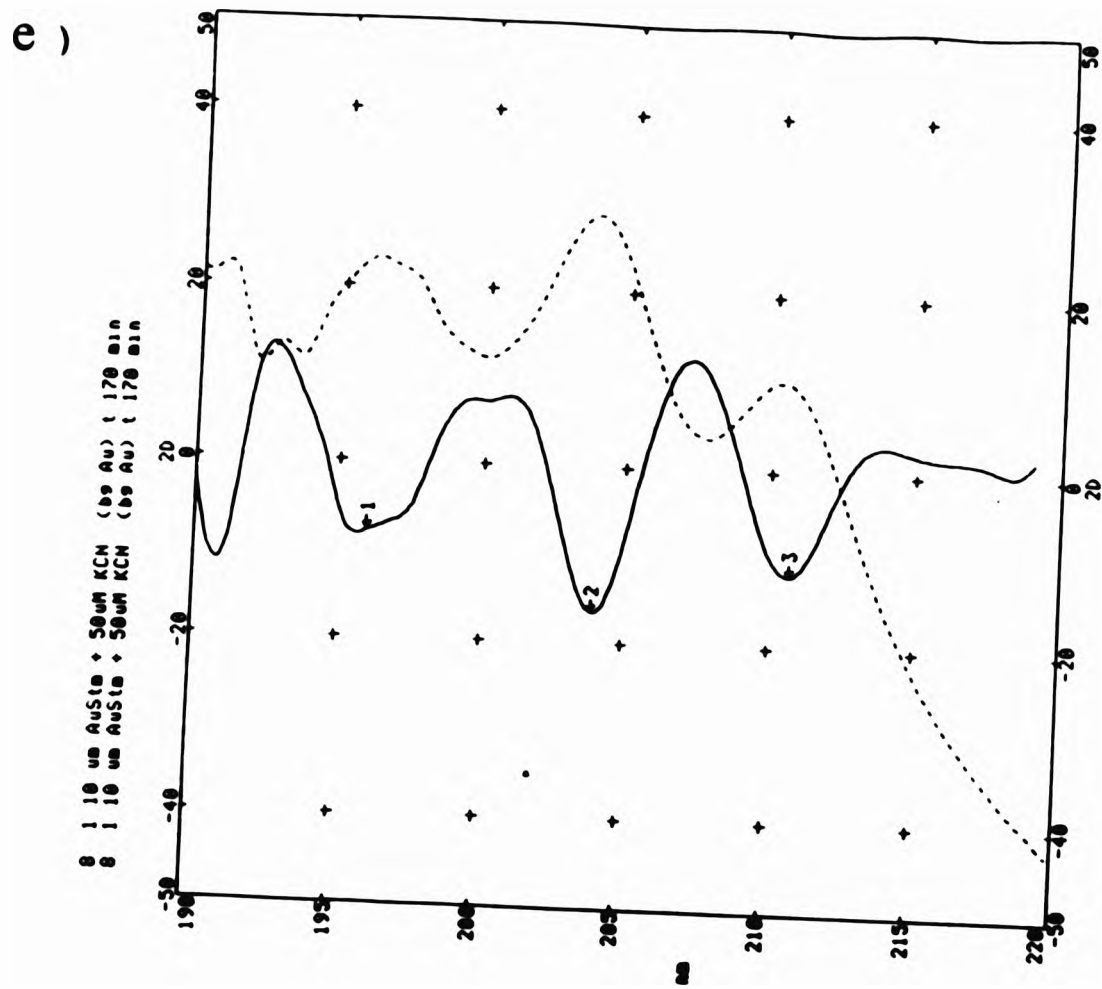
c)



d)

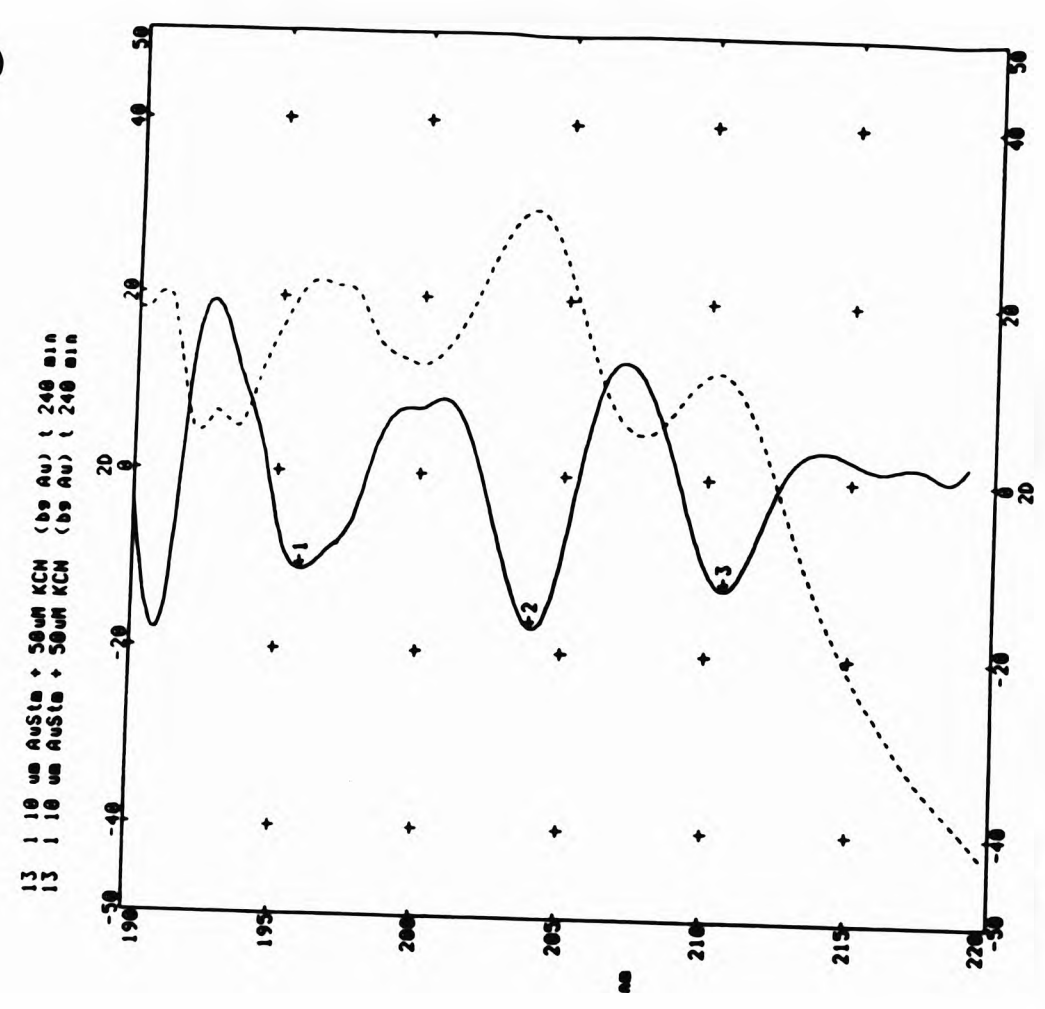


c) UV Spectrum After 90 mins and d) After 120 mins.

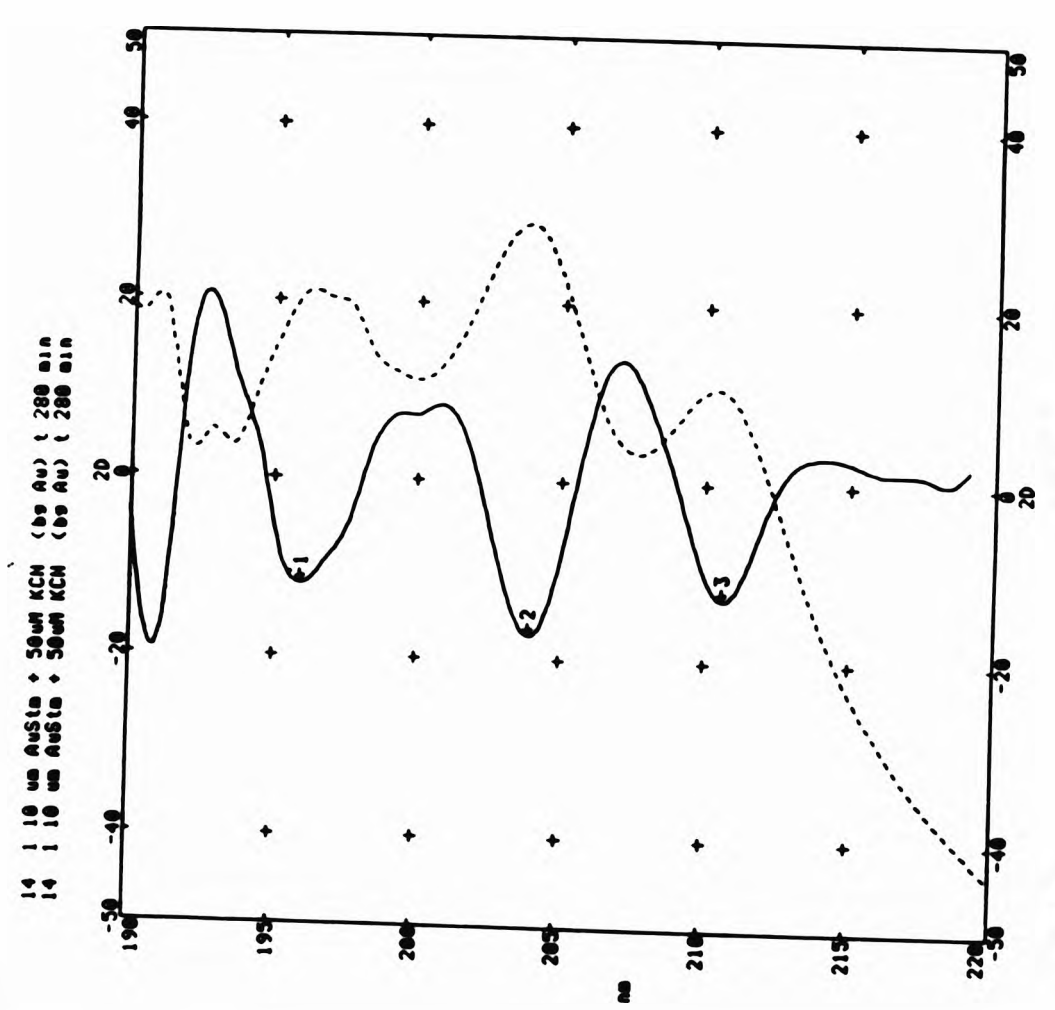


e) UV Spectrum After 170 min and f) After 200 mins.

g)



h)



g) UV Spectrum After 240 min and h) After 280 mins.

that the absorbance at 211 nm due to the formation of $K[Au(CN)_2]$ increases in intensity with time. The greatest increase occurs between 0-120 minutes after the addition of excess potassium cyanide. Since it is impractical to wait 120 minutes after the addition of cyanide before chromatographing the solution, a compromise is made and the mixture is left to react for 40 minutes before introduction onto the HPLC column. As can be seen a high sensitivity is achieved with the detection limit for $K[Au(CN)_2]$ at $1.0 \times 10^{-6} \text{ mol dm}^{-3}$. This is of a value at and below that which can be expected to be found in patients being injected with gold therapeutic agents ($1.5\text{-}4.0 \times 10^{-6} \text{ mol dm}^{-3}$).

3.5 CONCLUSION

For the purposes of detecting the low molecular weight "free" gold (I) present in rheumatoid arthritis patients undergoing chrysotherapy, the formation of the stable compound potassium dicyanoaurate, $K[Au(CN)_2]$, has been achieved by reacting the gold containing drug disodium aurothiomalate with excess potassium cyanide. The compound is formed almost instantaneously and is one of the most stable to be found in gold(I) chemistry. The peak for $K[Au(CN)_2]$ is clearly separated by HPLC and detectable at 211 nm by an on-line UV detector. A good standard curve is achieved with resorcinol as the internal standard, down to low concentrations, suitable for quantification of the "free" gold (I) in relevant biological samples.

The high sensitivity achieved and the stability of the formed compound make this method suitable for quantifying low molecular gold in ultrafiltrate biological samples obtained from RA patients undergoing chrysotherapy.

that the absorbance at 211 nm due to the formation of $K[Au(CN)_2]$ increases in intensity with time. The greatest increase occurs between 0-120 minutes after the addition of excess potassium cyanide. Since it is impractical to wait 120 minutes after the addition of cyanide before chromatographing the solution, a compromise is made and the mixture is left to react for 40 minutes before introduction onto the HPLC column. As can be seen a high sensitivity is achieved with the detection limit for $K[Au(CN)_2]$ at $1.0 \times 10^{-6} \text{ mol dm}^{-3}$. This is of a value at and below that which can be expected to be found in patients being injected with gold therapeutic agents ($1.5-4.0 \times 10^{-6} \text{ mol dm}^{-3}$).

3.5 CONCLUSION

For the purposes of detecting the low molecular weight "free" gold (I) present in rheumatoid arthritis patients undergoing chrysotherapy, the formation of the stable compound potassium dicyanoaurate, $K[Au(CN)_2]$, has been achieved by reacting the gold containing drug disodium aurothiomalate with excess potassium cyanide. The compound is formed almost instantaneously and is one of the most stable to be found in gold(I) chemistry. The peak for $K[Au(CN)_2]$ is clearly separated by HPLC and detectable at 211 nm by an on-line UV detector. A good standard curve is achieved with resorcinol as the internal standard, down to low concentrations, suitable for quantification of the "free" gold (I) in relevant biological samples.

The high sensitivity achieved and the stability of the formed compound make this method suitable for quantifying low molecular gold in ultrafiltrate biological samples obtained from RA patients undergoing chrysotherapy.

CHAPTER 4

**DEVELOPMENT OF AN ANALYTICAL METHOD FOR THE
DETECTION OF LOW MOLECULAR WEIGHT GOLD (I)
PRESENT IN BIOLOGICAL FLUIDS OF RHEUMATOID
ARTHRITIS PATIENTS UNDERGOING CHRYSOTHERAPY**

4.1 INTRODUCTION

As mentioned in the introduction, studies of the molecular pharmacology of gold drugs have established that both protein-bound and ultrafilterable (low-molecular weight) species of gold are found in blood plasma and synovial fluid following the parenteral administration of aurothiomalate^{38,39,114}. The fate of the gold between the time of administration and that of excretion is of primary importance in understanding the mechanism of gold (I) action in rheumatoid patients undergoing chrysotherapy. There is therefore a need to find an efficient, sensitive and selective analytical method for the study of gold (I) drugs *in vivo*.

A number of analytical methods have been used to monitor gold levels, both protein bound and non-protein bound in human blood plasma, using disodium aurothiomalate pre-labelled with ¹⁹⁵Au *in vitro*⁴⁰, and *in vivo*, using flame¹¹⁵ and electrothermal¹¹⁶ atomic absorption spectrometry, and neutron activation analysis¹¹⁷. Ward *et al*¹¹⁸ determined gold fractions by all three methods. Time consuming pre-treatment precluded all the analyses. Flame and electrothermal atomic absorption analysis was reported to give relatively low sensitivity, particularly in the measurement of the low-molecular weight gold (I) fractions. Flame atomic absorption requires large sample volumes and minimal dilution is required for a sensitive signal. Poor efficiency of the nebuliser-burner system was noted. Electrothermal atomic absorption suffers from matrix interference. Kamel *et al*¹¹⁹ determined blood serum gold levels in proteins separated by electrophoresis using carbon furnace atomic absorption spectrometry.

Work done by Rayner *et al*³⁹ involved the separation and detection of both protein bound and low-molecular weight gold species by a technique which incorporated a combination of fast protein liquid chromatography and eluant analysis by flame atomic absorption spectroscopy. The system was supplemented by continuous electronic absorption detection at 254 nm. Their results indicated that more than 50% of the gold is associated with a peak identified as serum albumin after a 5 minute incubation period and by 30 minutes more than 90% is found associated with the albumin. The FPLC method used in the Rayner analysis gave rise to broad peaks relative to analytical HPLC peaks. This in turn lessens the detection limits capable of being analysed.

The form in which a drug circulates invariably influences its biological effect and it has been shown that for many drugs the unbound fraction is of prime importance¹²⁰. With the administration of aurothiomalate, the relatively low levels of non-protein bound, low-molecular weight gold (I) present in plasma and synovial fluid are likely to play an important role in the attainment of an equilibrium of gold amongst the protein binding sites and hence be of vital importance in the understanding of the drug action itself. For this reason a rapid, highly sensitive and selective methodology needs to be developed to measure the low levels of non-protein bound gold in blood plasma and synovial fluid of rheumatoid arthritis patients undergoing gold (I) thiolate therapy. The HPLC method developed in Chapter 3 was employed to measure the low-molecular gold fraction of the biological fluids after removal of protein-bound gold moieties by use of an ultrafiltration device. Atomic absorption spectrophotometry was used as a corroborative analytical method.

4.2 MATERIALS AND METHODS

Disodium aurothiomalate was obtained from Rhone-Polenc (Dagenham, Essex). The potassium dicyanoaurate was obtained from Fluka (Gillingham, Dorset) and resorcinol, potassium dihydrogen phosphate were purchased from Sigma Chemical Company. All the chemicals used were of an analytical grade. Gold chloride for the AA standard work was of a Spectrosol grade and was obtained from BDH. Any other chemicals used were of the highest grade available.

4.2.1 Instrumentation

Chromatographic experiments were performed using apparatus as described in 3.2.1 and a column as described in 3.3.1.

For atomic absorption work a Varian SpectrAA 10/20 spectrophotometer autosampler was used in conjunction with a Varian GTA 96 graphite tube atomiser. A gold hollow cathode lamp was utilised and unless stated otherwise was run at 8 mA.

Ultrafiltration of the samples was carried out using a Centrifree™ Micropartition System (product number 4104) purchased from Amicon Ltd (Stonehouse, Gloucestershire).

4.2.2 Preparation of Biological Samples

1.0 mL of the biological samples were centrifuged at 3200 rpm for 25 minutes in a micropartition system. The micropartition system (Figure 4.1) is a disposable ultrafiltration device which prepares a protein free filtrate. The sample (1.0 mL) is placed in a sample reservoir at the end of which is an anisotropic, hydrophilic membrane. The membrane exhibits high permselectivity due to narrow pore size distribution. Under centrifugal force the protein component of the sample is unable to pass through the membrane. The filtrate containing the free ligands collects in the ultrafiltrate cup whilst the protein bound ligand and other macromolecules which are substantially larger than the membrane skin pores remain behind. The filtrate can then be analysed without further pretreatment. Over 99.9% of the serum protein can be removed this way.

4.2.3 Method

Relevant biological samples were provided by the Bone and Joint Research Unit at The Royal London Hospital Medical College. Samples were obtained from rheumatoid arthritis patients undergoing gold therapy, who had previously reached steady-state levels (cumulative doses of 10-50 mg of Myocrisin per week over a 6-12 week period of time¹²¹). Plasma and synovial fluid was taken from patients at various times after a gold injection. The samples were taken between 1/2-24 hours after a Myocrisin injection. After collection, the biological fluids were immediately frozen at -20°C to prevent further reaction of aurothiomalate with endogenous thiol groups.

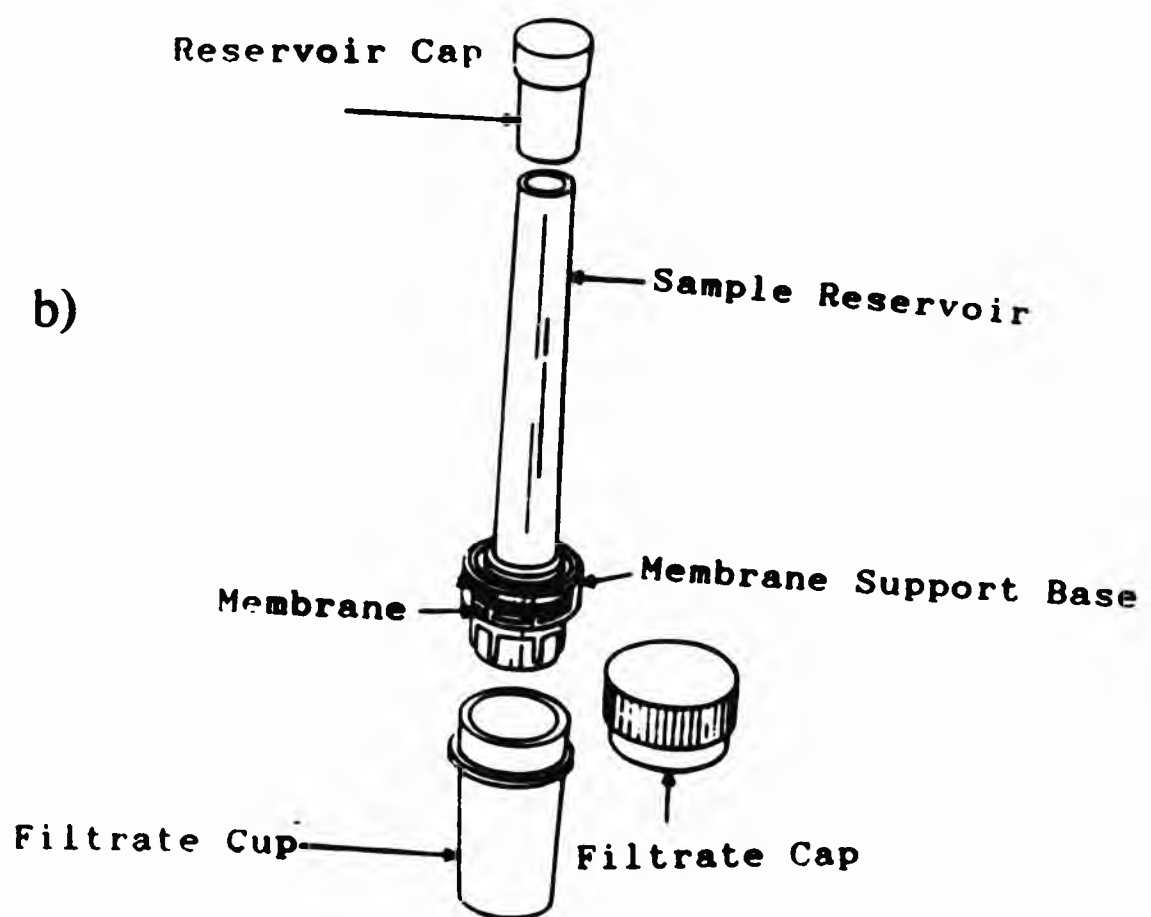
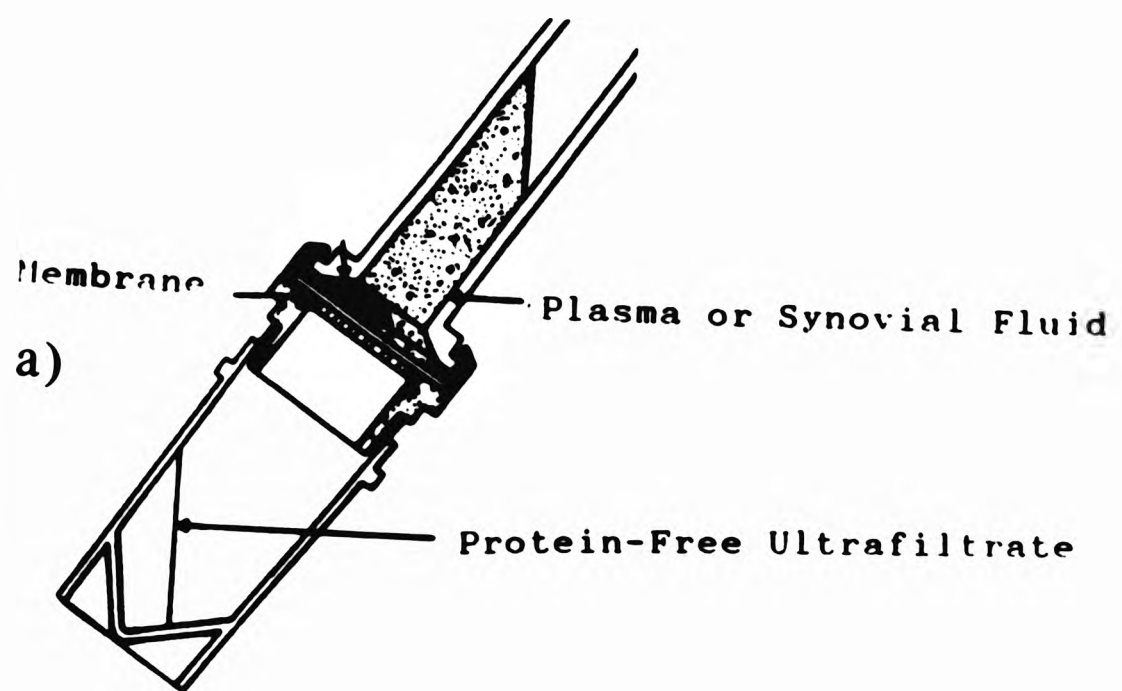


Figure 4.1 a) Diagram of the Ultrafiltration of Biological Fluids by the Micropartition System. b) Diagram of the Micropartition Component Parts.

The biological samples (blood serum and/or synovial fluid) were thawed out at room temperature from the freezer. It was presumed that no significant decomposition of the sample had occurred whilst frozen. On thawing 1.0 mL of the biological sample was pipetted into a micropartition device which was then centrifuged at 3200rpm for 25 minutes. The resultant ultrafiltrate (about 80 μL) was utilised for analytical HPLC and AA work.

4.2.4 HPLC Procedure

80 μL of the resultant ultrafiltrate was pipetted into 20 μL of 5.0×10^{-4} mol dm^{-3} potassium cyanide (final concentration 1.0×10^{-4} mol dm^{-3}) and left to react for 30 minutes at room temperature. This mixture was then split into two equal aliquots. To one 50 μL aliquot, 15 μL of water and 5 μL of 3.5×10^{-4} mol dm^{-3} resorcinol (final concentration 2.5×10^{-5} mol dm^{-3}) was added. To the other 50 μL aliquot, 15 μL of 1.0×10^{-5} mol dm^{-3} potassium dicyanoaurate (final concentration 23.08×10^{-6} mol dm^{-3}) and 5 μL of 3.5×10^{-4} mol dm^{-3} resorcinol was added. Hence the second aliquot was "spiked" in order to identify the dicyanoaurate peak in the biological sample.

The two samples were injected onto the HPLC column through a 50 μL injection loop. The flow rate was 1 mL/min and the mobile phase was an aqueous solution of potassium dihydrogen phosphate (0.15 mol dm^{-3} , pH 6.5). The UV detector was set at 211 nm, the λ_{max} for of the potassium dicyanoaurate ($\text{KAu}(\text{CN})_2$) (refer to Chapter 3). The chart speed was set at 1 cm/min. A standard was run prior to each analysis as a check and a fresh calibration curve was constructed every two weeks.

The volume of synovial fluid in a normal joint is relatively small and in an arthritic joint the volume increases but the viscosity of the synovial fluid decreases. This small volume accompanied by pain experienced by the patient when having synovial fluid withdrawn through a large needle, make it impossible and impractical to collect a large amount of sample. As only 1.0 mL of biological sample was collected from the patients, only about 80 μ L of ultrafiltrate was yielded. This volume of ultrafiltrate did not allow for duplicate runs to be carried out on the same biological sample.

4.2.5 Atomic Absorption

The program for the AA spectrophotometer was set up as follows:

Instrument Mode	Absorbance
Calibration Mode	Concentration
Measurement Mode	Peak Height
Lamp Position	1
Lamp Current (mA)	8
Band Pass (nm)	1.0
Wavelength (nm)	242.8
Sample Introduction	Sampler Automixing
Time Constant	0.05
Measurement Time (sec)	1.0
Replicates	2
Background Correction	OFF

The furnace parameters of the spectrophotometer were set up as below:

Step No.	Temp °C	Time (sec)	Gas Flow (L/min)
1.	85	5.0	3.0
2.	95	40.0	3.0
3.	120	10.0	3.0
4.	500	5.0	3.0
5.	500	5.0	3.0
6.	500	2.0	0.0
7.	2600	1.2	0.0
8.	2600	2.0	0.0
9.	2600	2.0	3.0

The gas type was argon.

Gold standards were prepared with Spectrosol grade gold chloride (1.0 mL = 1.0 mg Au = 5.08 mmol/L) and the standard curve was set up. Ultrafiltrate samples were then analysed for gold concentration.

The samples were dried for the first 55 seconds of the analysis at up to 120°C and were then ashed for 12 seconds at 500°C, and atomised at 2600°C.

4.3 RESULTS AND DISCUSSION

A number of difficulties were experienced in setting up a viable quantitative analysis of the biological samples by HPLC. Baseline drift was experienced with the high sensitivity required and the column had to be conditioned by flushing through with HPLC grade water overnight. Normal problems associated with HPLC such as the presence of air bubbles within the column and pressure fluctuations were exacerbated by the small volume of samples making reanalysis of affected samples unfeasible. Injecting numerous biological samples over an extended period of time onto the HPLC column, caused the column to become contaminated with a variety of biological fluid constituents. This would be indicated by the splitting of peaks. To alleviate this problem the contaminated stationary phase at the top of the column was removed and the column repacked. Repacking would become more frequent as the age of the column increased. After about every 6 months a new column was purchased.

Figure 4.2 shows a typical chromatogram of an "unspiked" synovial fluid filtrate from a RA patient undergoing chrysotherapy that has been reacted with excess potassium cyanide. It is expected that any "free" unreacted gold present in the biological ultrafiltrate would react with the excess cyanide to form the stable compound potassium dicyanoaurate ($\text{KAu}(\text{CN})_2$)¹⁰⁹. From preliminary standard work (Chapter 3) it has been shown that $\text{KAu}(\text{CN})_2$ has a average retention time (t_R) of 8.0 minutes. Peak A seemed likely to be due to $\text{KAu}(\text{CN})_2$. In order to confirm this the sample was spiked with a known amount of a dicyanoaurate standard. The chromatogram of the spiked sample is shown in Figure 4.3. As the only change noted was the increase in peak height this indicates that peak A is due to the formation of the dicyanoaurate complex in the presence of excess cyanide.

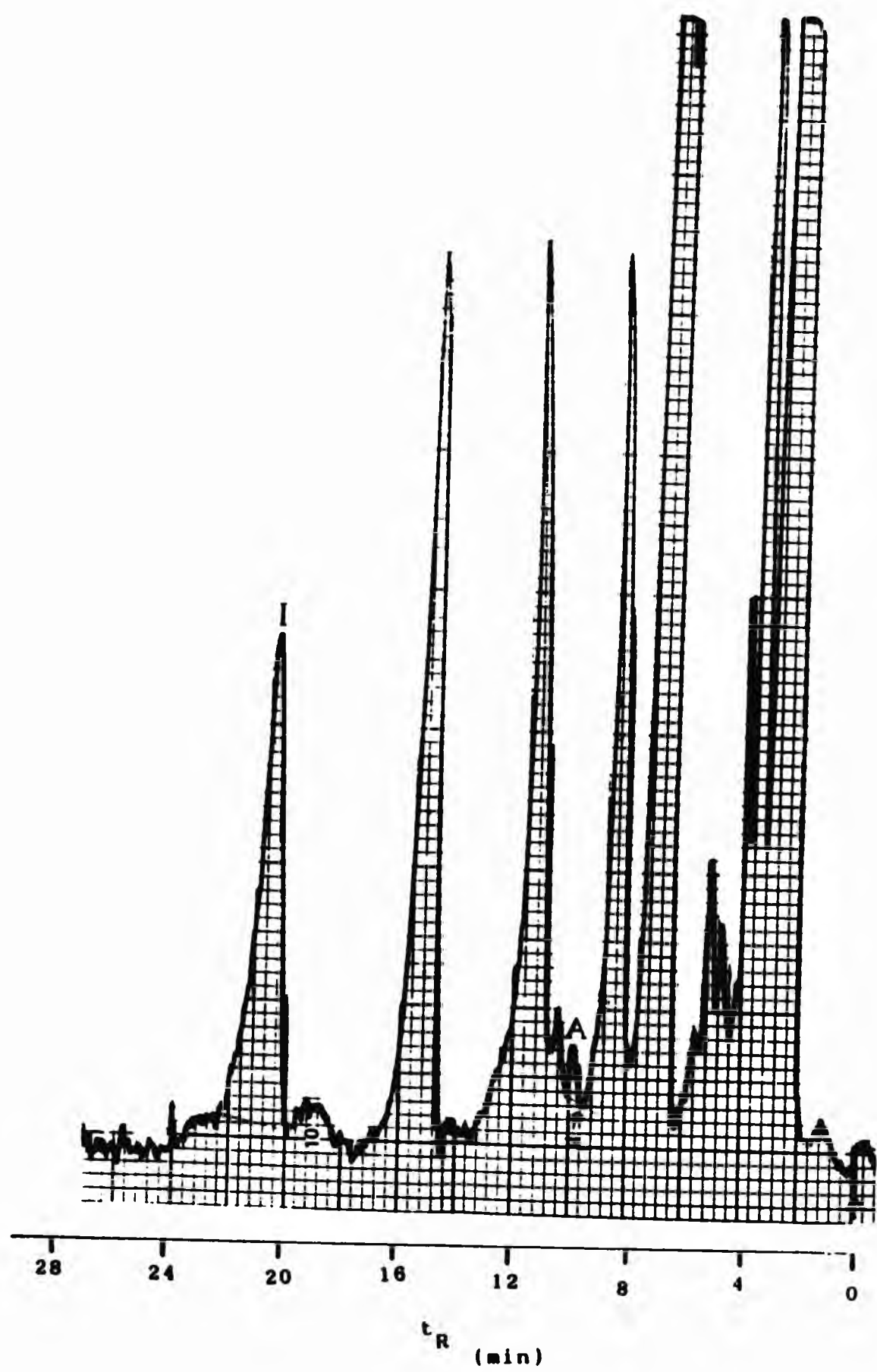


Figure 4.2 HPLC Chromatogram of RA Chrysotherapy Synovial Fluid Ultrafiltrate (Sample AK31/1) with Excess Potassium Cyanide ($1.00 \times 10^{-4} \text{ mol dm}^{-3}$) and Internal Standard Resorcinol ($2.5 \times 10^{-5} \text{ mol dm}^{-3}$). Mobile Phase: 0.15 mol dm^{-3} Potassium Dihydrogen Phosphate (pH 6.5), Flow Rate: 1 ml/min, UV Detector Wavelength: 211 nm, Sensitivity Response Factor, $R = 0.01$, Chart Speed: 0.5 cm/min. Peak A = KAu(CN)_2 ($t_R = 10.6 \text{ min}$), Peak I = Internal Standard (Resorcinol).

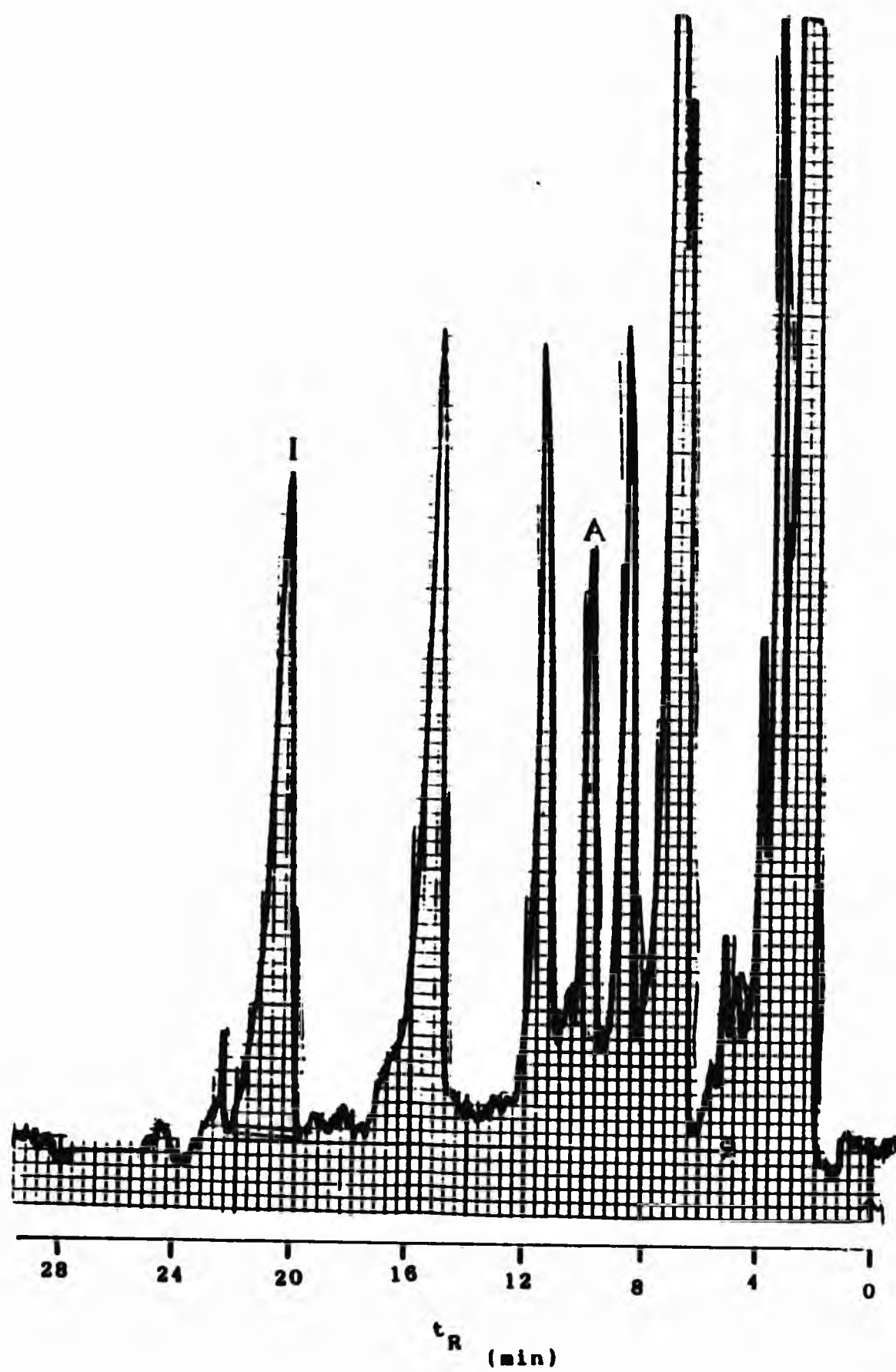


Figure 4.3 HPLC Chromatogram of RA Chrysotherapy Synovial Fluid Ultrafiltrate (Sample AK31/1) with Excess Potassium Cyanide ($1.00 \times 10^{-4} \text{ mol dm}^{-3}$) and Internal Standard Resorcinol ($2.5 \times 10^{-5} \text{ mol dm}^{-3}$) "Spiked" with $2.5 \times 10^{-5} \text{ mol dm}^{-3}$ Potassium Dicyanoaurate Standard ($\text{KAu}(\text{CN})_2$). Mobile Phase: 0.15 mol dm^{-3} Potassium Dihydrogen Phosphate (pH 6.5), Flow Rate: 1 ml/min , UV Detector Wavelength: 211 nm , Sensitivity Response Factor, $R = 0.01$, Chart Speed: 0.5 cm/min . Peak A = "Spiked" $\text{KAu}(\text{CN})_2$ ($t_R = 10.6 \text{ min}$), Peak I = Internal Standard (Resorcinol).

To further confirm this assignment the relative retention, α , of peak A, compared to the internal standard (resorcinol) was calculated for both the chromatograms.

$$\alpha, \text{ Relative Retention} = \frac{\text{Retention Time of Compound of Interest}}{\text{Retention Time of Internal Standard}}$$

Peak A	α , Relative Retention
Unspiked A	2.04
Spiked A	2.04

Table 4.1 Relative retentions of A, $\text{KAu}(\text{CN})_2$

It can therefore be concluded that peak A in fig. 4.3 is attributable to the presence of dicyanoaurate in synovial fluid ultrafiltrate which is formed in the presence of low-molecular weight "free" gold with excess cyanide. A further 15 ultrafiltrate samples were analysed by HPLC giving similar results. The average relative retention was 1.99 with a standard deviation of 0.21.

4.3.1 Quantitative Analysis

Quantitative analysis of the samples was achieved by calculating the area of $\text{KAu}(\text{CN})_2$ peak relative to the area of the internal standard peak. A standard calibration graph was prepared as detailed in chapter 3 and the concentration of low molecular weight gold in the biological sample was calculated after taking into account actual volume of ultrafiltrate over total injection volume.

A_x/A_{IS}	"Free" Gold Concentration from Standard Curve /10 ⁻⁶ mol dm ⁻³	"Free" Gold Concentration after Volume Correction /10 ⁻⁶ mol dm ⁻³
0.042	0.95	1.70

Table 4.2 Table shows Concentration of Low Molecular Gold present in Synovial Fluid of a RA patient Undergoing Chrysotherapy as Calculated from Chromatograms in Figs. 4.2 and 4.3.

Other synovial fluid samples were analysed and the results are shown in Table 4.3. It can be seen that the concentration of "free" gold in the synovial fluid samples is in the range of 1.70-3.01 x 10⁻⁶ mol dm⁻³. The average concentration was found to be 2.48 x 10⁻⁶ mol dm⁻³.

Sample	Concentration of "free" Gold /10 ⁻⁶ mol dm ⁻³
AK31/1	1.70
PG5/3	2.95
A1/5	3.01
LH5/3	3.00
AK5/3	1.85
AK22/8	2.74
PG13/1	2.11

Table 4.3 Concentration of Low Molecular Weight Gold in Synovial Fluid Samples from RA Patients Undergoing Chrysotherapy as Calculated from HPLC Chromatograms by Standard Additions Method. The Standard Deviation is 0.57 and the Mean Concentration is 2.48 x 10⁻⁶ mol dm⁻³.

4.3.2 Atomic Absorption Results

To verify the quantitative results obtained by HPLC analysis, RA synovial fluid samples were analysed by atomic absorption spectroscopy. After the setting up of a standard curve, synovial ultrafiltrate was analysed and the results are shown in Table 4.4.

Sample	Conc (ppb)	Mean Abs
Blank	0.00	0.007
Standard 1	4.00	0.590
Standard 2	8.00	0.116
Standard 3	12.00	0.171
Standard 4	16.00	0.220
Standard 5	20.00	0.256
Sample 1	14.46	0.202
Sample 2	13.06	0.184

Table 4.4 The absorbance of standards and of the synovial fluid ultrafiltrates as measured by atomic absorption spectroscopy. Sample 1 and sample 2 are labelled LH 29/1 and PG 19/2 respectively.

From Table 4.4 the concentration of gold present in the ultrafiltrates was calculated in mol dm⁻³ taking into account the dilution of the original sample. The results are shown in Table 4.5.

Sample	Concentration /10 ⁶ mol dm ⁻³
Sample 1	2.20
Sample 2	1.99

Table 4.5 showing the concentration of low molecular weight gold in representative synovial fluid samples.

Further synovial ultrafiltrate was analysed by AA and the results are seen in Table 4.6. The average concentration is 2.16×10^{-6} mol dm⁻³.

Sample	Concentration of "free" Gold /10 ⁶ mol dm ⁻³
LH29/1	2.20
PG19/2	1.99
PG23/1/90	2.91
PG5/3/91	1.91
LH22/8	1.77

Table 4.6 Concentration of Low Molecular Weight Gold in Synovial Fluid of Patients Undergoing Gold Therapy as Calculated By Atomic Absorption Spectrometry. The Standard Deviation is 0.45 and the Mean Gold Value is 2.16×10^{-6} mol dm⁻³.

From the concentrations calculated by both HPLC and AA it can be seen that the concentration of free unbound gold in synovial fluid is in the region of 2.0×10^{-6} mol dm⁻³, which correlates well with previously documented data⁸.

4.3.3 Analysis of Plasma

Blood plasma ultrafiltrate was also analysed for low molecular weight gold content by both HPLC and AA analysis. The HPLC results are seen in Table 4.7. Samples were taken both before and after a weekly 50 mg aurothiomalate injection.

Sample Pre/Post Au Injection	Concentration of "free" Gold /10 ⁵ mol dm ⁻³
Pre 50 mg (FH12/3)	4.62
Pre 50 mg (DB6/5)	5.11
Post 50 mg (1/2 Hr) (FH12/3)	11.90
Post 50 mg (1/2 Hr) (DB6/5)	12.80
Post 50 mg (1 Hr) (FH12/3)	7.30

Table 4.7 Concentration of Low Molecular Weight Gold in Blood Plasma of Patients Undergoing Chrysotherapy as Calculated by HPLC with Standard Additions Method. The Standard Deviation for Pre Injection is 0.35 and Post Injection is 2.95.

Pre injection readings show an average concentration of $4.87 \times 10^{-6} \text{ mol dm}^{-3}$. Comparing the level of low molecular weight gold found in the synovial fluid samples, with the levels found in the plasma by HPLC analysis gives a ratio of 1:2 respectively. This result ties in with previous results⁴⁴ that quote the synovial fluid to plasma "free" gold ratio is 1:1.8.

It is seen that post injection plasma samples (1/2 hour post injection) show quite a large increase in "free" (non-protein bound) gold concentration as expected (up to a $7.69 \times 10^{-6} \text{ mol dm}^{-3}$ increase). There is a 2.5 fold increase in the "free" gold level in plasma samples taken 30 minutes post injection. These results concur with those obtained by Danpure et al³⁸, who reported that the concentration of unbound gold increases 2-5 fold after an aurothiomalate injection, reaching a maximum level 10-30 minutes post injection. The uptake of the aurothiomalate by albumin in human blood plasma is slow^{11,12}, but eventually most of the gold injected becomes albumin bound (80-90%), and the level of low molecular weight "free" gold decreases accordingly. Rayner et al³⁹ observed that after a reaction time of 55 minutes nearly all the gold was albumin bound (Figure 4.4). Other workers³⁸ found that the binding plateau for albumin was not reached for 5 hours. The post injection plasma sample taken 1 hour after administration of aurothiomalate, shows the non-protein bound gold level falling to $7.30 \times 10^{-6} \text{ mol dm}^{-3}$ as the gold becomes predominately albumin bound and a steady state is eventually attained again.

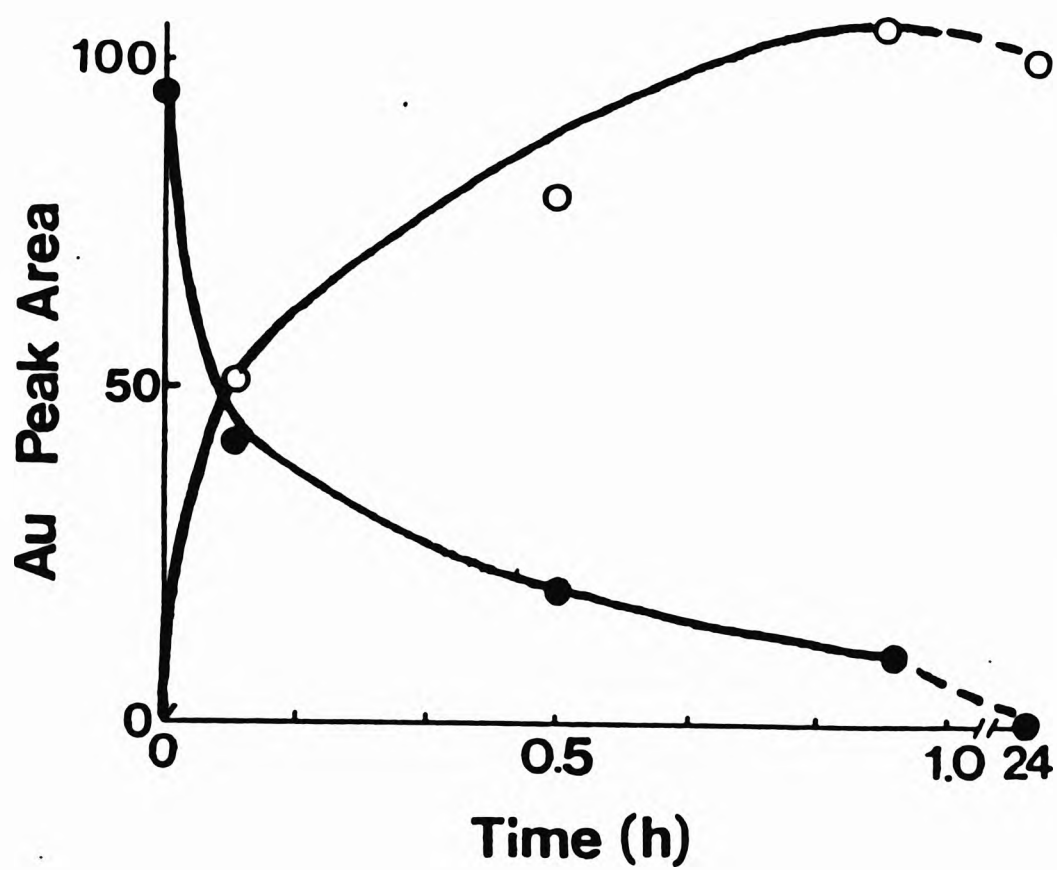


Figure 4.4 Plots of the decrease in concentration of non-protein bound, "free" gold with time (●) and the increase in the concentration of albumin bound gold with time (○) after administration of disodium aurothiomalate (final concentration $4.0 \times 10^{-5} \text{ mol dm}^{-3}$) to human plasma as shown by Rayner *et al*³⁹.

Table 4.8 shows the results of plasma analysis by atomic absorption spectroscopy.

Sample	Ultrafiltrate [Au] /10 ⁻⁶ mol dm ⁻³	Total [Au] /10 ⁻⁶ mol dm ⁻³
Pre 50 mg Au injection	3.28	3.44
Post 50 mg Au injection (1 Hr)	3.86	4.24

Table 4.8 Concentration of Gold in Ultrafiltrate and Whole Plasma Sample as Analysed by AA. Standard deviation is 0.43.

Both the ultrafiltrate (unbound gold content) and the whole plasma sample (total gold content) were analysed by AA. The pre injection unbound gold content plasma sample from this patient is somewhat lower than the plasma sample analysed by HPLC. The level of unbound gold in the post injection plasma ultrafiltrate sample taken 1 hour after the aurothiomalate injection ($3.86 \times 10^{-6} \text{ mol dm}^{-3}$) is only slightly higher than the pre injection level ($3.28 \times 10^{-6} \text{ mol dm}^{-3}$). This is due to the fact that 1 hour after the aurothiomalate injection the relatively slow uptake of aurothiomalate by albumin had taken place and the gold levels had almost reached a steady state again. This would account for the relatively close values obtained for both the pre and post injection ultrafiltrate samples.

The values obtained by AA for total gold content of plasma (Table 4.8) are very low indeed and are deemed unreliable as no clean-up or digestion of the biological sample was made prior to aspiration. This leads to matrix interference from the large protein molecules present and also sample introduction problems. To attempt to evaluate plasma total gold content the sample has to be treated and digested. This investigation centered on the concentrations of only the unbound low molecular weight gold found in biological fluids of RA patients undergoing chrysotherapy, so analysis of total gold content was not further pursued.

Table 4.9 shows the concentrations of unbound gold from plasma ultrafiltrates as analysed by atomic absorption. The levels are lower than those recorded on plasma analysis by HPLC.

Sample	Concentration of "free" Gold /10 ⁻⁶ mol dm ⁻³
PG15/1	3.24
PG23/1/90	3.33
PG5/2/91	2.91
PG5/3/91	1.91
LH26/2	3.54

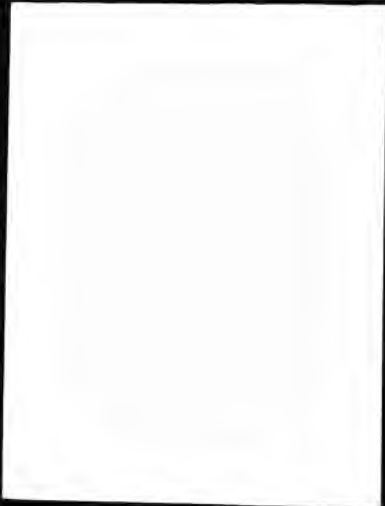
Table 4.9 Concentration of Low Molecular Weight Gold in Blood Plasma of RA Patients Undergoing Gold Treatment as Analysed by AA. The Standard deviation is 0.64 and the mean Gold Value is 2.99×10^{-6} mol dm⁻³.

4.4 CONCLUSION

The concentration of unbound, low molecular weight gold in blood plasma is thought to make up approximately 5% of the total gold content. However, previous investigations into the levels of "free" gold found in rheumatoid arthritis patients undergoing gold therapy have been contradictory. Campion *et al*¹²² have reported levels of 8-10% unbound gold, 2-4 weeks after 50 mg aurothiomalate injections whilst Kamel *et al*¹¹⁹ failed to detect any in some samples.

Although the concentration of low molecular gold is small (relative to the total gold content) and appears to vary widely, it is thought to play an important role in the attainment of equilibrium, transport processes and excretion of gold. The rate of interaction however, between aurothiomalate and albumin *in vivo* might be expected to play a key role in the size and the duration of peaks attributable to the unbound gold.

In this study it has been found that the level of unbound gold in synovial fluid is in the region of $2.0 \times 10^{-6} \text{ mol dm}^{-3}$. These results are consistent when analysed by both HPLC and atomic absorption spectroscopy. The plasma studies analysed by HPLC show that unbound gold is present in plasma in roughly double the quantity ($4.0 \times 10^{-6} \text{ mol dm}^{-3}$) to that found in synovial fluid, which tallies with the results obtained by other workers⁴⁴. The concentration of unbound gold rises by a factor of about 2.5 times after a 50 mg aurothiomalate injection as expected. The plasma results analysed by atomic absorption are found to be lower than those analysed by HPLC. However more samples need to be analysed by both methods to ascertain if this is a trend. In this study HPLC was used as the primary analytical method for non-protein bound gold analysis in biological fluids and



atomic absorption spectroscopy analysis was utilised for corroboration. The AA results for synovial fluid corroborated well with those obtained by HPLC, but discrepancies were observed with the analysis of the plasma samples. AA analysis of the biological fluids suffered due to matrix effects and sample introduction problems and further pre-treatment and digestion of the samples is needed before analysis. However, the HPLC analysis provided a relatively quick analytical method for "free" gold analysis *in vivo* with very little need for pre-treatment of the samples. In addition the HPLC is a relatively affordable piece of equipment commonly found in laboratories and as such this method might be developed for routine medical analysis.

The distribution of gold in biological fluids has been studied *in vivo*^{38,115-118}. Previous work on low molecular weight gold in human plasma has been analysed by neutron activation analysis, with fractionation of plasma by gel exclusion chromatography prior to analysis. This pre-requisite is very time consuming and gives a poor recovery of gold from the column. A less time consuming analytical method which could be used efficiently in a averagely equiped medical laboratory would therefore be of value. After overcoming initial problems, in this study HPLC was succssesfully used as a sensitive and selective analytical tool for low molecular weight analysis of gold in rheumatoid arthritis patients undergoing gold therapy.

CHAPTER 5

**INVESTIGATION OF THE MOLECULAR NATURE OF
IMPLANT-DERIVED TITANIUM (III) AND TITANIUM (IV)
IONS IN TISSUE AND SYNOVIAL FLUID ADJACENT TO
TITANIUM-ALLOY HIP PROSTHESES**

5.1 INTRODUCTION

Titanium alloy implants have been extensively used in hip replacement surgery because of their biocompatibility, due to the presence of an inert titanium oxide layer on the implant surface^{123,124}. However, the inertness of titanium in the biological environment has to be reviewed as on revision surgery for failed hip implants, dark staining of the tissue adjacent to the titanium prostheses has been observed in a number of cases.

5.1.1 Black Staining

The presence of a blue-black discolouration, due to titanium metal ions, has been reported to be present in tissue adjacent to the titanium alloy prostheses¹²⁵⁻¹³⁶. This unpredictable and occasional clinical finding of darkly stained soft tissues around the implant has given rise to the term "metallosis"^{129,130,135}. This can be defined as aseptic fibrosis, local necrosis or loosening of a device secondary to metallic corrosion and release of wear debris. Numerous workers have described this clinical observation, with no clear explanation or predictable occurrence.

Witt and Swann¹²⁷ reported 13 total hip replacements (17.3 %) needing revision surgery because of loosening, after an average of 2 years after implantation. They noted that soft tissues around the prostheses were darkly coloured and that a proliferative membrane had infiltrated the cement and bone interface. Agins *et al*¹²⁶ also noted this phenomenon and reported histiocytic and plasma cell reaction in the pseudocapsular tissue with the utilisation of Ti-6Al-4V (titanium-6% aluminium-4% vanadium) prostheses and ultra high weight polyethylene. A

number of researchers examined the dark tissue histologically, metallurgically and clinically. Goodman *et al*¹³⁷ studied the histological reaction to titanium alloy in rabbit tibia, whilst Rae¹³⁸ investigated the biological response to titanium and its alloy Ti-6Al-4V, by exposing primary cultures of human synovial fibroblasts and mouse peritoneal macrophages to them. Microscopically the cells appeared unaffected but a small release of lactate dehydrogenase (LDH) was noted, indicating some cell damage. The mechanism by which titanium and its alloy cause the release of LDH is unclear. There are 2 possibilities; i) the effects may be due to the action of the soluble metal or ii) to the particles themselves.

Witt and Swan¹²⁷ also reported that, on microscopic examination, the dark tissue was composed of fibroblastic tissue with extracellular dark fragments, also present within the histiocytes and foreign body giant cells. Microbiologically they found the culture negative. Black¹²⁹ stated that all metals, with the exception of maybe titanium and Ti-6Al-4V, are biologically active. Whilst these materials he deemed as being biocompatible in block form, he speculated that when present in particulate form, they induced a macrophage response by causing affected cells to release lysosomal enzymes, collagenase and interleukin, and prostaglandins. Agins *et al*¹²⁶ found the cytoplasm of a few synovial cells and most of the histiocytes contained a number of black, opaque, irregular particles with an approximate diameter of 1-2 μm . They also carried out atomic absorption analysis on the stained tissue and found that the average concentrations of titanium to be ~ 1,000 $\mu\text{g/g}$, of aluminium ~ 100 $\mu\text{g/g}$ and of vanadium ~ 70 $\mu\text{g/g}$. For all the metals the expected concentration was taken to be 0 $\mu\text{g/g}$. The ratio of the 3 metals in the soft tissue, was found to be similar to the ratio of them within the prostheses. Other workers^{128,138} however, reported that the two ratios do not correlate. Indeed, Lalor *et al*¹²⁸, found a complete absence of aluminium or vanadium within the affected tissues. This may be due to the fact that the 3 metals are handled differently *in vivo* and have differing solubilities. Animal studies¹⁴³ have

shown that vanadium is very soluble and passes through the kidneys very quickly, whilst titanium is insoluble and remains in the tissues. Aluminium is more soluble than titanium and may be transported away from the implant site. The presence of titanium was also confirmed by energy-dispersive spectroscopy, where the affected tissue samples gave the characteristic titanium double peak at 15 kV^{128,140}. Meachim and Williams¹³⁹ estimated titanium concentration by neutron activation analysis. They concluded that there was no correlation between titanium concentration and the time the implant had been in the body.

5.1.2 Oxide Needle Model

Solar *et al*¹⁴¹ tried to explain the dark tissue phenomenon found adjacent to failed titanium alloy hip replacements by proposing a model for the surface corrosion and wear of the alloy. The model proposes that the titanium alloy achieves a microscopically rough surface due to the mechanical polishing at the manufacture of the implants. The oxide that forms on the surface, is composed of oxide needles at the surface irregularities and of a smooth planar oxide (Figure 5.1).

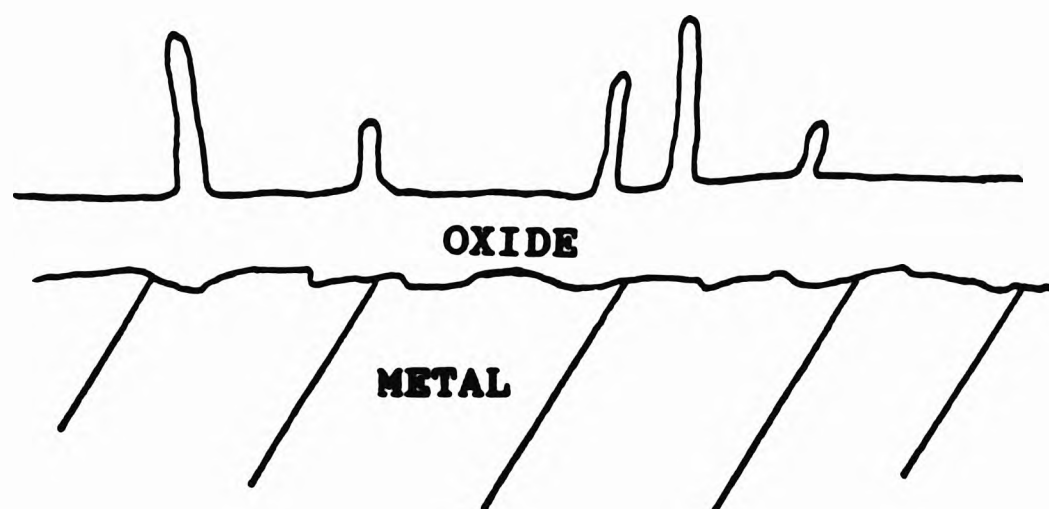


Figure 5.1: Oxide needle model

The oxide needles can be broken off by friction or can dissolve *in vivo*. This could account for the varying presence of titanium sometimes found in soft tissues. Mindell and Pollack¹⁴² describe similar titanium oxide needles in their study of titanium thin film oxidation (they observed needles approximately 500 Å long and with diameters of 75-200 Å).

Overall titanium is still considered to be the most biocompatible metal for implant manufacture. Major histological responses in the tissue have been noted consistent with either allergy or chronic inflammation. In the failed hip prostheses, copious metallic staining may form, which may be irritating to the adjacent tissues prompting immunological responses.

5.1.3 Titanium Gels

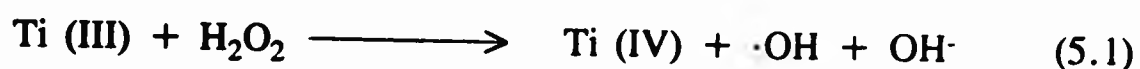
The sensitivity to titanium as described by Lalor *et al*¹²⁸ indicates that there is a deleterious proliferation of Ti (III)/Ti (IV) species present in tissue adjacent to the implant and in the synovial fluid and the synovium. To date little work has been carried out to determine the exact chemical nature of the titanium present. The *in vivo* corrosion of titanium in all likelihood involves a complex series of interdependent dissolution, acid-base and chelation reactions.

To further complicate the bioinorganic chemistry of titanium, Tengvall *et al*¹⁴⁴⁻¹⁴⁶ have reported the presence of a clear yellowish green gel, when metallic titanium is in the presence of hydrogen peroxide (H₂O₂) *in vitro*. They have suggested that this gel is also generated *in vivo* from the reaction of the implant titanium metal with the H₂O₂, which is formed at the surgery site due to a respiratory burst of

phagocytosing cells, or an inflammatory response caused by the surgical trauma at the time of implantation. This gel contains superoxide radicals coordinated to titanium (IV) and appears to be composed of four different Ti (IV) species; $\text{Ti(IV)O}_2^{2-}(\text{OH}^-)_x$, $\text{Ti(IV)O}_2^-(\text{OH}^-)_x$, $\text{Ti(IV)(OH}^-)_4$, $\text{Ti(IV)O}_2 \cdot n\text{H}_2\text{O}$.


The superoxotitanium (IV) component, $\text{Ti(IV)O}_2^-(\text{OH}^-)_x$ has a redox potential, $E_0 > 0.77 \text{ V}$, possibly as high as 1.7 V at pH 4 demonstrating its powerful oxidising properties. The gel readily oxidises superoxide to molecular oxygen, reduced glutathione, probably to its corresponding glutathiol, and Fe(II) to Fe(III)²⁸.

Sensitivity to titanium metal may be brought about by the release of the redox-active titanium (III) species from the prostheses, as this metal ion promotes the generation of the highly reactive hydroxyl radical ($\cdot\text{OH}$) from the hydrogen peroxide (H_2O_2) produced at the implant site by the phagocytic cells as a result of the surgical trauma (equation 5.1).



The peroxidation of the membrane polyunsaturated fatty acids by the hydroxyl radical, leads to cell and tissue damage and this highly reactive radical has the ability to modify the structure of the implant-localised proteins, so inducing immunological responses.

As the chemical speciation of metal ions *in vivo* is important, the precise chemical nature of titanium (III) and titanium (IV) complexes within biological matrices (implant-localised tissue and knee-joint synovial fluid) have been studied in the following work by FTIR and high field proton NMR spectroscopy. Tissue samples obtained from joints containing titanium alloy implants, were seen to contain a



localised blue-black deposit which appears to consist of a polynuclear Ti (III) oxo/hydroxo complex. The production of this species was simulated *in vitro*, by the use of synthetic routes which involved its precipitation, from aqueous Ti (III) solution with biologically-relevant bases. FTIR spectra of the synthesised complexes and of dried titanium-containing tissue were run. The molecular nature of non-protein bound, implant derived, titanium (IV) in knee joint synovial fluid, was assessed by addition of increasing concentrations of Ti (IV) to the rheumatoid synovial fluid and following the reactions by high field proton, Hahn spin-echo NMR.

5.2 MATERIALS AND METHODS

5.2.1 Reagents

Titanium potassium oxalate (dipotassium titanium (IV) oxyoxalate $K_2TiO(C_2O_4)_2$) was purchased from Hopkin and Williams Ltd. Zinc powder, titanium (IV) oxysulphate dihydrate ($TiOSO_4 \cdot 2H_2O$), titanium (IV) sulphate solution (15% w/v $Ti(SO_4)_2$), titanium (III) trichloride ($TiCl_3$), sodium hydroxide (NaOH), sodium carbonate (Na_2CO_3), potassium dihydrogen phosphate (KH_2PO_4), disodium hydrogen phosphate (Na_2HPO_4) and calcium chloride ($CaCl_2$) were all of the highest grade, analytical if possible and were purchased from Aldrich. Analar trisodium citrate was obtained from Sigma Chemicals.

5.2.2 Methods

5.2.2.1 Reduction of Titanium (IV) Complexes and Chemical Modification of Reduction Products with Endogenous Anionic Ligands

5.2.2.1.1 Preparation of a Dark-blue Multinuclear Titanium (III) Oxo/Hydroxo Complex with Titanium (IV) Oxysulphate

a) Precipitation with Sodium Hydroxide

0.75g of zinc powder was added to 5.0 cm³ of 0.75 mol dm⁻³ titanium (IV) oxysulphate ($TiO(SO_4)$), which contained 23 % w/v sulphuric acid (H_2SO_4). This reaction mixture was left for 30 minutes at ambient temperature. During this time

hydrogen gas evolved continuously and a deep violet colour developed in the solution. At the end of this period the colour was stable and no further gas evolved. The reaction was assumed to be complete. The final pH of the solution was found to be 5. A 1.0 mL sample of the dark violet solution was taken and mixed with sodium hydroxide solution (0.10 mol dm^{-3} , 10.0 mL). A dark blue coloured precipitate formed. This was filtered, washed three times in degassed, distilled water and dried under vacuum. It was noted that the dark blue precipitate had a multicoloured "metallic" sheen on its surface. Fourier transform infra-red (FTIR) spectroscopy was employed to obtain the spectrum of the precipitate in the range $400\text{-}4000 \text{ cm}^{-1}$. This spectrum showed a series of diffuse absorption bands found at 1143 , 1048 and 990 cm^{-1} , with a less well defined "shoulder" at 1213 cm^{-1} (Figure 5.2). These bands are characteristic of Ti (III)-sulphato complexes (mono- or bidentate co-ordination of sulphate), which can be presumed to be associated with polynuclear Ti (III) oxo/hydroxo complexes. The lower region of the FTIR spectrum displayed sharp absorption bands at 637 and 617 cm^{-1} . Exposure of the blue solid to atmospheric oxygen ($>72 \text{ hr}$) resulted in loss of colour. This was assumed to be due to the slow rate of transformation of Ti (III) to Ti (IV).

b) Measurement of the Titanium Concentration of the Precipitate

A standard curve was constructed by using varying concentrations of Ti (IV) oxysulphate ($\text{TiOSO}_4 \cdot 2\text{H}_2\text{O}$). Ti (IV) oxysulphate solutions of concentrations $0.50 \text{ mmol dm}^{-3}$, $0.75 \text{ mmol dm}^{-3}$, $1.50 \text{ mmol dm}^{-3}$, $2.50 \text{ mmol dm}^{-3}$ and $3.00 \text{ mmol dm}^{-3}$ were made up in 20.0 cm^3 of 1:1 1.80 mol dm^{-3} hydrochloric acid and 0.14 mol dm^{-3} hydrogen peroxide. The solutions were left to stand for 2 hr and became orange in colour, with the colour intensity increasing with increasing concentration. UV spectra of the solutions were then run at $200\text{-}600 \text{ nm}$ (speed 125 nm/min).

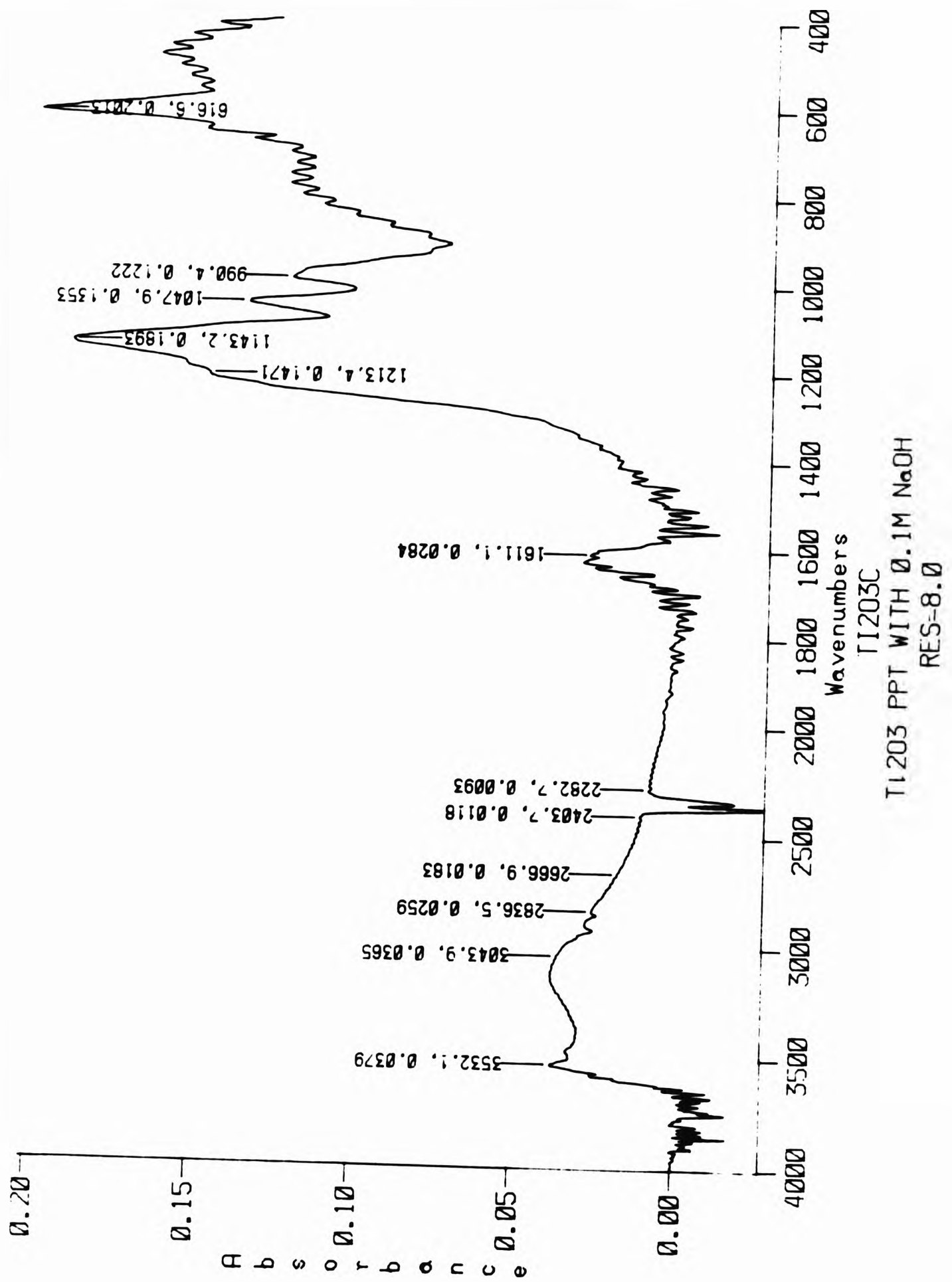


Figure 5.2 FTIR Spectrum of Blue Titanium (III) Oxo/Hydroxo Complex Prepared with Titanium (IV) Oxysulphate and Sodium Hydroxide.

5.0 mg of the precipitate was treated similarly to the Ti (IV) standard solution. The solution was also left for 2 hr before an UV absorbance spectrum was taken at 200-600 nm. A graph was plotted from the standards of absorbance at λ_{\max} (413 nm) versus concentration. A straight line graph was obtained which obeyed the Beer Lambert law, where $A = \epsilon cl$ (ϵ = extinction coefficient, c = concentration and l = cell path length). Using this graph and knowing the absorbance at λ_{\max} obtained by the prepared precipitate, its concentration and hence its titanium content was calculated. The solid was found to have 56 % titanium.

c) Precipitation with Sodium Carbonate

The dark violet coloured Ti (III) solution was prepared as in a), by the reduction of titanium (IV) oxysulphate (Ti(IV)OSO₄) with the Zn/HCl system. The solution was left for 30 min and then 1.0 mL of it was taken and to it was added 10.0 mL of 0.10 mol dm⁻³ sodium carbonate solution (Na₂CO₃). A dark blue precipitate was formed which was filtered, washed 3 times in deaerated water and dried in vacuum in a desiccator. A FTIR spectrum of the sample was run (Figure 5.3) which showed absorption bands at 1112 cm⁻¹ and 993 cm⁻¹, suggesting that the Ti (III) sulphato species are associated with the product prior to its loss of colour (oxygen dependant). As with the -OH precipitated complex, the 850-400 cm⁻¹ region of the spectrum showed sharp Ti (III)-O stretches at 637 and 619 cm⁻¹. Elemental CHN analysis gave 0.20 % carbon and 1.65 % hydrogen. The occurrence of carbon can be accounted for by the presence of the carbonate anion, which could be co-ordinated to the titanium or may just be present as a non co-ordinated impurity due to excess sodium carbonate (Na₂CO₃), existed as a co-precipitate or possibly adsorbed on the surface of the precipitate. On prolonged exposure to air (> 72 hr) the dark blue precipitate lost its colour and became white as the Ti (III) was oxidised by O₂ to Ti (IV).

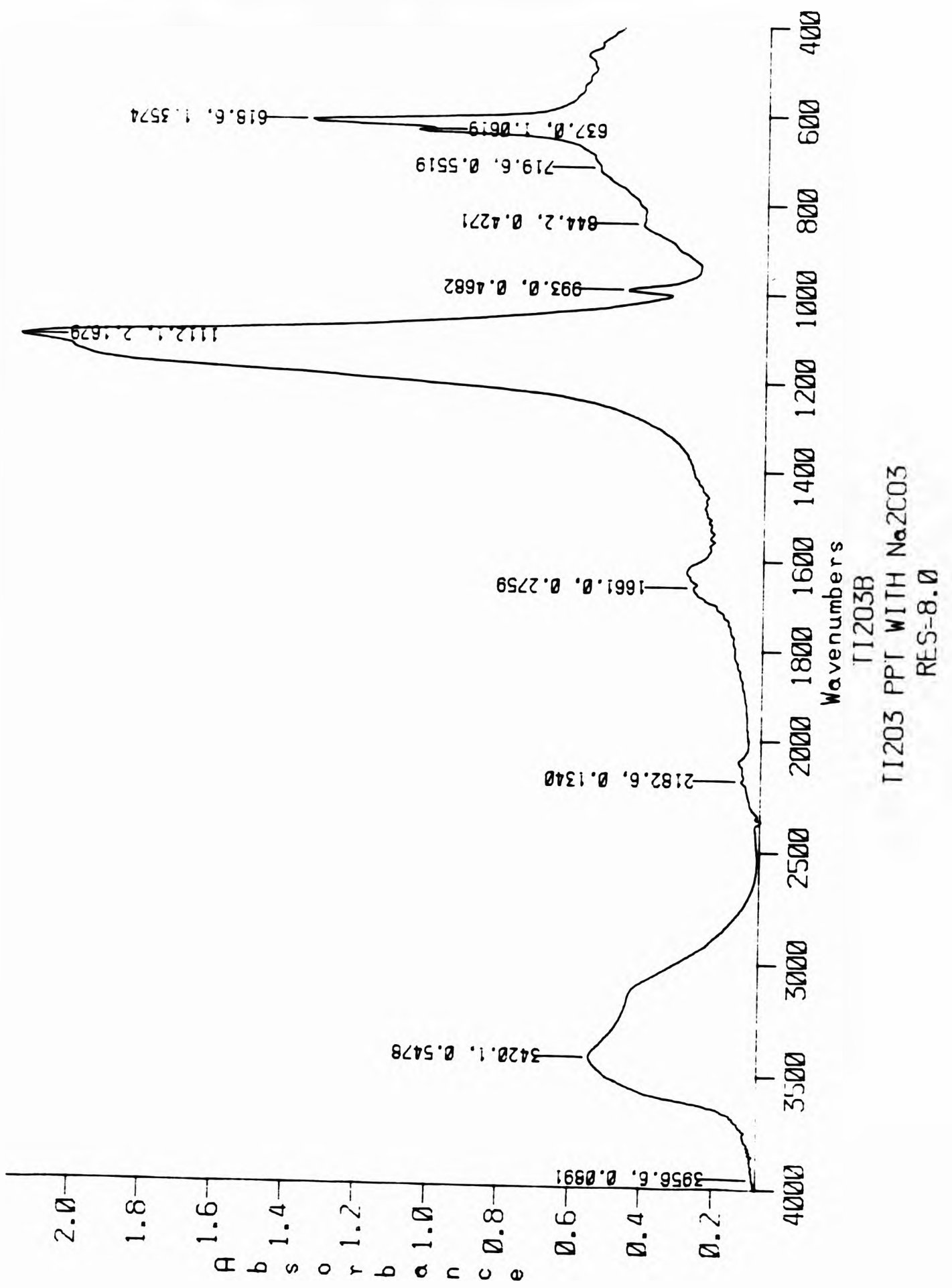


Figure 5.3 FTIR Spectrum of Blue Titanium (III) Oxo/Hydroxo Complex Prepared with Titanium (IV) Oxysulphate and Sodium Carbonate.

d) Precipitation with Inorganic Phosphate

To 1.0 mL of violet coloured Ti (III) solution, obtained as in a) and b), 10.0 mL of an aqueous solution of phosphate buffer, pH 7.41 ($8.70 \times 10^{-3} \text{ mol.dm}^{-3}$ of KH_2PO_4 , $3.04 \times 10^{-2} \text{ mol dm}^{-3}$ Na_2HPO_4) was added¹⁶⁵. A pale blue precipitate was obtained, which was filtered, washed 3 times with distilled, degassed water and left to dry under vacuum in a desiccator. The precipitate rapidly lost colour and was converted to a white Ti(IV) containing solid on exposure to air. A FTIR spectrum of the autoxidised white solid was run and a strong absorption band at 1038 cm^{-1} was seen which confirmed the presence of phosphate (Figure 5.4). The lower region of the spectrum ($850\text{--}400 \text{ cm}^{-1}$) showed a number of overlapping bands including ones at 730, 607, and 500 cm^{-1} , which were different from the bands obtained with the solid precipitated by sodium carbonate or sodium hydroxide. Elemental CHN analysis gave 0.00 % C and 1.65 % H.

5.2.2.1.2. Preparation of a Dark Blue Coloured Ti (III) Precipitate Using Titanium (IV) Potassium Oxalate (oxyoxalate)

a) Precipitation with Sodium Carbonate

To 10.0 mL of 0.10 mol dm^{-3} titanium (IV) potassium oxalate ($\text{K}_2\text{Ti}^{\text{IV}}\text{O}(\text{C}_2\text{O}_4)_2$) 1.5g of zinc powder was added, followed by 3.0 mL of 2.00 mol dm^{-3} hydrochloric acid. The liquid changed from a clear to an orange-brown colour as the Ti (IV) was reduced to Ti (III) (presumably forming mono- or/and bis oxalato Ti (III) complexes). Gas, presumed to be hydrogen was seen to evolve. The reaction mixture was left at ambient temperature for 30 minutes until the zinc powder settled. 3.0 mL of this reduced solution was placed in a test tube and

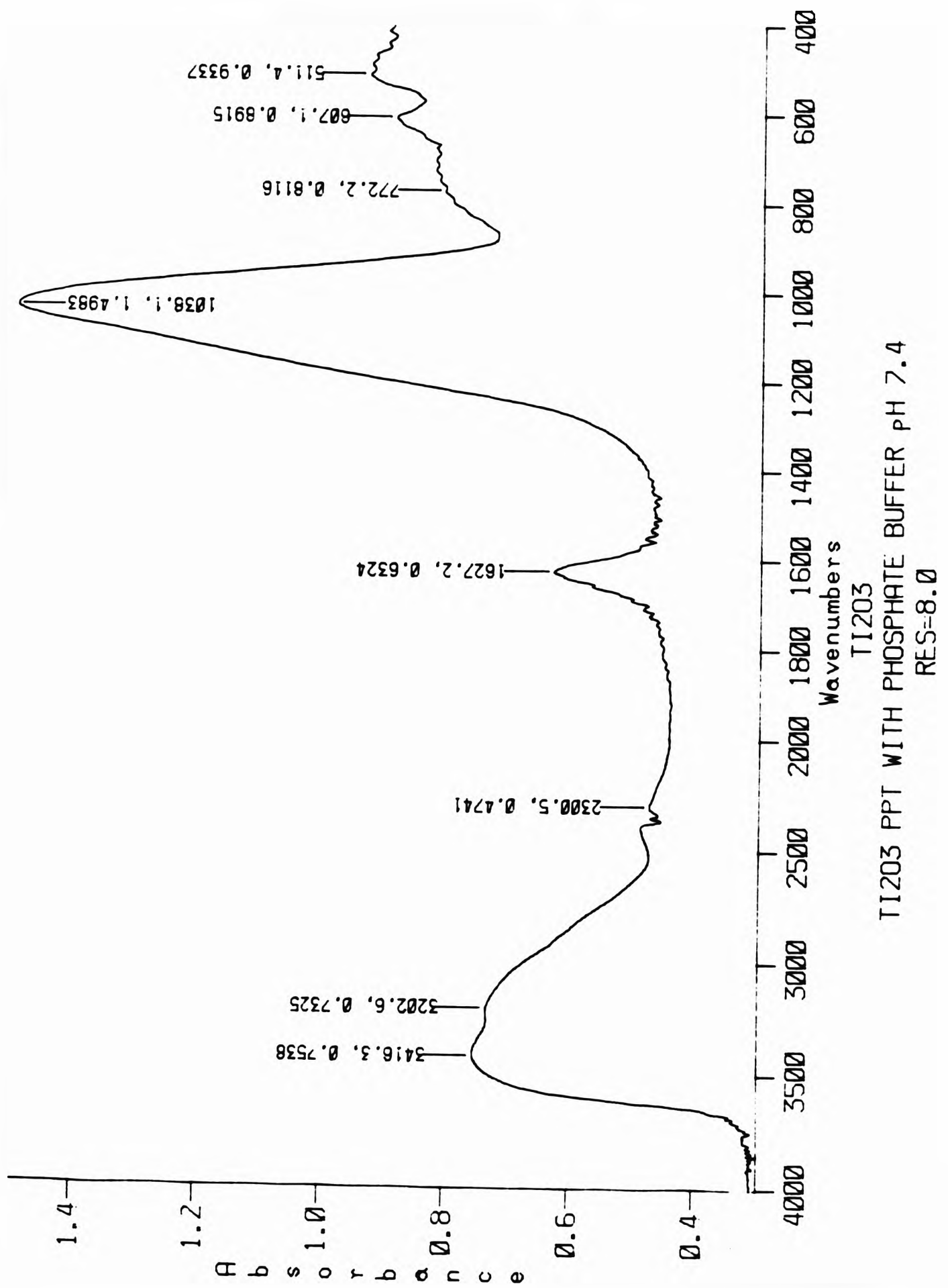


Figure 5.4 FTIR Spectrum of Blue Titanium (III) Oxo/Hydroxo Complex Prepared with Titanium (IV) Oxysulphate and Phosphate Buffer pH 7.4.

treated with 10.0 mL of 0.10 mol dm⁻³ sodium carbonate solution. A dark blue precipitate was formed, suspended in a now clear solution. The solid was filtered, washed with plenty of degassed water and dried under vacuum. Elemental CHN analysis gave results of 6.12 % C and 1.61 % H.

b) Precipitation with Sodium Hydroxide

The reduced titanium (III) orange-brown solution was prepared as previously described in a), and 10.0 mL of 0.10 mol dm⁻³ sodium hydroxide was added to 3.0 mL of the Ti (III) solution to yield a dark blue precipitate, which was dried and collected as before. Elemental CHN analysis performed on the solid gave readings of 4.44 % C and 1.43 % H.

The precipitate obtained with the CO₃²⁻ anion had a higher percentage of carbon compared with that obtained with sodium hydroxide, indicating the presence of carbonate as either a co-ordinated or/and unco-ordinated anion. FTIR spectra of the two precipitates were run (Figures 5.5 and 5.6) and both exhibited an intense C=O stretching band (1632 cm⁻¹) and two lesser C=O stretches (1364 and 1319 cm⁻¹). A series of bands were also present at 822, 742, 603, 495 and 458 cm⁻¹, which correspond to Ti (III)-O, C-O and C-C stretching and chelate ring deformation.

Exposing the blue precipitates to air over a prolonged period, resulted in a loss of colour ascribed to the oxidation of the sample. On prolonged air exposure the complexes became brown in colour. FTIR spectra performed on the oxidised white samples looked similar to those of the unoxidised blue Ti (III) precipitates (Figure 5.7). The multinuclear Ti (III) species did however exhibit a broad band of medium intensity at 1511 cm⁻¹ which was not present in the corresponding

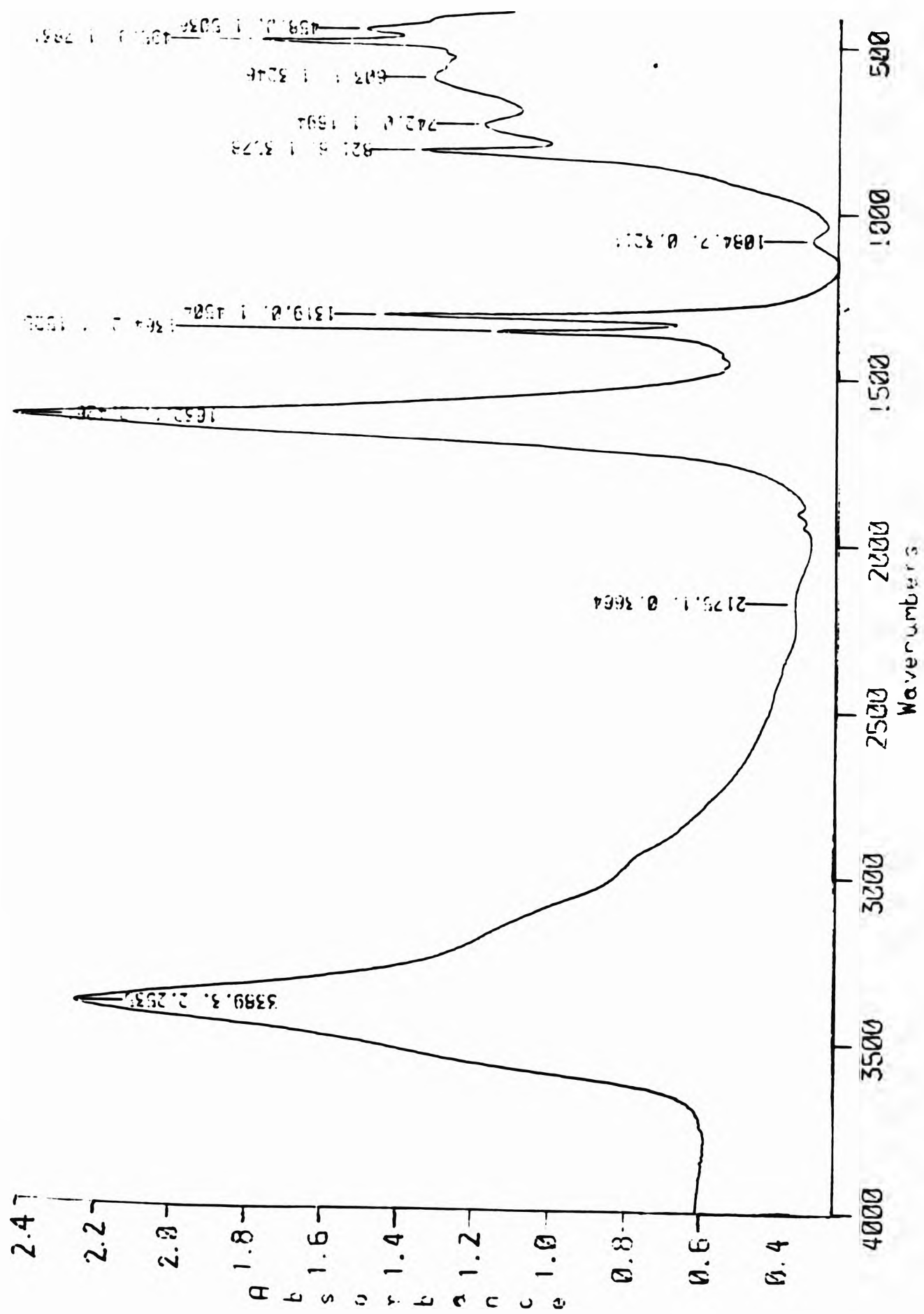


Figure 5.5 FTIR of Blue Titanium (III) Oxo/Hydroxo Complex Prepared with Titanium (IV) Potassium Oxalate and Sodium Carbonate.

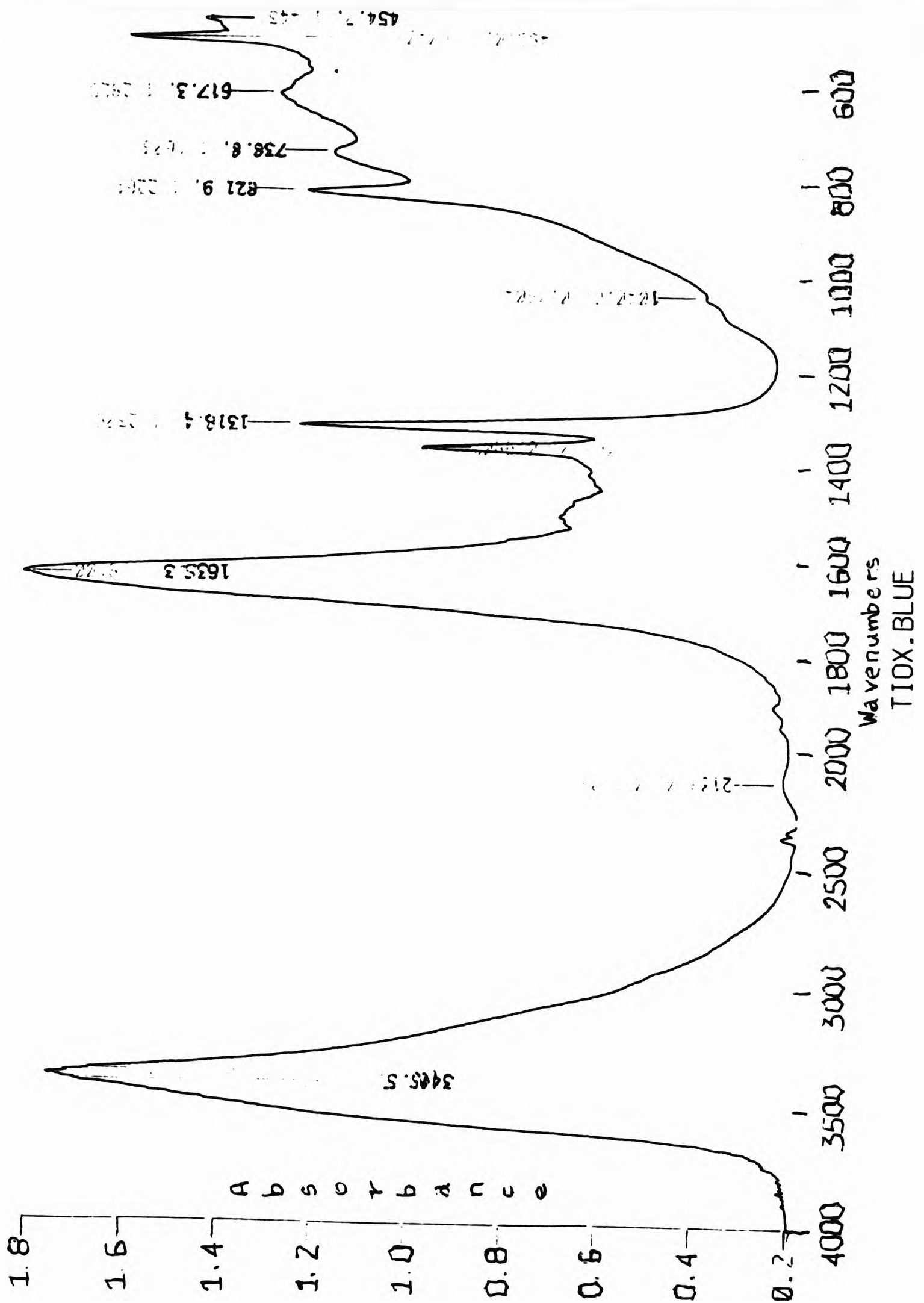


Figure 5.6 FTIR Spectrum of Blue Titanium (III) Oxo/Hydroxo Complex Prepared with Titanium (IV) Potassium Oxalate and Sodium Hydroxide.

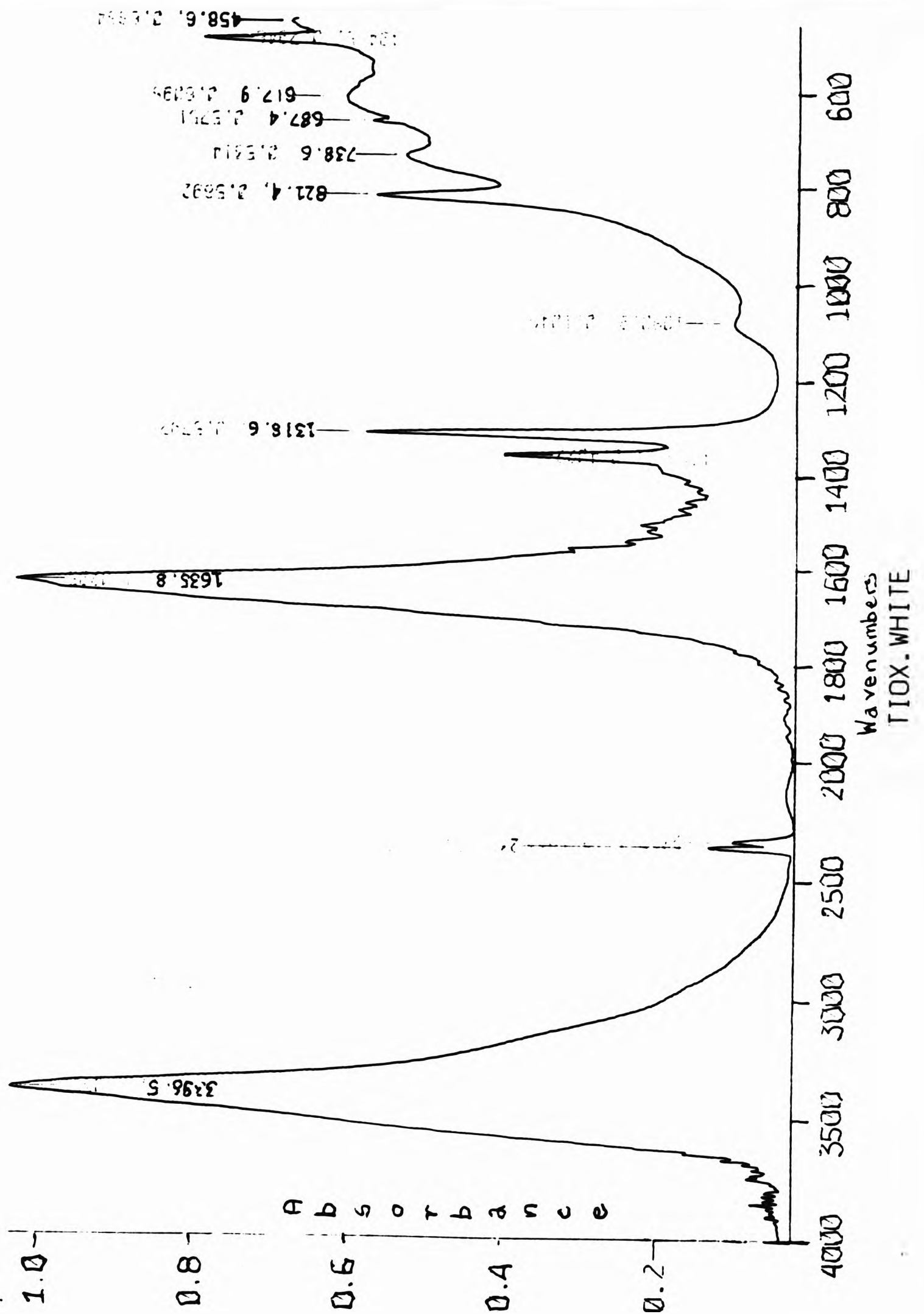


Figure 5.7 FTIR Spectrum of Oxidised (White) Titanium (III) Oxo/Hydroxo Complex Prepared with Titanium (IV) Potassium Oxalate and Sodium Hydroxide.

spectra of the oxidised solid. The brown solid, formed on further exposure to atmospheric oxygen, gave no significantly differing spectra.

c) Removal of Ti (IV) Co-ordinated Oxalate with Calcium Chloride

5.0 mL of 0.20 mol dm⁻³ calcium chloride (CaCl₂) was added to 5.0 mL of 0.10 mol dm⁻³ titanium (IV) potassium oxalate (K₂TiO(C₂O₄)₂). The white precipitate of calcium oxalate (CaC₂O₄) formed was filtered off and the clear supernatant was collected. To 5.0 mL of supernatant, 0.75g of zinc powder and 1.5 mL of 2.00 mol dm⁻³ hydrochloric acid (HCl) solution was added. The reaction was left to proceed at ambient temperature for 30 minutes during which hydrogen gas evolved. The solution became pale yellow in colour. To 3.0 mL of the solution, 12.0 mL of 0.10 mol dm⁻³ sodium hydroxide was added, resulting in the precipitation of a pale grey-blue solid which rapidly decolourised on exposure to air to give a white solid thought to contain titanium (IV). The precipitate was washed, filtered and dried under vacuum in a desiccator. The white calcium oxalate precipitate only formed in the neutral solution. When attempting to reduce the titanium (IV)-oxalate complex first, by adding the zinc and aqueous hydrochloric acid, the solution turned orange-brown as expected, but on addition of the calcium chloride to this acidic medium, no calcium oxalate precipitate formed.

d) Addition of Citrate

1.0 mL of 0.50 mol dm⁻³ trisodium citrate solution was added to 1.0 mL of 0.20 mol dm⁻³ titanium (IV) potassium oxalate and the mixture was left for 30 minutes. Then 2.0 mL of 0.20 mol dm⁻³ of calcium chloride was added to the solution and was allowed to stand for 15 minutes. The white precipitate of calcium oxalate

formed was filtered off and 0.45g of zinc and 0.9 mL of 0.20 mol dm⁻³ hydrochloric acid was added to 3.0 mL of the remaining supernatant. The reaction was allowed to proceed for 1 hour as hydrogen gas evolved. The solution changed colour from pale brown, through violet to deep purple, indicating complex formation and the transfer of Ti (III) from oxalate to citrate. To 3.0 mL of this solution, 18.0 mL of 0.10 mol dm⁻³ sodium hydroxide was added in order to precipitate a deep purple solid, which redissolved on addition of excess sodium hydroxide solution.

e) Precipitation with Phosphate

1.5g of zinc powder and 3.0 mL of 2.00 mol dm⁻³ hydrochloric acid were added to 10.0 mL of 0.10 mol dm⁻³ titanium (IV) potassium oxalate (K₂Ti^{IV}O(C₂O₄)₂) and allowed to stand for 30 minutes. Hydrogen gas evolved and the solution turned orange-brown in colour. To 3.0 mL of this solution was added 20.0 mL of phosphate buffer pH 7.41 which was prepared as described earlier. A violet-grey precipitate was formed, which faded in colour when allowed to remain in the supernatant for 30 min. The white solid, thus obtained was filtered, washed in degased, distilled water and dried in vacuum.

5.2.2.2 Tissue Samples

During revision surgery of patients with aseptically loosened hip prostheses, acetabular tissue samples were taken. Metal debris was seen to be present in the tissues sampled. The prostheses had high density polyethylene acetabular components, backed with chrome-cobalt (Cr-Co) alloy. Ti-6Al-4V alloy screws were used to fix the acetabular component to the skeleton.

The samples obtained were snap frozen by placing the fresh tissue in a sterilin cryotube, immersing the sealed tube into liquid nitrogen, and storing it at -70°C until needed for experimental work. Alternatively the tissue samples were fixed in 10 % formol saline (2.5 dm³ formaldehyde (Infracem), 212.5g NaCl (Sigma), diluted to 22.5 dm³ with distilled water) for 3 days. The tissue sample was then washed in a trihydroxymethylamine (BDH) buffered solution for 15 min, followed by washing in distilled water for 15 min to remove excess formol saline.

5.2.2.3 Synovial Fluid Samples

Knee-joint synovial fluid samples from rheumatoid patients with knee inflammations were aspirated into plastic tubes ($n = 5$). After collection, the samples were sent to the laboratory packed in ice, where they were centrifuged at 2,500 rpm for a duration of 15 minutes in order to remove the cells and debris. The resulting supernatant was stored at -70°C for a maximum of 14 days.

5.2.2.4 FTIR Spectroscopic Analysis of Prepared Titanium Ion Complex Precipitates and Titanium Ion Containing Deposits from Failed Hip Implant Tissue Samples

FTIR spectra of the prepared titanium (III) and/or titanium (IV) complexes were run, as well as the spectrum of commercially available titanium (IV) dioxide (TiO_2). A frozen tissue sample was defrosted at room temperature and the localised dark blue titanium containing deposit was manually extracted with tweezers and weighed. The sample was dried in vacuum in a desiccator. A

normal, weighed tissue sample with no blue deposit was also dried and treated in the same way as the affected sample. KBr discs of the dried samples to be examined (ca. 2 % w/w relative to KBr) were prepared by grinding with a pestle and mortar. The spectra were recorded using a Digilab FTS 40 spectrometer. All the samples were scanned 16 times before the spectra were run and a resolution of 8 was used.

5.2.2.5 NMR Measurements

0.07 mL of D₂O was added to 0.60 mL of synovial fluid in a 5 mm diameter NMR tube, in order to provide a field-frequency lock. The Hahn spin-echo sequence (time delay, $t_D = 60$ ms) was applied to the sample in order to suppress the broad protein resonances and continuous secondary irradiation at the water frequency was applied to suppress the intense water signal. The Hahn spin-echo was carried out 128-212 times. The external reference for the synovial fluid spectra was sodium-3-(trimethylsilyl)-1-propane-sulphonate (TSP, $\delta=0$).

Single pulse spectra of chemical model systems were also obtained. The pulse angle was 30-40° and the time delay between pulses was 3 seconds, in order to allow complete spin-lattice (T_1) relaxation of the protons within the sample. As before, the external reference was TSP.

In both cases the proton NMR measurements were carried out on a JEOL JNM-GSX spectrometer operating in quadrature detection mode at 500 MHz for ¹H and at a probe temperature of 25°C.

5.3 RESULTS AND DISCUSSIONS

The presence of blue-black discolorations in tissues adjacent to failed hip implants, discovered during revision surgery, has been reported previously. The discoloured tissue has been shown to contain titanium³². Although the discolouration can be due to naturally occurring titanium dioxide (TiO₂) in the presence of impurities, the blue-black colour of the tissues sampled and that of the redox-dependent precipitates formed suggests that it occurs due to Ti (III) and/or a mixed Ti (III)/Ti (IV) complex. The localised deposit may consist of one or more complexes of titanium (III) bound to an anionic ligand that would be found in the human body, e.g. carbonate, phosphate or oxalate. A number of such ligands, including the hydroxide ion, were used to precipitate Ti (III) and/or Ti (III)/Ti (IV) complexes and the resultant precipitates colour was compared to that of the discoloured tissue sample.

A redox-active dark blue precipitate whose colour closely resembled that of the localised discolouration found on the failed hip implant tissue samples, was produced by reduction of titanium IV oxysulphate to titanium (III), with Zn/HCl, followed by subsequent precipitation with excess hydroxide or carbonate ions. The solid is probably an insoluble polynuclear titanium (III)-oxo and/or hydroxo complex or the hydrated mixed oxide of titanium (III) and titanium (IV), Ti₃O₅.nH₂O. The titanium content of the precipitate was calculated to be 56% which is consistent with the polynuclear Ti (III) species with an approximate ratio of titanium:oxygen as 1:2.

Both the blue/black deposit isolated from the implant localised tissue samples and the synthesised dark blue precipitate discoloured on exposure to air (>72 hrs), becoming white in colour as oxidation to titanium (IV) occurred, the hydrated titanium (IV) oxide, TiO₂.nH₂O presumably being formed.

The precipitate formed with carbonate was observed to oxidise more rapidly than the hydroxide-formed solid.

A phosphate buffer (pH 7.4) was used to precipitate a pale grey-blue Ti (III) solid. The titanium (III) was generated by the reduction of titanium (IV) oxysulphate ($\text{Ti}^{\text{IV}}\text{OSO}_4$) with a Zn/HCl system. The solid contains one or more Ti (III)-phosphate complexes even though some of the Ti (III) oxo/hydroxo complexes were also probably present. The pH may also have affected the precipitation and the formation of the complexes. The phosphate induced titanium (III) precipitate oxidised even more rapidly on exposure to air than the previously prepared complexes.

As the oxalate anion is a metal ion chelator and is therefore physiologically relevant, titanium potassium oxalate ($\text{K}_2\text{TiO}(\text{C}_2\text{O}_4)_2$) was used as the starting titanium (IV) salt. The precipitate was obtained as previously by reducing the Ti (IV) with a Zn/HCl system and then the dark-blue solid was dropped out of the solution by the addition of sodium hydroxide. The characteristic blue colour, similar to that obtained with titanium (IV) oxysulphate, indicates that the multinuclear titanium (III) oxo/hydroxo complex or the hydrated mixed titanium (III)/titanium (IV) oxide, $\text{Ti}_3\text{O}_5 \cdot n\text{H}_2\text{O}$ was formed. The elemental CHN analysis gave the percentage of carbon as 4.44%, higher than expected suggesting the presence of Ti (III)-co-ordinated oxalate ion, as later confirmed by FTIR analysis of the dried sample.

A similar dark-blue precipitate was also formed with sodium carbonate as the precipitant. CHN elemental analysis of the solid derived in this way gave the carbon content as 6.12%; higher than that obtained with sodium hydroxide. This increased carbon content indicates the solid contains a significant quantity of co-ordinated or non-co-ordinated carbonate ion.

Both the precipitates obtained with OH^- and CO_3^{2-} became white in colour on prolonged (> 72 hrs) exposure to atmospheric oxygen.

The removal of the oxalate anion, in the $\text{K}_2\text{TiO}(\text{C}_2\text{O}_4)_2$ solution, prior to reduction of Ti (IV) to Ti (III), was carried out by calcium chloride. The white precipitate of calcium oxalate ($\text{Ca}(\text{C}_2\text{O}_4)_2$) was removed and the resulting supernatant, after reduction with the Zn/HCl system, yielded a blue-grey precipitate on addition of NaOH. This product was unstable in air, as it quickly auto-oxidised. Colour of solid was unaffected by the continuous purging with nitrogen gas throughout the reaction.

The action of the endogenous chelator citrate on the colour and solubility of titanium (III) was also studied. A solution with the $[\text{TiO}(\text{C}_2\text{O}_4)_2]^{2-}$ anion was sequentially treated with a) 2.50 molar equivalents of trisodium citrate and b) 2.00 molar equivalents of calcium chloride (CaCl_2) to remove the oxalate in the form of insoluble calcium oxalate. The reduction of the supernatant with Zn/HCl yielded a deep purple solution, which on addition of sodium hydroxide, gave a purple precipitate, presumably a complex of one or more titanium (III)-citrate complexes. The precipitate redissolved on the addition of excess NaOH, and the solution became clear.

Treating the Zn/HCl reduced titanium oxalate solution with phosphate buffer, (pH 7.41) yielded a violet-grey precipitate, of probably one or more titanium (III)-phosphate complexes. The precipitate rapidly oxidised to white, on exposure to air.

Titanium (III) is a powerful reducing agent (the redox potential, E_0 of the $\text{Ti}^{\text{IV}}(\text{OH})_2^{2+}/\text{Ti}^{3+}$ system is estimated to be 7.7×10^{-3} V) and therefore the oxidation of the newly formed Ti (III) (or mixed Ti (III)/Ti (IV)) complexes are to be expected. The violet Ti (III) ions readily donate electrons to molecular oxygen. The hexaaquatitanium (III) complex ($[\text{Ti}(\text{H}_2\text{O})_6]^{3+}$) does not directly interact with molecular oxygen, even though O_2 does oxidise the hydroxotitanium (III) ion ($[\text{Ti}(\text{H}_2\text{O})_5(\text{OH})]^{2+}$) to Ti (IV) (TiO_2^+) by an outer-sphere pathway which generates the superoxide anion (O_2^-).

The reaction is slow at room temperature (second-order rate constant, $k_2 = 4.25 \text{ mol dm}^{-3} \text{ s}^{-1}$). The oxidation of the insoluble titanium (III) complex present as localised titanium deposits in tissue adjacent to failed Ti-6Al-4V alloy prostheses, may play a significant part in promoting the generation of reactive oxygen radicals *in vivo*. However, these reactions are expected to be retarded in the environment of the inflamed rheumatoid joint which has a diminished amount of oxygen in the tissues, i.e in a hypoxic environment.

On further exposure of the white titanium dioxide ($\text{TiO}_2 \cdot n\text{H}_2\text{O}$) solid (derived from the oxidation of the deep blue mixed Ti (III)/Ti (IV) oxide) to the atmosphere a yellow/brown discolouration was observed. This colour change was thought to be due to the presence of the white/yellow titanium (IV) hydroxide species in the product.

5.3.1 FTIR Spectroscopic Analysis

The titanium (III) compounds prepared (including the polynuclear titanium (IV) oxo/hydroxo complexes and their autoxidation products) were examined by FTIR spectroscopy to help elucidate their structure. The absorption bands displayed, as mentioned earlier, were attributable to Ti (III)-O stretches and to the multinuclear

species derived from titanium (IV) oxysulphate ($\text{Ti}^{(\text{IV})}\text{OSO}_4$) or titanium (IV) potassium oxalate ($\text{K}_2\text{Ti}^{(\text{IV})}\text{O}(\text{C}_2\text{O}_4)$) which contained titanium (III) co-ordinated to the respective sulphate or oxalate. The presence of oxalate was further implied by a carbon content of ca. 5%, as given by elemental CHN analysis.

The localised dark blue/black prosthesis-derived tissue samples were manually isolated from affected tissues obtained from patients undergoing revision surgery and were examined by FTIR spectroscopy. A typical FTIR spectrum of such a sample is shown in Figure 5.8. A very broad absorption band is seen in the lower region at $800\text{-}400\text{ cm}^{-1}$, which could be due to the presence of Ti (III)-O and/or Ti (IV)-O stretches. A FTIR spectrum of commercially available titanium (IV) oxide (TiO_2) was run and as seen in Figure 5.9, exhibited two intense bands at 672 and 532 cm^{-1} . This suggests that the Ti-O stretches present in the spectrum of the tissue sample could be attributed to Ti (IV)-O stretches of the $\text{TiO}_2\cdot n\text{H}_2\text{O}$ formed on the oxidation of the blue coloured titanium oxo/hydroxo complex, together with underlying Ti (III)-O stretching bands of the complex itself. The complex tissue sample spectrum also exhibits numerous other absorption bands, which can be tentatively assigned to endogenous protein, polysaccharide and other low molecular weight components.

The stretches at 1652 and 1636 cm^{-1} , are attributed to amide and C=O stretches arising from proteins. The regions of $1610\text{-}1550\text{ cm}^{-1}$ and $1420\text{-}1300\text{ cm}^{-1}$ indicate the respective antisymmetrical and symmetrical stretches of the carboxylate anion. The presence of overlapping bands in the $1150\text{-}1000\text{ cm}^{-1}$ region may point towards the presence of some titanium (III) or titanium (IV) co-ordinated phosphate. A typical spectrum of a synovial tissue sample derived from a patient with no joint prosthesis is shown in Figure 5.10 as a reference.

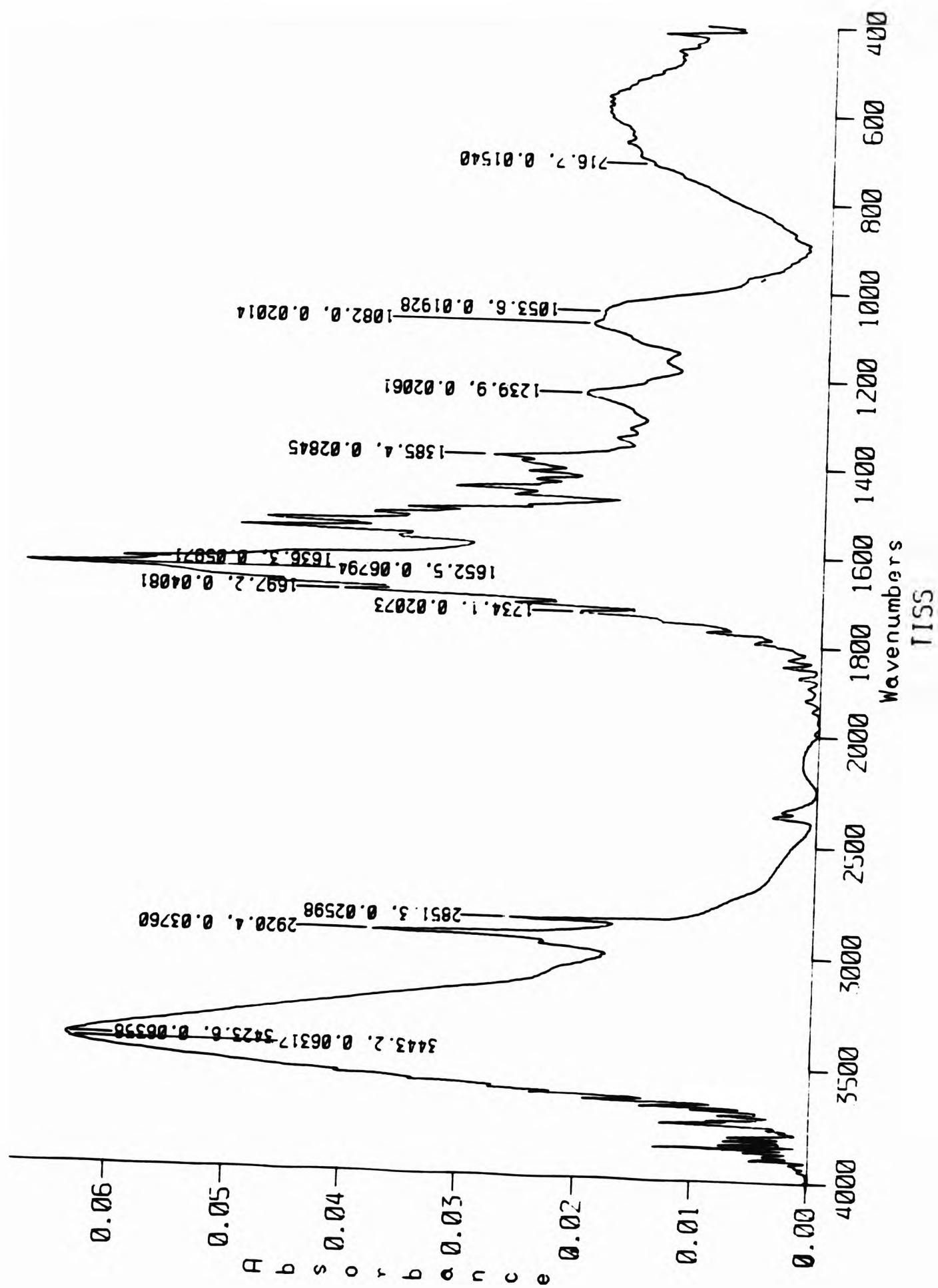


Figure 5.8 FTIR of a Localised Blue/Black Tissue Sample From a Patient Undergoing Revision Surgery for a Failed Titanium Alloy Hip Implant.

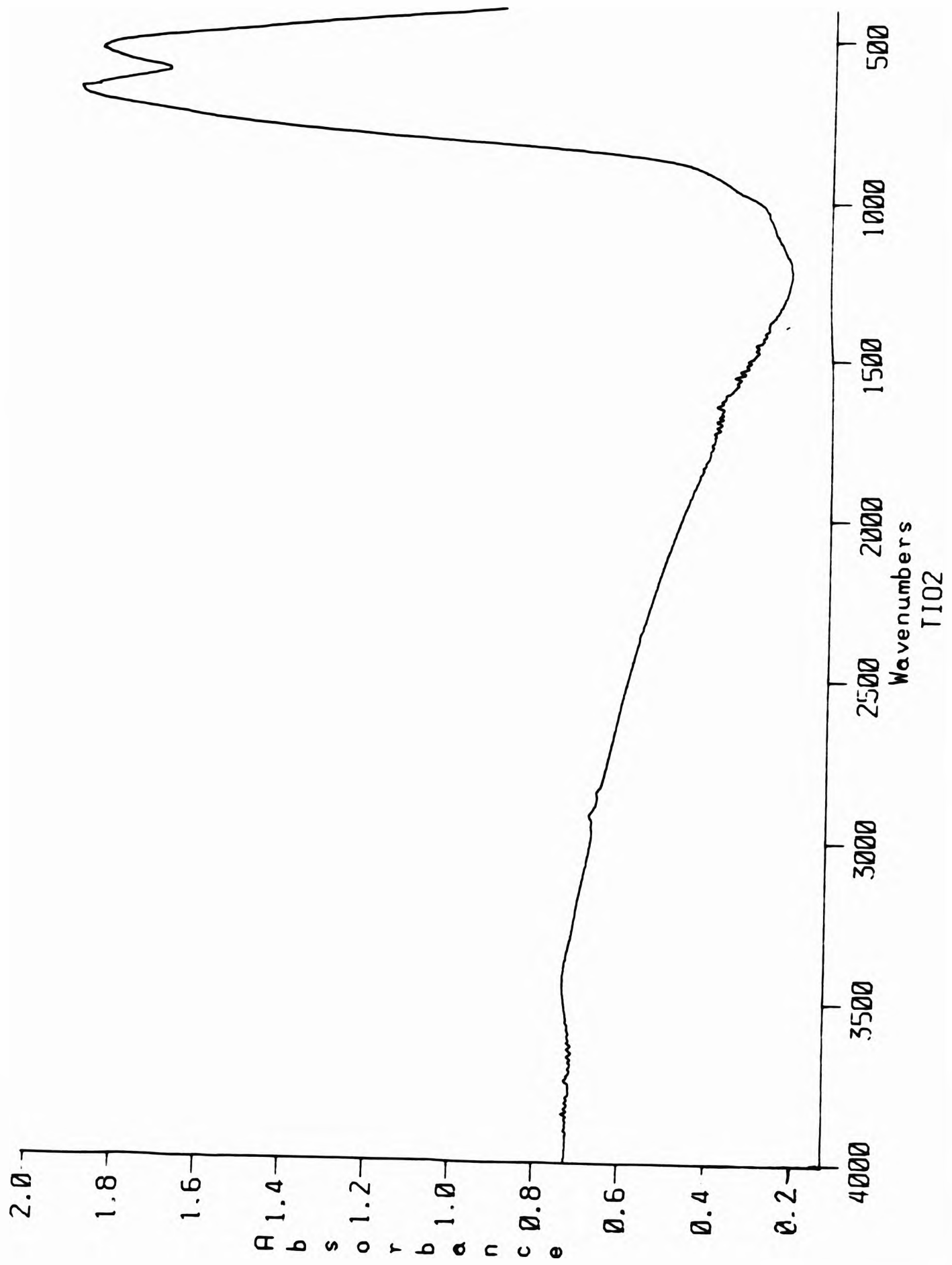


Figure 5.9 FTIR of Titanium Dioxide.

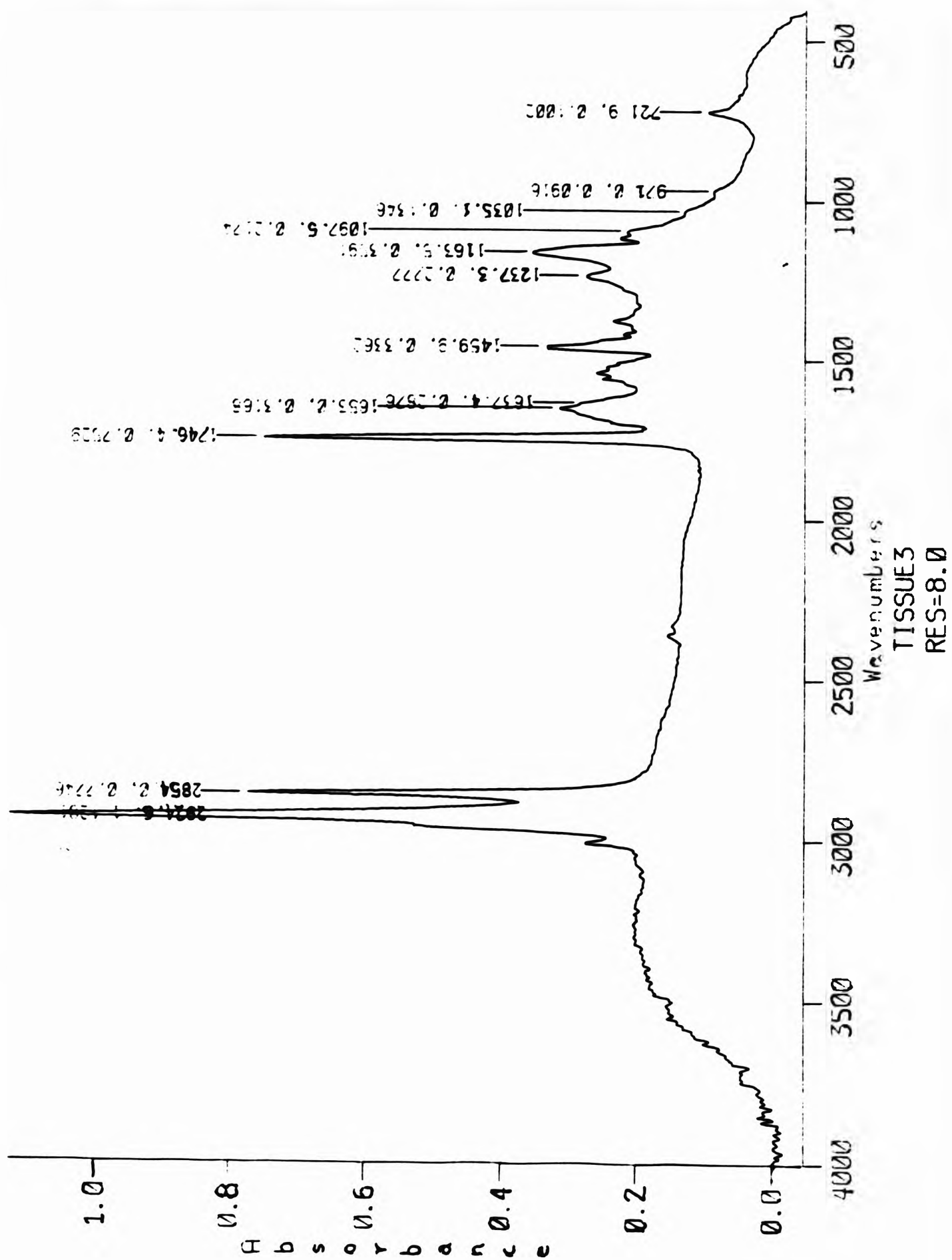


Figure 5.10 FTIR of Tissue Sample from a Patient with No Titanium Alloy Hip Implant.

5.3.2 High Field Proton Hahn Spin-echo NMR Analysis of Synovial Fluid Treated with Titanium (IV)

Hahn spin-echo was used to ascertain the molecular nature and speciation of the titanium (IV) ions in the synovial fluid surrounding the implant joint. Successive increasing concentrations of $[\text{Ti}^{\text{IV}}\text{O}(\text{C}_2\text{O}_4)_2]^{2-}$ (0.10 - $1.52 \times 10^{-3} \text{ mol dm}^{-3}$) solution were introduced to the synovial fluid samples (Figs. 5.11 and 5.12). A small amount of a white solid was seen to be precipitated. There was a notable broadening of the peaks attributable to the citrate $-\text{CH}_2-$. The peaks attributable to the succinate $-\text{CH}_2-$ and the acetate $-\text{CH}_3$ were seen to a lesser extent, as the time delay between the pulses was adjusted so as to be close to their spin-spin relaxation times. This indicates that these endogenous oxygen-donor ligands interact with the $[\text{TiO}(\text{C}_2\text{O}_4)_2]^{2-}$ to give rise to titanium (IV)-citrate and/or ternary titanium (IV)-citrate-succinate or titanium (IV)-citrate-acetate complexes by way of ligand substitution involving the release of one or both of the oxalate ligands from the titanium (IV) complexation sphere.

The initial formation of the transient white precipitate on addition of the titanium (IV) oxalate salt is consistent with the observed formation of insoluble calcium (II)-oxalate derived from the relatively high concentration (ca. $2 \times 10^{-3} \text{ mol dm}^{-3}$) of Ca^{2+} ions found within synovial fluid.

Subsequent addition of excess ascorbate ($1.00 \times 10^{-2} \text{ mol dm}^{-3}$) to the titanium (IV)-synovial fluid samples and equilibration for 45 minutes at ambient temperature produced a "sharpening" of the peaks attributable to citrate (Figure 5.13). This sharpening demonstrated the transfer of Ti (IV) from citrate to ascorbate. In this instance, ascorbate probably takes on the role of a bidentate oxygen donor ligand.

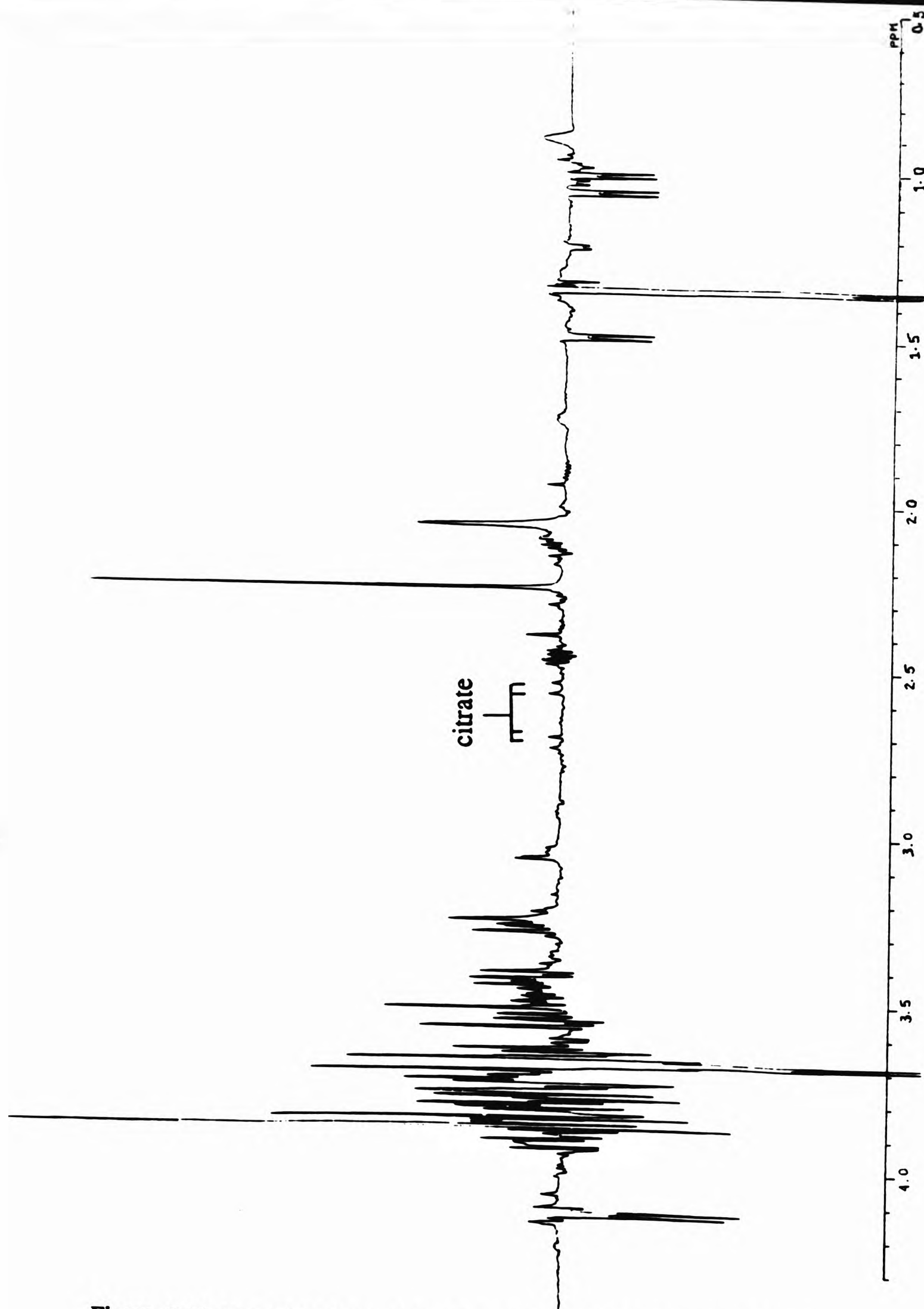


Figure 5.11 High Field Proton Hahn Spin Echo NMR of Synovial Fluid Treated with $1.55 \times 10^{-4} \text{ mol dm}^{-3}$ Titanium (IV) Potassium Oxalate.

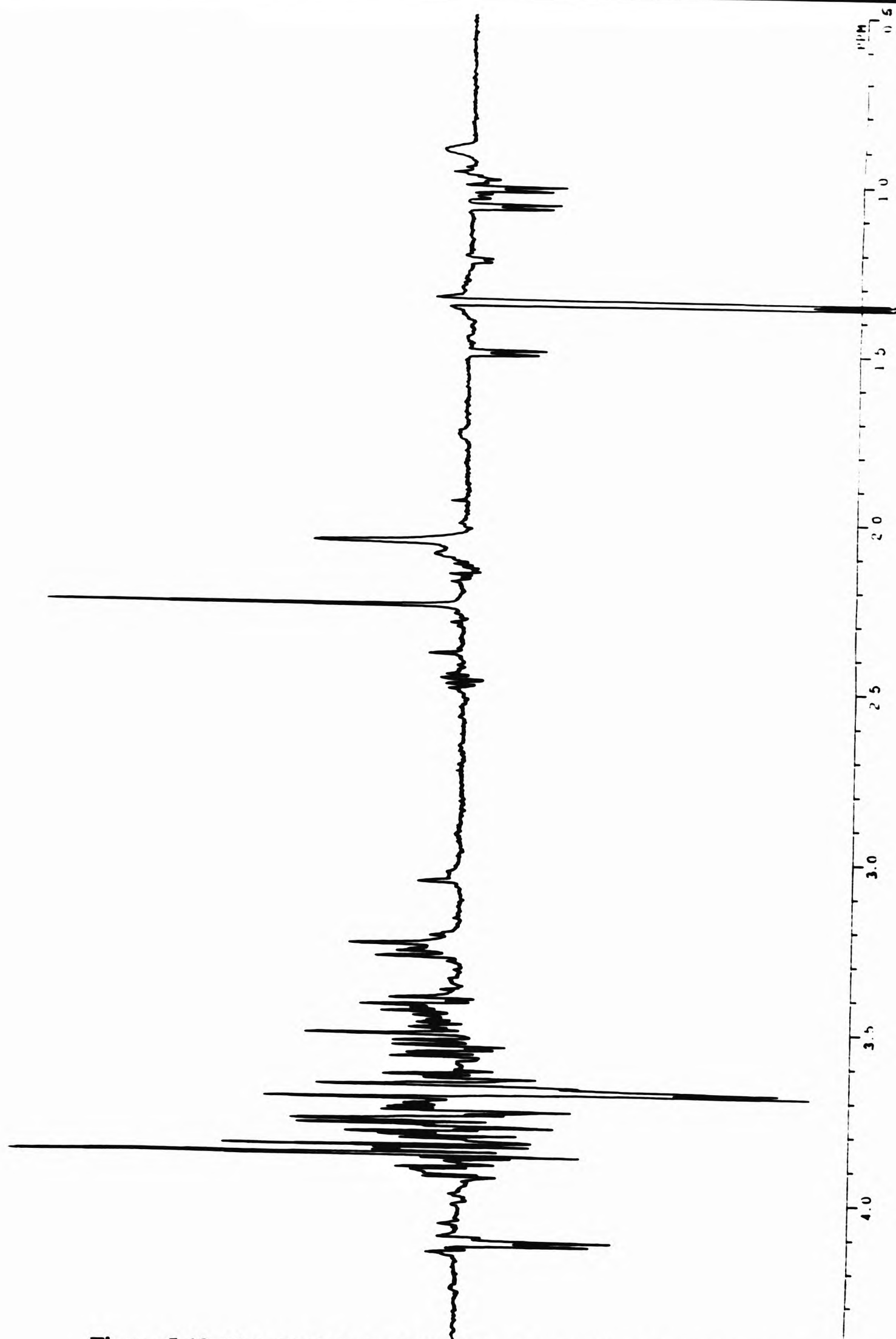


Figure 5.12 High Field Proton Hahn Spin Echo NMR of Synovial Fluid Treated with $1.52 \times 10^{-3} \text{ mol dm}^{-3}$ Titanium (IV) Potassium Oxalate.

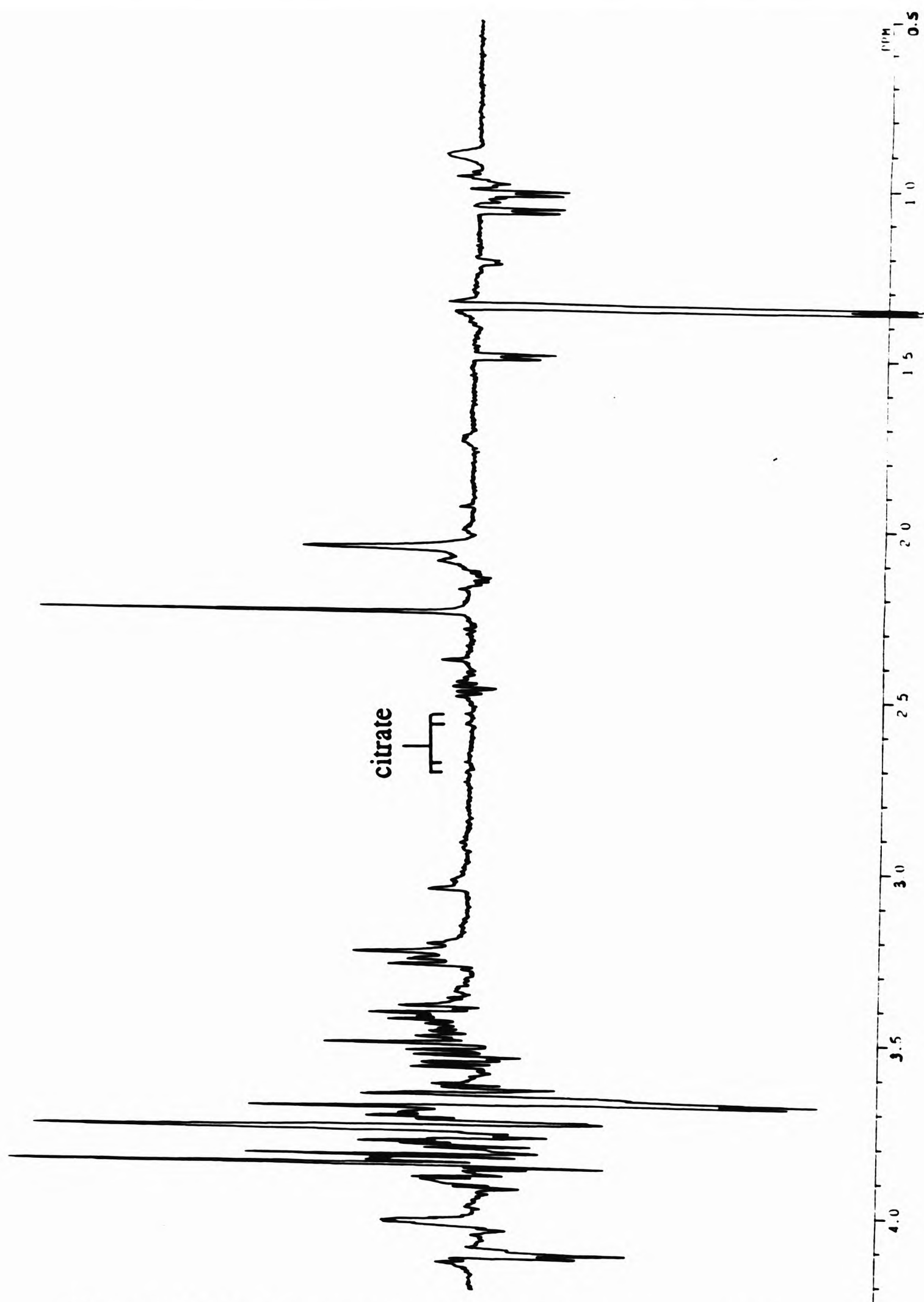


Figure 5.13 High Field Proton Hahn Spin Echo NMR of Synovial Fluid Treated with $1.52 \times 10^{-3} \text{ mol dm}^{-3}$ Titanium(IV) Potassium Oxalate and $1.00 \times 10^{-2} \text{ mol dm}^{-3}$ Ascorbate.

It has long been known that titanium forms an intensely orange complex with ascorbate¹⁴⁸ in aqueous solution. This orange colour was seen on the addition of excess ascorbate to the titanium-containing synovial fluid sample, indicating the formation of one or more titanium (IV)-ascorbate or ternary titanium (IV)-ascorbate-citrate complexes. The colour change occurs due to an oxygen-to-titanium (IV) (ligand to metal ion) charge transfer absorption band centered in the near UV region of the electromagnetic spectrum at ca. 360 nm.

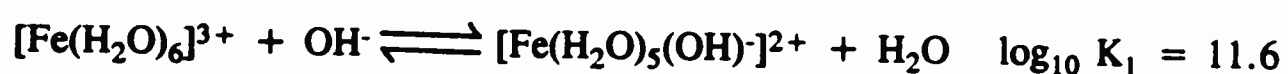
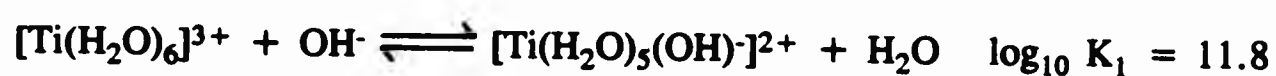
It has been postulated that the predominant titanium species in excess ascorbate is a tris-(ascorbato) Ti (IV) complex ($[\text{Ti}(\text{Asc})_3]^{2-}$), which is formed in aqueous solution at pH 4. The proposed octahedral complex is thought to have three 5-membered chelating rings, involving the neighbouring deprotonated hydroxyl oxygen atoms which act as donor atoms, and are found on the unsaturated heterocyclic ring of the ligand. The chelate is discouraged from undergoing an intramolecular redox reaction due to the stability of titanium (IV) relative to titanium (III), that is to say that the redox potential of the Ti (III)/Ti (IV) system is low.

In all the 5 synovial fluid samples studied, the ascorbate dependant resharping of the titanium broadened citrate resonances were reproducible. However, in every case the resharping of the citrate resonances did not reach completion, even on prolonged exposure (>24 hr) the peaks did not return to the state prior to treatment with titanium (IV). This indicates that ascorbate has a lower affinity for Ti (IV) than citrate.

5.4 CONCLUSION

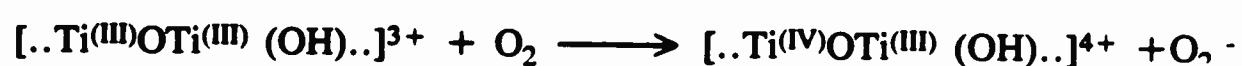
The coloured titanium (III) oxo/hydroxo complexes were produced relatively easily from the implant derived Ti (III) ions and this is not surprising considering the hydrolysis of the hexaaqua cation ($[\text{Ti}(\text{H}_2\text{O})_6]^{3+}$) is thermodynamically favoured. Pecsok and Fletcher¹⁵⁰ reported the rapid formation of such a polynuclear titanium (III)-oxo/hydroxo species at pH values above 3.5, which were more sensitive to oxidation than either Ti^{3+} or TiOH^{2+} . They also showed that electronic absorption spectra of aqueous solutions of these species gave a number of diffuse bands which spanned the entire visible region of the spectra. The bands were responsible for the stability of the black colour of the solutions upon the addition of the chelator sodium tartrate.

As with the polynuclear titanium (III) species synthesised, iron (III) chelate complexes also readily polymerise to form the multinuclear iron (III)-oxo/hydroxo species. The two metals have in common similar hydrolytic equilibria as illustrated:



The polynuclear titanium (III) complex derived from the titanium alloy prosthesis, manifests itself as a localised, insoluble deposit in the interface tissue, since the physiological pH readily facilitates precipitation of such a species. However in the inflamed joint environment, it is possible that chelators such as phosphate, sulphate, citrate or oxalate (oxalate is present only in very low levels in normal biological fluids; $\mu\text{mol}.\text{dm}^{-3}$ or below in normal human plasma) are capable of retaining some of the titanium (III)-oxo/hydroxo polymers in solution.

The relatively rapid oxidation of the synthetically produced Ti (III)-oxo/hydroxo complexes, upon exposure to air is significant in view of its potential ability to generate the superoxide anion by electron transfer to molecular oxygen *in vivo*:-



Reactions such as these, are however retarded in an anoxic environment and as the titanium is detected as Ti (III) rather than Ti (IV) when newly isolated from the tissue sample, this indicates that a reduction, such as expressed, occurs to a limited extent, if at all. Indeed, the abnormal profile of a chronically inflamed joint is partly characterised by the hypoxic (diminished oxygen) environment of the joint, and as such would retard the radical generating pathways. The titanium may be partly stabilised by the reducing environment of the biological matrices due to the presence of electron donors such as thiols in the form of cysteine or glutathione.

Polynuclear titanium (III)-oxo/hydroxo complexes may promote the destructive generation of $\cdot OH$ radicals from peroxide (H_2O_2) even though the relative insolubility of such a titanium (III) species at a physiologically relevant pH, will likely modulate the extent of these reactions *in vivo*.

Tengvall *et al*¹⁴⁵, suggested that as well as the production of the oxidising $Ti(IV)O_2 \cdot (OH)_y$ species from the reactions of titanium (IV) with protonated superoxide (HO_2), or $Ti(IV)O_2^{2-} (OH)_x$ with the $\cdot OH$ radical, the oxidant may also form due to the direct interaction of titanium (III) from the implant with molecular oxygen. This reaction pathway could also be brought about due to an increase in oxygen pressure, derived from titanium metal mediated hydrogen peroxide decomposition.

The relatively rapid autoxidation of the titanium (III)-oxo/hydroxo complex reported in this work supports the hypothesis that the superoxotitanium (IV) component is derived from Ti (III).

Also possibly present in the affected tissue, is the dark blue coloured mixed titanium (III)/titanium (IV) oxide (Ti_3O_5) and it may significantly contribute to the distinctive blue/black colour observed. It has been reported that the thermal oxidation of titanium metal gives rise to a layered structure consisting of TiO , Ti_2O_3 , Ti_3O_5 and TiO_2 in the given order, from the oxide interface to the surface. The lower titanium oxides are formed first and their potentially continuous oxidation and regeneration is likely to have important biological consequences for the bone-implant interface of the titanium prosthesis. The hypoxic environment of the inflamed rheumatic joint may promote the lifetime of such species *in vivo*.

Treating rheumatoid synovial fluid samples with increasing concentrations of titanium (IV) and following the reactions using Hahn spin-echo NMR spectroscopy, provided evidence that citrate, acting as a tetradentate oxygen donor ligand complexes with non-protein bound titanium. A significant amount of the titanium (IV) is probably derived from the autoxidation of polynuclear Ti (III)-oxo-hydroxo species *in vivo*. There was an observable broadening of citrate resonances on addition of $0.10-1.03 \times 10^{-3} \text{ mol dm}^{-3}$ Ti (IV) to the synovial fluid samples. The resonances due to succinate and acetate were broadened to a lesser extent. The NMR spectra suggest that the non-protein bound, low-molecular mass titanium (IV) is mainly present as titanium (IV)-citrate complexes. The relatively low level of broadening observed in the succinate and acetate resonances, is probably due to their involvement with titanium (IV) and citrate in the formation of ternary Ti (IV)-citrate-succinate and Ti (IV)-citrate-acetate complexes. Even though the amount of citrate present in rheumatoid synovial fluid will significantly

vary between patients (ca. $0.5-4.5 \times 10^{-4} \text{ mol dm}^{-3}$), it is expected to be present in excess compared to the level of implant derived Ti(IV) *in vivo*, so facilitating the formation of titanium (IV)-complexes.

Considering the prevalence of Ti(IV)-O in titanium (IV) chemistry it is not surprising that the endogenous citrate molecules complex with titanium (IV). Recently work has been carried out using proton NMR spectroscopy, showing the ability of citrate to complex with low-molecular mass (non-transferrin bound) iron (III) in rheumatoid synovial fluid¹⁴⁹.

Incubating the titanium (IV) loaded synovial fluid with excess ascorbate produced changes in the citrate resonances. This demonstrates that the titanium (IV) is partially transferred from the citrate to the ascorbate ligand under the experimental conditions. The concentrations of the (reduced) ascorbate within the rheumatoid synovial fluid are, however, depleted due to the fact that ascorbic acid is prone to oxidative damage by way of highly reactive oxygen radicals (e.g. $\cdot\text{OH}$ radicals). Indeed, the concentration of ascorbate in synovial fluid (ca. $8.0 \times 10^{-6} \text{ mol dm}^{-3}$) has been shown to be notably lower than that of dehydroascorbate (ca. $3.3 \times 10^{-5} \text{ mol dm}^{-3}$). Therefore the concentrations of ascorbate in rheumatoid synovial fluid are of a level which would greatly limit its ability to compete with other endogenous chelating ligands such as citrate.

In conclusion, this work has gone some way in identifying the chemical nature of titanium metal as found in the previously observed and reported phenomenon, of staining of the tissue adjacent to failed hip prosthesis implants. FTIR and NMR has been used to provide an overview of the prosthesis derived titanium (III) and titanium (IV) species. The proliferation of these species may be harmful and by an understanding of their chemical nature, therapeutic agents may be investigated which may chelate with the redox active metal ions.

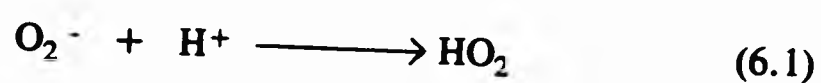
CHAPTER 6

**SPECIATION OF NON-TRANSFERRIN BOUND IRON IN
SYNOVIAL FLUID OF RHEUMATOID ARTHRITIS PATIENTS
BY PROTON HAHN SPIN-ECHO NMR.**

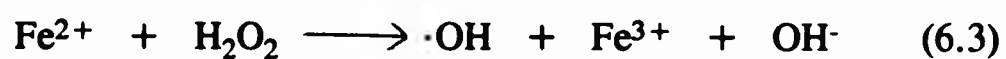
6.1 INTRODUCTION

It has been reported¹⁵¹ that the knee joint synovial fluid of rheumatoid arthritis patients contains non-transferrin bound iron. The iron is redox-active and can readily act as a catalyst to promote the production of the hydroxyl radical ($\cdot\text{OH}$) from the superoxide radical ion (O_2^-) and hydrogen peroxide (H_2O_2) which are released from inflamed sites by activated polymorphnuclear leucocytes and macrophages¹⁵².

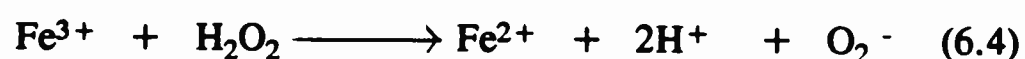
The one-electron reduction of oxygen (O_2) produces the superoxide radical ion, O_2^- . Superoxide is formed in almost all aerobic cells, a major source being the "leakage" of electrons on to O_2 from various components of the cellular electron transport chains. An elevated oxygen concentration increases the O_2^- production by activated phagocytic cells. The superoxide radical undergoes a dismutation reaction, which at physiological pH occurs in two stages:



Hydrogen peroxide, H_2O_2 , is produced from the superoxide radical ion by a non-enzymic or an enzymic superoxide dismutase (SOD) catalysed dismutation reaction. The O_2 and H_2O_2 are relatively poorly reactive in themselves, in aqueous solution, but the iron dependent decomposition of hydrogen peroxide generates the highly reactive hydroxyl radical, $\cdot\text{OH}$. The so-called Fenton reaction (Equation 6.3) follows the production of the hydroxyl radical from the H_2O_2 which occurs only in the presence of iron.



Traces of Fe^{3+} can react further with H_2O_2 :



Overall the reaction taking place can be summarised in the metal-catalysed Haber-Weiss reaction (6.5).



The hydroxyl radical readily reacts with molecules at or close to its site of formation, modifying the existing biomolecules with deleterious effect. These degradation products can stimulate synovitis and can be responsible for progressive joint destruction^{153,154}. For this reason it is important to investigate the chemical nature of the non-transferrin-bound iron.

For many years it has been known that there are abnormalities in the iron metabolism of rheumatoid arthritis patients^{155,156}. There is a rapid fall in the total iron content of blood plasma at the onset of inflammation. This is followed by a drop in haemoglobin concentration and an increased deposition of iron proteins in the synovial membrane and fluid¹⁵⁷. The iron in the synovial fluid is largely present within ferritin. Halliwell *et al*¹⁵⁸ reported the presence of "free" iron within RA synovial fluid by development of a specific test that detects non-protein bound iron in biological fluids. This test makes use of bleomycin, an anti-tumour antibiotic which degrades DNA. The degradation by bleomycin is absolutely dependant on the presence of Fe^{2+} ions and so the rate of degradation can be used to assess the "free" iron content of the system. They reported that the small but

significant amount of non-transferrin bound iron, is enough to allow the formation of the $\cdot\text{OH}$ from O_2^- and H_2O_2 generated by the phagocytes in the rheumatoid joint.

Halliwell, Gutteridge and Blake¹⁵⁹ postulated that the formation of hydroxyl radicals is at least partly responsible for cartilage damage. They hypothesised that the presence of the "free" iron was due to a creation of a microenvironment by the "sliding over" of phagocytes over cell surfaces, the pH of which can fall to 5 or below. This acidic environment would facilitate the release of iron from transferrin and would account for the presence of the non-protein bound iron.

As the role of iron in free radical generation is very important, it would be beneficial to investigate the speciation of the "free" iron in the biological system. It has been reported that the chromatographic fractionation of biological fluids leads to protein degradation and to metal ion release¹⁶⁰. The development of an alternative analytical method would therefore be appropriate. Ideally this method would involve little or no pre-treatment. To this purpose nuclear magnetic resonance (NMR) spectroscopy was investigated as a possible alternative method for the metal speciation of the low-molecular weight iron. This technique has been successfully utilised for the study of biological fluids and has been found to be useful in providing details on the concentration and mobility of many low-molecular mass metabolites in biological fluids¹⁶¹. By using Hahn spin-echo NMR and desferrioxamine, a strong hexadentate iron (III) chelator, the low molecular weight, non-transferrin bound iron present in the synovial fluid of rheumatoid patients can be speciated as described in the following work.

6.2 MATERIALS AND METHODS

6.2.1 Materials

Desferrioxamine (Desferal, desferrioxamine B methanesulphonate) was provided by Ciba-Geigy, and analytical grade iron (III) chloride was obtained from BDH Pharmaceuticals.

Proton NMR spectra were obtained on a JEOL GSX-500 NMR spectrometer operating at 500 MHz.

6.2.2 Methods

Knee joint synovial fluid from rheumatoid arthritis patients was drawn into heparinised tubes (n=9). Heparin is a drug used for its anti-coagulant properties. It is a polysaccharide composed of D-glucosamine and D-glucuronic acid units, with N- and O- sulphate esters. It is obtained from beef liver, lung or small intestine.

The samples were centrifuged at 400g for 15 minutes and were then either used for analysis within a few hours of collection, or were stored at -70°C until needed. Serum samples were prepared by letting the freshly obtained blood, from non-heparinised tubes, clot. These serum samples were stored at -70°C also. Control experiments carried out at the Royal London Medical School showed that

none of the criteria studied changed significantly during storage. The preparation of the biological samples prior to their analytical investigation, was carried out by the staff at the Bone and Joint Unit, at The Royal London Medical School.

6.2.3 NMR Measurements

A portion of knee joint synovial fluid (0.60 mL) was introduced to a 5 mm diameter NMR tube and to it was added 0.20 mL of deuterium oxide (D_2O) to provide a frequency lock. A Hahn spin-echo pulse sequence, $D[90^\circ x - T - 180^\circ y - T - \text{collect}]_n$ was performed, where $n = 342-354$. The value of $T = 60$ ms; this being the time after which all the resonances due to the high molecular weight proteins have relaxed and are therefore removed from the spectrum. As explained in Chapter 2, this pulse sequence "cleans up" the spectra by the removal of broad signals due to proteins. A gated secondary irradiation was applied at the water frequency to remove the intense water signal from the spectrum. The samples were run using sodium-3-(trimethylsilyl)-1-propane-sulphonate (TSP), $\delta = 0$ ppm) as an external reference.

On completion of this measurement, 0.02 mL of the iron chelating drug desferrioxamine (3.00×10^{-4} mol dm^{-3}) was added to the NMR tube which was left for over 6 hours, to allow equilibration to take place. After this time another NMR spectrum was run using the same protocol.

6.3 RESULTS AND DISCUSSION

Figure 6.1 shows the proton Hahn spin-echo NMR spectrum of a typical synovial fluid sample from a patient with rheumatoid arthritis. Figure 6.2 shows the difference in the intensity of the peaks attributable to citrate before and after addition and incubation with desferrioxamine. It can be seen that there is a small but reproducible increase in the characteristic citrate resonances when desferrioxamine is present. This result would suggest that some of the low molecular weight non-transferrin bound iron present in the synovial fluid is bound to the citrate. To reaffirm this observation, iron (III) chloride ($1.00 \times 10^{-4} \text{ mol dm}^{-3}$) was added to the sample which was then incubated for 2 hours. A localised NMR spectrum was run. From figure 6.3 it can be seen that the addition of the iron (III) led to a marked broadening of the characteristic AB coupling pattern of the citrate resonances. The addition of a higher concentration of iron (III) chloride ($2.00 \times 10^{-4} \text{ mol dm}^{-3}$) to the synovial sample led to the disappearance of the citrate resonances from the spectrum altogether. Similar results were obtained from five different samples studied.

The resonances of other potential chelators of the iron (III), such as acetate and glutamine, were virtually unchanged by the addition of the iron (III) chloride, even at the higher concentration. This would seem to indicate that citrate is a highly selective chelating ligand of non-transferrin bound iron in synovial fluid.

The iron (III)-loaded samples were subsequently treated and incubated (6h) with an excess of desferrioxamine ($2.5 \times 10^{-4} \text{ mol dm}^{-3}$). A spectrum obtained showed that the citrate resonances reappeared, demonstrating the transfer of the low molecular weight iron from the citrate ligand to the iron chelating drug desferrioxamine.

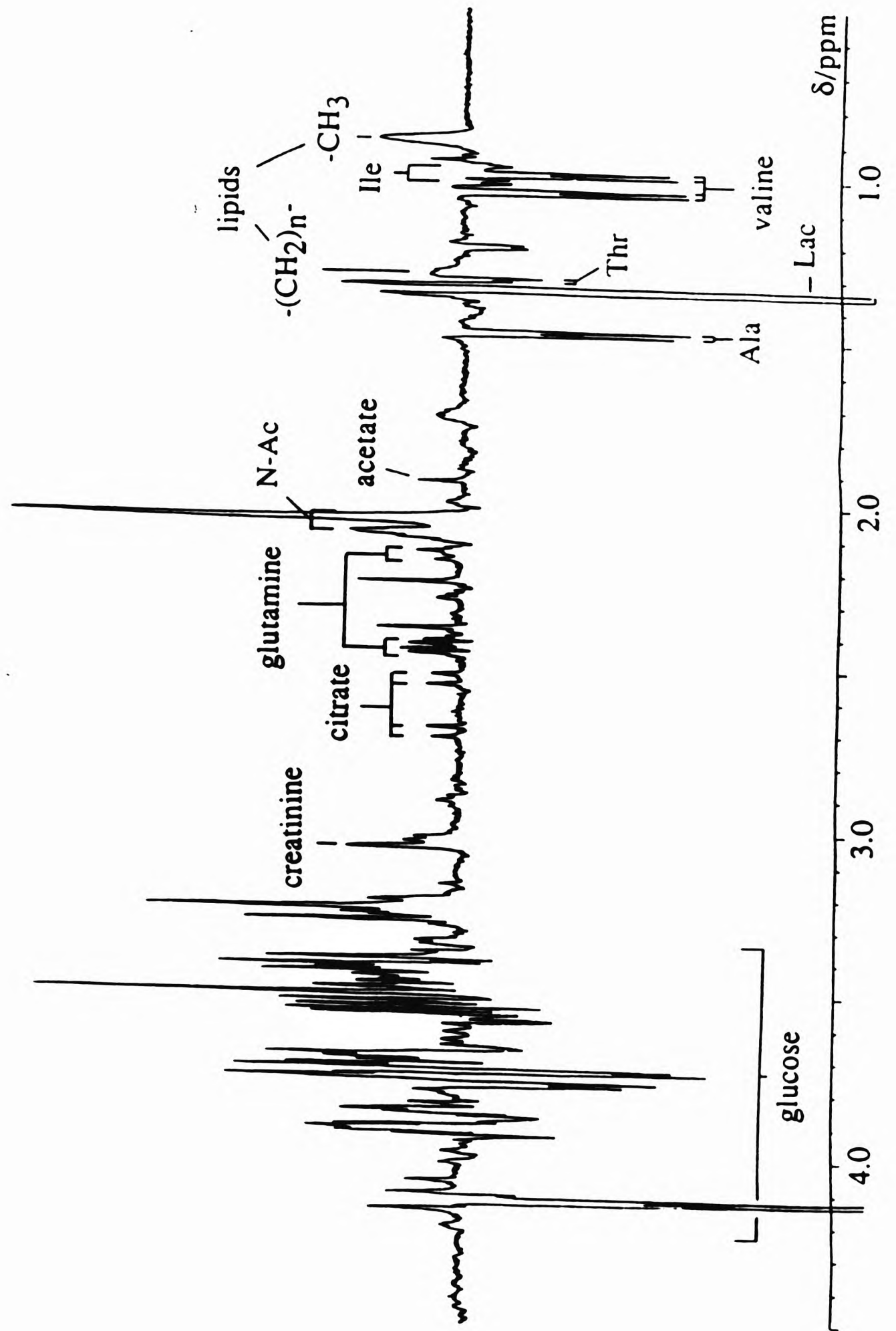


Figure 6.1 500 MHz Proton Spin-echo NMR Spectra of a Typical Synovial Fluid Sample from a Rheumatoid Arthritis Patient.

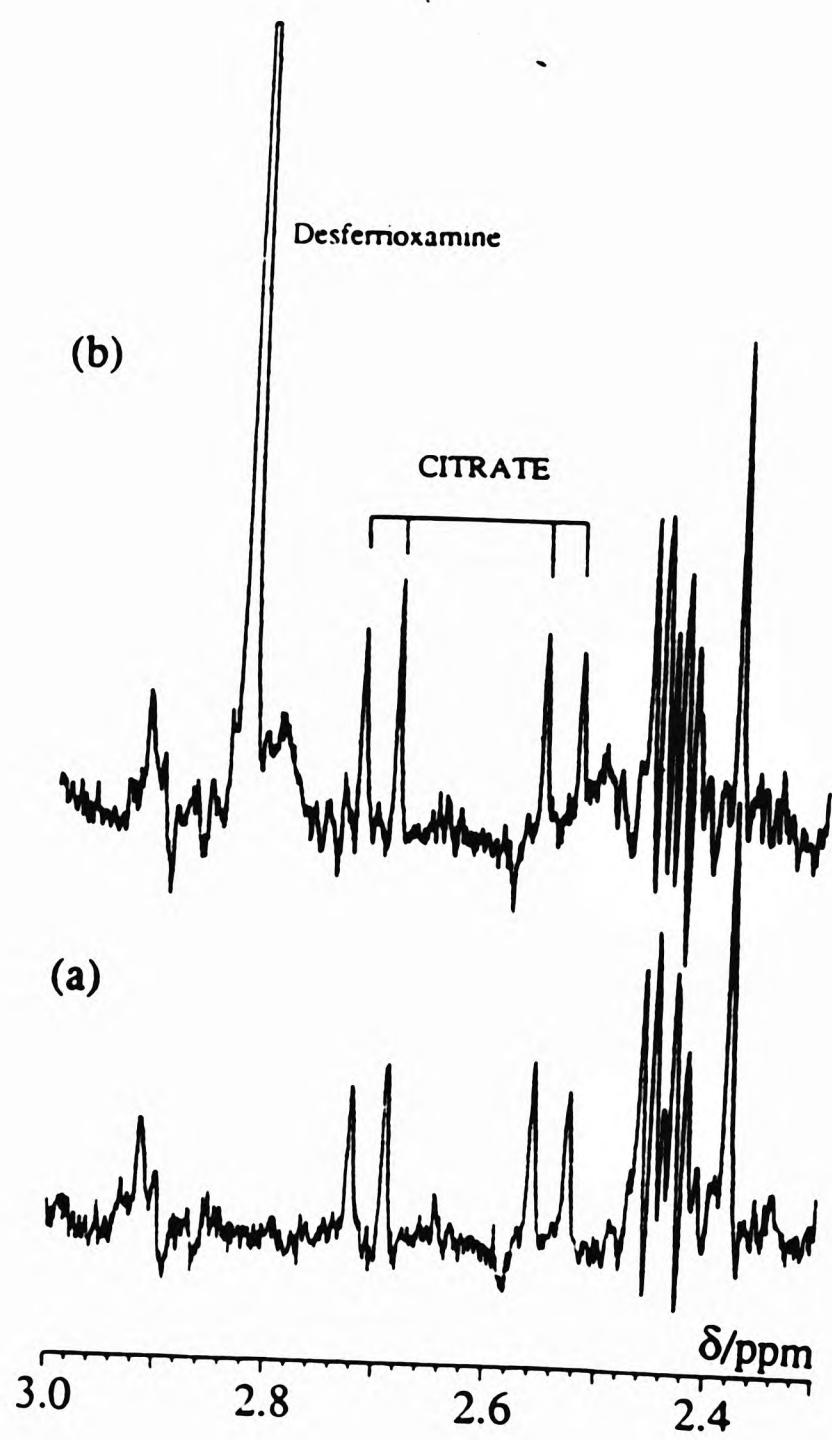


Figure 6.2 500 MHz Proton Spin-echo NMR Spectra of a Typical Sample of Rheumatoid Synovial Fluid (a) Before and (b) After Equilibration with $2.00 \times 10^{-4} \text{ mol dm}^{-3}$ Desferrioxamine.

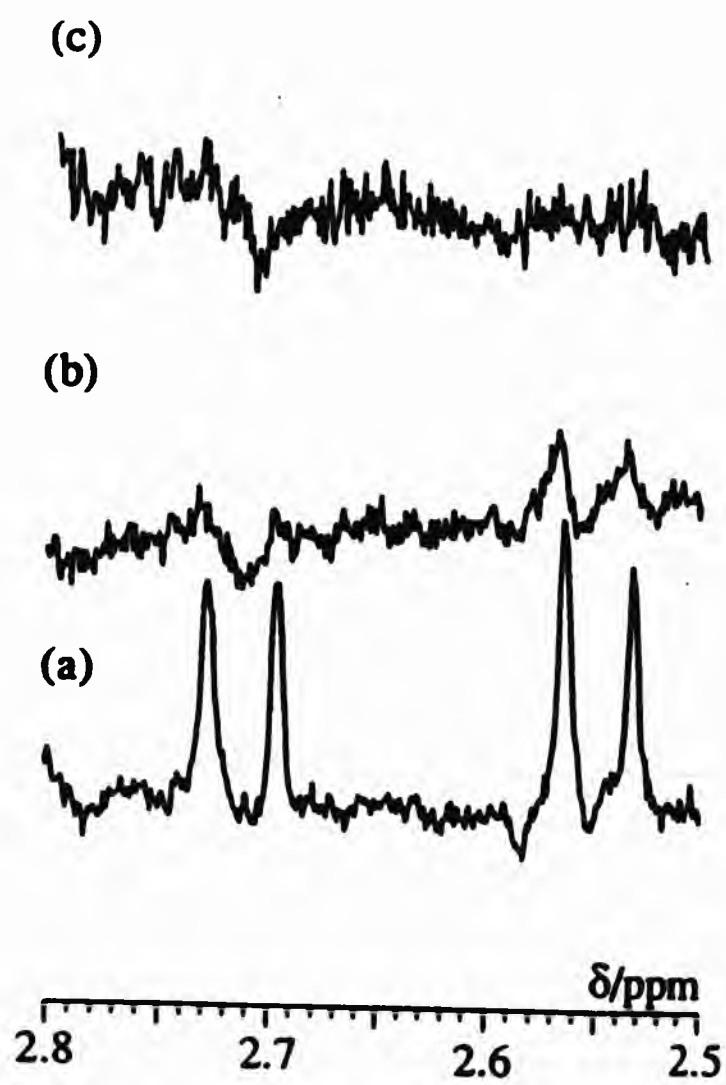


Figure 6.3 500 MHz Proton Spin-echo NMR Spectra of a Typical Sample of Rheumatoid Synovial fluid (a) Untreated Sample (b) With the Addition of 1.00×10^{-4} mol dm⁻³ Iron (III) and (c) With the Addition of 2.00×10^{-4} mol dm⁻³ Iron (III). The Iron Added was in the Form of $TiCl_3$.

The changes in the citrate resonances, within a synovial fluid sample incubated with desferrioxamine, demonstrate the ability of citrate to chelate these low levels of non-transferrin bound iron (ca. $1-8 \times 10^{-6} \text{ mol dm}^{-3}$)¹⁵⁶. This function is very important since the iron can act as a potential catalyst within the biological fluid. As already mentioned, Halliwell and Gutteridge¹⁵⁹ explained the presence of low molecular weight iron in rheumatoid synovial fluid by the drop in pH of the environment, which facilitates the release of iron from transferrin. Further studies¹⁶² proposed that the iron could be liberated from ferritin by chelators such as citrate and acetate. High resolution proton NMR and HPLC work by Grootveld *et al*¹⁶³ indicated that the low molecular weight iron (III) is present as an iron-citrate and/or ternary iron-citrate-acetate complex. In this study however there was no indication that the acetate ligand was acting as a chelator of the non-transferrin bound iron (III).

The levels of non-protein bound citrate, that are detected by NMR in synovial fluid samples, can vary widely both between, and within patients (ca. $0.5-4.5 \times 10^{-4} \text{ mol dm}^{-3}$). Citrate is always present in excess compared to the non-transferrin bound iron. At a neutral pH, the main iron (III)-citrate complex formed is likely to be iron (III)-monocitrate, with all the three carboxylate groups and the hydroxyl group deprotonated. At a more acidic pH, the 1:2 $[\text{Fe}(\text{citrate})_2]^{5-}$ complex forms, and is present as 40 mol % fraction of the total iron concentration at pH 5 in an isolated iron (III)-citrate system¹⁶⁴. It seems probable that the iron-citrate complexes form a major component of the catalytic, low molecular weight iron in synovial fluid.

6.4 CONCLUSION

It can be seen that proton Hahn spin-echo NMR spectroscopy provides us with an invaluable analytical tool with which to study the speciation of the metal ions such as iron (III) within synovial fluid from rheumatoid arthritis patients. With a minimum of sample treatment, metal ion abnormalities of inflammatory joints have been followed. It can be concluded that the low molecular weight iron present in the rheumatoid joint, which is deleterious to its surroundings because of its ability to readily promote production of free radicals, is present as a low molecular mass iron (III)-citrate complex. The harmful presence of the "free" iron can be controlled by the application of the drug desferrioxamine (Desferal), which as shown in this work effectively chelates the potentially catalytic iron.

CHAPTER 7
CONCLUSIONS

CONCLUSIONS

Bone and joint disease is the most common ailment amongst the elderly population. Much research has been done to investigate the causes and mode of action of effective drugs to control the disease, especially in the field of rheumatoid arthritis. As this study shows, metal ions, particularly low molecular weight ions, play an important role in bone and joint disease, whether they are present naturally within the biological environment, or are introduced, as is the case with gold containing drugs and titanium alloy implants. The speciation of the relevant 'free' metal ions will go a long way in helping us to elucidate what is happening in the diseased tissues.

Chrysotherapy with gold containing drugs such as disodium aurothiomalate, have been known to induce remission in rheumatoid arthritis sufferers. Most of the gold is protein bound in the body, but 5-10% of the gold is present as low molecular weight gold. This gold is of interest as it would seem to play an important role in the attainment of chemical equilibrium and in transport processes.

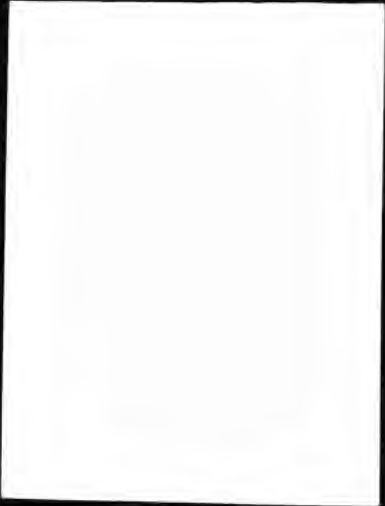
Initial work with the formation of a spectroscopically active Au-dithizonate complex was abandoned after the realisation of the instability of the complex and therefore its unsuitability for the development of a working low molecular gold analysis method.

Using HPLC and atomic absorption spectroscopy as a corroborative tool, a viable qualitative and quantitative analytical method was set up which was used to measure the levels of low molecular weight gold in plasma and synovial fluid obtained from rheumatoid arthritis patients undergoing a course of chrysotherapy. The synovial fluid was found to have in the region of 2.0×10^{-6} mol dm⁻³ of

low molecular weight gold and plasma samples about 4.0×10^{-6} mol dm⁻³ of the non-protein bound gold. This study derived a relatively speedy method for the detection of non-protein bound gold by complexing the gold with cyanide and detecting the resultant dicyanoaurate complex. The method provided an analysis which was sensitive enough for detection of gold at the biologically relevant levels with very little need for pre-treatment. Further work should be done on an effective and quick method for the analysis of protein bound gold.

Titanium implants used in hip replacements, have been employed for many years because of their inert properties. However in failed hip replacement operations, dark staining in tissue adjacent to the prostheses has been noticed in some cases. FTIR was used in this study to show that the dark stained tissue contained Ti complexes, thought to be a mixture of Ti(III)/Ti(IV) complexes. Furthermore Ti(III) complexes were synthesised in vitro which displayed the dark blue colour as seen in the tissue samples. NMR studies carried out gave evidence that non-protein bound Ti(IV) is mainly present in the form of a Ti(IV)-citrate complex. The work carried out, helped to identify the chemical nature of the Ti metal found in the stained tissue. These metal ions may be harmful and further work would need to be carried out to find a suitable chelator to act as a therapeutic agent.

The abnormalities in the iron metabolism of RA patients has been known for many years. The presence of non-protein bound iron in RA synovial fluid has been documented. As the presence of the 'free' iron encourages free radical generation which is deleterious to the biological system it is important to speciate the metal ion. NMR provided an analytical tool with which to study the speciation of Fe with the minimum of sample pre-treatment. It was seen that the free iron was present in synovial fluid as a low molecular mass Fe(III)-citrate complex. Application of the drug desferrioxamine, successfully chelated the free iron. Further work would include the quantifying of the free iron.



The 'free' low molecular weight, or non-protein bound metal ions, present in bone and joint diseased tissues and fluids are of importance because of their more reactive nature and greater 'mobility' compared to protein-bound metal moieties. It is therefore very probable that they play a pivotal role in any therapeutic or deleterious effects due to the presence of metal ions within bone and joint diseased systems, and as such their study is of interest.

In this study a wide range of analytical methods were employed, including HPLC, AA spectroscopy FTIR and NMR. These analytical tools allowed the study of a differing range of 'free' metal ions encountered in bone and joint disease, and so in some way increased the understanding of the metals role and action within the biological system of the diseased tissue.

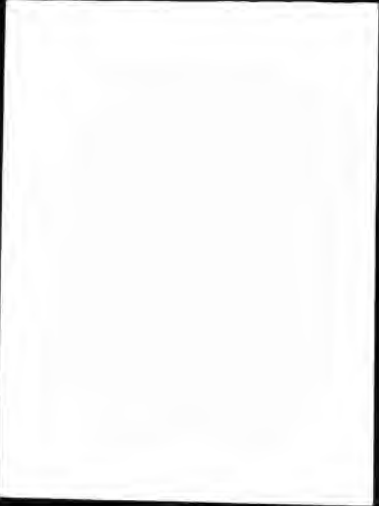


REFERENCES

1. M.N. Hughes, "The Inorganic Chemistry of Biological Processes",
Second Edition, John Wiley and Sons, London, (1985).
2. A.B. Sabin, J. Warren, *J. Bact.*, 40, 823, (1940).
3. D.A. Gerber, *Arthritis and Rheumatism*, 19, 593, (1976).
4. D.A. Gerber, *J. Pharm. Exp. Ther.*, 143, 137, (1964).
5. G.B. Bluhm, *J. Rheum. Suppl.*, 8, 10, (1982).
6. G. Meachim, D.F. Williams, *J. Biomed. Mater. Res.*, 10, 555,
(1973).
7. D.F. Williams, G. Meachim, *J. Biomed. Mater. Res. Symp. No.5, Part
1*, (1974).
8. R.J. Solar, S.R. Pollack, E. Korostoff, *J. Biomed. Mater. Res.*,
13, 217, (1979).
9. P.A. Lalor, P.A. Revell, A.B. Gray, S. Wright, G.T. Railton,
M.A.R. Freeman, *J. Bone Joint Surg. [Br]*, 73-B, 25, (1991).
10. P.G. Bullough, F. Bansall, F. Betts, E.A. Salvati, *J. Bone Joint
Surg. [Br]*, 72-B, 533, (1990).
11. J. Black, H. Sherk, J. Bonino, W.R. Rostoker, F. Schajowicz, J.O.
Galante, *J. Bone Joint Surg. [Am]*, 72-A, 126, (1990).
12. K.D. Rainsford, K. Brune, M.W. Whitehouse, *Agents and Actions
Supps.*, 8, (1981).
13. J.R.J. Sorenson, *Prog. Med. Chem.* 15, 211, (1978).
14. R.M. Mason, *Diseases of Joints*, "Prices Textbook of the Practice of
Medicine", Ed. R.B. Scott, 12th Ed., Oxford University Press,
(1978).
15. J.L. Decker, D.G. Malone, B. Haraoui, S.M. Wahl, L. Schrieber,
J.H. Klippel, A.D. Steinberg, R.L. Wilder, *Ann. Int. Med.*, 101,
810, (1984).
16. A. Engstrom-Laurent, R. Hallgren, *Ann. Rheum. Dis.*, 44, 83, (1985)

17. G.B. Bluhm, *J. Rheumat.*, Suppl. 8, 10, (1982).
18. B.S. Nepom, U. Malhorta, D.A Schwartz, J.W. Nettles, J.G. Schaller, P. Concannon, *Arth. Rheum.*, 34, 1254, (1991).
19. B. Gudbjornsson, A. Zak, F. Niklasson, R. Hallgren, *Ann. Rheum. Dis.*, 50, 669, (1991).
20. J.B. Weinberg, A.M.M. Pippen, C.S. Greenberg, *Clin. Orth. Rel. Res.*, No. 271, 305, ((1991).
21. N.R. Matheson, *Biochem. Biophys. Res. Commun.*, 108, 259, (1982).
22. N.R. Matheson, P.S. Wong, M. Schuyler, J. Travis, *Biochem.*, 20, 331, (1981).
23. B. Halliwell, J.M.C. Gutteridge, D.R. Blake, *Phil. Trans. Roy. Soc. (London)*, 311, 650, (1985).
24. D.R. Blake, P. Merry, J. Unsworth, B. Kidd, J.M. Outhwaite, R. Ballard, C.J. Morris, L. Gray, J. Lunec, *Lancet*, i, 289, (1989).
25. P. Merry, P.G. Winyard, C.J. Morris, M. Grootveld, D.R. Blake, *Ann. Rheum. Dis.*, 48, 864, (1989).
26. B.M. Sutton, "Gold and Silver in Medicine - Metal Chemotheurapeutic Agents", Chap. 18, pg 355-369, *Am. Chem. Soc.* (1983).
27. P.D. Hart, *Brit. Med. J.*, 2, 805, (1946).
28. J. Forestier, *B. Soc. Med. Hosp.*, 53, 323, (1929).
29. J. Forestier, *J. Lab. Clin. Med.*, 20, 827, (1935).
30. ERC Trial, *Ann. Rheum. Dis.*, 20, 315, (1961).
31. T.J Constable, A.P. Crockson, R.A. Crockson and B. McConkey, *The Lancet*, May 24, 1176, (1975).
32. Goodman and Gilman, "The Pharmacological Basis of Theurapeutics", 7th Edition, Macmillan Publishing Company, New York, (1985).
33. M.C. Grootveld, M.T. Razi, P.J. Sadler, *Clin. Rheum.*, 351, 5, (1984).
34. P.J. Sadler, *J. Rheum.*, 9, 71, (1982).

35. D.H. Brown, W.E. Smith, *Chem. Soc. Rev.*, 9, 217, (1980).
36. A.K.H. Sa'ady, K. Moss, C.A. McAuliffe, R.V. Parish, *J. Chem. Soc. Dalton Trans.*, 1609, (1984).
37. M.C. Grootveld, P.J. Sadler, *J. Inorg. Chem.*, 19, 51, (1983).
38. C.J. Danpure, D.A. Fyfe, J.M. Gumpel, *Ann. Rheum. Dis.*, 38, 364, (1979).
39. M.H. Rayner, M. Grootveld, P.J. Sadler, *Int. J. Clin. Pharm. Res.*, IX(6), 377, (1989).
40. C.J. Danpure, *Biochem. Soc. Trans.*, 4, 161, (1976).
41. C.F. Shaw, G. Schmitz, H.O. Thompson, P. Witkeiwicz, *J. Inorg. Biochem.*, 10, 317, (1974).
42. F.N. Ghadially, *J. Rheumatol.*, 6, 25, (1979).
43. C.F. Shaw, *Inorg. Perspect. Biol. Med.*, 2, 287, (1979).
44. R.C. Gerber, H.E. Paulus, R. Bluestone, *Arthritis Rheum.*, 15, 625, (1972).
45. C.F. Shaw, N. Schaeffer-Memmel, D. Krawczak, *J. Inorg. Biochem.*, 26, 185, (1986).
46. D.A. Gerber, *J. Immunol.*, 92, 885, (1964).
47. D.A. Gerber, *Arthritis and Rheumatism*, 19, 593, (1976).
48. A. Wildfeuer, *Drug Res.*, 33, No. 5, 780, (1983).
49. M. Harth, P.A. Keown, J. Orange, *J. Rheum.*, Supp. No. 11, 10, 76, (1983).
50. M.J. DiMartino, D.T. Waltz, *Inflammation*, 2, 131, (1977).
51. D. Burkhardt, R.W. Stephens, P. Ghosh, T.K.F. Taylor, *Agents and Actions*, 8, 251, (1978).
52. R.S. Ennis, J.L. Granada, A.S. Posner, *Arth. Rheum.*, 11, 756, (1968).
53. S.K. Mallya, H.E. Van Wart, *Biochem. Biophys. Res. Comm.*, 144, 101, (1987).

- 
54. K.J. Stone, S.J. Mather, P.P Gibson, *Prostaglandins*, 10, 241, (1975).
 55. S. Norn, *Acta Pharm. Tox.*, 22, 369, (1985).
 56. D.T. Waltz, D.E. Griswold, *Inflammation*, 3, No. 2, 117, (1978).
 57. H.G. Parkes, M.C. Grootveld, E.B. Henderson, A. Farrell, D.R. Blake, *J. Pharm. Biomed. Anal.* 9, (1), 75, (1991).
 58. P. Merry, M. Grootveld, J. Lunec, D.R. Blake, *Am. J. Clin. Nutr.*, 53, (1), 3625, (1991).
 59. M. Grootveld, E.B. Henderson, A. Farrell, D.R. Blake, H.G. Parkes, P. Haycock, *Biomed. J.*, 15, 273, (1991).
 60. D.P. Naughton, R. Haywood, D.R. Blake, S. Edmonds, G.E. Hawkes, M. Grootveld, *FEBS Lett.*, 332, 221, (1993).
 61. P.F. Maestro, *Acta Physiol. Scand.*, 492, 153, (1980).
 62. J. McCord, K. Wong, S.H. Stokes, *Acta Physiol. Scand.*, 492, 25, (1980).
 63. M. Grootveld, D.R. Blake, T. Sahinoglu, A.W. Claxson, P. Mapp, C. Stevens, R.E. Allen, A. Furst, *Free Rad. Res. Comm.*, 10, 199, (1991).
 64. M. Grootveld, A.W. Claxson, D. Naughton, M. Whelan, A. Furst, D.R. Blake, *Agents Actions Suppl.*, 32, 65, (1991).
 65. E.J. Corey, M.M. Mehrotra, A.U. Khan, *Science*, 236, 68, (1987).
 66. E. Jellum, E. Munthe, G. Guldal, J. Aaseth, *Ann. Rheum. Dis.*, 39, 155, (1980).
 67. D.F. Williams, *Med. Prog. Technol.*, 4, 31, (1976).
 68. B.J. Kasemo, *Prosthet. Dent.*, 49, 832, (1983).
 69. G.H. Hille, *J. Mater.*, 1, 21, (1966).
 70. R.T. Bothe, L.E Beaton, H.A. Davenport, *Surg. Gynecol. Obstet.*, 71, 49, (1940).
 71. J. Lausmaa, *Acta Orthop. Scand.*, 59, 199, (1988).


72. D. Nicholls, "Complexes and First Row Transition Elements", Goodman and Gilman, Macmillan Press Ltd., (1974).
73. J.J. Lingare, "Analytical Chemistry of Selected Metallic Elements", Reinhold Publishing Company, (1966).
74. K.G. Strid, *Acta Orthop. Scand.*, 59, 197, (1988).
75. J. Harms, E. Mausle, *Biocomp. Implant Orthop.*, 144, 236, (1980).
76. V.A. Memoli, J.L. Woodman, R.M. Urban, J.O. Galante, *Acta Orthop. Scand.*, 59, 202, (1988).
77. T. Albrektsson, P.I. Branemark, Hansson, H.A., B. Kasemo, K. Larsson, I. Lundstrom, D. McQueen, R. Skalak, *Ann. Biomed. Eng.*, 11, 1, (1983).
78. L. Linder, T. Albrektsson, P.I. Branemark, H.A. Hansson, B. Ivarsson, U. Jonsson, I. Lundstrom, *Acta Orthop. Scand.*, 54, 1, (1983).
79. B. Halliwell, J.M.C. Gutteridge, *Molec. Asp. Med.*, 8, 89, (1985).
80. S.F. Wong, B. Halliwell, R. Richmond, W.R. Skowroneck, *J. Inorg. Biochem.*, 14, 127, (1981).
81. J.M.C. Gutteridge, D.A. Rowley, B. Halliwell, *Biochem. J.*, 199, 263, (1981).
82. J.E. Harrison, R.J. Hoare, "Metals in Biochemistry", Chapman and Hall, London, (1980).
83. D.T Day, *Proc. Am. Phil. Soc.*, 36, 112, (1897).
84. M.S. Tswett, *Ber. Deut. Bot. Ges.*, 24, 384, (1906).
85. A.J.P. Martin, R.L.M. Syngé, *Biochem. J.*, 35, 1358, (1941).
86. A.T. James, A.J.P. Martin, *Biochem. J.*, 50, 679, (1952).
87. G.A. Howard, A.J.P. Martin, *Biochem. J.* 46, 532, (1950).
88. L.R. Snyder, *Anal. Chem.*, 39, 698, (1967).
89. R.P.W. Scott, J.G. Lawrence, *J. Chromatog. Sci.*, 7, 65, (1969).
90. J.J. Kirkland, *Anal. Chem.*, 40, 391, (1968).

91. H.N.M. Stewart, S.G. Perry, *J. Chromatog.*, 37, 97, (1968).
92. I. Halasz, I. Sebastian, *Angew. Chem. Int. Edn.*, 84, 453, (1969).
93. R.S. Deelder, P.J.W.M. Claassen, P.J.H. Hendricks, *J. Chromatog.*, 91, 201, (1974).
94. B.L. Karger, L.R. Snyder, C. Horvath, "An Introduction to Separation Science", Wiley-Interscience Publication, New York, (1973).
95. R.G. Pearson, *Science*, 151, 172, (1966).
96. J. van Deemter, F.J. Zuiderweg, A. Klinkenberg, *Chem. Eng. Sci.*, 5, 271, (1956).
97. G.D. Christian, J.E. O'Reilly, "Instrumental Analysis", 2nd Edn., Alley and Bacon, Inc., (1986).
98. D.A. Skoog, "Principles of Instrumental Analysis", 3rd Edn., Saunders College Publishing, (1984).
99. J.R. Bales, D.P. Higham, I. Howe, J.K. Nicholson, P.J. Sadler, *Clin. Chem.*, 30, 426, (1984).
100. D.L. Rabenstein, T.T. Nakashima, *Anal. Chem.*, 51, 1465, (1979).
101. J.K. Sanders, B.K. Hunter, "Modern NMR Spectroscopy - A Guide for Chemists", Oxford University Press, (1987).
102. E.L. Hahn, *Phys. Rev.*, 80, 580, (1950).
103. H. Fischer, *Agnew. Chem.*, 50, 230, (1937).
104. R.S. Young, *Analyst*, 76, 49, (1951).
105. L. Erdey, G. Rady, *Z. Anal. Chem.*, 135, 141, (1952).
106. G.G. Graham, T.M. Haavisto, C.D. McNaught, G.D. Champion, *J. Rheum.*, 9, 527, (1982).
107. D.W. James, N.W. Ludvigsen, L.G. Cleland, S.C. Milazzo, *J. Rheum.*, 9, 532, (1982).
108. G.G. Graham, T.M. Haaviasto, H.M. Jones, G.D. Champion, *Biochem. Pharmacol.*, 33, 1257, (1984).

109. G.G. Graham, J.R. Bales, M.C. Grootveld, P.J. Sadler,
J. Inorg. Chem., 25, 163, (1985).
110. W.R. Mason, J. Am. Chem. Soc., 95, 3573, (1973).
111. P.R. Haddad, N.E. Rochester, Anal. Chem., 60, 536, (1988).
112. D.A. Beardsly, G.B. Briscoe, J. Ruzicka, M. Williams, Analyst,
90, 328, (1965).
113. G. Lewis, C.F. Shaw, Inorg. Chem., 25, 58, (1986).
114. E.C. McQueen, P.W. Dykes, Ann. Rheum. Dis., 28, 437, (1969).
115. A.A. Deitz, H.M. Rubenstein, Ann. Rheum. Dis., 32, 124, (1973).
116. F.J. Maessen, F.D. Posma, J. Balke, Anal. Chem., 46, 1445,
(1974).
117. J.P. Vacik, J.E. Christian, J. Pharm. Sci., 50, 225, (1961).
118. R.J. Ward, C.J. Danpure, D.A. Fyfe, Clinica Chimica Acta, 81, 87,
(1977).
119. H. Kamel, D.H. Brown, J.M. Ottaway, W.E. Smith, Analyst, 102,
645, (1977).
120. A. Goldstein, Pharm. Rev., 1, 625, (1949).
121. R.C. Blodgett, M.A. Heuer, R.G. Pietrusko, Seminars in Arthritis
and Rheumatism, 13, 25, (1984).
122. D.A. Campion, R. Olsen, A. Bohan, R. Bluestone, J. Rheum., 1,
112, (1974).
123. R. Hazan, R. Brener, U. Oron, Biomaterials, 14, 570, (1993).
124. D.S. Sutherland, P.D. Forshaw, G.C. Allen, I.T. Brown, K.R.
Williams, Biomaterials, 14, 893, (1993).
125. J.T. Scales, J. Bone and Joint Surg.[Br], 73-B, 534, (1991).
126. H.J. Agins, N.W. Alcock, M. Bansal, E.A. Salvati, P.D. Wilson,
P.M. Pellicci, P.G. Bullough, J. Bone and Joint Surg.[Am], 73-A,
347, (1988).

127. J.D. Witt, M. Swann, *J.Bone and Joint Surg.[Br]*, 73-B, 559, (1991).
128. P.A. Lalor, P.A. Revell, A.B. Gray, S. Wright, G.T. Railton, M.A.R. Freeman, *J.Bone and Joint Surg.[Br]*, 73-B, 25, (1991).
129. J. Black, *J.Bone and Joint Surg.[Br]*, 70-B, 517, (1988).
130. J. Black, H. Sherk, J. Bonino, W.R. Rostoker, F. Schajwicz, J.O Galante, *J.Bone and Joint Surg.[Am]*, 72-A, 126, (1990).
131. G.S. Leventhal, *J.Bone and Joint Surg.[Am]*, 33-A, 473, (1951).
132. H. McKellop, I. Clarke, K. Markoff, H. Amstutz, *Orth.Trans*, 3, (1979).
133. C.P. Case, V.G. Langkamer, C. James, A.J. Kemp, P.F. Heap, L. Solomon, *J. Bone and Joint Surg.[Br]*, 76-B, 701, (1994).
134. J.K. La Budde, J.F. Orosz, T.A. Bonfiglio, V.D. Pellegrini, *J. Arthrop.*, 9, 291, (1994).
135. P.G. Bullough, *J. Bone and Joint Surg.[Br]*, 76-B, 687, (1994).
136. H. Ronningen, *Acta Orthop. Scand.*, 59, 221, (1988).
137. S.B. Goodman, J.A. Davidson, V.L. Fornasier, *Biomaterials*, 14, 723, (1993).
138. T. Rae, *Biomaterials*, 7, 30, (1986).
139. G. Meachim, D.F. Williams, *J.Biomed.Mater.Res.*, 7, 555, (1973).
140. J.C. Coelho Filho, R.A. Moreira, P.R. Crocker, D.A. Levison, B. Corrin, *Histopathology*, 19, 190, (1991).
141. R.J. Solar, S.R. Pollack, E. Korostoff, *J.Biomed.Mater.Res.*, 13, 217, (1979).
142. M.J. Mindell, S.R. Pollack, *Acta Met.*, 17, 1441, (1969).
143. S.A. Brown, R.W. Margevicius, K. Merrit, *Clinical Implant Materials. Advances in Biomaterials. Vol. IX, Elsevier* (1990).
144. P. Tengvall, H. Elwing, I. Lundstrom, *J.Colloid Interface Sci.*, 130, 405, (1989).

145. P. Tengvall, I. Lundstrom, L. Sjokvist, H. Elwing, L.M. Bjursten, *Biomaterials*, 10, 118, (1989).
146. P. Tengvall, I. Lundstrom, *Clin. Mater.*, 9, 115, (1992).
147. V.M. Berdnikov, L.L. Makarshin, L.S. Ryvkina, *React. Kinet. Catal. Lett.*, 9, 205, (1978).
148. E. Hines, D.F. Boltz, *Anal.Chem.* 24, 6, (1952).
149. H.G. Parkes, R.E. Allen, A. Furst, D.R. Blake, M.C. Grootveld, *Pharm. and Biomed. Anal.*, 9, 1, (1991).
150. R.L. Pecsok, A.N. Fletcher, 1, 155, (1962).
151. D. Rowley, J.M.C. Gutteridge, D. Blake, M. Farr, B. Halliwell, *Clin. Sci.*, 66, 691, (1984).
152. B. Halliwell, *FEBS Lett.*, 92, 321, (1978).
153. J. Lunec, A. Wakefield, S. Brailsford, D.R. Blake, "Free Radical Damage in Disease" (C. Rice-Evans, Ed.), Richlieu Press, London, (1986).
154. S.D. Hewitt, J. Lunec, C.J. Morris, D.R. Blake, *Ann. Rheum. Dis.*, 46, 866, (1987).
155. K.D. Muirden, *Aust. Ann. Med.*, 2, 97, (1970).
156. A.A.H. Lawson, E.T. Owen, A.G. Mowat, *Ann. Rheum. Dis.*, 26, 552, (1976).
157. D.R. Blake, N.D. Hall, P.A. Bacon, P. Dieppe, B.Halliwell, J.M.C. Gutteridge, *Lancet*, ii, 1142, (1981).
158. J.M.C. Gutteridge, D.A Rowley, B. Halliwell, *Biochem. J.*, 199, 2635, (1981).
159. B. Halliwell, J.M.C. Gutteridge, *Molec. Aspects. Med.*, 8, 89, (1985).
160. J.M.C. Gutteridge P.G. Winyard D.R. Blake J. Lunec, S. Brailsford, B. Halliwell, *Biochem. J.*, 230, 517, (1985).

- 
161. J.R. Bales, D.P. Higham, I. Howe, J.K. Nicholson, P.J. Sadler,
Clin. Chem., 30, 426, (1984).
 162. M.J. O'Connell, R.J. Ward, H. Baum, J. Peters, Biochem. J.,
260, 903, (1987).
 163. M.C. Grootveld, J.D. Bell, B. Halliwell, O.I. Aruoma, A. Bomford,
P.J. Sadler, J. Biol. Chem., 264, 4417, (1989).
 164. R.B. Martin, J. Inorg. Biochem., 28, 181, (1986).
 165. CRC Handbook of Chemistry and Physics (51st edition, 1970-71, Chemical
Rubber Co.).

Papers Published

M. Grootveld, D.R. Blake, T. Sahinoglou, A.W. Claxson, P.Mapp, C. Stevens, R.E. Allen, A. Furst, *Free Rad. Res. Comm.*, 10, 199, (1990).

H.G. Parkes, R.E. Allen, A. Furst, D.R. Blake, M.C. Grootveld, *J. Pharm. Biomed. Anal.*, 9, 29, (1991).

M. Grootveld, A.W. Claxson, A. Furst, D.R. Blake, *Agents Actions Suppl.*, 32, 77, (1991).

M. Grootveld, A.W. Claxson, D. Naughton, M. Whelan, A. Furst, D.R. Blake, *Agents Actions Suppl.*, 32, 65, (1991).

Abstracts presented at the Barcelona 1990 International Conference on Inflammation:

M. Grootveld, A. Furst, P.Revell, D.R. Blake, 'Speciation of Implant-Derived Titanium (III) and Titanium (IV) Ions from Samples Obtained from Patients with Joint Prostheses Containing Titanium-Aluminium-Vanadium Alloy'.

M. Grootveld, A. Furst, R.E. Allen, D. Naughton, D.R. Blake, 'The Chemical Nature of Non-Transferrin-Bound Iron Ions in Synovial Fluid from Patients with Rheumatoid Arthritis: Characterisation by Proton Nuclear Magnetic Resonance (NMR) Spectroscopy'.

THE BRITISH LIBRARY

BRITISH THESIS SERVICE

TITLE AN ANALYTICAL STUDY OF THE ROLE SELECTED
METAL IONS IN BONE AND JOINT DISEASES

AUTHOR Alexandra
FURST

DEGREE Ph.D

**AWARDING
BODY** University of North London

DATE 1995

**THESIS
NUMBER** DX189641

THIS THESIS HAS BEEN MICROFILMED EXACTLY AS RECEIVED

The quality of this reproduction is dependent upon the quality of the original thesis submitted for microfilming. Every effort has been made to ensure the highest quality of reproduction. Some pages may have indistinct print, especially if the original papers were poorly produced or if awarding body sent an inferior copy. If pages are missing, please contact the awarding body which granted the degree.

Previously copyrighted materials (journals articles, published texts etc.) are not filmed.

This copy of the thesis has been supplied on condition that anyone who consults it is understood to recognise that its copyright rests with its author and that no information derived from it may be published without the author's prior written consent.

Reproduction of this thesis, other than as permitted under the United Kingdom Copyright Designs and Patents Act 1988, or under specific agreement with the copyright holder, is prohibited.

DX

189641